NAVAL POSTGRADUATE SCHOOL
Monterey, California

THESIS

EFFECTS OF POWER PULSATIONS ON NATURAL CONVECTION FROM DISCRETE HEAT SOURCES

by

Stephen Larsen

DECEMBER 1991

Thesis Advisor: Yogendra Joshi

Approved for public release: Distribution is unlimited

REPORT DOCUMENTATION PAGE

Form Approved
OMB No 0704-0188

1. REPORT SECURITY CLASSIFICATION: Unclassified	1b. RESTRICTIVE MARKINGS
2. SECURITY CLASSIFICATION AUTHORITY	3. DISTRIBUTION/AVAILABILITY OF REPORT: Approved for public release: Distribution is unlimited
2b. DECLASSIFICATION/DOWNGRADING SCHEDULE	
4. PERFORMING ORGANIZATION REPORT NUMBER(S)	5. MONITORING ORGANIZATION REPORT NUMBER(S)
6a. NAME OF PERFORMING ORGANIZATION: Naval Postgraduate School; 6b. OFFICE SYMBOL (If applicable): ME	7a. NAME OF MONITORING ORGANIZATION: Naval Postgraduate School
6c. ADDRESS (City, State and ZIP Code): Monterey, CA 93943-5000	7b. ADDRESS (City, State, and ZIP Code): Monterey, CA 93943-5000
8a. NAME OF FUNDING/SPONSORING ORGANIZATION; 8b. OFFICE SYMBOL (If applicable)	9. PROCUREMENT INSTRUMENT IDENTIFICATION NUMBER
8c. ADDRESS (City, State, and ZIP Code)	10. SOURCE OF FUNDING NUMBER: PROGRAM ELEMENT NO. / PROJECT NO. / TASK NO. / WORK UNIT ACCESSION NO.

11. TITLE (Include Security Classification)

EFFECTS OF POWER PULSATIONS ON NATURAL CONVECTION FROM DISCRETE HEAT SOURCES

12. PERSONAL AUTHORS
STEPHEN LARSEN

13a. TYPE OF REPORT	13b. TIME COVERED	14. DATE OF REPORT (Year, Month, Day)	15. PAGE COUNT
Master's Thesis	FROM_____ TO_____	DECEMBER 1991	286

16. SUPPLEMENTARY NOTATION
The views expressed are those of the author and do not reflect the official policy or position of the Department of Defense or the U.S. Government

17. COSATI CODES			18. SUBJECT TERMS (Continue on reverse if necessary and identify by block numbers)
IELD	GROUP	SUB-GROUP	liquid immersion cooling, power pulsation, temperature variation

19. ABSTRACT (Continue on reverse if necessary and identify by block numbers)

The natural convection heat transfer response of an array of heaters flush mounted on a vertical test surface in water to periodic input power has been investigated. Two types of periodic input power variations were examined: a triangular wave and an approximate square wave. The resulting heater temperatures over several cycles were measured for mean values of 0.5, 1.0, 2.0, and 3.0 watts and varying amplitudes. The frequency of the input power pattern was also varied, from 0.025 to 0.1 Hz. The measured heater temperatures were compared with the responses for steady input power equal to the mean of the periodic input.

20. DISTRIBUTION/AVAILABILITY OF ABSTRACT	21. ABSTRACT SECURITY CLASSIFICATION	
XX UNCLASSIFIED/UNLIMITED __ SAME AS RPT __ DTIC USERS	unclassified	
22a. NAME OF RESPONSIBLE INDIVIDUAL: Yogendra Joshi	22b. TELEPHONE (Include Area Code): (646-3400	22c. OFFICE SYMBOL: ME/Jo

Approved for public release: Distribution is unlimited

Effects of Power Pulsations on Natural Convection From Discrete Heat Sources

by

Stephen Larsen
Lieutenant, United States Navy
B.S., University of Nebraska, Lincoln, 1984

Submitted in partial fulfillment of the
requirements for the degree of

MASTER OF SCIENCE
IN MECHANICAL ENGINEERING

from the

NAVAL POSTGRADUATE SCHOOL

DECEMBER 1991

Author: 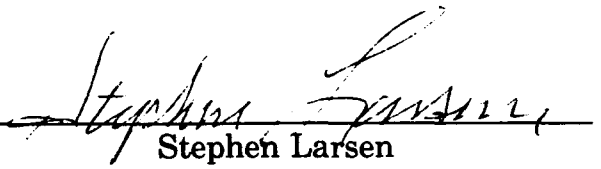
Stephen Larsen

Approved by: 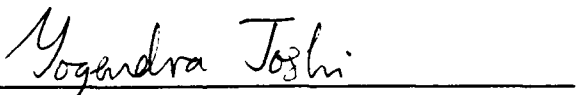
Yogendra Joshi, Thesis Advisor

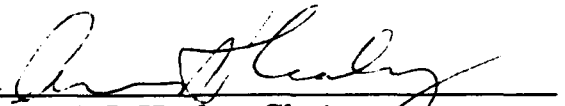
A.J. Healey, Chairman
Department of Mechanical Engineering

ABSTRACT

The natural convection heat transfer response of an array of heaters flush mounted on a vertical test surface in water to periodic input power has been investigated. Two types of periodic input power variations were examined: a triangular wave and an approximate square wave. The resulting heater temperatures over several cycles were measured for mean values of 0.5, 1.0, 2.0, and 3.0 watts and varying amplitudes. The frequency of the input power pattern was also varied, from 0.025 to 0.1 Hz. The measured heater temperatures were compared with the responses for steady input power equal to the mean of the periodic input.

TABLE OF CONTENTS

LIST OF TABLES

LIST OF FIGURES

NOMENCLATURE

A	Surface area of each element
β	Expansion coefficient
g	gravity
k	Thermal conductivity
L	Area divided by the perimeter
Q	Rate of energy output from each element
Q_{conv}	Net rate of energy input from each element to the fluid
R_L	Lead resistance
R_p	Precision resistor resistance
T_{amb}	Ambient temperature
T	temperature of the element
V_L	Voltage measured over the leads and heater [Volts]
V_T	Voltage over the precision resistor, leads and heater [Volts]
ν	Kinematic viscosity

ACKNOWLEDGMENTS

First of all, I would like to thank Professor Joshi for the assistance and insight which he provided me throughout this project. Secondly, I would like to thank my wife for her patience and understanding during this time. Thirdly, I would like to thank Tom Christian for his technical assistance. Finally, I would like to give my special thanks to Jim Scholfield. Jim on several occasions bridged the gap between design and reality. His suggestions always enhanced design and made the accomplishment of this project possible in a timely fashion.

I. INTRODUCTION

As electronic components become increasingly smaller, the volumetric power generation rates escalate and the problem of their thermal management becomes even more challenging. The greatest constraint to further advances in decreasing the feature size and increasing functional capability of electronic components could be the unavailability of appropriate heat removal techniques. The performance and reliability of microelectronic components is a function of junction temperature. The average failure rates of microelectronic components increase exponentially with junction temperature increase; Bar-Cohen and Kraus [Ref. 1].

Direct liquid cooling has emerged as one of the most promising thermal management techniques for overcoming this barrier; Bar-Cohen [Ref. 2]. The advantages of liquid cooling have been demonstrated for over 40 years in macroelectronic components, yet its use for cooling microelectronic components is relatively new.

There are three types of liquid cooling techniques that can be employed; boiling, forced convection, and natural convention. Initiation of boiling with dielectric fluids is complicated by the highly wetting nature of these liquids. Forced convection can produce higher heat dissipation rates, however, it may present its own set of problems with reliability and higher costs. Even though

natural convection cooling typically allows lower heat dissipation rates than the first two methods, it has the advantages of simplicity of design, low operation cost due to no outside power requirements and minimum maintenance, absence of noise and high reliability. Also, in the event of a mechanical failure, natural convection may be the only method of cooling available [Refs. 3, 4, 5].

Natural convection originates when a body force acts on a fluid in which there are density gradients. The net effect is a buoyancy force, which induces free convection currents. In the most common case, the density gradient is due to a temperature gradient, and the body force is due to the gravitational field.

A. SUMMARY OF LITERATURE

Baker [Ref. 6] studied the heat transfer characteristics of flush mounted heat sources on vertical surface in several liquids. Park and Bergles [Ref. 7] investigated both flush and protruding arrangements in water and R-113. Bar-Cohen and Schweitzer [Ref. 8] presented correlations for natural convection in a vertical channel dissipating uniform heat flux from the sides. Kelleher *et. al.* [Ref. 9] conducted flow visualization and heat transfer measurements for natural convection from a long heated protrusion on a vertical insulated wall of a rectangular chamber filled with water. Lee *et. al.* [Ref 10] supported Kelleher's findings with a computational investigation.

Joshi *et. al.* [Ref. 11] presented flow visualizations and component surface temperature measurements for natural convection cooling of a three by three array of discrete heated protrusions on the vertical wall of a rectangular enclosure filled with a dielectric liquid. Joshi *et. al.* presented experimental studies of the heat transfer and flow characteristics of a column of protruding heat sources, [Ref. 12] on a vertical surface and within a vertical channel, [Ref. 13]. Sathe and Joshi [Ref. 4] reported results of a numerical investigation of natural convection flow and heat transfer arising from a protruding heat source on a vertical plate within an enclosure. Joshi and Paje [Ref. 14] reported experimental results of natural convection heat transfer from a commercially available semiconductor device package.

Joshi and Knight [Ref. 15] studied the natural convection from a single column of eight in-line, rectangular heat sources flush mounted on one wall of a vertical channel immersed in water. Gaiser [Ref. 16] examined natural convection adjacent to a three column array of 15 per column uniformly heated components flush mounted on a vertical flat plate in water. Haukenes [Ref. 5] reported results of a numerical investigation of two dimensional natural convection flow and heat transfer from a substrate-mounted flush heat source immersed in a liquid filled square enclosure. Akdeniz [Ref. 17] investigated the natural convection heat transfer from an array of heaters flush mounted on a vertical test surface in response to both step and periodic input power.

B. PRESENT STUDY

The investigation reported here is a continuation of the studies of Gaiser [Ref. 16], Haukenes [Ref. 5], and Akdeniz [Ref. 17]. As stated above, Akdeniz [Ref. 17] presented the changes in the natural convection flow and heat transfer characteristics of a three column array of 45 flush mounted heaters on a vertical test surface. In his study, power to the bottom heater of the center column oscillated with time while power to all the other heaters was kept constant. The present experimental study was conducted with the same test surface as in [Ref. 16, 5, and 17], however, the entire center column was powered in a time periodic fashion while the side columns of heaters remained unpowered.

Specifically, the natural convection heat transfer response of a column of heaters flush mounted on a vertical test surface in water to periodic input power has been investigated. Two types of periodic input power variations were examined: a triangular wave and an approximate square wave. The resulting heater temperatures over several cycles were measured for mean values of 0.5, 1.0, 2.0, and 3.0 watts and varying amplitudes. The frequency of the input power patterns was also varied, from 0.025 to 0.1 Hz. The measured heater temperatures were compared with the responses for steady input power equal to the mean of the periodic input.

C. OBJECTIVES

The particular objectives of this investigation were:

- To examine the effects of power pulsation on the heat transfer characteristics for the selected conditions.
- To determine if any enhancement of heat transfer occurs due to the input power variations.

II. EXPERIMENT

A. EXPERIMENTAL APPARATUS

The experimental apparatus is described in detail by Gaiser [Ref. 16]. Additions and modifications to the apparatus were discussed by Haukenes [Ref. 5] and Akdeniz [Ref. 17]. The following is a brief summary of the above with emphasis on the additional changes to reflect the current status of the apparatus.

The apparatus itself is sub-divided into four separate assemblies; test surface assembly, power supply assembly, data acquisition/reduction unit, and the deaerating assembly, as seen in Figure 1. The first three of these systems are interrelated through three distinct variables; the input power to the heater strips, the heater strip surface temperatures, and the ambient temperature of the bath. The last of these systems, the deaerating system is used separately to reduce the amount of entrained air and compressible gasses.

1. Test Surface Assembly

This consisted of a vertical test surface with 45 flush mounted heater strips placed on three columns of 15 each. The test surface is immersed in a one cubic meter plate glass tank filled with deionized water. The water is deionized by a series of filters attached externally to the tank. The test surface was constructed using a 31.75 cm x 31.75 cm x 1.11 cm plexiglass plate with

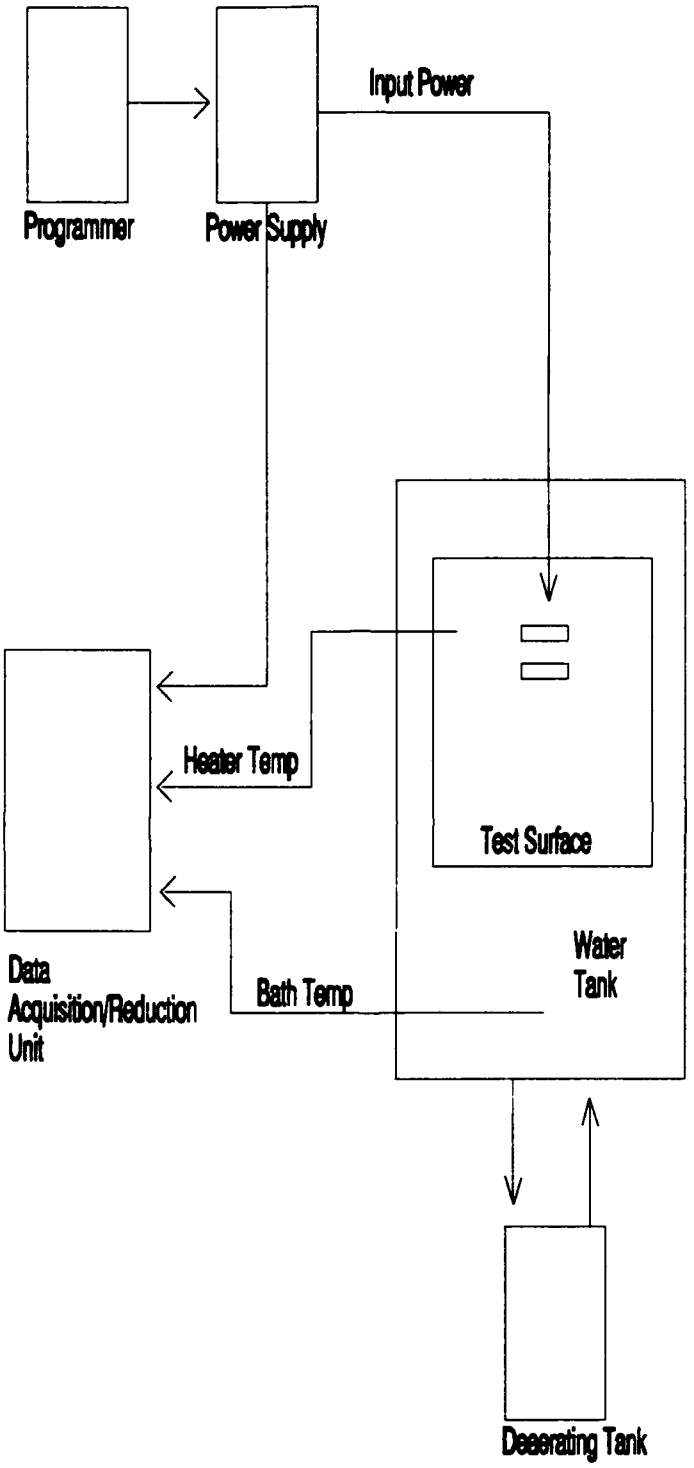

Figure 1. Experimental Apparatus.

3.58 cm x 0.79 cm slots milled out to a depth of 0.19 cm at each location where a heater strip was to be embedded. Figure 2 shows the front view of the test surface showing the location of each heater strip in the central column, powered in this investigation. Within each slot, a 0.79 cm diameter hole was drilled through the board in order to allow the heater strip power leads and thermocouple wires to pass through. Side and top views of a slot are shown in Figure 3. [Ref. 16]

Before mounting the heater strips to the board, two power leads and a 0.0076 cm copper-constantan thermocouple were attached to the back of each strip. The power leads were simply soldered onto the heater strip. A layer of Omega bond 101 high thermal conductivity adhesive was coated over the back of the heater strip to electrically isolate each thermocouple from the heater strip, while allowing for accurate temperature measurements. Once the strip was coated, an additional small drop of the adhesive was used to attach the thermocouple onto the center of the heater strip. [Ref.16]

2. Power Supply Assembly

The power supply assembly provided power to the individual heater strips. For this investigation only the central column was used as seen in Figure 2. An HP-85 computer was used in conjunction with an HP-59501 power supply programmer and a 0-40 Volt, 0-1.5 Amp HP-6298A D.C. power supply to control the power output of the center column of heaters. The HP-6298A power supply was connected to two of the six distribution panels. These

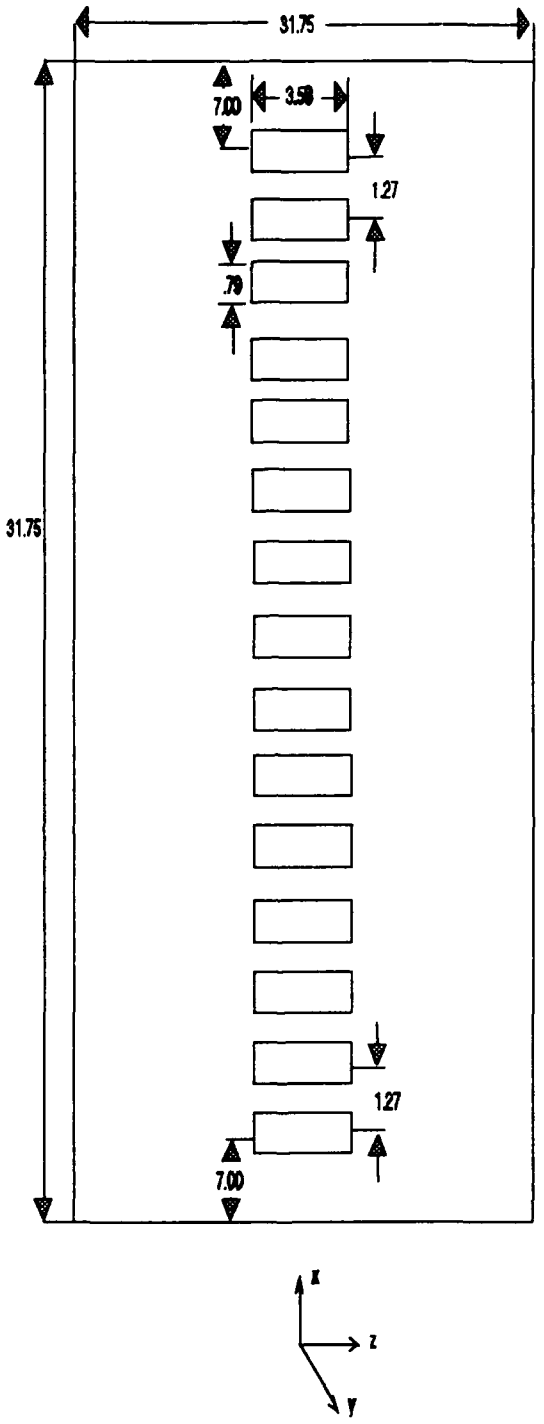

Figure 2. **Front View of Test Surfaces with Active Heaters. All Units in cm.**

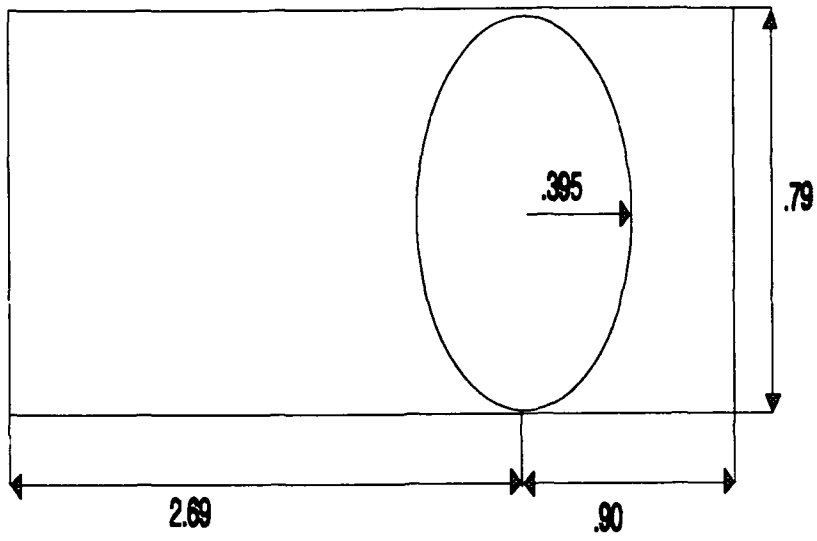

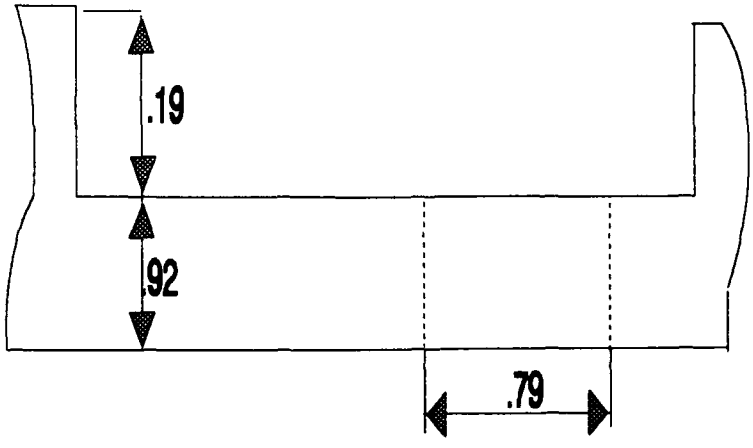

Figure 3. **Front and Side View of the Test Surface Heater Slots. All Units in cm.**

two distribution panels are the ones to which the center column of heaters are connected. Each distribution panel acts as an individual power supply for a specified number of heaters. Each panel supplies power to either seven or eight heaters. If only seven heaters were connected to a particular panel, a ten ohm resistor was used to equilibrate the total power requirement of the panel as compared with an eight heater panel.

Figure 4 shows the power distribution panel. Each heater on a panel was connected in series with a 2.01 ohm 1% precision resistor. The heater and resistor pair was then connected in parallel to two copper wire bus bars, previously referred to as distribution panels. Additional 1% and 5% precision resistors were connected in parallel with the original 1% precision resistors in order to approximate a constant input power for all heaters.

The data acquisition system measures the total voltage drop across the bus, V_T, and the voltage drop for each heater including the leads, V_L. Using these two measured quantities the power output for each heater was determined using the following formula:

$$Power = \left(\frac{V_L(R_p - R_L) - V_T R_L}{R_p^2} \right) (V_T - V_L)$$

Where R_p is the precision resistor resistance and R_L is the heater resistance plus lead resistance. [Ref. 5]

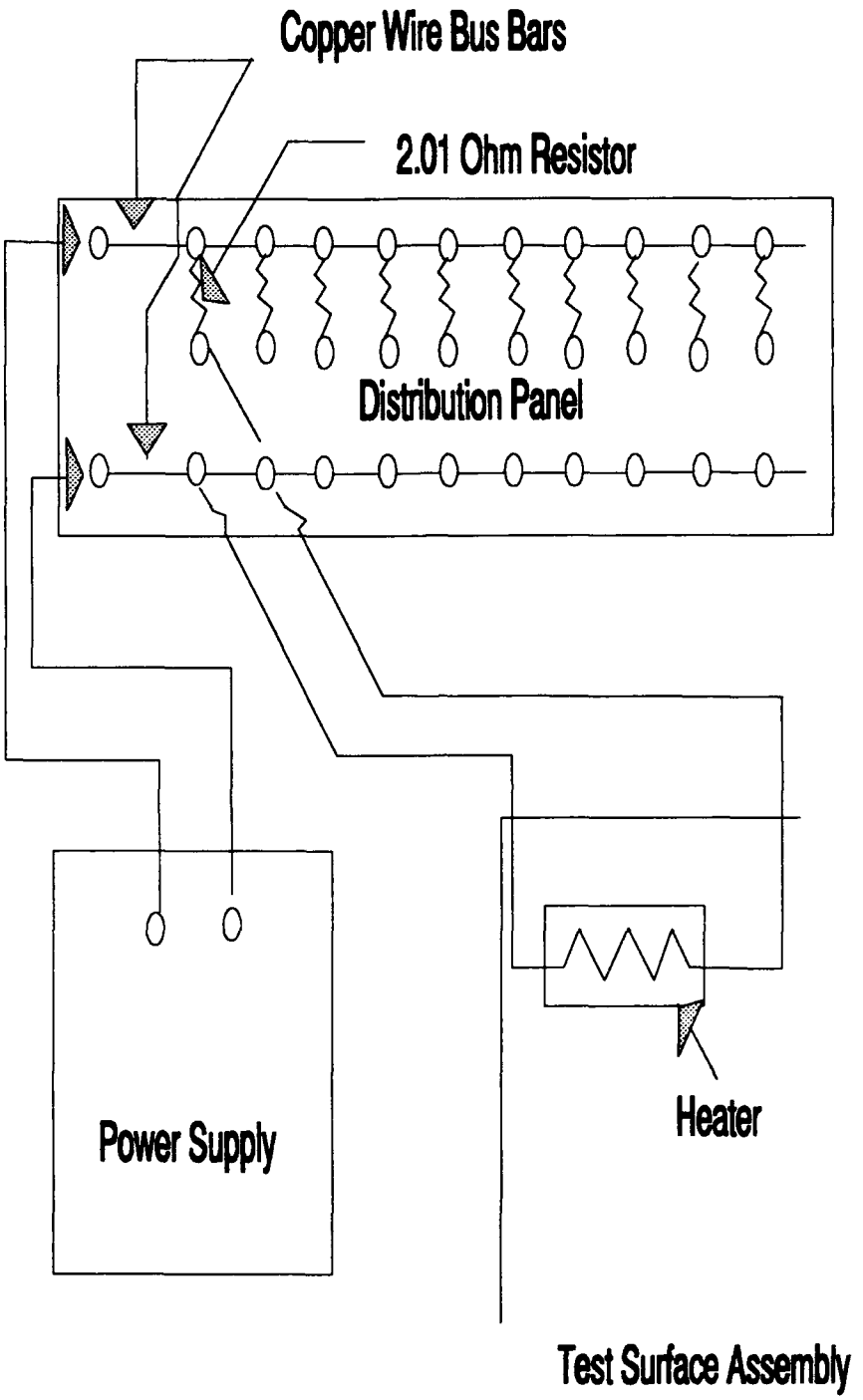

Figure 4. Power Distrimbution Panel.

3. Acquisition/Reduction Unit

The data acquisition/reduction unit was made up of an HP 3852A Data Acquisition unit, an HP 9153 Computer system, and an IBM clone personal computer. This system initiates, records and processes all data from the test surface and power assembly. When tasked by the HP 9153 Computer system, the HP 3852A Data Acquisition unit reads the thermocouple voltages, and the appropriate voltages for the determination of heater powers.

This data was then transmitted into the HP 9153 Computer system which processed it into temperatures and power measurements. The temperature readings were further manipulated by taking the difference between the ambient temperature and the temperature of the heater. The power readings were processed as per the discussion above.

This data, once processed, was transferred to an IBM clone personal computer. This was accomplished by printing the data directly to the RS-232 port of the HP 9153 Computer system, which was connected to the RS-232 IBM computer via a cable. The statement used for the HP 9153 computer to transmit through the RS-232 port was "printer is 9". The HP 9153 computer automatically converted the data file into ASCII file format prior to printing it to the RS-232 port. The data was received into the IBM computer by using a communication program. Once received by the IBM computer, the data was imported into a spread sheet program which was used for graphics. The data files were imported as a comma & "" delimited file. The data file had to be

formatted to be imported this way. This was accomplished using an editor within the IBM clone computer.

4. Deaerating Assembly

The deaerating assembly was composed of a vacuum pump, discharge pump, a heating element, and the deaerating tank, see Figure 5. The deaerating tank can be used in conjunction with the filtration system. The filtration system, consisting of four cartridges, is used to ensure the purity by maintaining the resistivity of the tank water at 0.7 megaohm-cm or above. This is achieved through periodic recirculation of the tank water.

The bath water from the tank was vacuum dragged into the deaerating tank through a nozzle. The vacuum was manually regulated to be between 68 and 85 KPa. A heating element within the deaerating tank heats the water to 10 - 15 K above the bulk temperature in the test tank. The temperature within the deaerating tank is maintained by regulating the flow rate through the tank by the discharge pump. Flow rates between 900 milliliters per minute to 1500 milliliters per minute were the norm.

Float switches were used to maintain the water level within a range around the nominal level. The capacity of the deaerating tank was 60.6 liters and the tank was nominally maintained to be half full. This was done to provide complete coverage of the panel heating element. The tank itself was elevated 1.83 meters above the floor to provide sufficient head for the discharge pump.

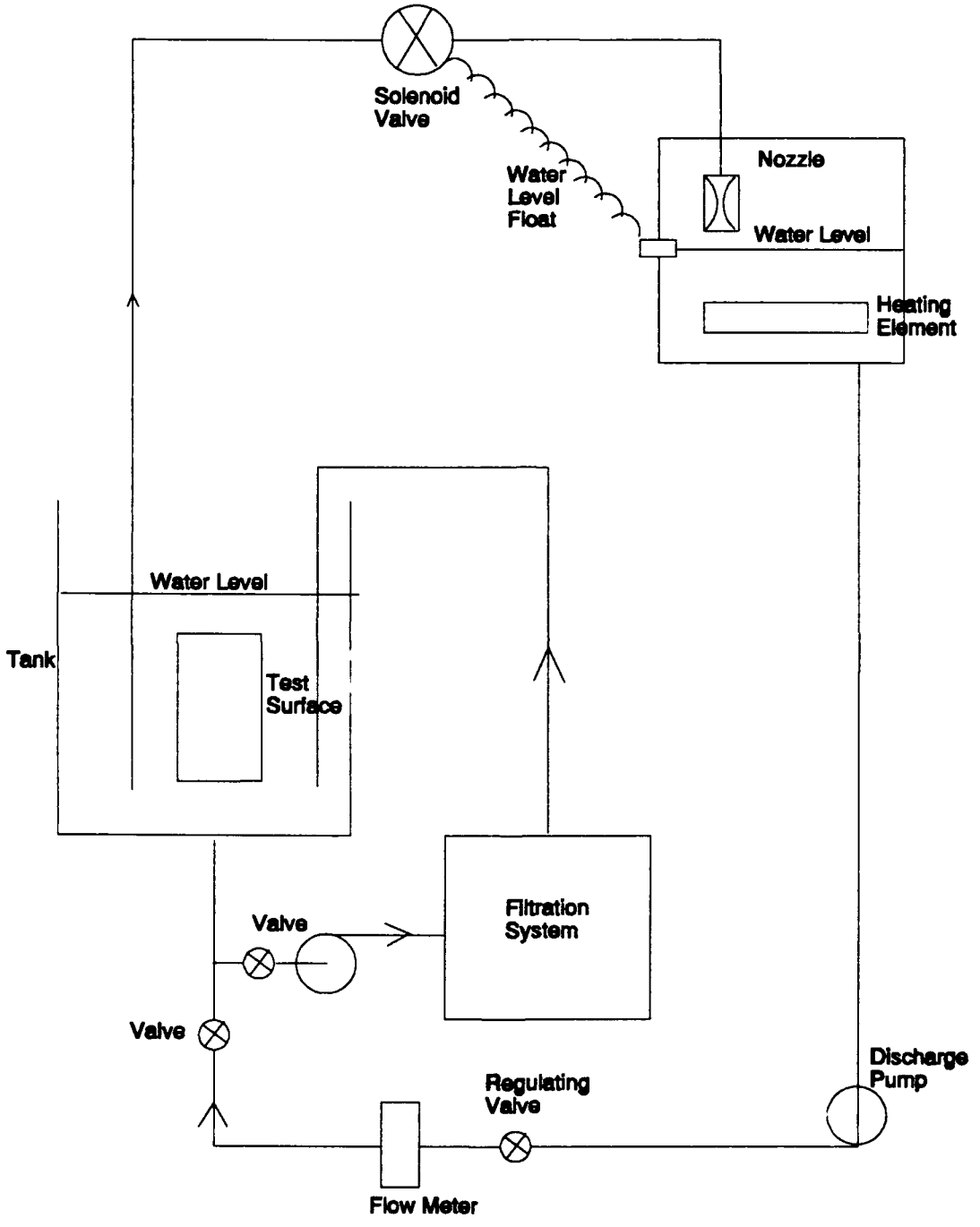

Figure 5. Deaerating System.

B. EXPERIMENTAL PROCEDURE

In preparing for a series of experiments, the mechanical stirrer would be run for five to ten minutes to dissipate prior stratification within the test tank. Crushed ice was placed into the thermocouple reference bath. Typically the data acquisition unit and the HP computers were left on. Only the IBM computer and the power supply were secured. Quiescence was achieved within the test tank prior to powering any of the heaters. This would take approximately 30 minutes.

Once the bath was ready, the power supply was energized and the program to generate appropriate periodic power input patterns through the heaters was loaded and run (see Appendix D). Another 10 to 12 minutes were needed to ensure that steady state conditions were reached prior to taking any temperature measurements. Once steady conditions were achieved, the data acquisition program was started and periodic temperature measurements over five minutes were taken.

The effects of two different type of periodic input power patterns were examined: a triangular pattern and an approximate square wave pattern. Measurements at three locations along the test surface were obtained for each run. These measurements were obtained for four mean input power levels, each for three amplitudes and three frequencies of pulsation. The

corresponding steady state measurements for the selected mean power levels were also made.

III. EXPERIMENTAL RESULTS

A. DESCRIPTION OF DATA

As previously mentioned, the test surface consisted of three columns of 15 heaters, numbered as in Figure 6. Only the center column of heaters was used for this study, heaters 16 through 30. Three different configurations of the center column of heaters were used, see Figure 7. In configuration A, all 15 heaters were powered uniformly. In configuration B, only the top 13 heaters were powered uniformly, thus leaving heater 29 and 30 de-energized. Configuration C is a further modification of heater configuration B, de-energizing the top heater, heater 16. This left 12 heaters heated. The reason for the modifications was to the failure of some heaters due to prolonged periodic input power through them.

Contained within Appendix A is a complete listing of all runs performed for this study. All graphical data is presented within Appendix B. The captions for each figure contained within Appendix B refer to a heater configuration, using a three digit alphanumeric format. The first digit is a letter, either A, B, or C, which references the number of active heaters as stated above, see Figure 7. The second and third digits are numbers which denote the heater number, as seen in Figure 6. For example, heater configuration B21 means that the top

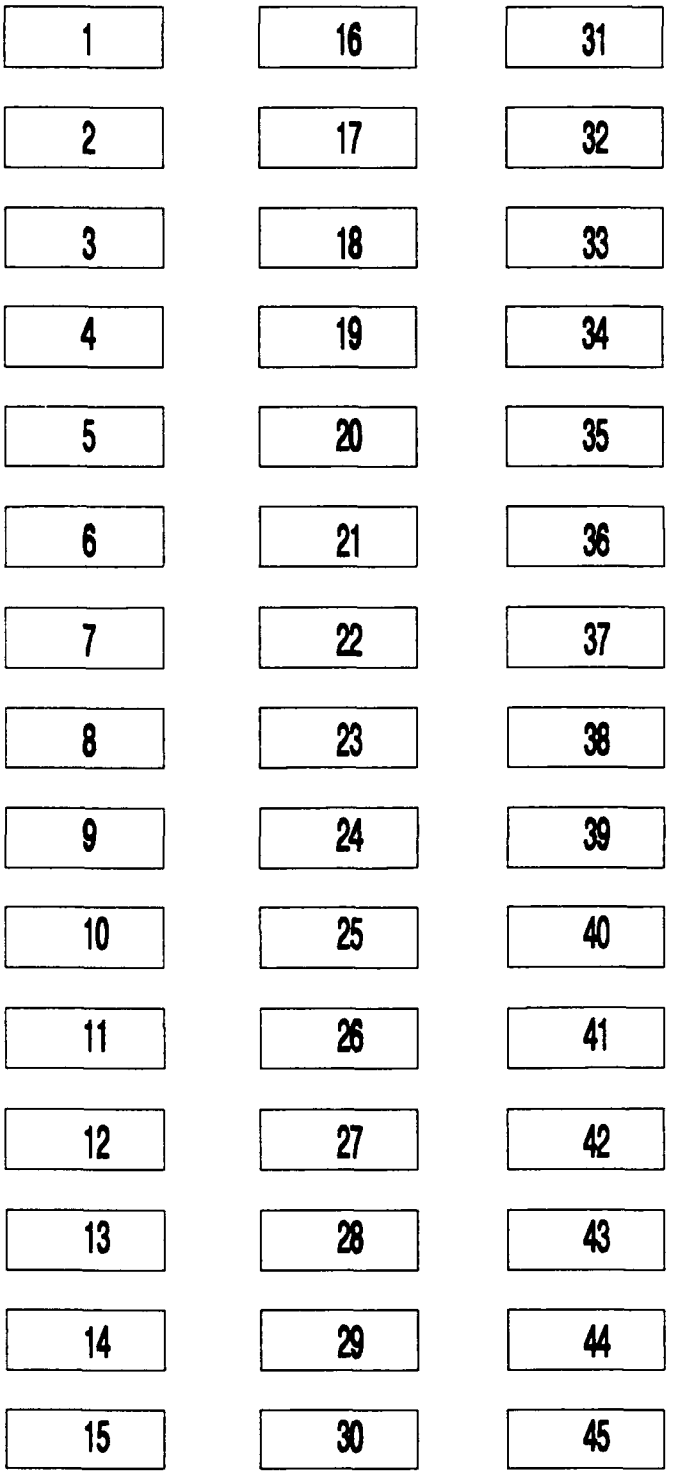

Figure 6. View of Test Surface.

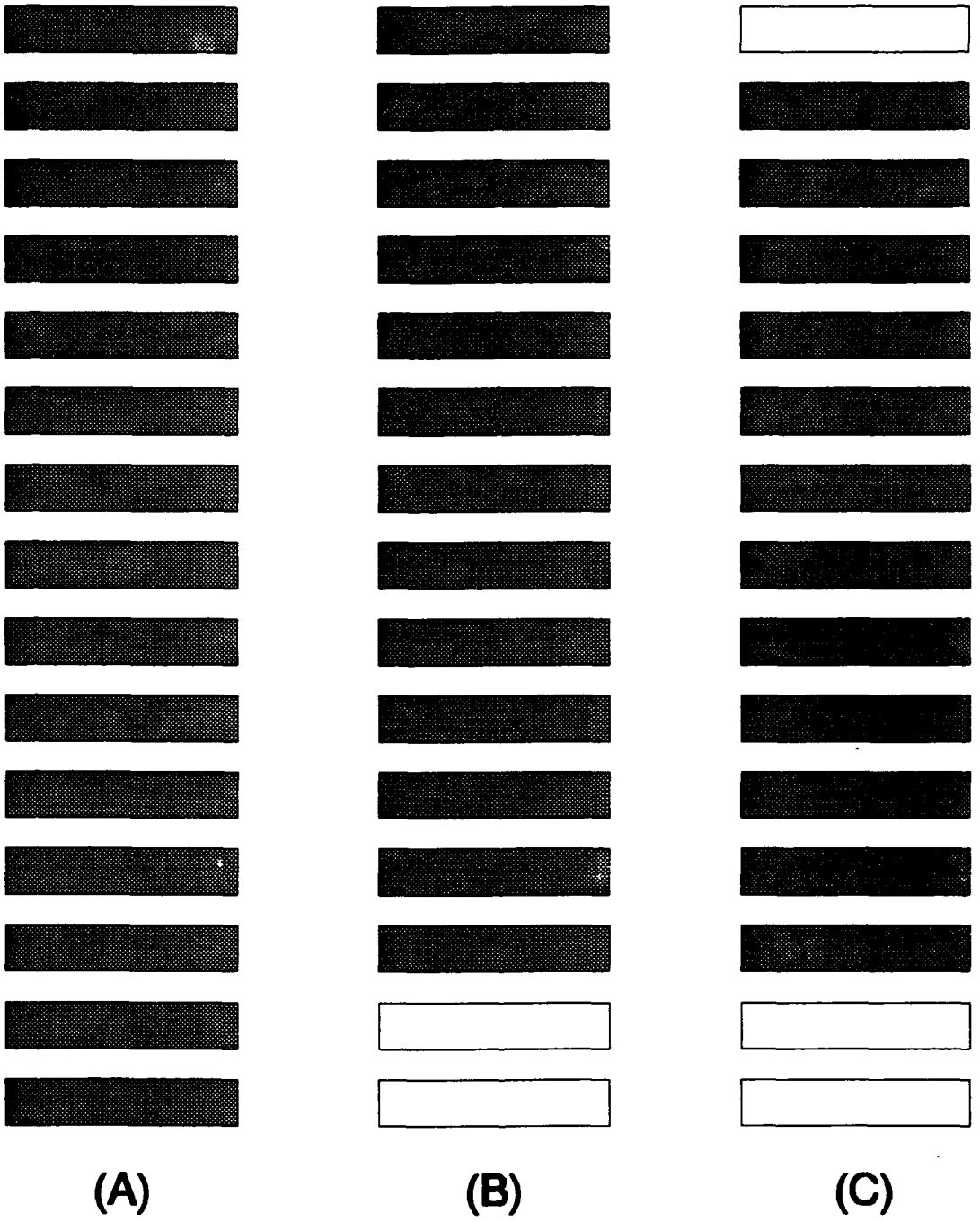

Figure 7. Heater Configurations A, B, and C.

13 heaters where heated and the heater of interest is heater number 21, or the middle heater.

For this investigation, measurements at three heater locations were made for each run near the top, middle and bottom of the column, in order to determine the downstream effects on the heat characteristics. Table I, shows which heaters were used near the top, middle, and, bottom locations for each of the heater configurations.

TABLE I. DESIGNATION OF TOP, MIDDLE AND BOTTOM HEATERS FOR DIFFERENT HEATER CONFIGURATIONS

HEATER	HEATER CONFIGURATION		
	A	B	C
TOP	16	16	17
MIDDLE	23	21	21
BOTTOM	30	28	28

Each of the figures found in Appendix B are numbered with a two letter code. The first letter denotes a specific mean power input and amplitude. The second letter designates a specific heater, top, middle, or bottom, and frequency at which the input power pattern was applied. This can be seen in Table II and Table III. It takes a grouping of three figures to represent a single run. A run represents a grouping of figures where only the heater of interest changes for a given set of power input parameters. The second letter designation for the figures, A, B, and C, constitutes one run. E, D, and F constitutes the next run,

and G, H, and I constitutes the last run. These groupings are divided up by the frequency at which the power pattern is applied.

TABLE II. FIRST LETTER DESIGNATION OF FIGURE CODE

First Letter Designation	Mean Value of Power Input	Amplitude	Power Pattern
A	2	0.5	Triangular
B	2	1	Triangular
C	2	2	Triangular
D	0.5	0.5	Triangular
E	1	0.5	Triangular
F	1	1	Triangular
G	3	0.5	Triangular
H	3	1	Triangular
I	3	2	Triangular
J	2	0.5	Square
K	2	1	Square
L	2	2	Square
M	0.5	0.5	Square
N	1	0.5	Square
O	1	1	Square
P	3	0.5	Square
Q	3	1	Square
R	3	2	Square

To obtain all the data for a single run, each experiment had to be repeated a total of six different times. This allowed gathering the necessary

TABLE III. SECOND LETTER DESIGNATION FOR FIGURE CODE

Second Letter Designation	Heater	Frequency
A	Top	0.100
B	Middle	0.100
C	Bottom	0.100
D	Top	0.050
E	Middle	0.050
F	Bottom	0.050
G	Top	0.025
H	Middle	0.025
I	Bottom	0.025

input power and temperature data on three different heaters with pulsating and steady input powers. The pulsating and steady programs for the HP 85 computer are contained within Appendix D. The data are presented one heater per graph. This was done to enhance readability.

For all discussion of the data two definitions are needed. The first being heat transfer enhancement; where the mean cyclic temperature response is less than the steady temperature response. The second being significant heat transfer enhancement; where the maximum cyclic temperature response is less than the steady temperature response.

B. DISCUSSION OF TRIANGULAR WAVE DATA

The baseline run for the triangular wave data was arbitrarily taken to be; mean value power input of 2.0 watts, amplitude of 1.0 watts, and a frequency of 0.050 Hz, see Figures BD-BF.

The amplitude of the cyclic temperature response as a percentage of the steady temperature response ranges from 6.7% at the top heater to 16.8% at the bottom heater, where the amplitude of input power is 50% of the mean power input. There are some damping effects evident from the temperature response. The damping effects are more pronounced at the top heater than the bottom or middle heaters. There seems to be little change in the damping effects between the middle heater and the bottom heater. Minimizing the amplitude of the temperature response is desirable for application purposes. The frequency of the cyclic temperature response matches that of the power input, however, as expected there was a phase lag. Also, for the top heater the cyclic temperature response, is slightly lower than the steady temperature response implying some heat transfer enhancement. The pulsation of the power input seems to have a more dramatic effect on the top heater than the bottom heater, where there seems to be little to no heat transfer enhancement. This trend will become more dramatic later on.

1. Effects of the Amplitude of Power Pulsation

Figures CD-CF present results for mean input of 2.0 watts, amplitude of 2.0 watts and a frequency of 0.025 Hz. These figures are an

increase in the amplitude of 1.0 watts compared to the baseline conditions. For these conditions the heat transfer enhancement is more pronounced than the base line case. For the top heater the mean cyclic temperature response, is 6 K lower than the steady temperature response. The top heater sees the greatest enhancement and the bottom heater the least. For the top and middle heaters, the maximum cyclic temperature response is clearly lower than the steady temperature response. Note, the maximum cyclic temperature response for the top and middle heaters are very close. For the bottom heater, the mean of the cyclic temperature response is significantly lower than the steady temperature response. Still, the maximum cyclic temperature response is higher than the steady temperature response.

Figures AD-AF present results for mean input of 2.0 watts, amplitude of 0.5 watts and a frequency of 0.050 Hz. These figures are a decrease in the amplitude of 0.5 watts compared to the baseline case. The heat transfer enhancement effects due to this pulsation are negligible. The amplitude of the temperature response is less than in the baseline case.

It can be readily seen that as the amplitude to mean power ratio approaches one, significant heat transfer enhancement takes place. The importance of this ratio will be demonstrated again later on with different input powers.

2. Effects of the Frequency of Pulsation

Figures BA-BC present results for mean input of 2.0 watts, amplitude of 1.0 watts and a frequency of 0.100 Hz. These figures are an increase in the frequency by a factor of two from the baseline case. The first effect noticed is the damping of the temperature response. The amplitude response of the top heater drops from 6.7% in the base line case to 3.7%, and bottom heater drops from 16.8% to 6.4%. Some increase in enhancement is noted by increasing the frequency. Figure BA shows a slightly lower mean cyclic temperature response than the steady temperature response.

Figures BG-BI present a decrease in the frequency of the pulsation of the input power from 0.050 to 0.025 Hz. The effects of damping were diminished. The temperature amplitude at the top heater jumped from 6.7% to 10% and for the bottom heater from 16.8% to 20.5%. With the decreased frequency the thermal inertia of the surface and thermocouple becomes less important. No significant heat transfer enhancement was noted at the bottom heater location. A slight enhancement at the top heater was noted, but less than in the base line case.

In summary, as the frequency of the power pulsation is increased the amplitude of the temperature response decreases and there is a slight heat transfer enhancement. As stated previously, smaller amplitudes of the temperature response are desirable for applications purposes.

3. Effects of the Mean Input Power

Figures HD-HF present results for a mean input of 3.0 watts, amplitude 1.0 watts and a frequency of 0.050 Hz. These figures are an increase in the mean input power of 1.0 watts from the baseline case. It is readily seen that the amplitude of the temperature response remains unchanged from the baseline case for the top and bottom heater locations. For the middle heater location the amplitude of the temperature response is slightly larger. This may be due to the fact that heater configuration B for this run was used instead of heater configuration A for the baseline run resulting in minor differences in the response times of the embedded surface thermocouple. The frequency response still matches that of the input power for all three heaters. The drop in temperature is more pronounced for the top heater than in the base line case.

Figures FD-FF present results for a mean input of 1.0 watts, amplitude of 1.0 watts and a frequency of 0.050 Hz. Heat transfer enhancement is seen for all three heaters. The greatest enhancement occurred for the top heater location. Note heater configuration B was used for this run. The frequency response matches that of the input power, and temperature amplitudes are approximately the same as that of the baseline case. The middle heater location has a slightly larger temperature amplitude than in the baseline case, probably due to the different heater configuration. For the top heater location there is approximately a 4 K difference between the mean of

the cyclic temperature response and the steady temperature response, see Figure FD.

The effects of the mean power are two fold. First as a ratio of the amplitude to mean power level. Also, the mean power level is important as an independent variable. The larger the mean power input the more vigorous the base flow is which is more prone to amplification of disturbances. These influences can be seen in Figures FD-FF and Figures HD-HF. In Figures FD-FF the amplitude to mean power ratio is equal to one. Significant heat transfer enhancement is occurring. In Figures HD-HF, the amplitude to mean power input ratio is equal to 0.33, still greater heat transfer enhancement can be seen than in the baseline case where the amplitude to mean power ratio is equal to 0.50. This is accounted for by the higher mean input power than the baseline case.

4. Combined of Effects

It is also important to examine more than one variation to the input power pulsation, (e.g. increase the frequency and the amplitude of the input power keeping the mean input the same).

a. Varying Amplitude and Frequency

Figures CA-CC present results for mean input of 2.0 watts, amplitude of 2.0 watts and a frequency of 0.100 Hz. These figures are an increase in the amplitude of 1.0 watts and an increase of the input frequency

by a factor of two from the baseline case. There was significant heat transfer enhancement for all three heater locations. Significant heat transfer enhancement was previously defined as the maximum cyclic temperature response being less than the steady temperature response. The amplitude of the temperature response is greater than the baseline case, however, less than if the amplitude of the input power alone was increased, see Figures CD-CF.

Figures CG-CI present results for mean input of 2.0 watts, amplitude of 2.0 watts and a frequency of 0.025 Hz. These figures are an increase in the amplitude of 1.0 watts and a decrease of the input frequency by a factor of two from the baseline case. Heat transfer enhancement was observed for all three heater locations. For the middle and bottom heater locations the mean cyclic temperature response was well below the steady temperature response. As expected, the amplitude of the cyclic temperature response was significantly larger than the baseline case and greater than if the frequency of the pulsation alone was decreased, see Figures BG-BI.

Figures AA-AC present results for mean input of 2.0 watts, amplitude of 0.5 watts and a frequency of 0.100 Hz. These figures are a decrease in the amplitude of 0.5 watts and an increase of the input frequency by a factor of two from the baseline case. Heat transfer enhancement was found for the top and bottom heater locations. The maximum cyclic temperature response for the top heater location coincided with the steady temperature response. For the middle heater the mean cyclic temperature

response was equal to the steady temperature response indicating no heat transfer enhancement. For the bottom heater location the mean cyclic temperature response was slightly lower than the steady temperature response. The amplitude of the temperature response was significantly smaller than the baseline case for all three heater locations tested.

Figures AG-AI present results for mean input of 2.0 watts, amplitude of 0.5 watts and a frequency of 0.025 Hz. These figures are a decrease in the amplitude of 0.5 watts and a decrease of the input frequency by a factor of two from the baseline case. No heat transfer enhancement was found for any of the three heater locations. The amplitude of the temperature response was slightly less than the baseline case.

The variation of amplitude and frequency act independently of each other. In fact, the benefits of higher amplitudes and higher frequencies to the heat transfer appear to be additive.

b. Varying Amplitude and Mean Input Power

Figures ID-IF present results for mean input of 3.0 watts, amplitude of 2.0 watts and a frequency of 0.050 Hz. These figures are an increase in the amplitude of 1.0 watts and an increase of the mean power of 1.0 watts from the baseline case. Heat transfer enhancement is seen for all three heater locations and significant heat transfer enhancement occurs for the top heater location. As expected, the amplitude of the temperature response is greater than the baseline case.

Figures GD-GF present results for mean input of 3.0 watts, amplitude of 0.5 watts and a frequency of 0.050 Hz. These figures are a decrease in the amplitude of 0.5 watts and an increase of the mean power of 1.0 watts from the baseline case. The top and middle heater locations demonstrate some heat transfer enhancement, more so for the top heater. The bottom heater shows no heat transfer enhancement and even a slight decrease in the heat transfer. The amplitude of the temperature response is less than in the baseline case. The amplitude of the temperature is greatest for the middle heater, of the three heater locations. Note heater configuration B was used in this case and typically smaller amplitudes of the temperature response for the bottom heater location were found than for heater configuration A.

Figures ED-EF present results for mean input of 1.0 watts, amplitude of 0.5 watts and a frequency of 0.050 Hz. These figures are a decrease in the amplitude of 0.5 watts and a decrease of the mean power of 1.0 watts from the baseline case. The heat transfer enhancement at the top heater location is greater than for the baseline case. Here the maximum cyclic temperature response is equal to the steady temperature response. While in the baseline case it was greater than the steady temperature response. The temperature response for the middle and bottom heater locations is approximately the same as that of the baseline case. As expected, the amplitude of the temperature response was less than for the baseline case.

Figures DD-DF present results for mean input of 0.5 watts, amplitude of 0.5 watts and a frequency of 0.050 Hz. These figures are a decrease in the amplitude of 1.5 watts and a decrease of the mean power of 0.5 watts from the baseline case. For all three heater locations heat transfer enhancement was seen. Significant heat transfer enhancement was seen for the top heater location. Once again, this emphasizes the importance of the increase in the amplitude to mean power ratio for heat transfer enhancement. The amplitude of the temperature, as expected, is less than in the baseline case.

c. Varying Frequency and Mean Input Power

Figures HA-HC present results for mean input of 3.0 watts, amplitude of 1.0 watts and a frequency of 0.100 Hz. These conditions are an increase in the mean power input of 1.0 watts and an increase of the input frequency by a factor of two from the baseline case. There was heat transfer enhancement for all three heater locations with significant enhancement for the top heater location. The amplitude of the temperature response was less than that of the baseline case.

Figures HG-HI present results for mean input of 3.0 watts, amplitude of 1.0 watts and a frequency of 0.025 Hz. These conditions are an increase in the mean power input of 1.0 watts and a decrease of the input frequency by a factor of two from the baseline case. Only the top and middle heater locations presented a slight heat transfer enhancement. As expected,

the amplitude of the temperature response was greater than that of the baseline case.

Figures FA-FC present results for mean input of 1.0 watts, amplitude of 1.0 watts and a frequency of 0.100 Hz. These figures are a decrease in the mean power input of 1.0 watts and an increase of the input frequency by a factor of two from the baseline case. Significant heat transfer enhancement was observed for all three heater locations. The amplitude of the temperature response is less than that of the baseline case. This run represents dramatic improvements to the heat transfer characteristics using lower mean power input and variations to the amplitude. Being able to use lower amplitudes and mean power inputs to achieve significant heat transfer enhancement, results in lower mean cyclic temperature responses. This type of enhancement to the heat transfer characteristics with lower input powers would be desirable for applications purposes, when such enhancement could be achieved by using auxiliary heaters with pulsed input power.

Figures FG-FI present results for mean input of 1.0 watts, amplitude of 1.0 watts and a frequency of 0.025 Hz. These figures display the effect of a decrease in the mean power input of 1.0 watts and a decrease of the input frequency by a factor of two from the baseline case. Heat transfer enhancement at all three heater locations is evident with significant enhancement for the top heater location. Amplitude of the temperature response was greater than the baseline case.

The frequency of the pulsating power has less of an effect on the heat transfer enhancement than the amplitude and mean power input does. Its greatest influence is on the amplitude of the temperature response.

d. Other Variations of Parameters

Figures DA-DC present results for mean input of 0.5 watts, amplitude of 0.5 watts and a frequency of 0.100 Hz. These parameters are a decrease in the amplitude of 0.5 watts, a decrease of the mean power of 1.5 watts, and an increase in the input frequency by a factor of two from the baseline case. There is significant heat transfer enhancement for all three heater locations. This again demonstrates the importance of the amplitude to mean power input ratio. As expected, the amplitude of the temperature response is less than in the baseline case. In addition, for the top heater location the mean cyclic temperature response is 20 K below the mean cyclic temperature response for the baseline case. The corresponding decrease 18.5 K and 14 K for the middle and bottom heater locations respectively. This is a significantly lower mean temperature response with greater heat transfer enhancement than the baseline case. Also, the mean cyclic temperature response for the middle and bottom heater locations are the same.

Figures EA-EC present results for mean input of 1.0 watts, amplitude of 0.5 watts and a frequency of 0.100 Hz. These values are a decrease in the amplitude of 0.5 watts, a decrease of the mean power of 1.0 watts, and an increase in the input frequency by a factor of two from the

baseline case. There is heat transfer enhancement for all three heater locations. Significant heat transfer enhancement occurs for the top heater location only. The amplitude of the temperature response is less than the baseline case.

Figures IA-IC present results for mean input of 3.0 watts, amplitude of 2.0 watts and a frequency of 0.100 Hz. These figures are an increase in the amplitude of 1.0 watts, an increase of the mean power of 1.0 watts, and an increase in the input frequency by a factor of two from the baseline case. There is heat transfer enhancement for all three heater locations with significant heat transfer enhancement for the top heater only. The amplitude of the temperature response is approximately the same as the baseline case. The reduced amplitude of the temperature response is a function of the higher frequency of the input power.

Figures GA-GC present results for mean input of 3.0 watts, amplitude of 0.5 watts and a frequency of 0.100 Hz. These figures are a decrease in the amplitude of 0.5 watts, an increase of the mean power of 1.0 watts, and an increase in the input frequency by a factor of two from the baseline case. There is heat transfer enhancement for all three heater locations. The mean cyclic temperature response is higher than the case just discussed, see Figures IA-IC, however, the maximum cyclic temperature responses are approximately the same. The amplitude of the temperature response is less than for the baseline case.

Figures DG-DI present results for mean input of 0.5 watts, amplitude of 0.5 watts and a frequency of 0.025 Hz. These result from a decrease in the amplitude of 0.5 watts, a decrease of the mean power of 1.5 watts, and a decrease in the input frequency by a factor of two from the baseline case. There is heat transfer enhancement for all three heater locations with significant heat transfer enhancement for the top heater location only. The amplitude of the temperature response is similar to that of the baseline case.

Figures EG-EI present results for a mean input of 1.0 watts, amplitude of 0.5 watts and a frequency of 0.025 Hz. These parameters are a decrease in the amplitude of 0.5 watts, a decrease of the mean power of 1.0 watts, and a decrease in the input frequency by a factor of two from the baseline case. There is heat transfer enhancement for all three heater locations. The amplitude of the temperature response is similar to that of the baseline case.

Figures GG-GI present results for mean input of 3.0 watts, amplitude of 0.5 watts and a frequency of 0.025 Hz. These parameters are a decrease in the amplitude of 0.5 watts, an increase of the mean power of 1.0 watts, and a decrease in the input frequency by a factor of two from the baseline case. There is heat transfer enhancement for all three heater locations. The amplitude of the temperature response is similar to that of the baseline case.

Figures IG-II presents results for mean input of 3.0 watts, amplitude of 2.0 watts and a frequency of 0.025 Hz. These values are an increase in the amplitude of 1.0 watts, an increase of the mean power of 1.0 watts, and a decrease in the input frequency by a factor of two from the baseline case. There is heat transfer enhancement for all three heater locations. The amplitude of the temperature response is much greater than that of the baseline case.

In examining these cases the amplitude to mean input power ratio was the dominant factor in producing heat transfer enhancement. Increase in the frequency of the input power provided some heat transfer enhancement, but more importantly it greatly influenced the amplitude of the temperature response. Higher mean power inputs provide some heat transfer enhancement. However they were a less dominant factor than the amplitude to mean power input ratio.

C. DISCUSSION OF SQUARE WAVE DATA

As was the case for the triangular wave data, the base line profile had a mean value power input of 2.0 watts, amplitude of 1.0 watts, and a frequency of 0.050 Hz, see Figures KD-KF.

Note the spikes in the power pulsation. These spikes were prevalent throughout the square wave data. The exact cause is inconclusive, however, it is believed that the spikes are due to the power supply hunting for the proper

voltage to match the control signal supplied by the programmer. The control signal produced by the programmer is the same as the desired output voltage. In examining the raw data, these spikes are caused at isolated points, in some cases two points out of a total of nine hundred data points for each run. These spikes did not seem to have an impact on the temperature responses.

The amplitude of the cyclic temperature response for the baseline case is 14.8% of the mean for the top heater location, 17.3% for the middle heater location and 18.4% for the bottom heater location. This is for a power amplitude 50% of the mean input. The amplitude of the temperature response for the baseline case of the triangular wave power pattern range from 6.7% at the top heater location to 16.8 % for the bottom heater location. The frequency of the cyclic temperature response matches that of the input power pulsation. There is a phase lag in the cyclic temperature response, but not as large as in the triangular power pattern. The mean cyclic temperature response coincides with the steady temperature response indicating no heat transfer enhancement due to power pulsation.

1. Effects of Amplitude of Power Pulsation

Figures LD-LF present results for mean input of 2.0 watts, amplitude of 2.0 watts and a frequency of 0.050 Hz. This is an increase of 1.0 watt to the baseline case. There is only a slight improvement in the heat transfer characteristics. The amplitude of the cyclic temperature response is increased to 32.6% for the top heater, 42.6% for the middle heater and 55.7%

for the bottom heater. The maximum value of the cyclic temperature response for the middle heater is actually higher than that of the top heater.

Figures JD-JF present results for mean input of 2.0 watts, amplitude of 0.5 watts and a frequency of 0.050 Hz. This is a decrease in the amplitude of 0.5 watts compared to the baseline case. There is no heat transfer enhancement for this case. The mean cyclic temperature response coincides with the steady temperature response for all three heater locations. The amplitude of the cyclic temperature response is decreased significantly to 8.35% for the top heater location, 10.7% for the middle heater location, and 10.2% for the bottom heater location. Once again, the maximum cyclic temperature response for the middle heater is higher than that of the top heater.

2. Effects of Time Period of Pulsation

Figures KA-KC present results for mean input of 2.0 watts, amplitude of 1.0 watts and a frequency of 0.100 Hz. This is an increase in the frequency of pulsation from the baseline case by a factor of two. There is no heat transfer enhancement for this case. The amplitude of the temperature response for the top heater location drops to 7.8% of the mean, 12.4% for the middle heater location, and 10.5% for the bottom heater location. The frequency of the cyclic temperature response matches that of the pulsating power input. The maximum cyclic temperature response for the middle heater location is slightly larger than that of the top heater.

Figures KG-KI present results for mean input of 2.0 watts, amplitude of 1.0 watts and a frequency of 0.025 Hz. This is a decrease in the frequency of pulsation from the baseline case by a factor of two. There is only a slight heat transfer enhancement for the top and middle heater locations and no enhancement for the bottom heater location. The amplitude of the temperature response of the top heater location jumps to 24.5%, the middle heater location to 27.5%, and the bottom heater location to 26.3%. The middle heater still has a slightly larger maximum cycle temperature than that of the top heater. Also noted was a drop in temperature at the end of each cycle. This effect is most prominent for the middle heater, Figure KH.

3. Effects of the Mean Input Power

Figures QD-QF present results for mean input of 3.0 watts, amplitude of 1.0 watts and a frequency of 0.050 Hz. This is an increase of 1.0 watt to the baseline case. The temperature amplitude for the middle and bottom heaters are approximately the same, while the top heater amplitude has decreased. The frequency of the cyclic temperature response matches that of the power input. The mean cyclic temperature response coincides with the steady temperature responses.

Figures OD-OF present results for mean input of 1.0 watts, amplitude of 1.0 watts and a frequency of 0.050 Hz. This is a decrease of 1.0 watt to the baseline case. By decreasing the mean power input to 1.0 watts, the amplitudes of the temperature response for all three heater locations are

approximately the same as in the base line case. The frequency response was unchanged. The mean of the cyclic temperature response is only slightly lower than the temperature response to the steady input for the top and middle heaters locations.

4. Combing of Effects

a. Varying Amplitude and Frequency

Figures LA-LC present results for mean input of 2.0 watts, amplitude of 2.0 watts and a frequency of 0.100 Hz. These figures are an increase in the amplitude of 1.0 watts and an increase of the input frequency by a factor of two from the baseline case. There is a slight heat transfer enhancement for all three heater locations. The amplitude of the temperature response is larger than the baseline case.

Figures LG-LI present results for mean input of 2.0 watts, amplitude of 2.0 watts and a frequency of 0.025 Hz. These figures are an increase in the amplitude of 1.0 watts and a decrease of the input frequency by a factor of two from the baseline case. For all three heater locations there is a slight heat transfer enhancement. Also, there is a large increase in the amplitude of the temperature response as compared to the baseline case.

Figures JA-JC present results for mean input of 2.0 watts, amplitude of 0.5 watts and a frequency of 0.100 Hz. These parameters are a decrease in the amplitude of 0.5 watts and an increase of the input frequency

by a factor of two from the baseline case. Only the top heater location demonstrates a slight enhancement to the heat transfer. As expected, the amplitude of the temperature response is less than the baseline case.

Figures JG-JI present results for mean input of 2.0 watts, amplitude of 0.5 watts and a frequency of 0.025 Hz. These values are a decrease in the amplitude of 0.5 watts and a decrease of the input frequency by a factor of two from the baseline case. No heat transfer enhancement for any of the three heater locations is noted. However, there is a dramatic drop in temperature at the end of each cycle, as was discussed early.

No significant enhancement to the heat transfer, as defined early, was found for any of the runs performed. The drop in temperature at the end of each cycle was apparent for amplitudes of 0.5 watts and an input frequency of 0.025 Hz. As for the triangular wave power pattern data, frequency of the input power had a influence over the amplitude of the temperature response. However, the amplitude to mean power input ratio did not bring about the dramatic effects seen with the triangular wave power pattern data.

b. Varying Amplitude and Mean Input Power

Figures RD-RF present results for mean input of 3.0 watts, amplitude of 2.0 watts and a frequency of 0.050 Hz. These values are an increase in the amplitude of 1.0 watts and an increase of the mean power of 1.0 watts from the baseline case. Only slight heat transfer enhancement can

be seen at all three heater locations. The amplitude of the temperature response is greater than the baseline case.

Figures PD-PF present results for mean input of 3.0 watts, amplitude of 0.5 watts and a frequency of 0.050 Hz. These values are a decrease in the amplitude of 0.5 watts and an increase of the mean power of 1.0 watts from the baseline case. No heat transfer enhancement was present for any of the three heater locations. For the top heater location there is a degrade in the heat transfer effects. The amplitude of the temperature response is less than the baseline case.

Figures ND-NF presents results for mean input of 1.0 watts, amplitude of 0.5 watts and a frequency of 0.050 Hz. These parameters are a decrease in the amplitude of 0.5 watts and a decrease of the mean power of 1.0 watts from the baseline case. All three heater locations demonstrated a slight enhancement to the heat transfer. The amplitude of the temperature response is less than the baseline.

Figures MD-MF present results for mean input of 0.5 watts, amplitude of 0.5 watts and a frequency of 0.050 Hz. These parameters are a decrease in the amplitude of 1.5 watts and a decrease of the mean power of 0.5 watts from the baseline case. No heat transfer enhancement for any of the three locations is seen. The amplitude of the temperature response is less than the baseline.

The effect of the amplitude of the power input was to increase the amplitude of the temperature response. The dramatic effects seen with triangular wave data were not seen here.

c. Varying Frequency and Mean Input Power

Figures QA-QC present results for mean input of 3.0 watts, amplitude of 1.0 watts and a frequency of 0.100 Hz. These values are an increase in the mean power input of 1.0 watts and an increase of the input frequency by a factor of two from the baseline case. None of the three of the heater locations demonstrated any heat transfer enhancement. The amplitude of the temperature response is less than the baseline case.

Figures QG-QI present results for mean input of 3.0 watts, amplitude of 1.0 watts and a frequency of 0.025 Hz. These parameters are an increase in the mean power input of 1.0 watts and a decrease of the input frequency by a factor of two from the baseline case. Only a slight heat transfer enhancement is seen for all three heater locations. There was a drop in temperature at the end of each cycle. The amplitude of the temperature response was greater than the baseline case.

Figures OA-OC present results for mean input of 1.0 watts, amplitude of 1.0 watts and a frequency of 0.100 Hz. These values are a decrease in the mean power input of 1.0 watts and an increase of the input frequency by a factor of two from the baseline case. A slight heat transfer

enhancement was observed for all three heater locations. The amplitude of the temperature response is less than the baseline case.

Figures OG-OI present results for mean input of 1.0 watts, amplitude of 1.0 watts and a frequency of 0.025 Hz. These parameters are a decrease in the mean power input of 1.0 watts and a decrease of the input frequency by a factor of two from the baseline case. A slight heat transfer enhancement is observed at all three heater locations. The amplitude of the temperature response is greater than the baseline case.

The last two cases discussed both had a mean power input of 1.0 watts and amplitude of 1.0 watts. Both of these cases displayed some heat transfer enhancement, implying that the amplitude to mean power input ratio of one does have some impact upon the heat transfer characteristics. However, this enhancement is small in comparison to the triangular wave data and only applies for mean power inputs equal to or greater than 1.0 watts. The large temperature drop at the end of the cycle found in Figures OG-OI, aided in the heat transfer enhancement. However, the maximum cyclic temperature response was not lessened.

d. Other Variations of Parameters

Figures MA-MC present results for mean input of 0.5 watts, amplitude of 0.5 watts and a frequency of 0.100 Hz. These values are a decrease in the amplitude of 0.5 watts, a decrease of the mean power of 1.5 watts, and an increase in the input frequency by a factor of two from the

baseline case. No heat transfer enhancement is seen for this case. The amplitude of the temperature response is less than the baseline case. Also, the mean cyclic temperature response is higher than the triangular wave data for identical parameters.

Figures NA-NC present results for mean input of 1.0 watts, amplitude of 0.5 watts and a frequency of 0.100 Hz. These values are a decrease in the amplitude of 0.5 watts, a decrease of the mean power of 1.0 watts, and an increase in the input frequency by a factor of two from the baseline case. There was a slight enhancement for all three heater locations. The amplitude of the temperature response is less than the baseline case.

Figures RA-RC present results for mean input of 3.0 watts, amplitude of 2.0 watts and a frequency of 0.100 Hz. These values are an increase in the amplitude of 1.0 watts, an increase of the mean power of 1.0 watts, and an increase in the input frequency by a factor of two from the baseline case. A slight heat transfer enhancement, approximately the same as in the previous case, is seen for all three heater locations. The amplitude of the temperature response is less than the baseline case for the top heater location, greater for the middle heater location, and approximately the same for the bottom heater. Heater configuration C was used for the baseline case while heater configuration B is used for this case with different locations of the heaters examined. This could explain the difference.

Figures PA-PC present results for mean input of 3.0 watts, amplitude of 0.5 watts and a frequency of 0.100 Hz. These parameters are a decrease in the amplitude of 0.5 watts, an increase of the mean power of 1.0 watts, and an increase in the input frequency by a factor of two from the baseline case. No heat transfer enhancement for any of the three heater locations is noted. The amplitude of the temperature response is much less than the baseline case.

Figures MG-MI present results for mean input of 0.5 watts, amplitude of 0.5 watts and a frequency of 0.025 Hz. These values are a decrease in the amplitude of 0.5 watts, a decrease of the mean power of 1.5 watts, and a decrease in the input frequency by a factor of two from the baseline case. No heat transfer enhancement is found for these conditions. The amplitude of the temperature response is approximately the same as the baseline case.

Figures NG-NI present results for a mean input of 1.0 watts, amplitude of 0.5 watts and a frequency of 0.025 Hz. These values are a decrease in the amplitude of 0.5 watts, a decrease of the mean power of 1.0 watts, and a decrease in the input frequency by a factor of two from the baseline case. Only slight heat transfer enhancement is seen here. The amplitude of the temperature response is approximately the same as in the baseline case. The middle heater location is starting to experience a temperature drop at the end of the cycle.

Figures PG-PI present results for mean input of 3.0 watts, amplitude of 0.5 watts and a frequency of 0.025 Hz. These values are a decrease in the amplitude of 0.5 watts, an increase of the mean power of 1.0 watts, and a decrease in the input frequency by a factor of two from the baseline case. All three heater locations demonstrate a temperature drop at the end of each cycle. The middle heater shows the most dramatic drop of the three heater locations. There is only a slight heat transfer enhancement seen for these three heater locations. The greatest enhancement is seen for the middle heater. The amplitude of the temperature response is slightly less than the baseline case.

Figures RG-RI present results for mean input of 3.0 watts, amplitude of 2.0 watts and a frequency of 0.025 Hz. These values are an increase in the amplitude of 1.0 watts, an increase of the mean power of 1.0 watts, and a decrease in the input frequency by a factor of two from the baseline case. Only a slight heat transfer enhancement are seen for these three heater locations. The middle heater shows a small temperature drop at the end of the cycle. The amplitude of the temperature response is much greater than in the baseline case.

These experiments reveal a much less pronounced trend for heat transfer enhancement then observed for the triangular wave. Large ratios of amplitude to mean power level have a minor but positive impact on the heat transfer characteristics. Frequency of the power pulsation has an effect on the

amplitude of the temperature response, but once again much less than for the triangular wave data. Higher mean power inputs influence the large temperature drops at the end of each cycle. However, this enhancement does not lead to significant heat transfer enhancement over the entire cycle.

D. NON DIMENSIONAL HEAT TRANSFER CHARACTERISTICS

Figure 8 presents a comparison of the steady data for the bottom heater location with previous investigations. The non dimensional data are calculated by defining the Nusselt number, Nu, and Grashof number, Gr as:

$$Nu = \frac{Q_{conv}L}{kA(T-T_{amb})}$$

where Q_{conv} was determined by the following equation

$$Q_{conv} = Q - Q_{cond}$$

Q_{cond} was estimated from [Ref. 16]

$$Gr = \frac{g\beta QL^4}{kA\nu^2}$$

Along with the present measurements also contained within Figure 8 is the applicable steady data from Haukenes [Ref. 5] and Akdeniz [Ref. 17], present measurements were obtained with the same test surface as used by there investigations. Also seen in Figure 8 is an empirical correlation from [Ref. 15]:

$$Nu^* = 1.11(Gr)^{0.12}$$

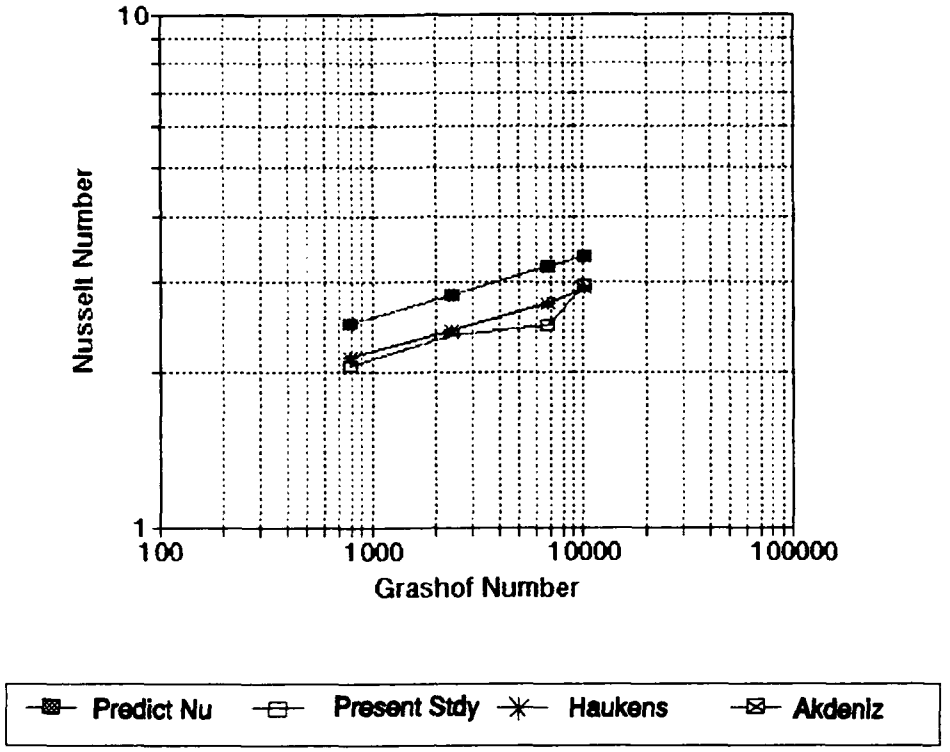

Figure 8. Comparison of Steady Data

The present data are in good agreement with those of Haukenes and Akdeniz for the same heater spacing. They are about 20% below the empirical equation. The lower Nu^* values are expected due to the reduced heater spacing in the present measurements compared to [Ref. 15] which results in larger interaction between heaters by substrate conduction.

Figures 9 and 10 are variations of the average Nusselt number with average Grashof number with amplitude of pulsation as a parameter. From the cyclic responses of heater temperature and power inputs, mean values were

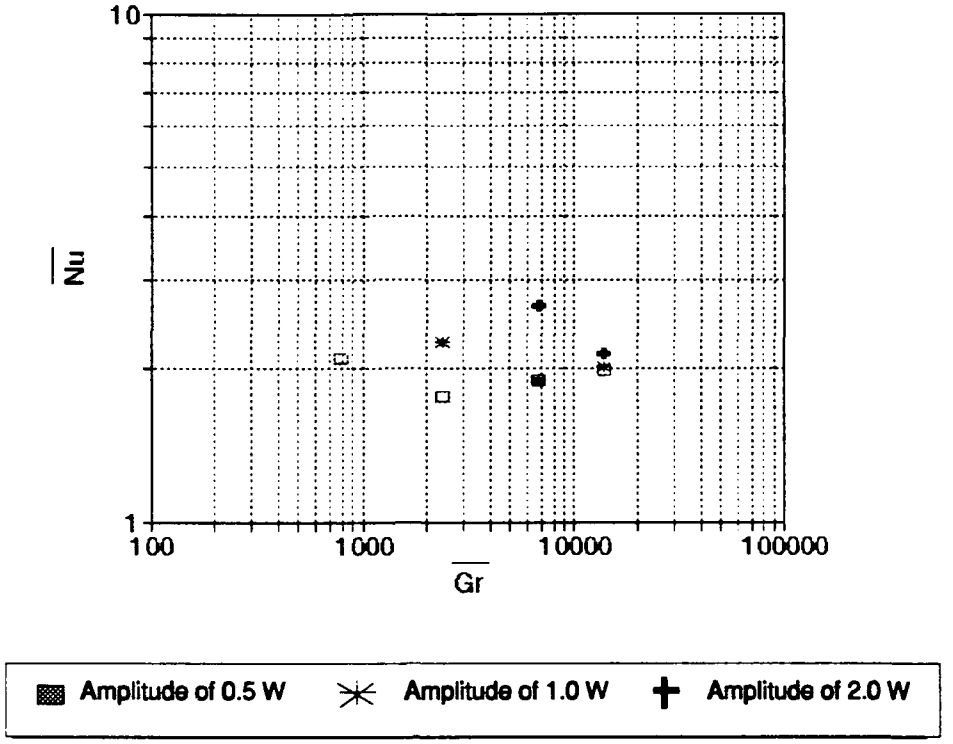

Figure 9. **Average Nusselt Number Versus Average Grashof Number for the Top Heater Location, Frequency of 0.050 Hz for Triangular Wave Power Pattern.**

determined. The average Nusselt number and average Grashof number were then determined as previously discussed based on these cycle averaged values. Figure 9 is for triangular wave power pattern and Figure 10 is for square wave power pattern. All points are for the top heater location and frequency of pulsation of 0.050 Hz, and varying mean input power levels. The upper three points for Figure 9 are for an amplitude to mean power input ratio of one. This dramatically illustrates the effect to the heat transfer characteristics as the

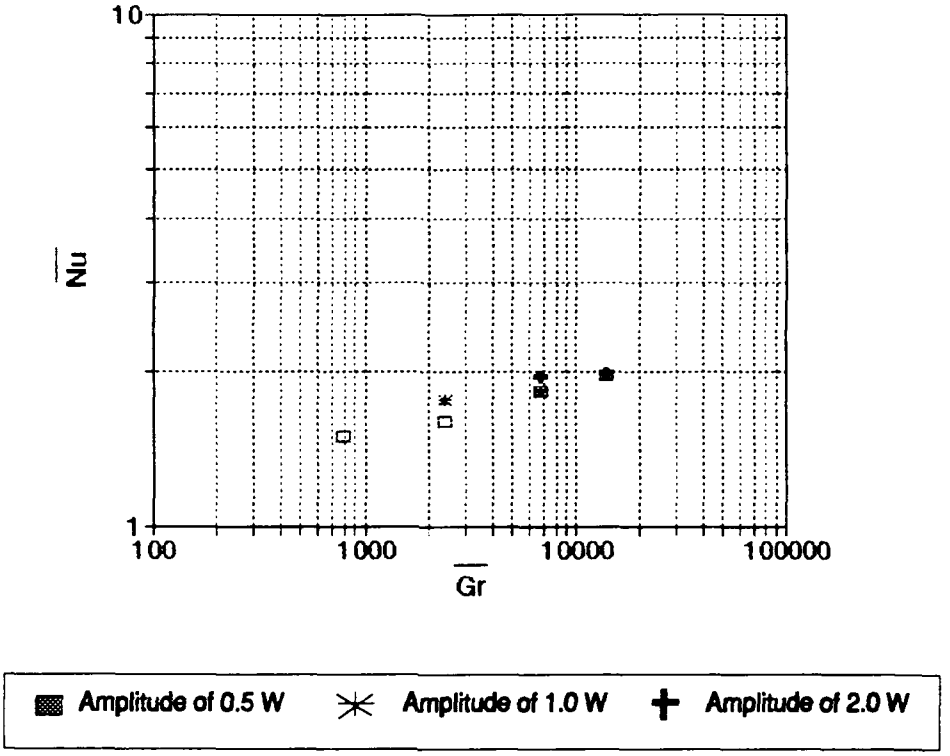

Figure 10. Average Nusselt Number Versus Average Grashof Number for the Top Heater Location, Frequency of 0.050 Hz for Square Wave Power Pattern.

amplitude to mean power input approaches one. There is the expected trend of increasing Nusselt number for higher Grashof number which indicates that more vigorous flows lead to higher heat transfer rates.

Unlike the triangular wave power pattern, Figure 9, there is no dramatic heat transfer enhancement seen for the square wave power pattern.

Uncertainty analysis is contained within Appendix E for the above calculations. No attempt was made to include the response time of the

thermocouple. Also, the uncertainty of the measurements of the physical dimensions of the heater, surface area and perimeter, were considered negligible compared to the uncertainty of the temperature and power measurements.

IV. CONCLUSIONS

In comparing the base line profiles of the two data sets, the square wave power pulsation produces less thermal damping effects than the triangular wave power pulsation. In addition, the degree of thermal damping effects are approximately the same for all the three heaters for the square wave power pulsation. Also the phase lag in the cyclic temperature response is more pronounced for the triangular wave power pattern.

With the triangular wave power pattern, significant enhancement to the heat transfer was achieved. This was most pronounced when the ratio of amplitude to mean power input was the greatest, for the upper heater, for increased frequency and for higher mean power inputs.

The square wave power input was only marginally effective in lowering the mean cyclic temperature response below the temperature response for the steady mean power level. However, dramatic temperature drops over part of the temperature response cycle were found for a frequency of 0.025 Hz, smaller amplitudes and higher mean power input values. This drop occurred at the end of each cycle. The maximum cyclic temperature response was never below the steady temperature response as in the triangular wave pattern.

With the ultimate objective of improving heat transfer characteristics for electronic components, triangular wave power pattern holds much promise. Square wave power patterns only produced marginal results. Specifically, the triangular wave pattern power pulsation provided improvements to the heat transfer characteristics;

- when the amplitude to mean power input approached one
- at higher mean power inputs (3.0 watts)
- at higher frequencies (0.100 Hz)

V. RECOMMENDATIONS

The following recommendations are made for further study:

1. Vary the pattern of the power input, starting with a sine wave pattern.

2. Investigate larger frequencies and higher mean power input levels for the triangular wave power pattern.

3. For square wave power pattern, further investigation is needed to determine the reason behind the large drop in temperature at the end of the cycle for higher mean input power levels, lower frequencies and lower amplitudes.

APPENDIX A: LIST OF RUNS

Figure Number	Mean Value	Amplitude	Frequency	Heater	Power Pattern
AA	2	0.5	0.100	Top	Triangular
AB	2	0.5	0.100	Middle	Triangular
AC	2	0.5	0.100	Bottom	Triangular
AD	2	0.5	0.050	Top	Triangular
AE	2	0.5	0.050	Middle	Triangular
AF	2	0.5	0.050	Bottom	Triangular
AG	2	0.5	0.025	Top	Triangular
AH	2	0.5	0.025	Middle	Triangular
AI	2	0.5	0.025	Bottom	Triangular
BA	2	1	0.100	Top	Triangular
BB	2	1	0.100	Middle	Triangular
BC	2	1	0.100	Bottom	Triangular
BD	2	1	0.050	Top	Triangular
BE	2	1	0.050	Middle	Triangular
BF	2	1	0.050	Bottom	Triangular
BG	2	1	0.025	Top	Triangular
BH	2	1	0.025	Middle	Triangular
BI	2	1	0.025	Bottom	Triangular
CA	2	2	0.100	Top	Triangular
CB	2	2	0.100	Middle	Triangular
CC	2	2	0.100	Bottom	Triangular
CD	2	2	0.050	Top	Triangular
CE	2	2	0.050	Middle	Triangular
CF	2	2	0.050	Bottom	Triangular
CG	2	2	0.025	Top	Triangular
CH	2	2	0.025	Middle	Triangular
CI	2	2	0.025	Bottom	Triangular

Figure Number	Mean Value	Amplitude	Frequency	Heater	Power Pattern
DA	0.5	0.5	0.100	Top	Triangular
DB	0.5	0.5	0.100	Middle	Triangular
DC	0.5	0.5	0.100	Bottom	Triangular
DD	0.5	0.5	0.050	Top	Triangular
DE	0.5	0.5	0.050	Middle	Triangular
DF	0.5	0.5	0.050	Bottom	Triangular
DG	0.5	0.5	0.025	Top	Triangular
DH	0.5	0.5	0.025	Middle	Triangular
DI	0.5	0.5	0.025	Bottom	Triangular
EA	1	0.5	0.100	Top	Triangular
EB	1	0.5	0.100	Middle	Triangular
EC	1	0.5	0.100	Bottom	Triangular
ED	1	0.5	0.050	Top	Triangular
EE	1	0.5	0.050	Middle	Triangular
EF	1	0.5	0.050	Bottom	Triangular
EG	1	0.5	0.025	Top	Triangular
EH	1	0.5	0.025	Middle	Triangular
EI	1	0.5	0.025	Bottom	Triangular
FA	1	1	0.100	Top	Triangular
FB	1	1	0.100	Middle	Triangular
FC	1	1	0.100	Bottom	Triangular
FD	1	1	0.050	Top	Triangular
FE	1	1	0.050	Middle	Triangular
FF	1	1	0.050	Bottom	Triangular
FG	1	1	0.025	Top	Triangular
FH	1	1	0.025	Middle	Triangular
FI	1	1	0.025	Bottom	Triangular

Figure Number	Mean Value	Amplitude	Frequency	Heater	Power Pattern
GA	3	0.5	0.100	Top	Triangular
GB	3	0.5	0.100	Middle	Triangular
GC	3	0.5	0.100	Bottom	Triangular
GD	3	0.5	0.050	Top	Triangular
GE	3	0.5	0.050	Middle	Triangular
GF	3	0.5	0.050	Bottom	Triangular
GG	3	0.5	0.025	Top	Triangular
GH	3	0.5	0.025	Middle	Triangular
GI	3	0.5	0.025	Bottom	Triangular
HA	3	1	0.100	Top	Triangular
HB	3	1	0.100	Middle	Triangular
HC	3	1	0.100	Bottom	Triangular
HD	3	1	0.050	Top	Triangular
HE	3	1	0.050	Middle	Triangular
HF	3	1	0.050	Bottom	Triangular
HG	3	1	0.025	Top	Triangular
HH	3	1	0.025	Middle	Triangular
HI	3	1	0.025	Bottom	Triangular
IA	3	2	0.100	Top	Triangular
IB	3	2	0.100	Middle	Triangular
IC	3	2	0.100	Bottom	Triangular
ID	3	2	0.050	Top	Triangular
IE	3	2	0.050	Middle	Triangular
IF	3	2	0.050	Bottom	Triangular
IG	3	2	0.025	Top	Triangular
IH	3	2	0.025	Middle	Triangular
II	3	2	0.025	Bottom	Triangular

Figure Number	Mean Value	Amplitude	Frequency	Heater	Power Pattern
JA	2	0.5	0.100	Top	Square
JB	2	0.5	0.100	Middle	Square
JC	2	0.5	0.100	Bottom	Square
JD	2	0.5	0.050	Top	Square
JE	2	0.5	0.050	Middle	Square
JF	2	0.5	0.050	Bottom	Square
JG	2	0.5	0.025	Top	Square
JH	2	0.5	0.025	Middle	Square
JI	2	0.5	0.025	Bottom	Square
KA	2	1	0.100	Top	Square
KB	2	1	0.100	Middle	Square
KC	2	1	0.100	Bottom	Square
KD	2	1	0.050	Top	Square
KE	2	1	0.050	Middle	Square
KF	2	1	0.050	Bottom	Square
KG	2	1	0.025	Top	Square
KH	2	1	0.025	Middle	Square
KI	2	1	0.025	Bottom	Square
LA	2	2	0.100	Top	Square
LB	2	2	0.100	Middle	Square
LC	2	2	0.100	Bottom	Square
LD	2	2	0.050	Top	Square
LE	2	2	0.050	Middle	Square
LF	2	2	0.050	Bottom	Square
LG	2	2	0.025	Top	Square
LH	2	2	0.025	Middle	Square
LI	2	2	0.025	Bottom	Square

Figure Number	Mean Value	Amplitude	Frequency	Heater	Power Pattern
MA	0.5	0.5	0.100	Top	Square
MB	0.5	0.5	0.100	Middle	Square
MC	0.5	0.5	0.100	Bottom	Square
MD	0.5	0.5	0.050	Top	Square
ME	0.5	0.5	0.050	Middle	Square
MF	0.5	0.5	0.050	Bottom	Square
MG	0.5	0.5	0.025	Top	Square
MH	0.5	0.5	0.025	Middle	Square
MI	0.5	0.5	0.025	Bottom	Square
NA	1	0.5	0.100	Top	Square
NB	1	0.5	0.100	Middle	Square
NC	1	0.5	0.100	Bottom	Square
ND	1	0.5	0.050	Top	Square
NE	1	0.5	0.050	Middle	Square
NF	1	0.5	0.050	Bottom	Square
NG	1	0.5	0.025	Top	Square
NH	1	0.5	0.025	Middle	Square
NI	1	0.5	0.025	Bottom	Square
OA	1	1	0.100	Top	Square
OB	1	1	0.100	Middle	Square
OC	1	1	0.100	Bottom	Square
OD	1	1	0.050	Top	Square
OE	1	1	0.050	Middle	Square
OF	1	1	0.050	Bottom	Square
OG	1	1	0.025	Top	Square
OH	1	1	0.025	Middle	Square
OI	1	1	0.025	Bottom	Square

Figure Number	Mean Value	Amplitude	Frequency	Heater	Power Pattern
PA	3	0.5	0.100	Top	Square
PB	3	0.5	0.100	Middle	Square
PC	3	0.5	0.100	Bottom	Square
PD	3	0.5	0.050	Top	Square
PE	3	0.5	0.050	Middle	Square
PF	3	0.5	0.050	Bottom	Square
PG	3	0.5	0.025	Top	Square
PH	3	0.5	0.025	Middle	Square
PI	3	0.5	0.025	Bottom	Square
QA	3	1	0.100	Top	Square
QB	3	1	0.100	Middle	Square
QC	3	1	0.100	Bottom	Square
QD	3	1	0.050	Top	Square
QE	3	1	0.050	Middle	Square
QF	3	1	0.050	Bottom	Square
QG	3	1	0.025	Top	Square
QH	3	1	0.025	Middle	Square
QI	3	1	0.025	Bottom	Square
RA	3	2	0.100	Top	Square
RB	3	2	0.100	Middle	Square
RC	3	2	0.100	Bottom	Square
RD	3	2	0.050	Top	Square
RE	3	2	0.050	Middle	Square
RF	3	2	0.050	Bottom	Square
RG	3	2	0.025	Top	Square
RH	3	2	0.025	Middle	Square
RI	3	2	0.025	Bottom	Square

APPENDIX B: REDUCE DATA

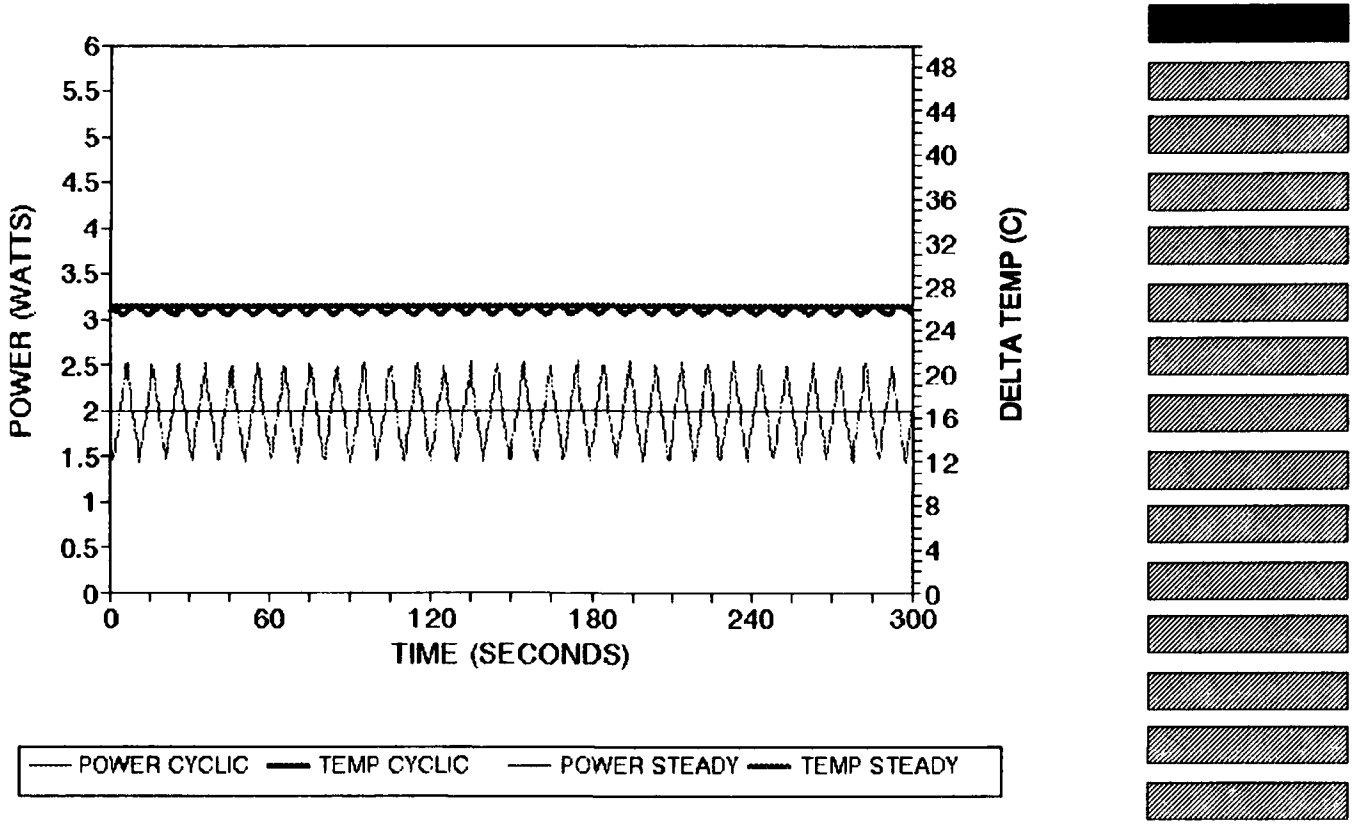

Figure AA. Time dependent transient power and delta temperature for triangular wave input, top heater, heater configuration A16, ambient temperature 20.0°C.

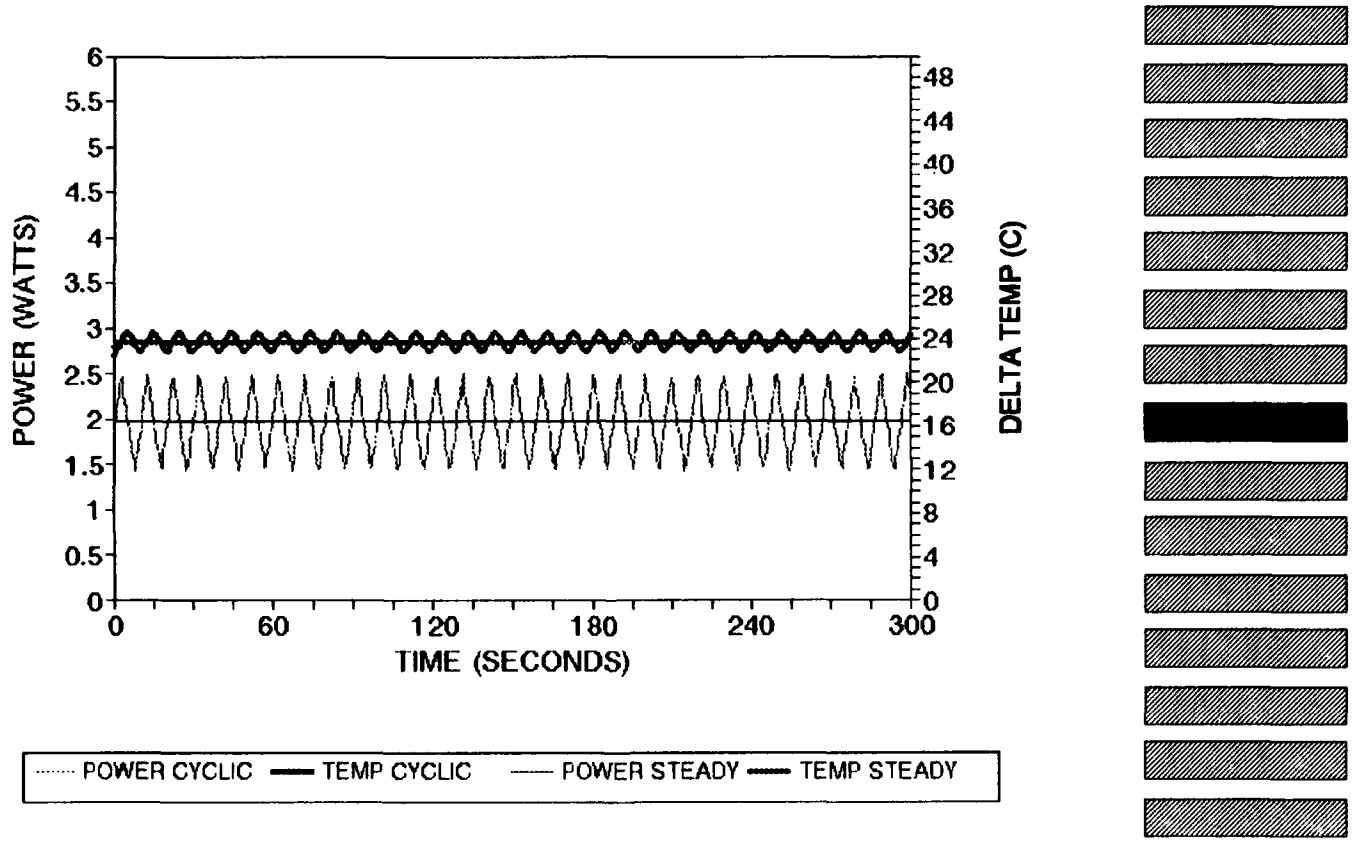

Figure AB. Time dependent transient power and delta temperature for triangular wave input, middle heater, heater configuration A23, ambient temperature 20.0°C.

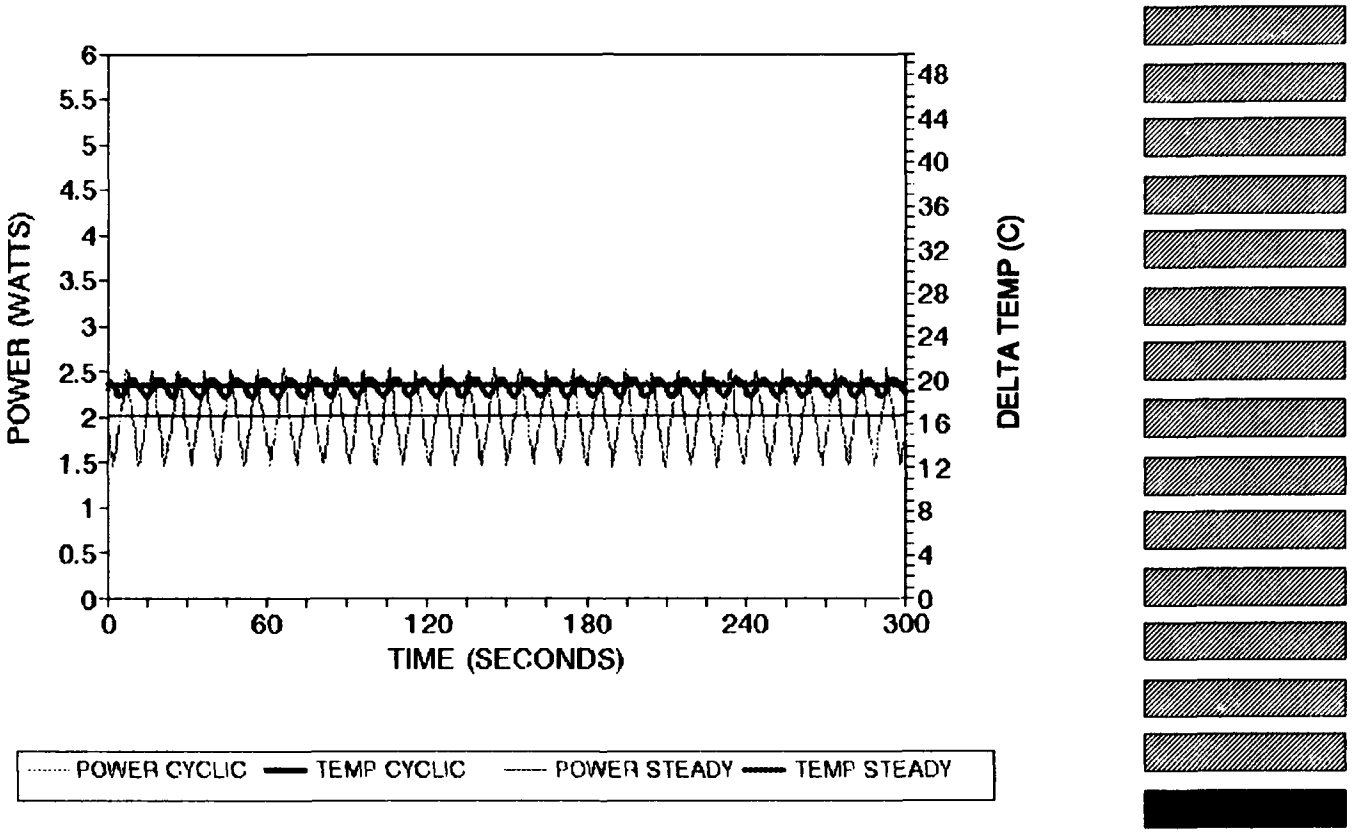

Figure AC. Time dependent transient power and delta temperature for triangular wave input, bottom heater, heater configuration A30, ambient temperature 20.0°C.

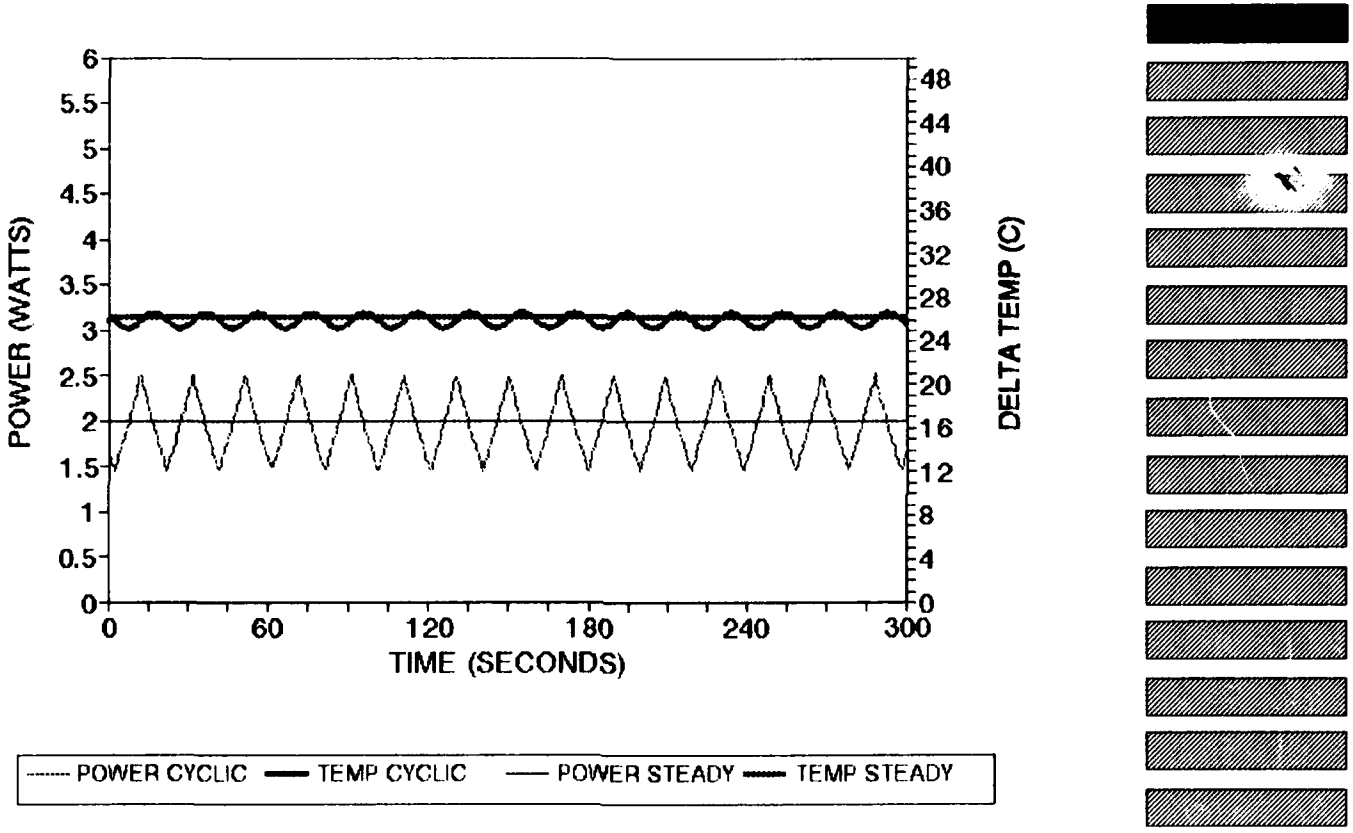

Figure AD. Time dependent transient power and delta temperature for triangular wave input, top heater, heater configuration A16, ambient temperature 20.0°C.

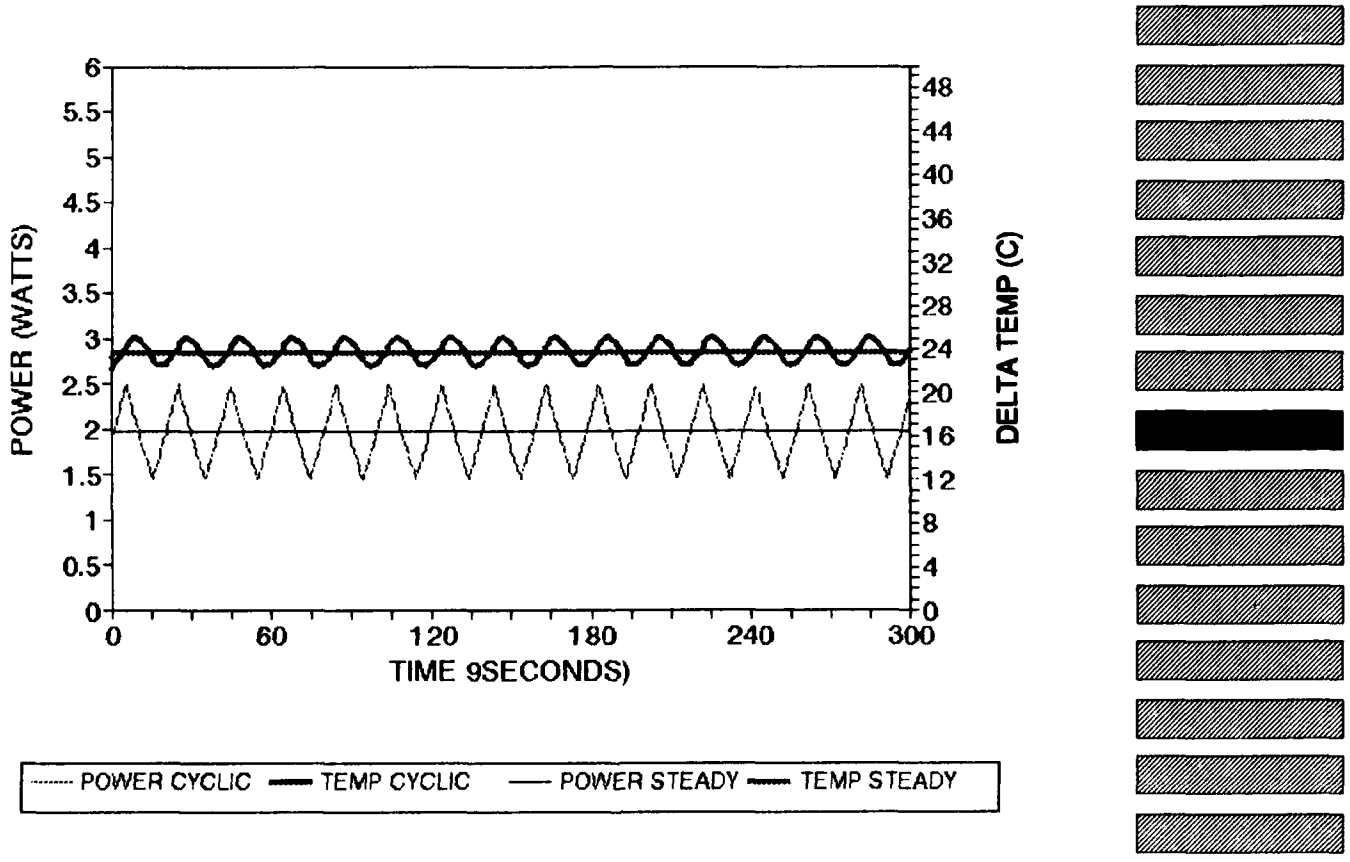

Figure AE. Time dependent transient power and delta temperature for triangular wave input, middle heater, heater configuration A23, ambient temperature 20.0°C.

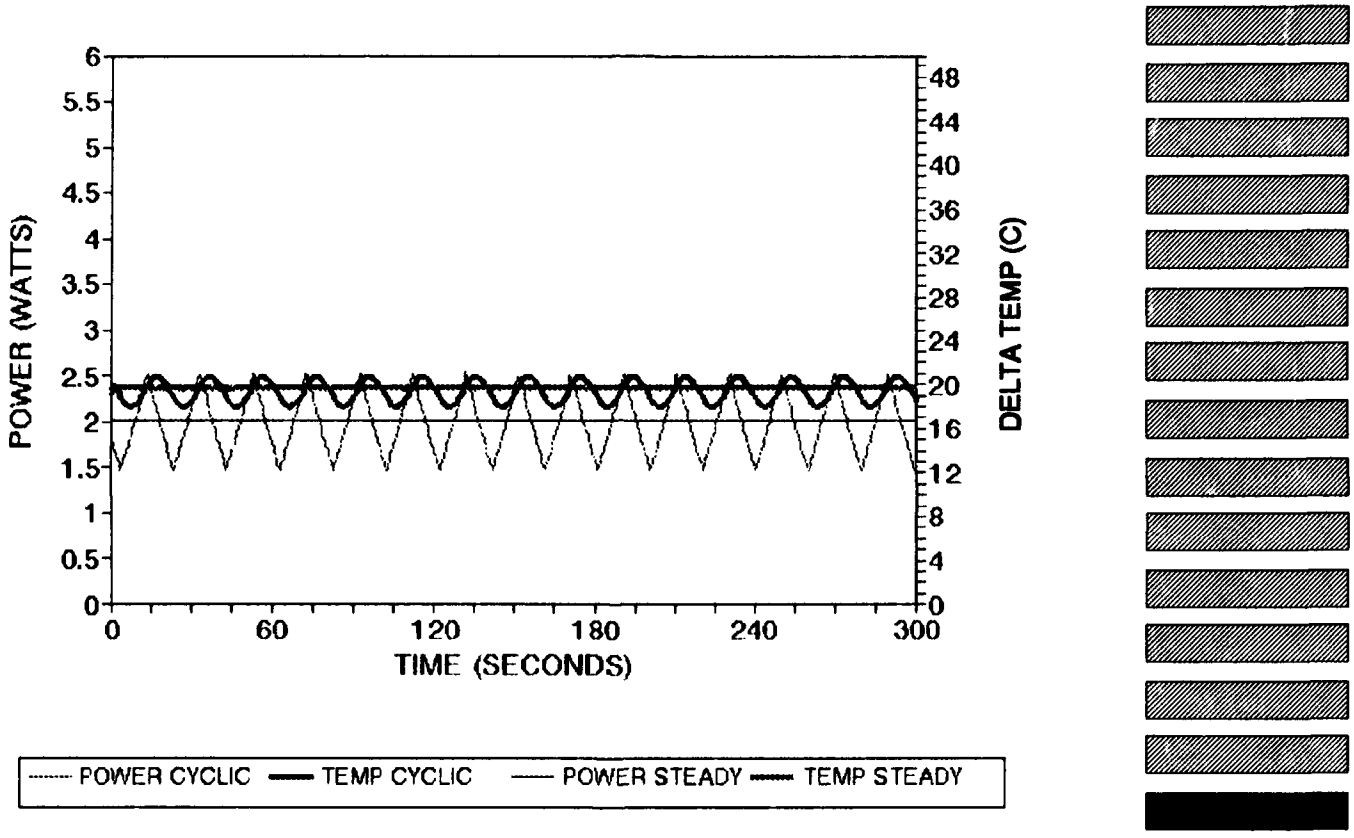

Figure AF. Time dependent transient power and delta temperature for triangular wave input, bottom heater, heater configuration A30, ambient temperature 20.0°C.

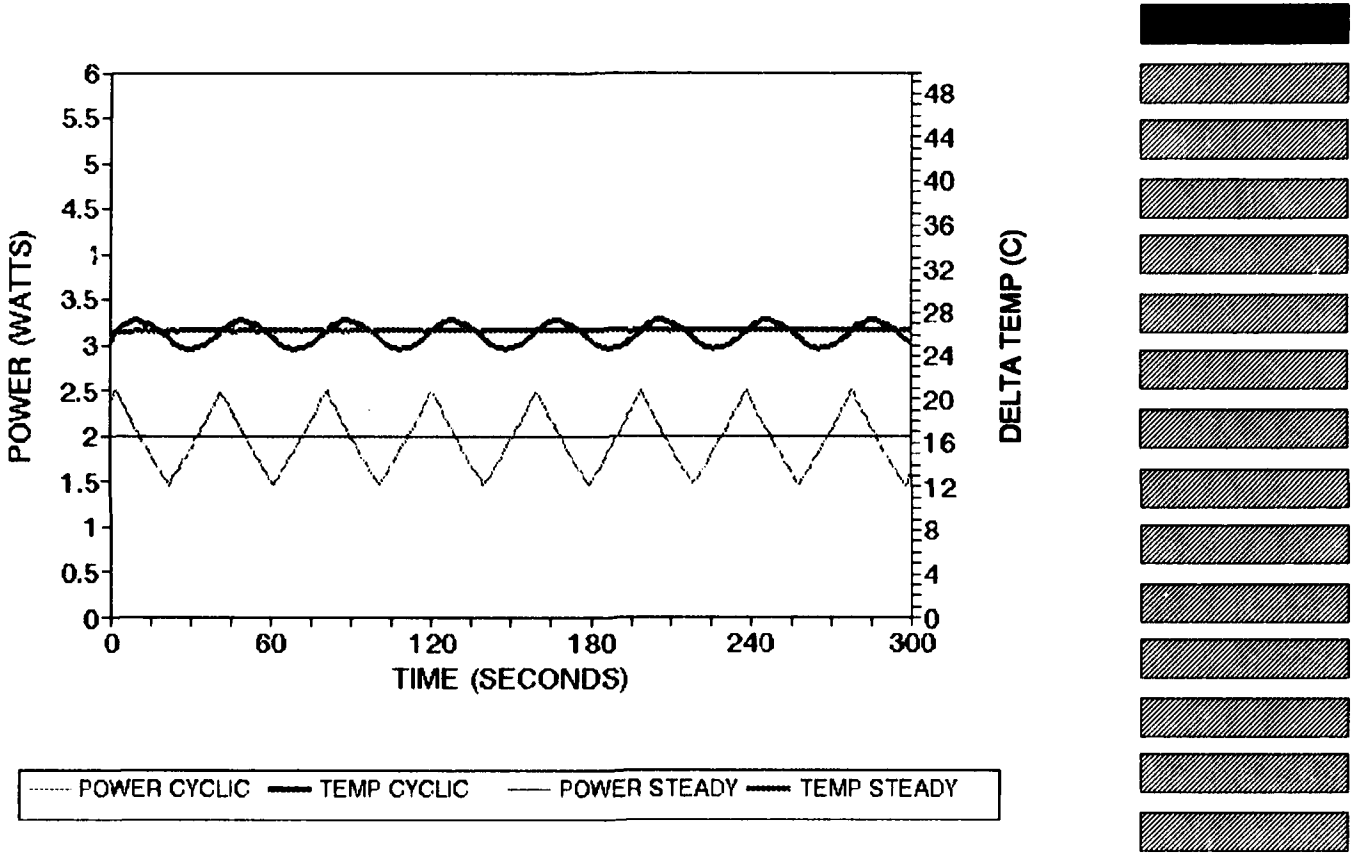

Figure AG. Time dependent transient power and delta temperature for triangular wave input, top heater, heater configuration A16, ambient temperature 20.0°C.

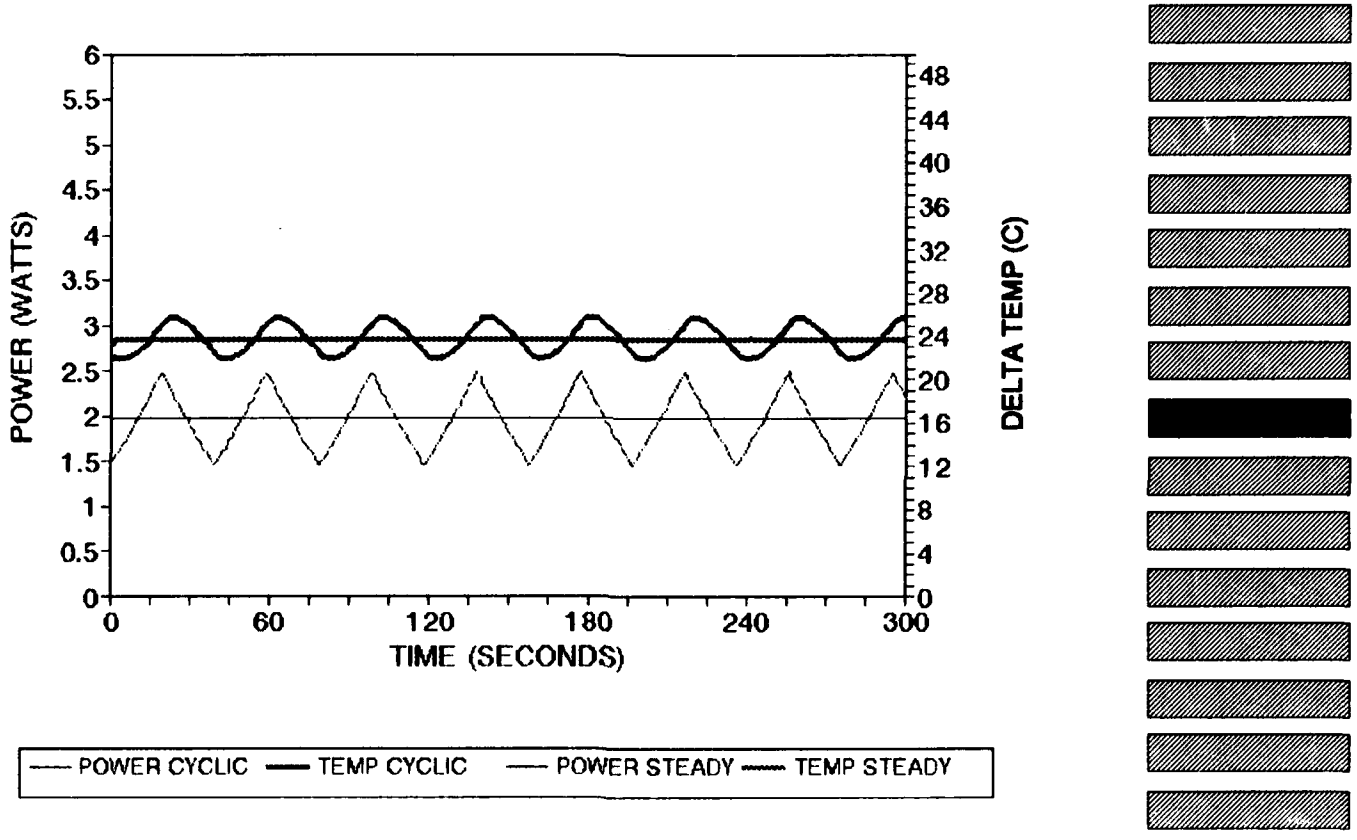

Figure AH. Time dependent transient power and delta temperature for triangular wave input, middle heater, heater configuration A23, ambient temperature 20.0°C.

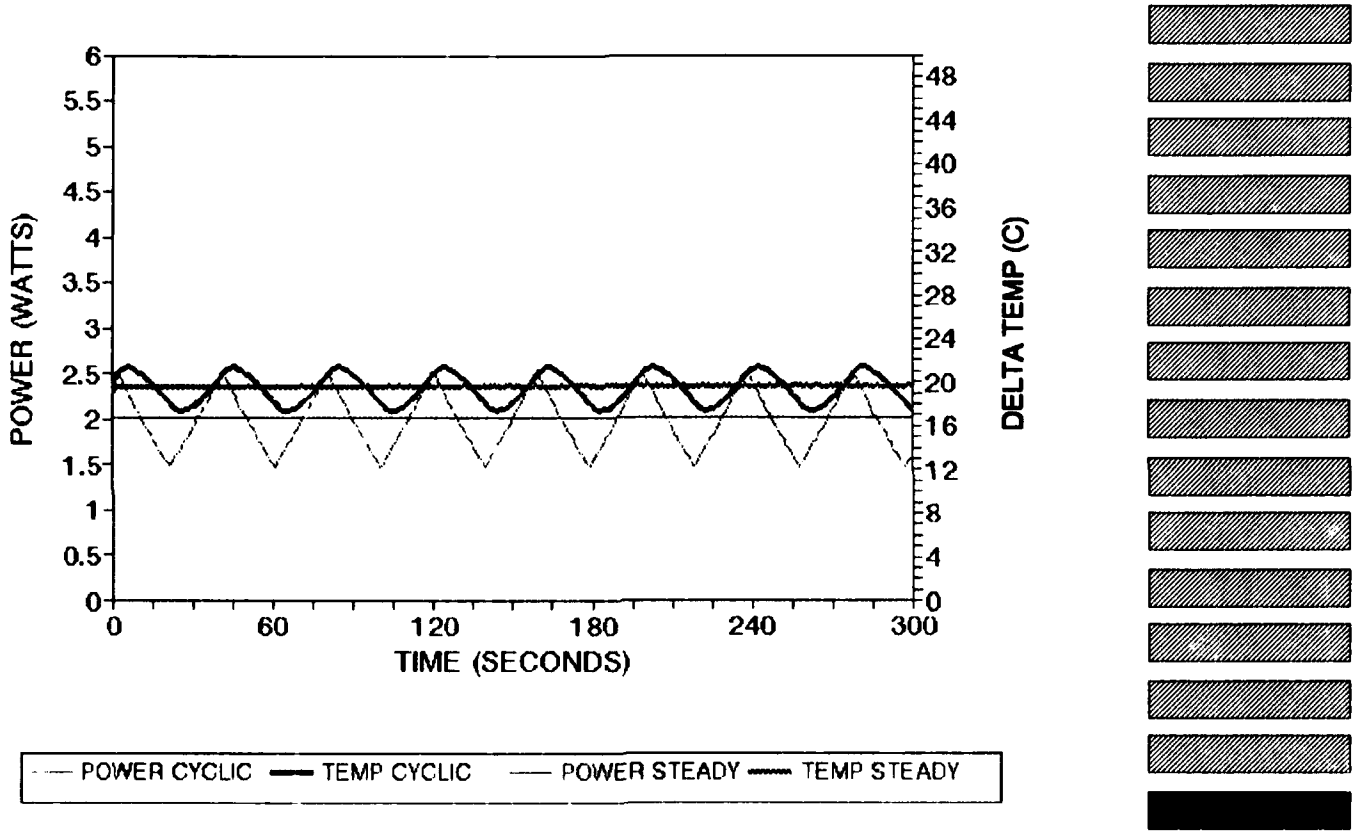

Figure AI. Time dependent transient power and delta temperature for triangular wave input, bottom heater, heater configuration A30, ambient temperature 20.0°C.

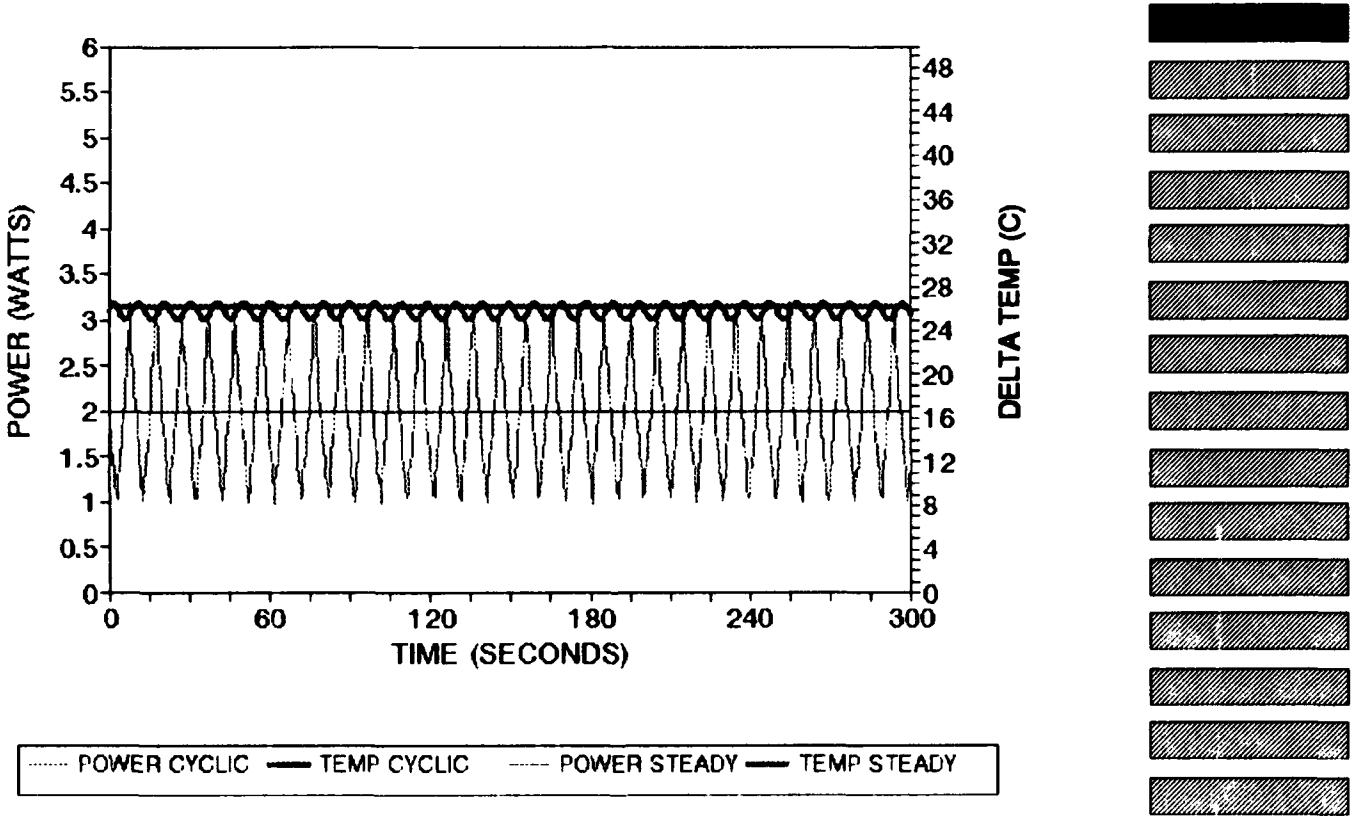

Figure BA. Time dependent transient power and delta temperature for triangular wave input, top heater, heater configuration A16, ambient temperature 20.0°C.

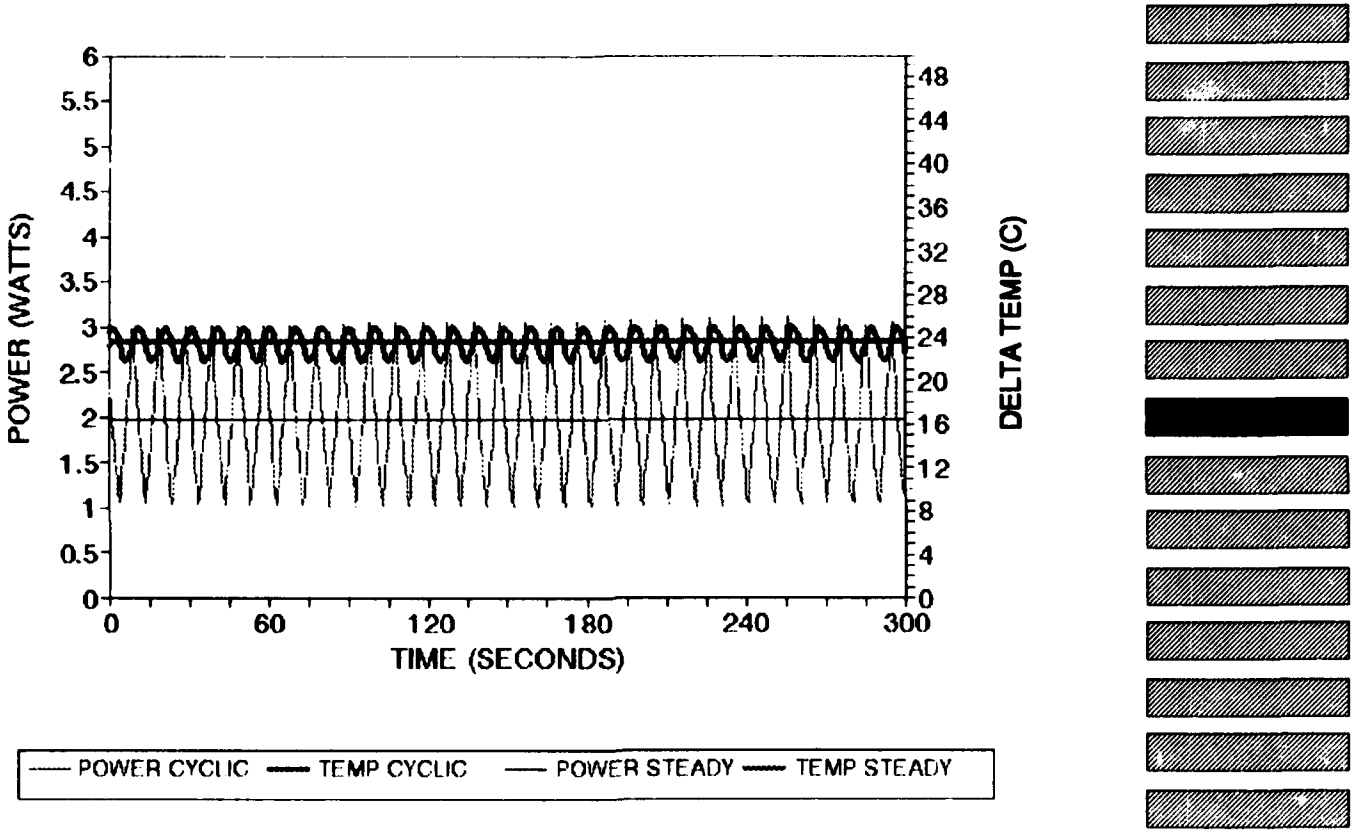

Figure BB. Time dependent transient power and delta temperature for triangular wave input, middle heater, heater configuration A23, ambient temperature 20.0°C.

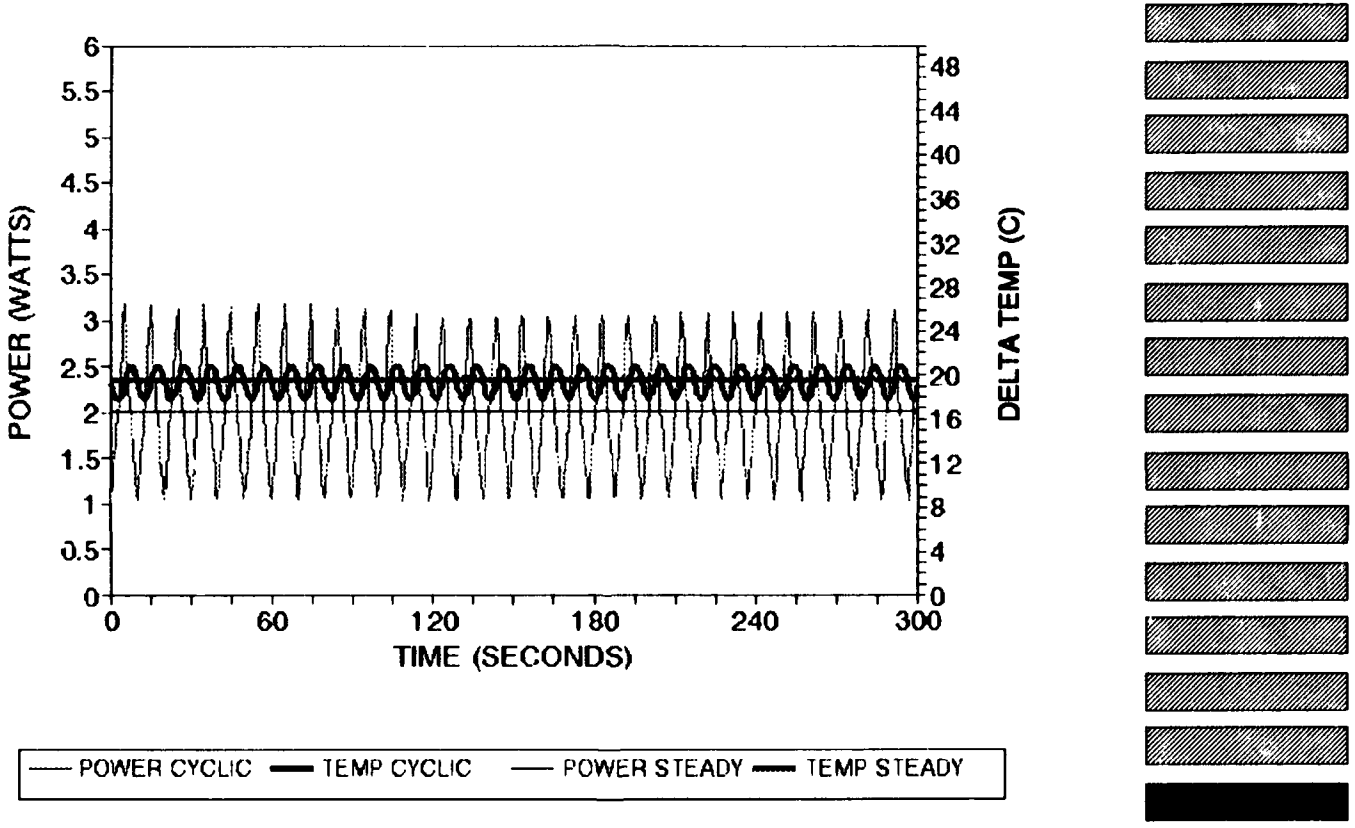

Figure BC. Time dependent transient power and delta temperature for triangular wave input, bottom heater, heater configuration A30, ambient temperature 20.0°C.

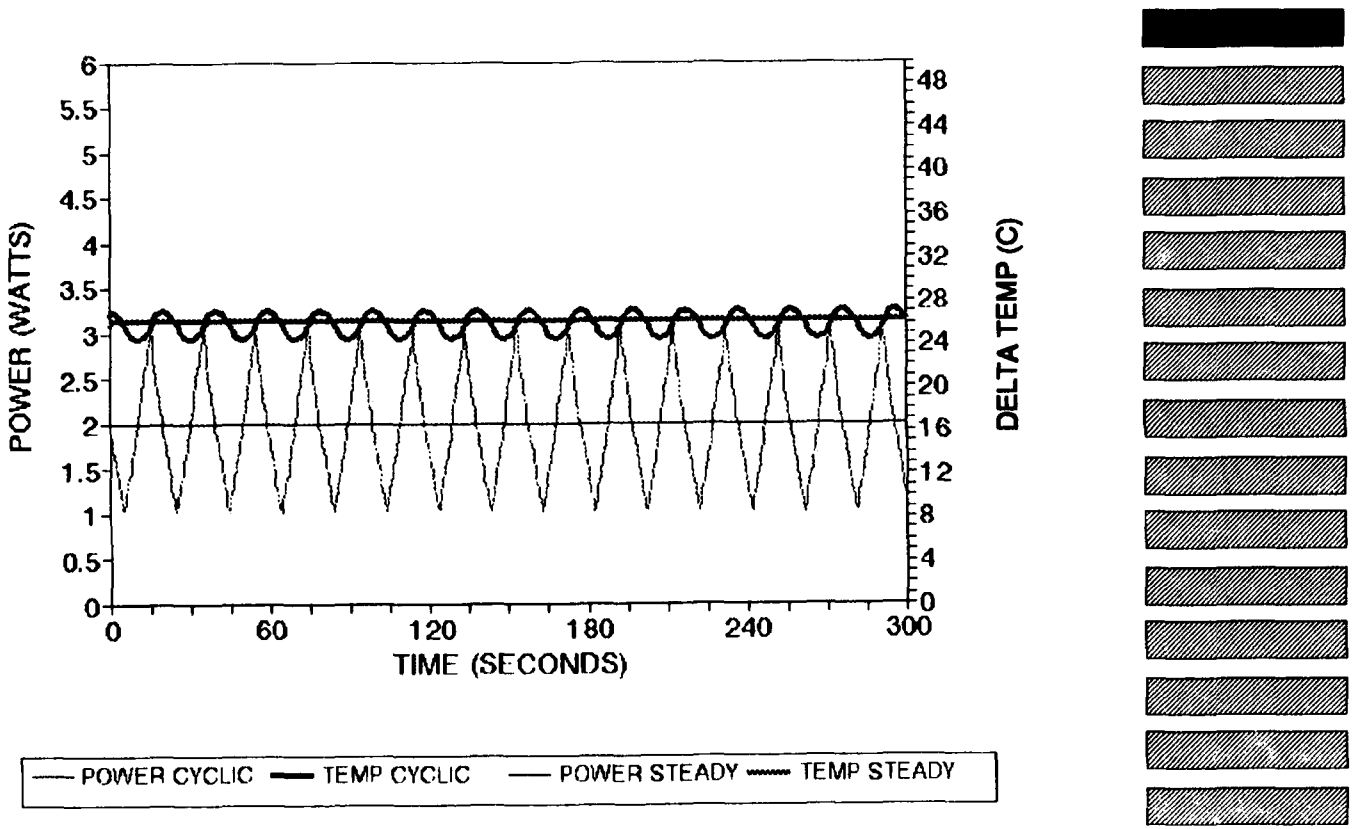

Figure BD. Time dependent transient power and delta temperature for triangular wave input, top heater, heater configuration A16, ambient temperature 20.0°C.

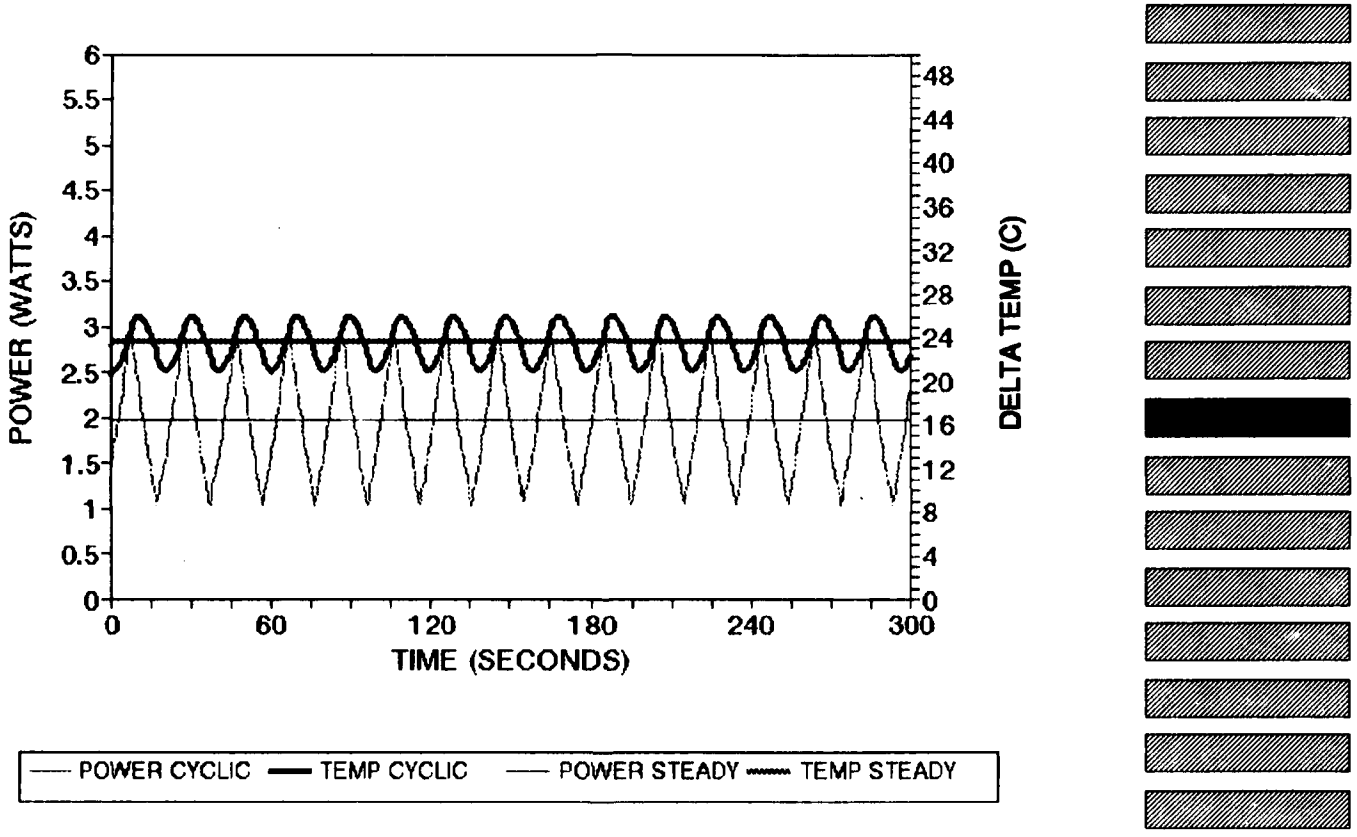

Figure BE. Time dependent transient power and delta temperature for triangular wave input, middle heater, heater configuration A23, ambient temperature 20.0°C.

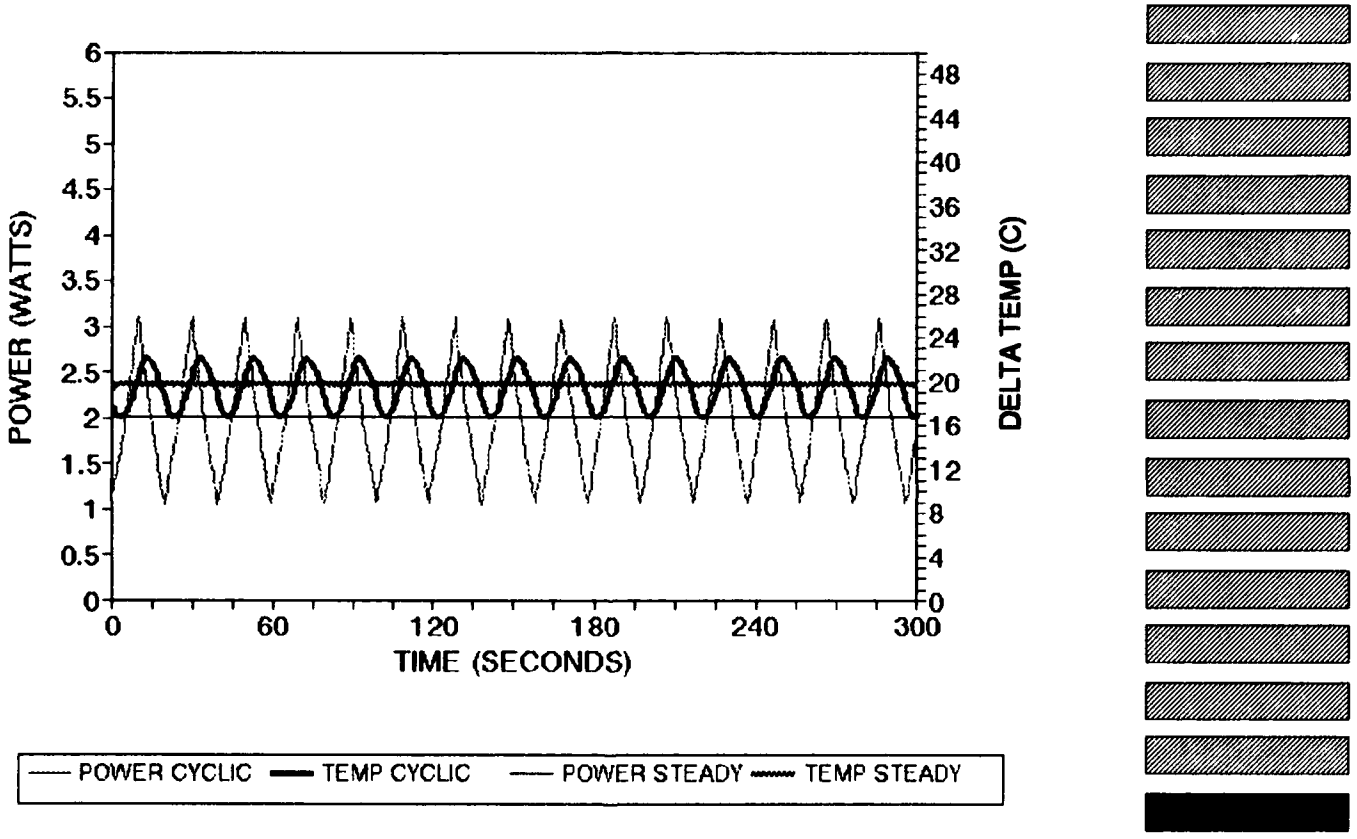

Figure BF. Time dependent transient power and delta temperature for triangular wave input, bottom heater, heater configuration A30, ambient temperature 20.0°C.

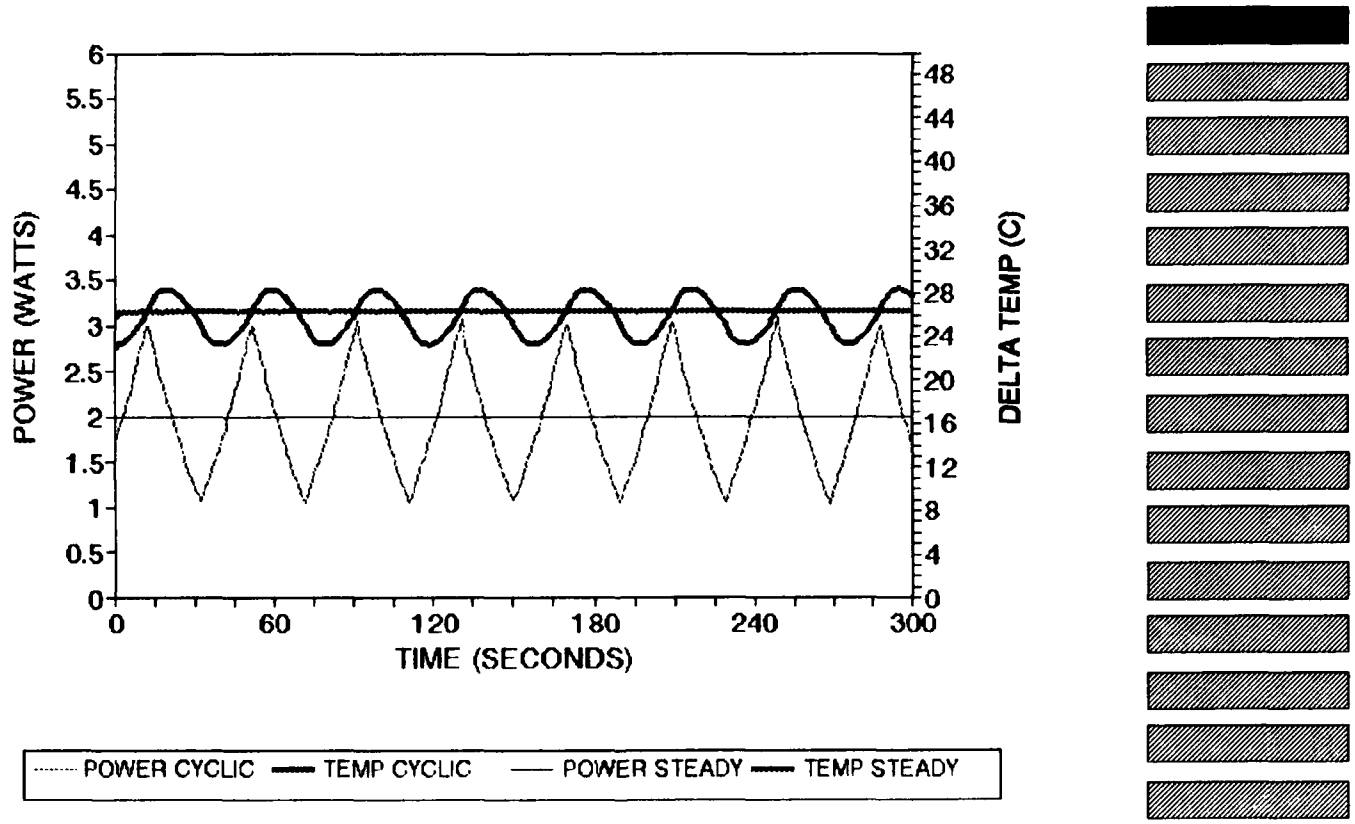

Figure BG. Time dependent transient power and delta temperature for triangular wave input, top heater, heater configuration A16, ambient temperature 20.0°C.

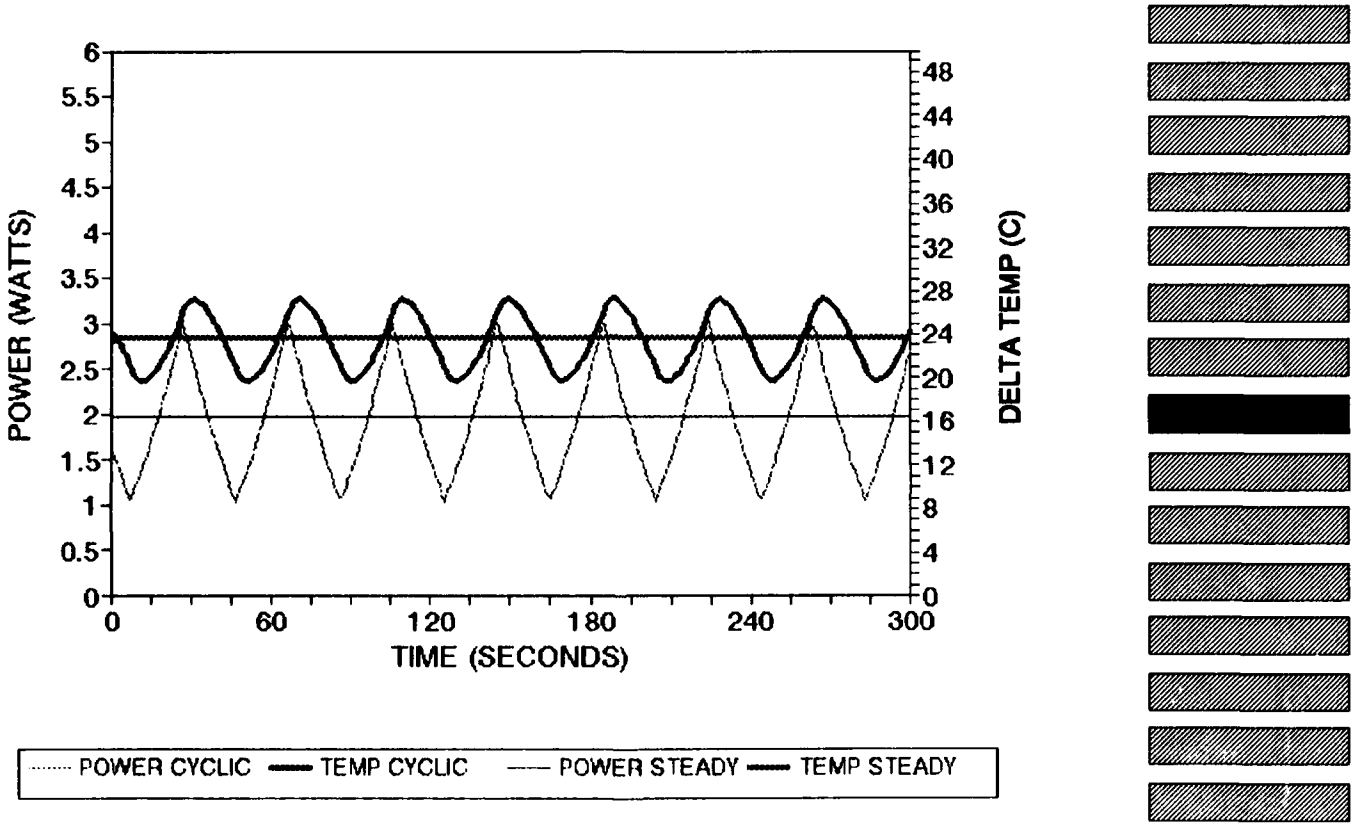

Figure BH. Time dependent transient power and delta temperature for triangular wave input, middle heater, heater configuration A23, ambient temperature 20.0°C.

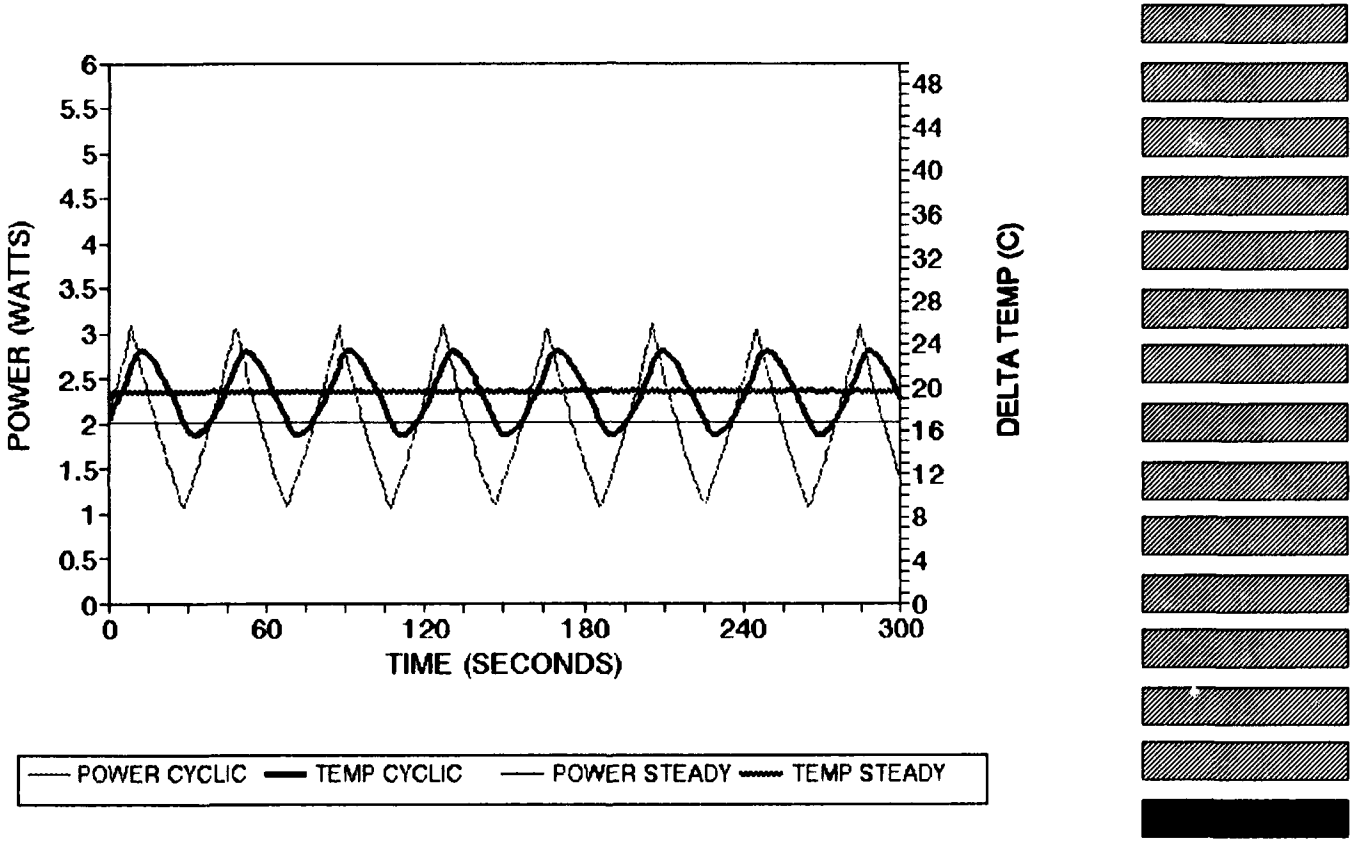

Figure BI. Time dependent transient power and delta temperature for triangular wave input, bottom heater, heater configuration A30, ambient temperature 19.9°C.

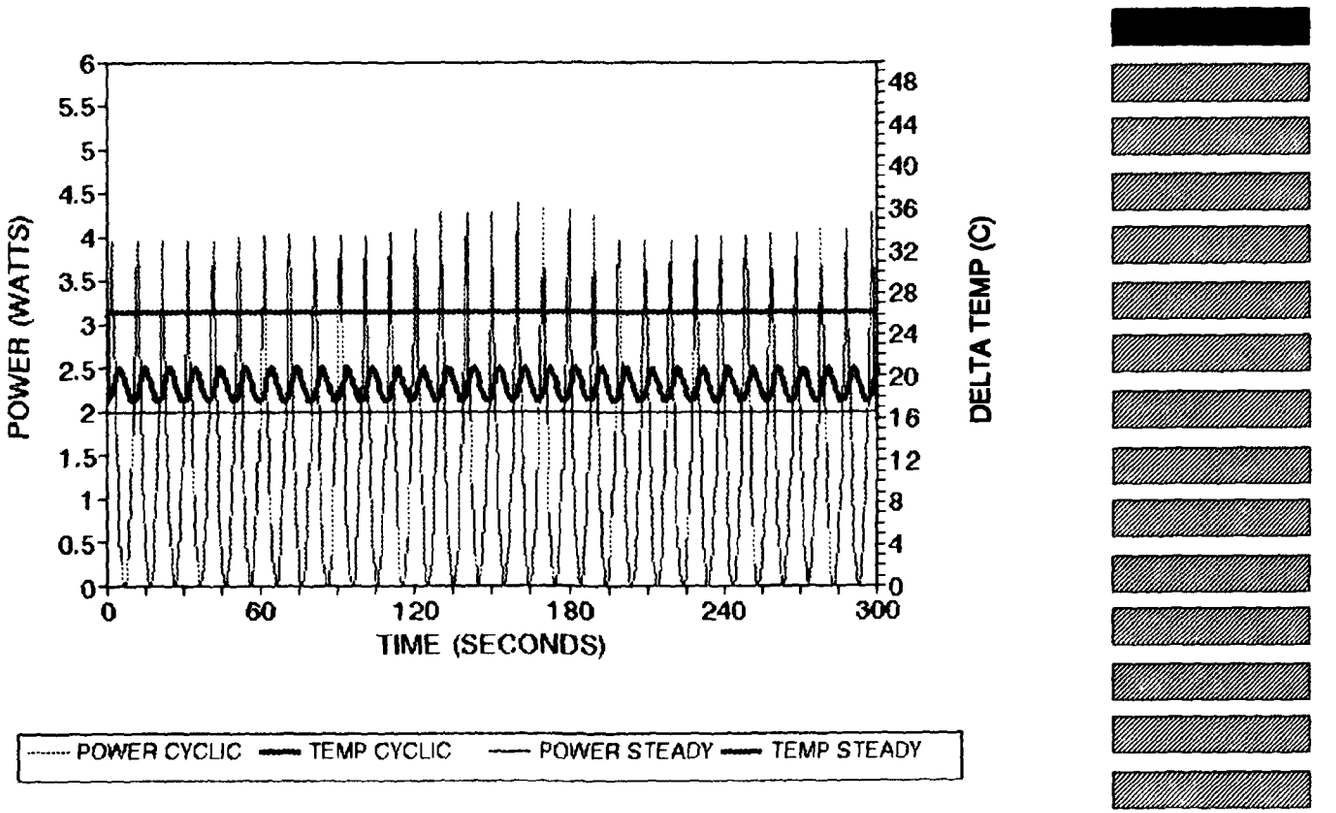

Figure CA. Time dependent transient power and delta temperature for triangular wave input, top heater, heater configuration A16, ambient temperature 19.9°C.

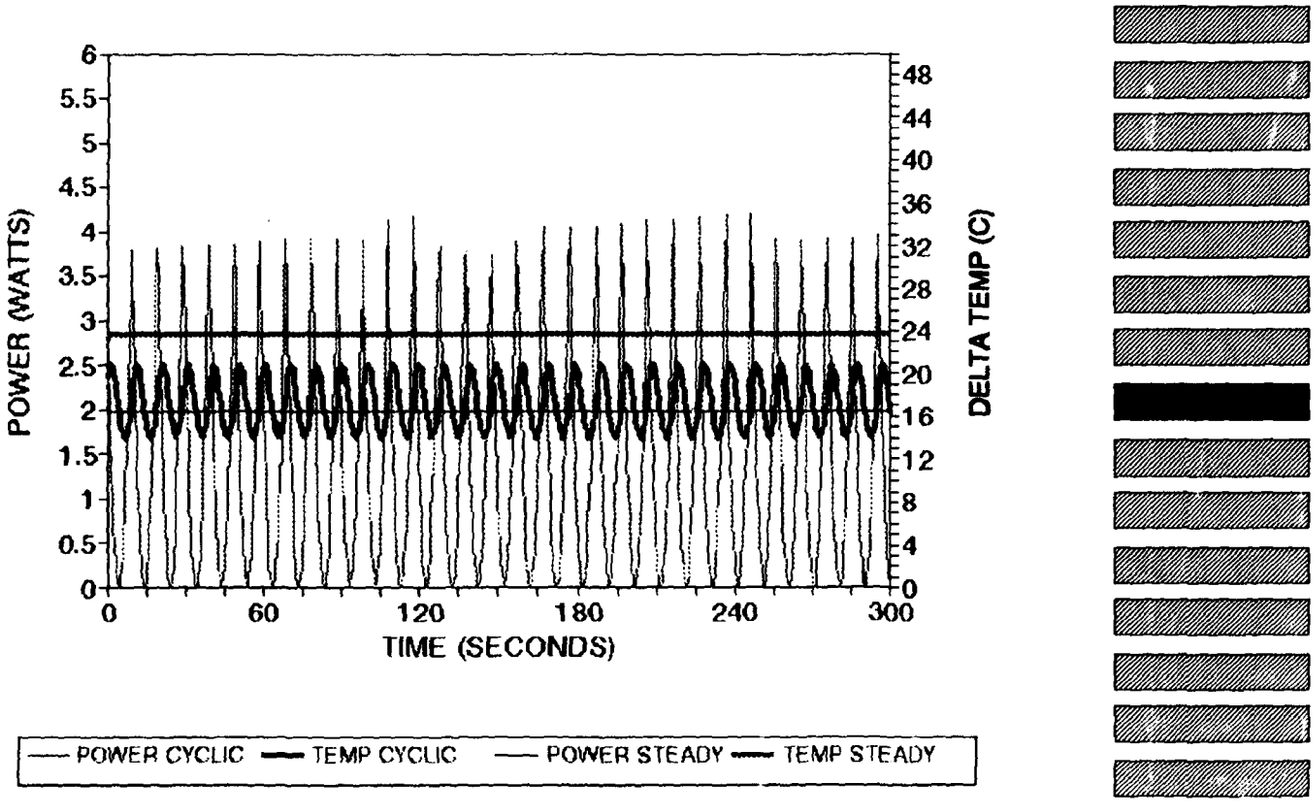

Figure CB. Time dependent transient power and delta temperature for triangular wave input, middle heater, heater configuration A23, ambient temperature 19.9°C.

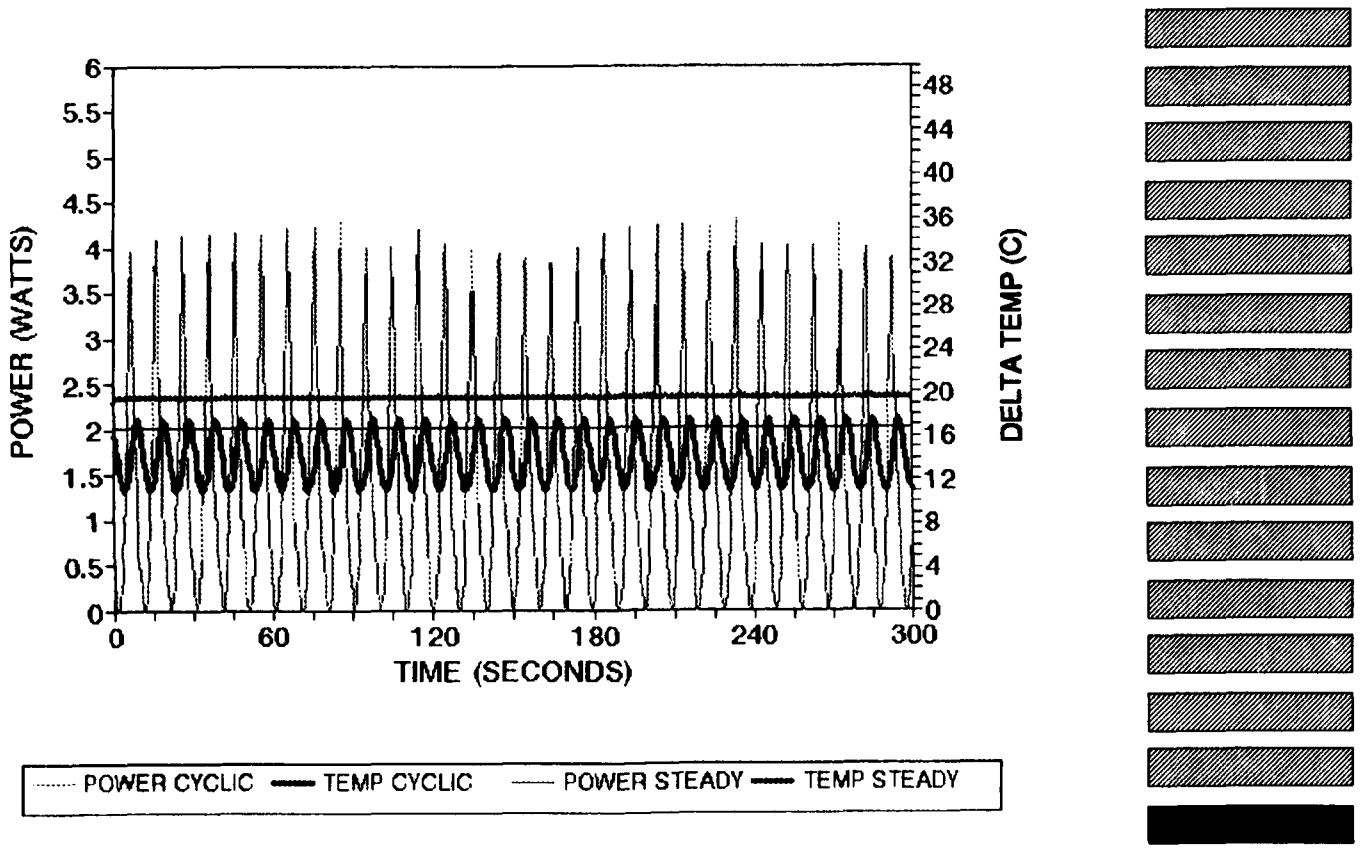

Figure CC. Time dependent transient power and delta temperature for triangular wave input, bottom heater, heater configuration A30, ambient temperature 19.9°C.

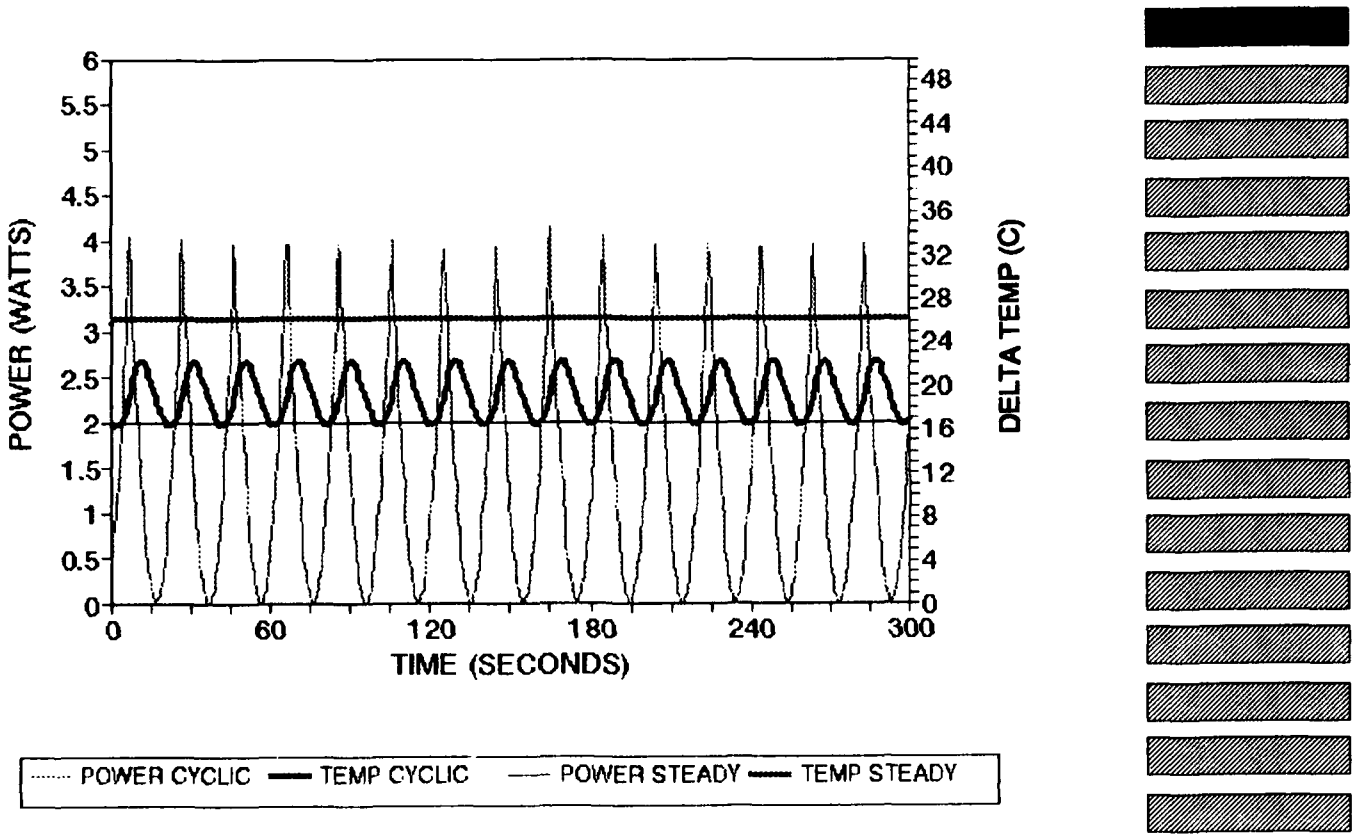

Figure CD. Time dependent transient power and delta temperature for triangular wave input, top heater, heater configuration A16, ambient temperature 20.0°C.

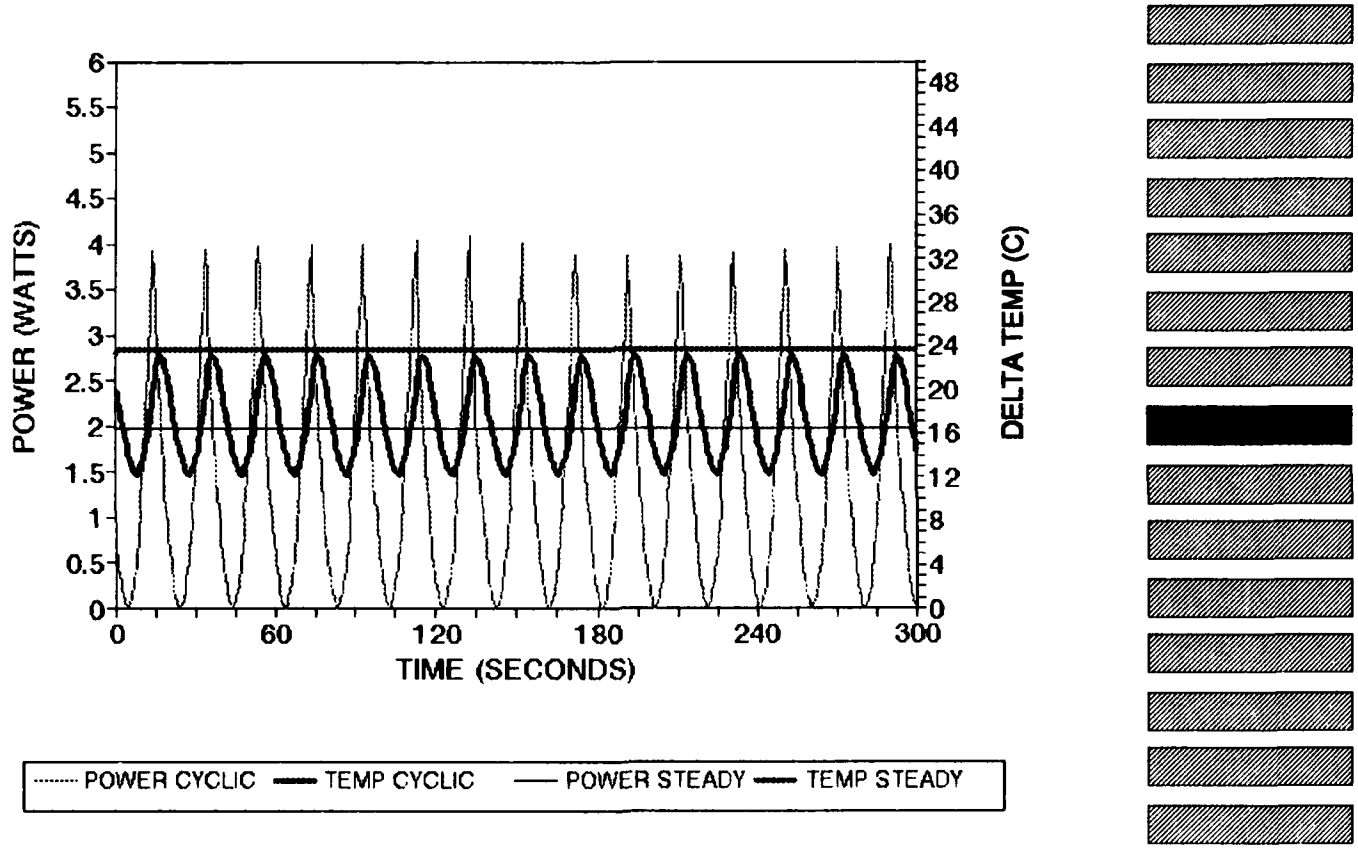

Figure CE. Time dependent transient power and delta temperature for triangular wave input, middle heater, heater configuration A23, ambient temperature 20.0°C.

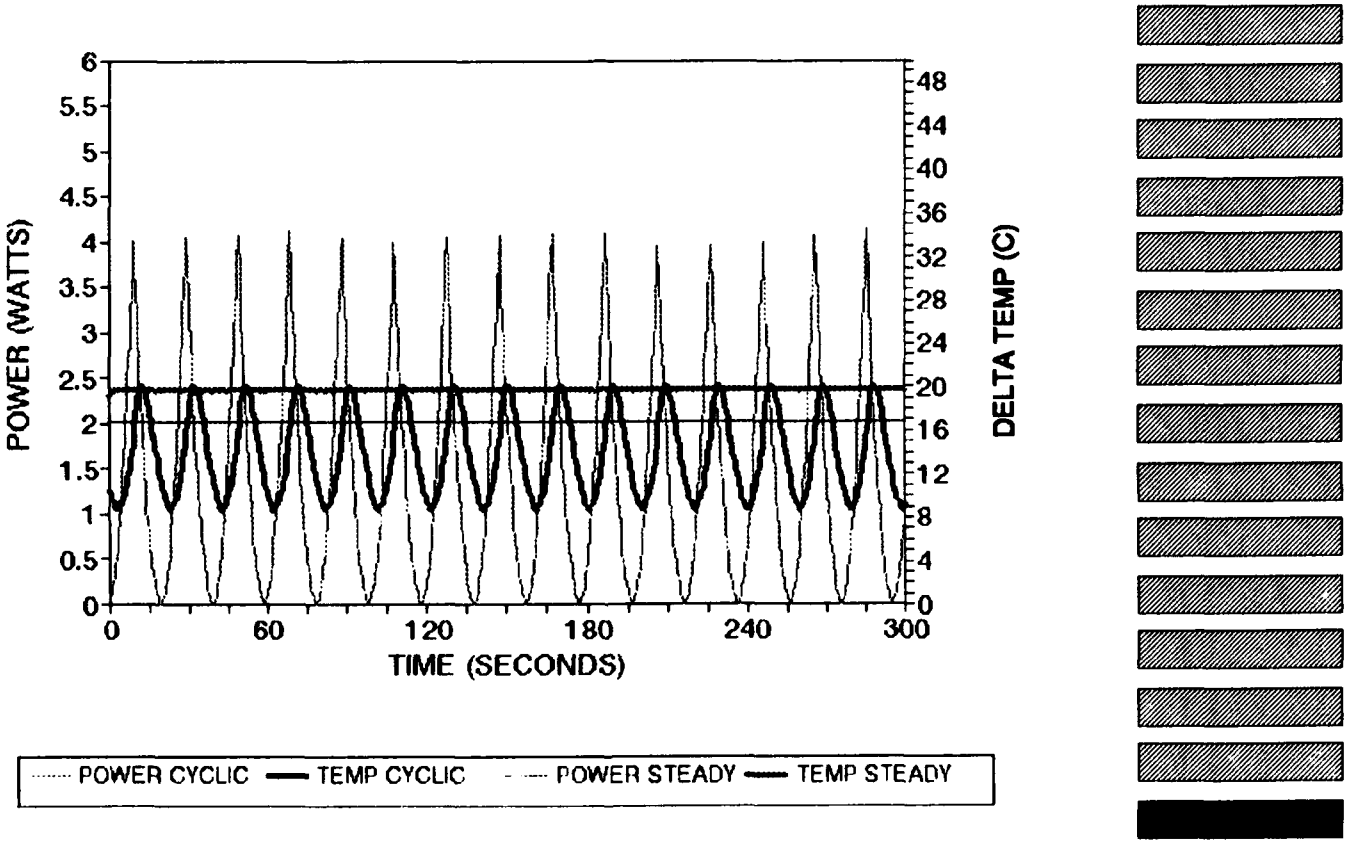

Figure CF. Time dependent transient power and delta temperature for triangular wave input, bottom heater, heater configuration A30, ambient temperature 20.0°C.

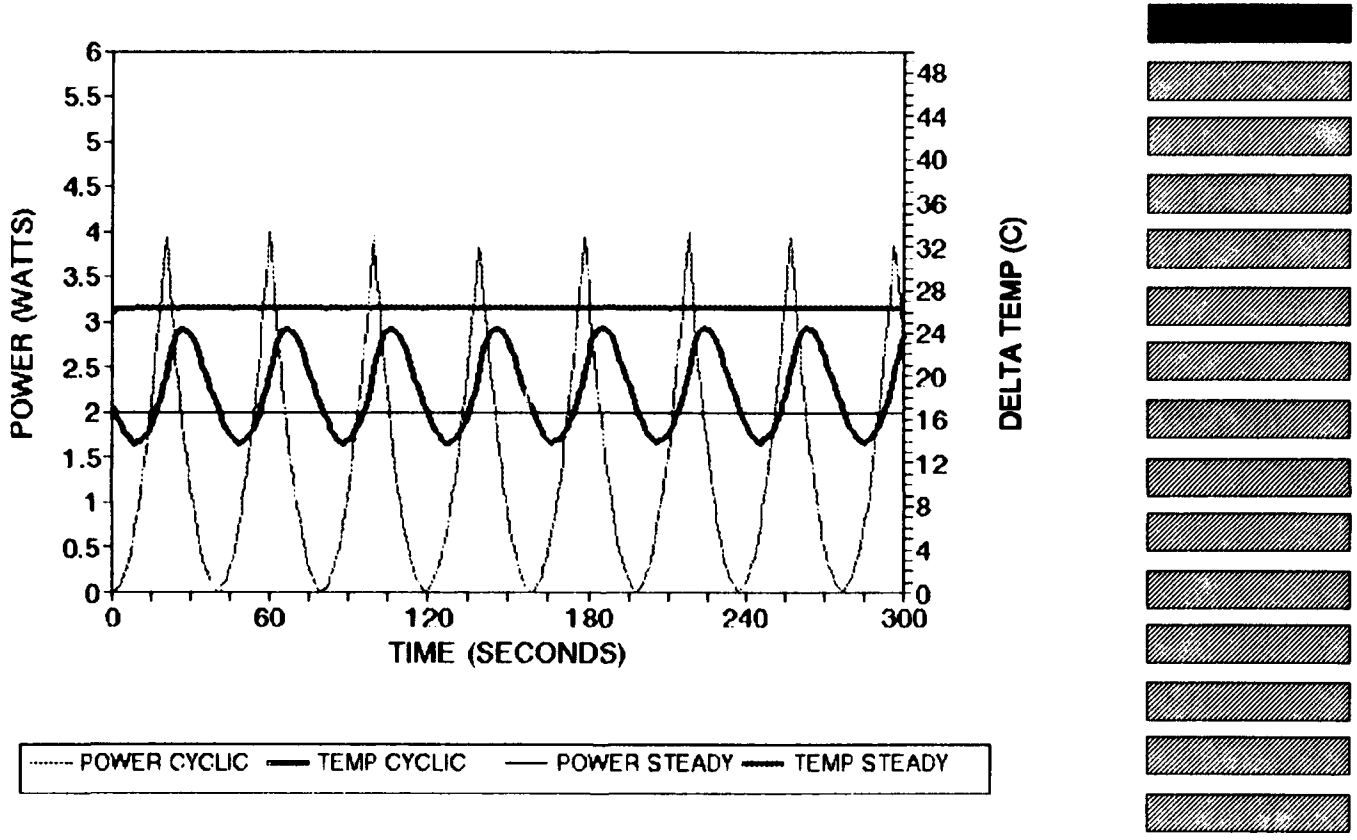

Figure CG. Time dependent transient power and delta temperature for triangular wave input, top heater, heater configuration A16, ambient temperature 20.0°C.

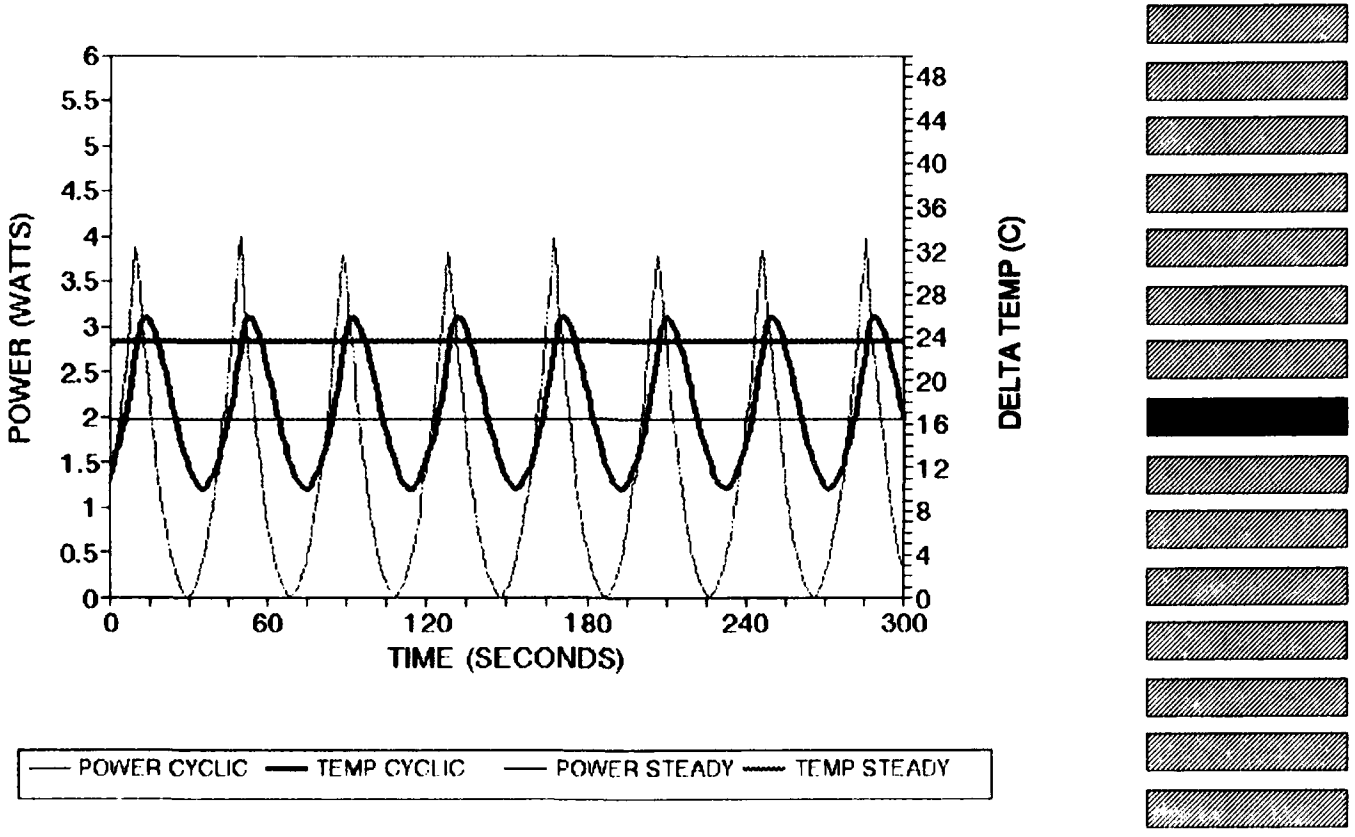

Figure CH. Time dependent transient power and delta temperature for triangular wave input, middle heater, heater configuration A23, ambient temperature 19.9°C.

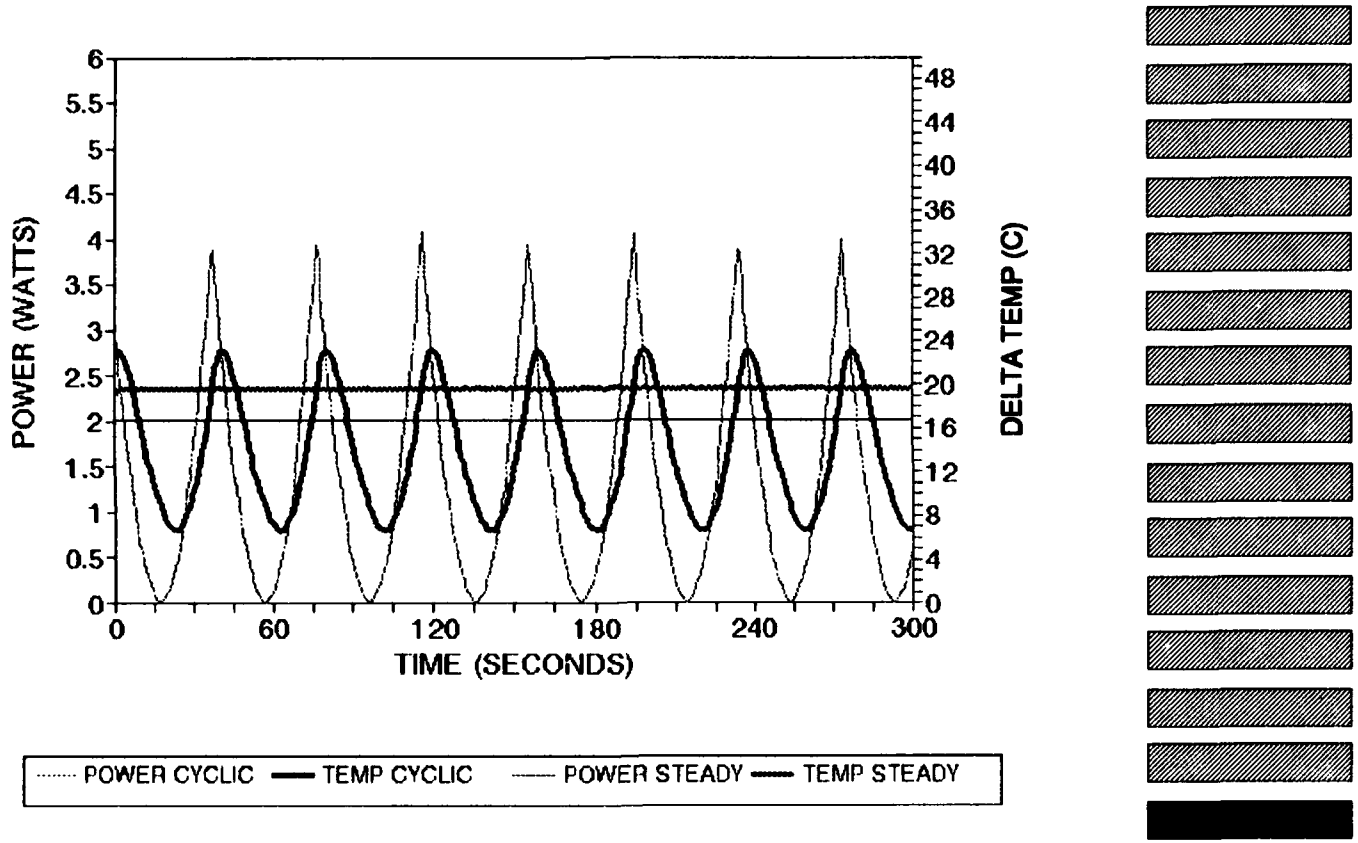

Figure CI. Time dependent transient power and delta temperature for triangular wave input, bottom heater, heater configuration A30, ambient temperature 20.0°C.

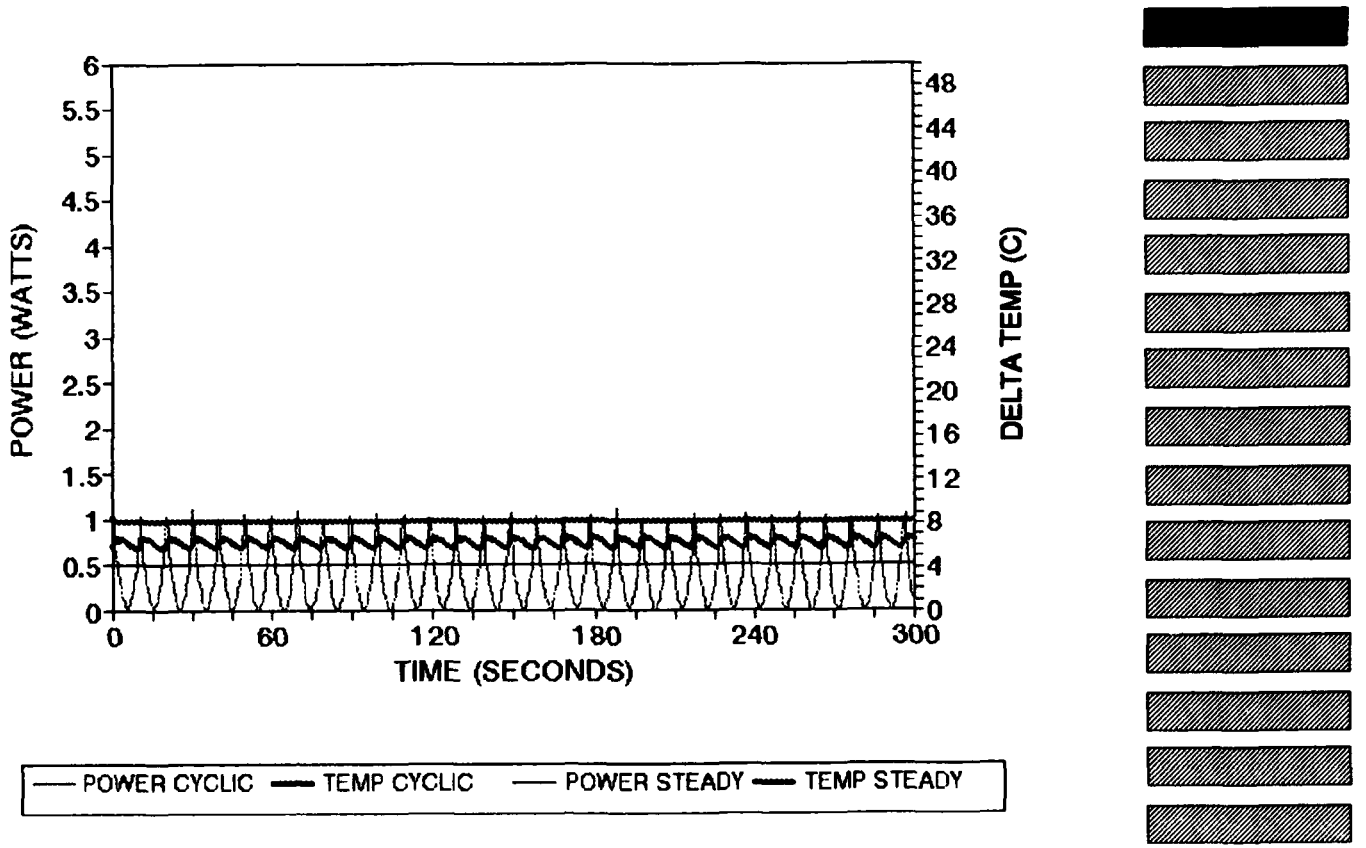

Figure DA. Time dependent transient power and delta temperature for triangular wave input, top heater, heater configuration A16, ambient temperature 19.2°C.

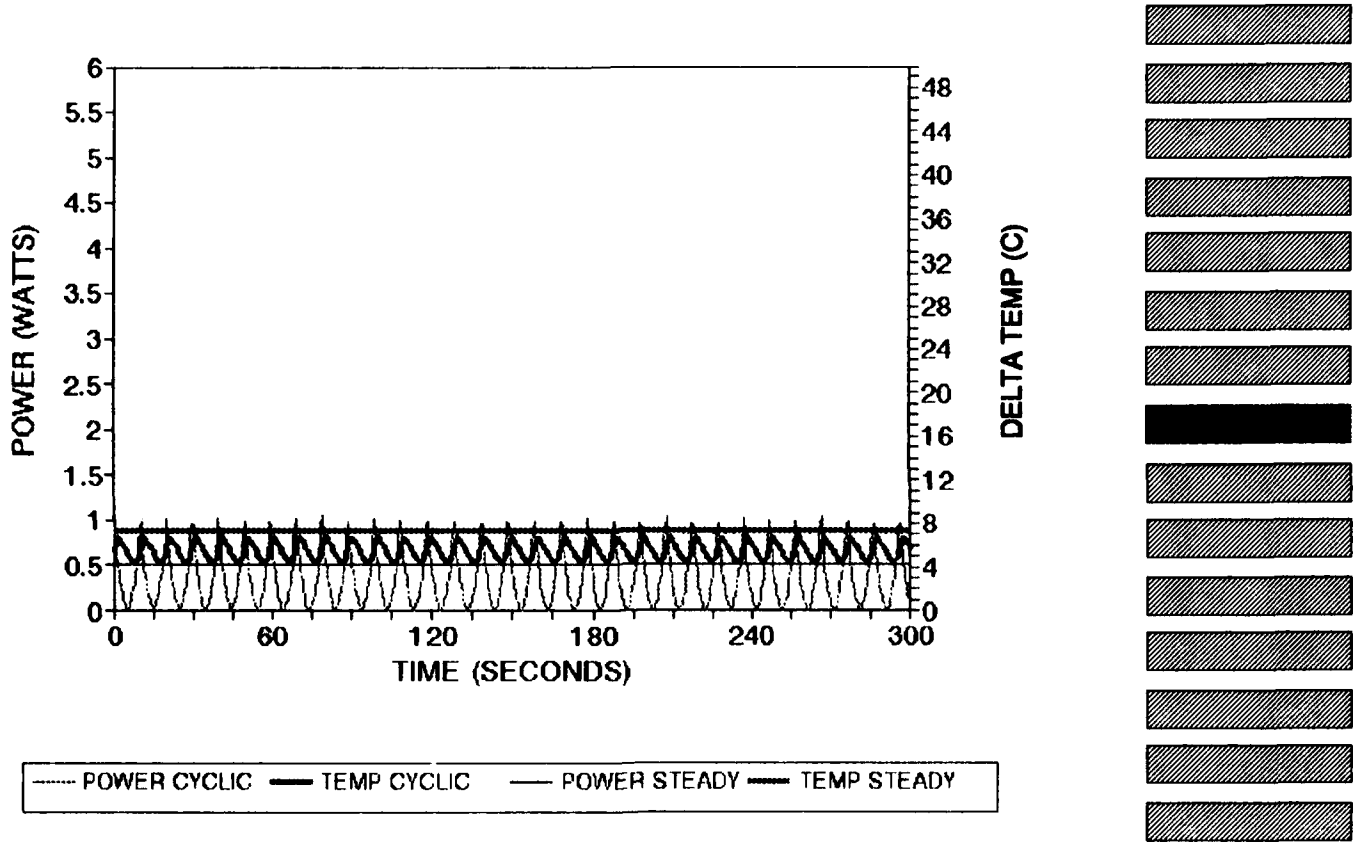

Figure DB. Time dependent transient power and delta temperature for triangular wave input, middle heater, heater configuration A23, ambient temperature 19.3°C.

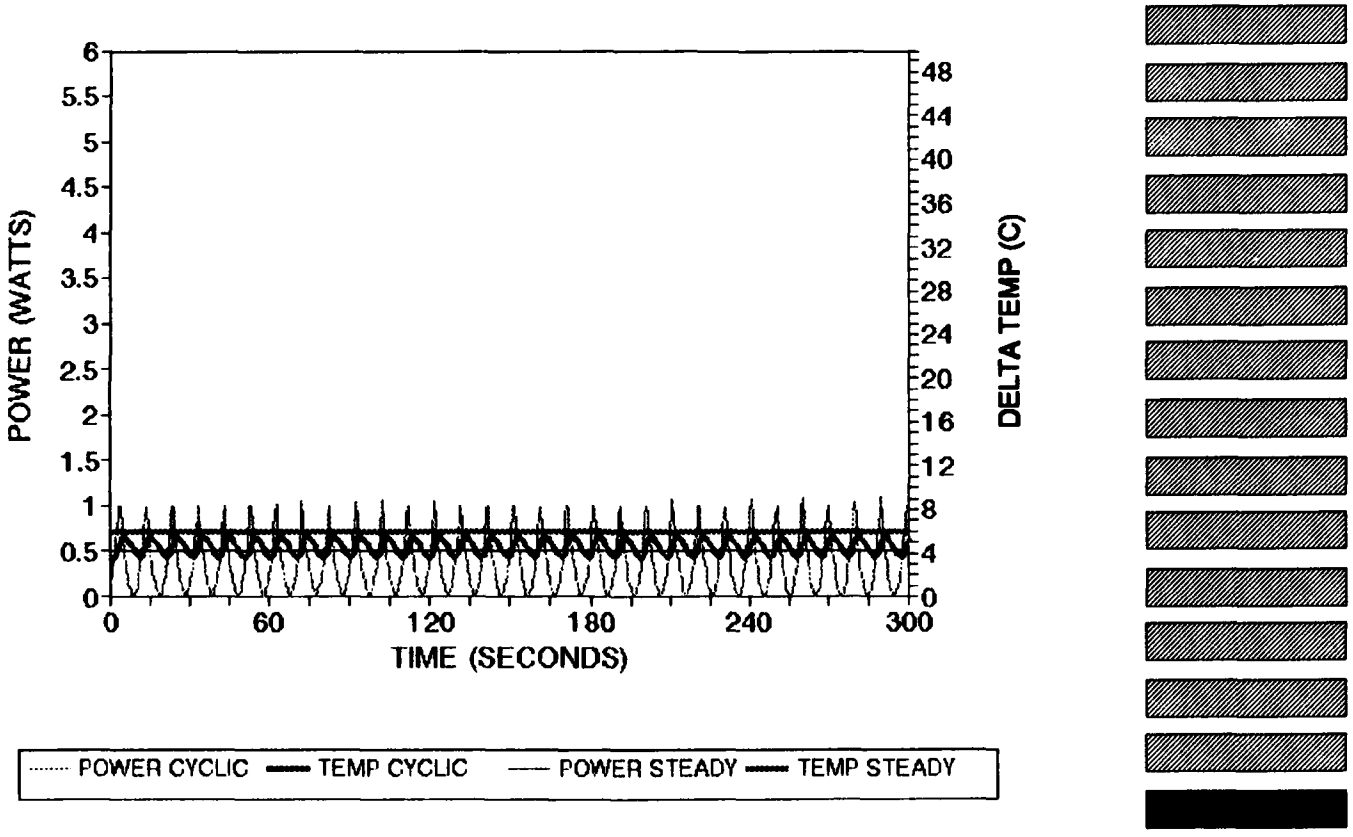

Figure DC. Time dependent transient power and delta temperature for triangular wave input, bottom heater, heater configuration A30, ambient temperature 19.3°C.

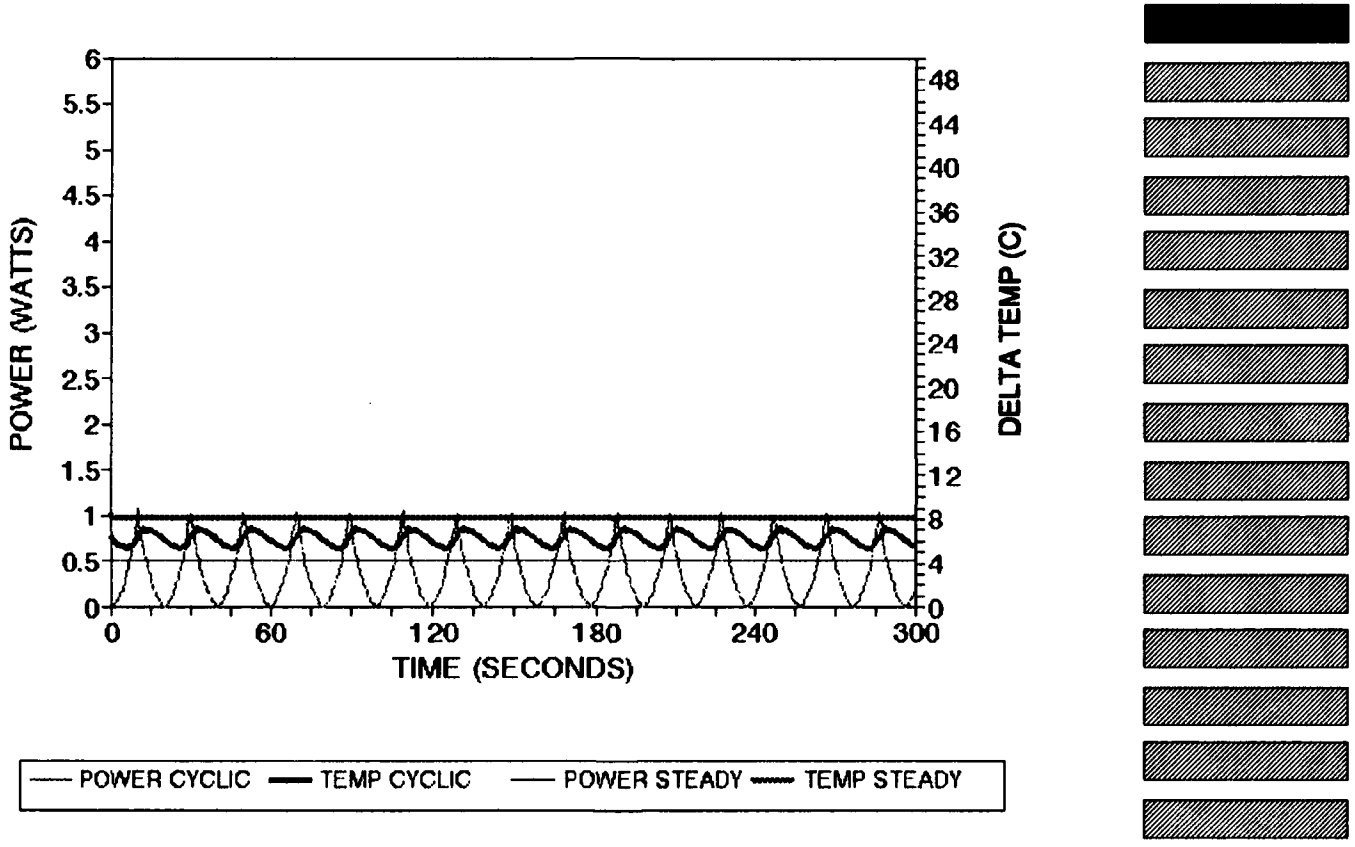

Figure DD. Time dependent transient power and delta temperature for triangular wave input, top heater, heater configuration A16, ambient temperature 19.3°C.

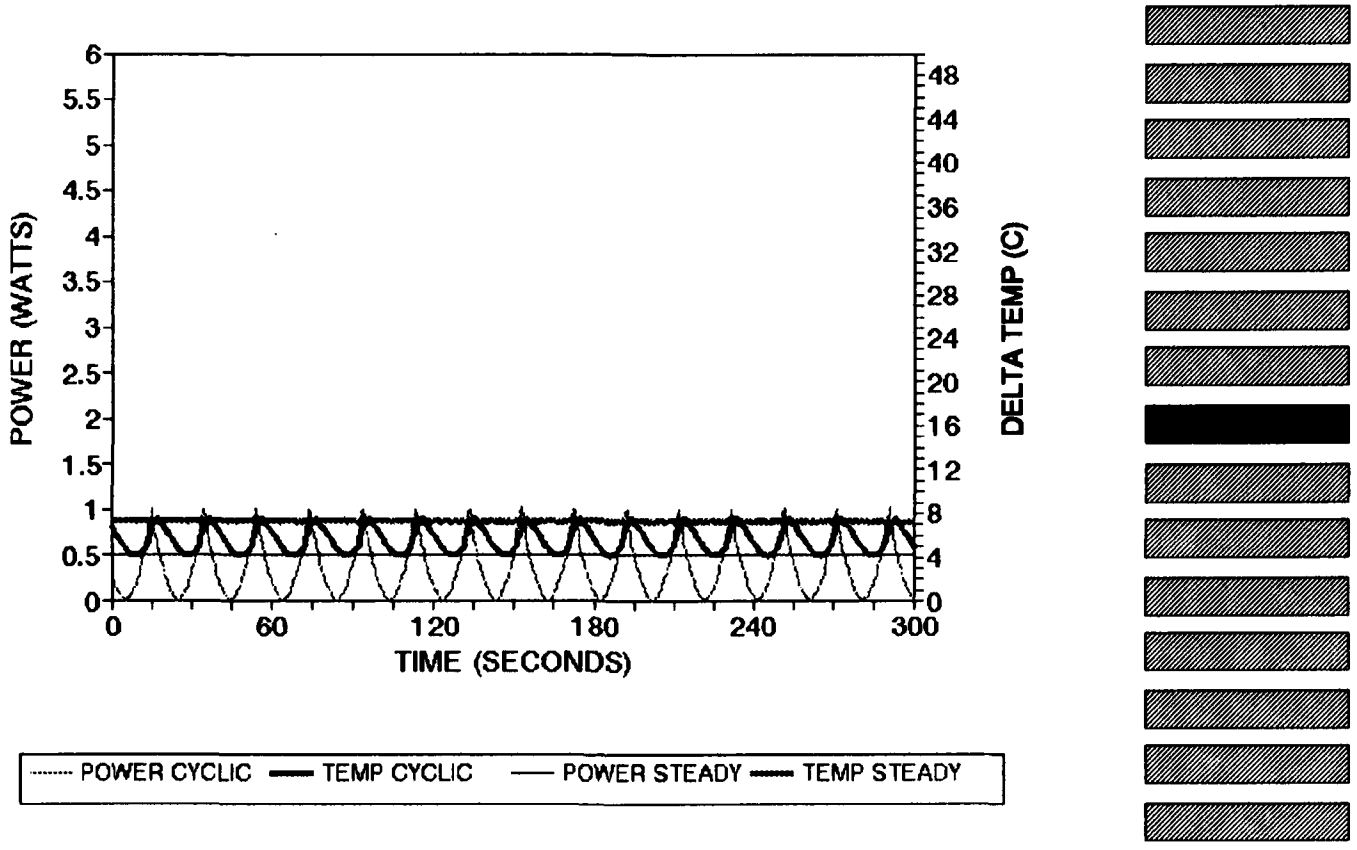

Figure DE. Time dependent transient power and delta temperature for triangular wave input, middle heater, heater configuration A23, ambient temperature 19.4°C.

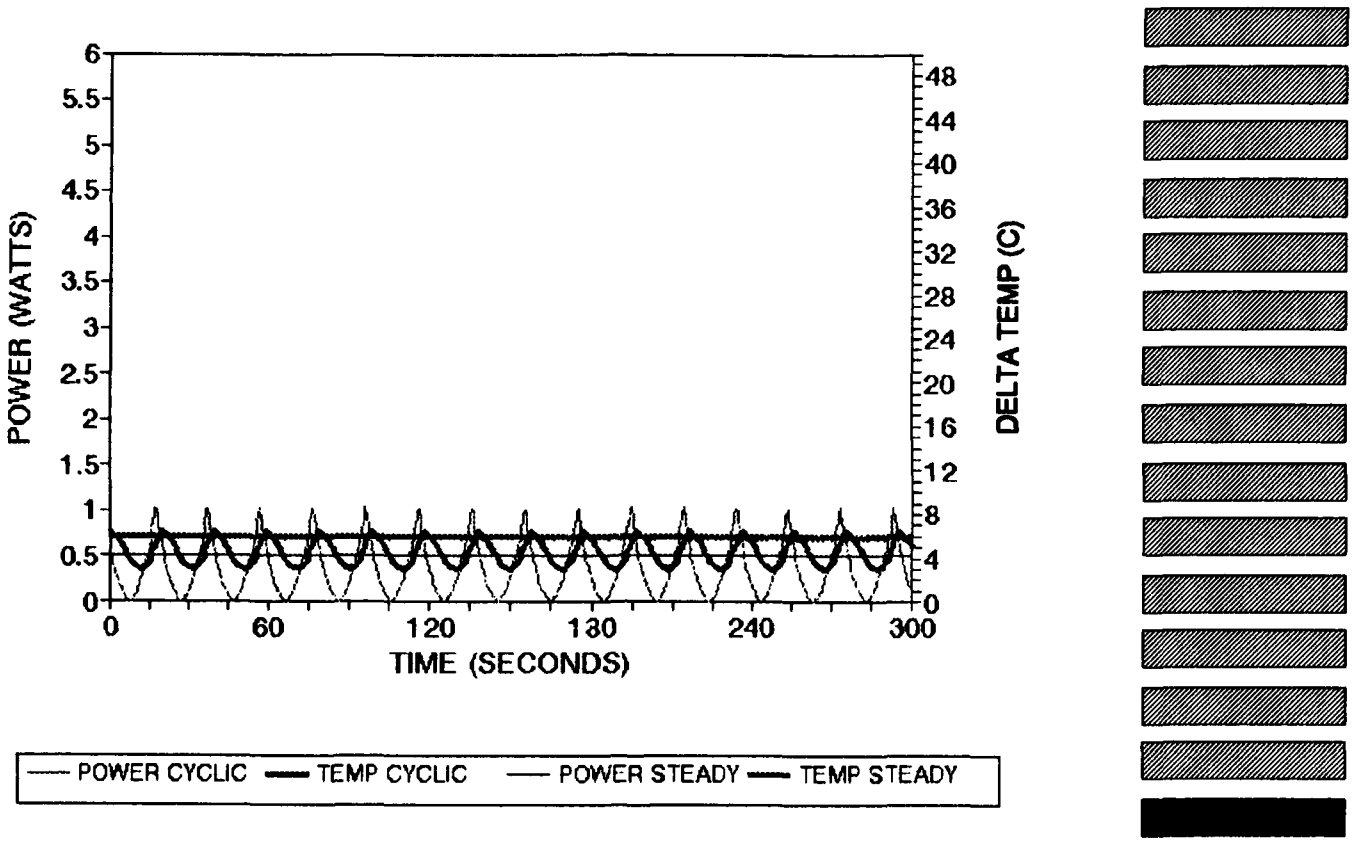

Figure DF. Time dependent transient power and delta temperature for triangular wave input, bottom heater, heater configuration A30, ambient temperature 19.2°C.

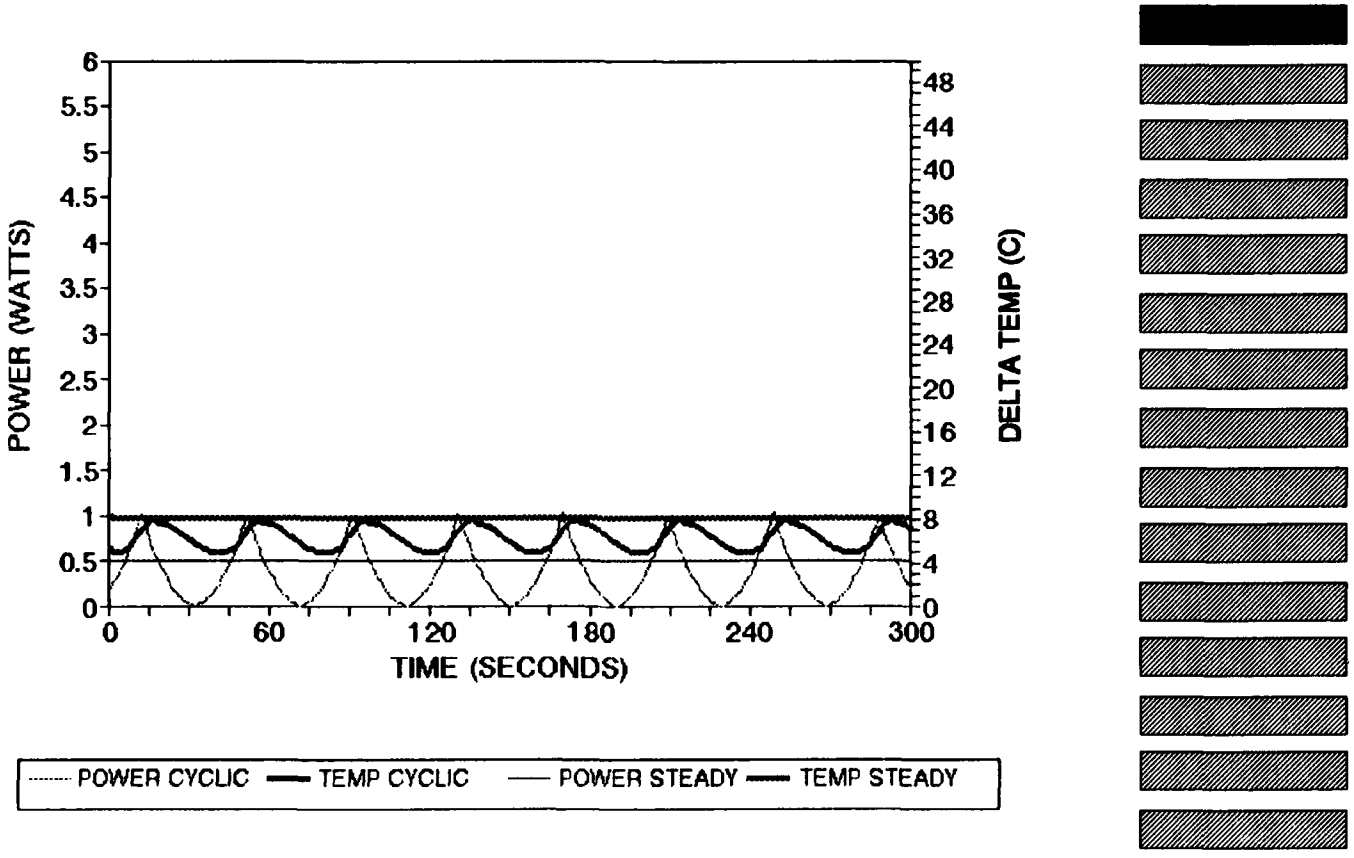

Figure DG. Time dependent transient power and delta temperature for triangular wave input, top heater, heater configuration A16, ambient temperature 19.4°C.

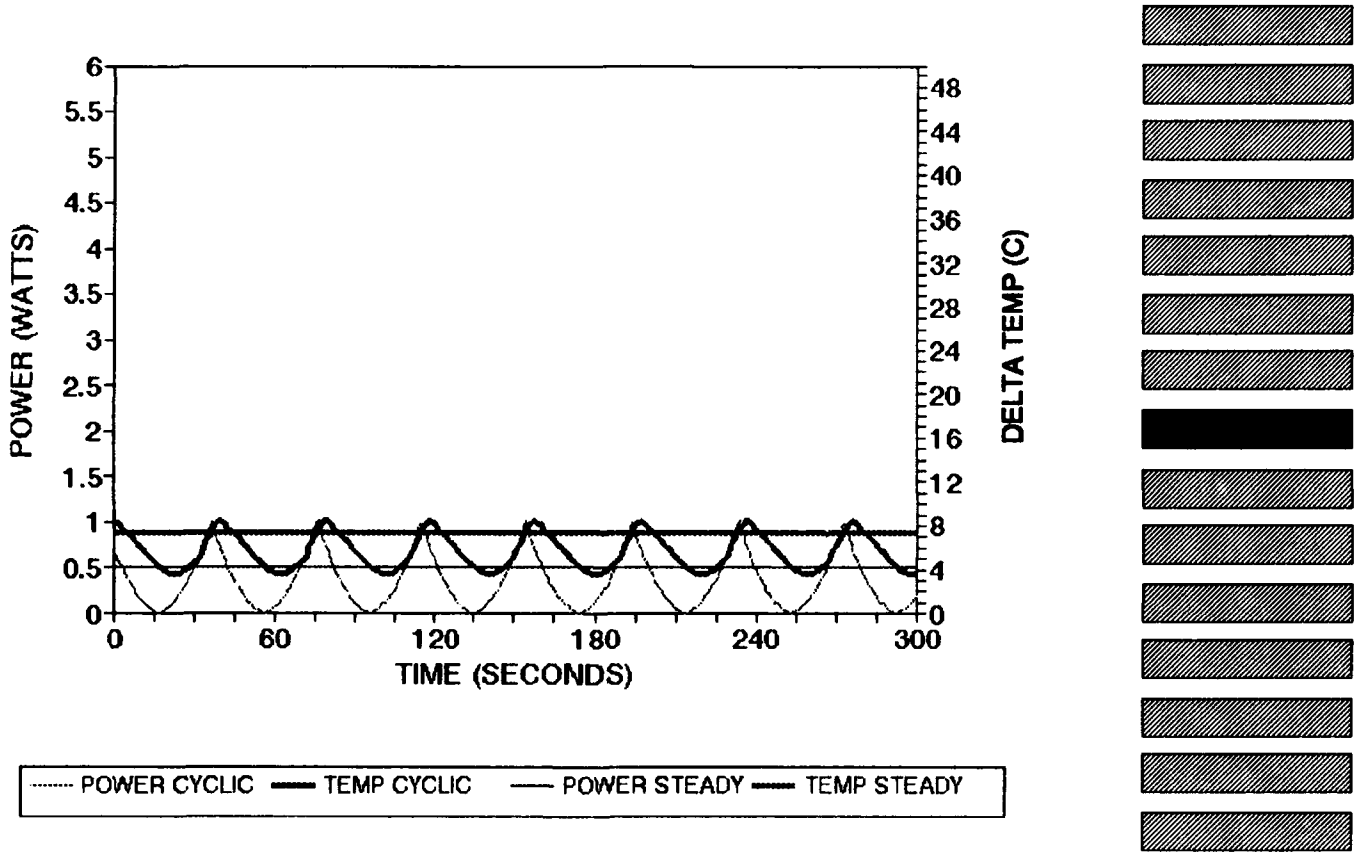

Figure DH. Time dependent transient power and delta temperature for triangular wave input, middle heater, heater configuration A23, ambient temperature 19.4°C.

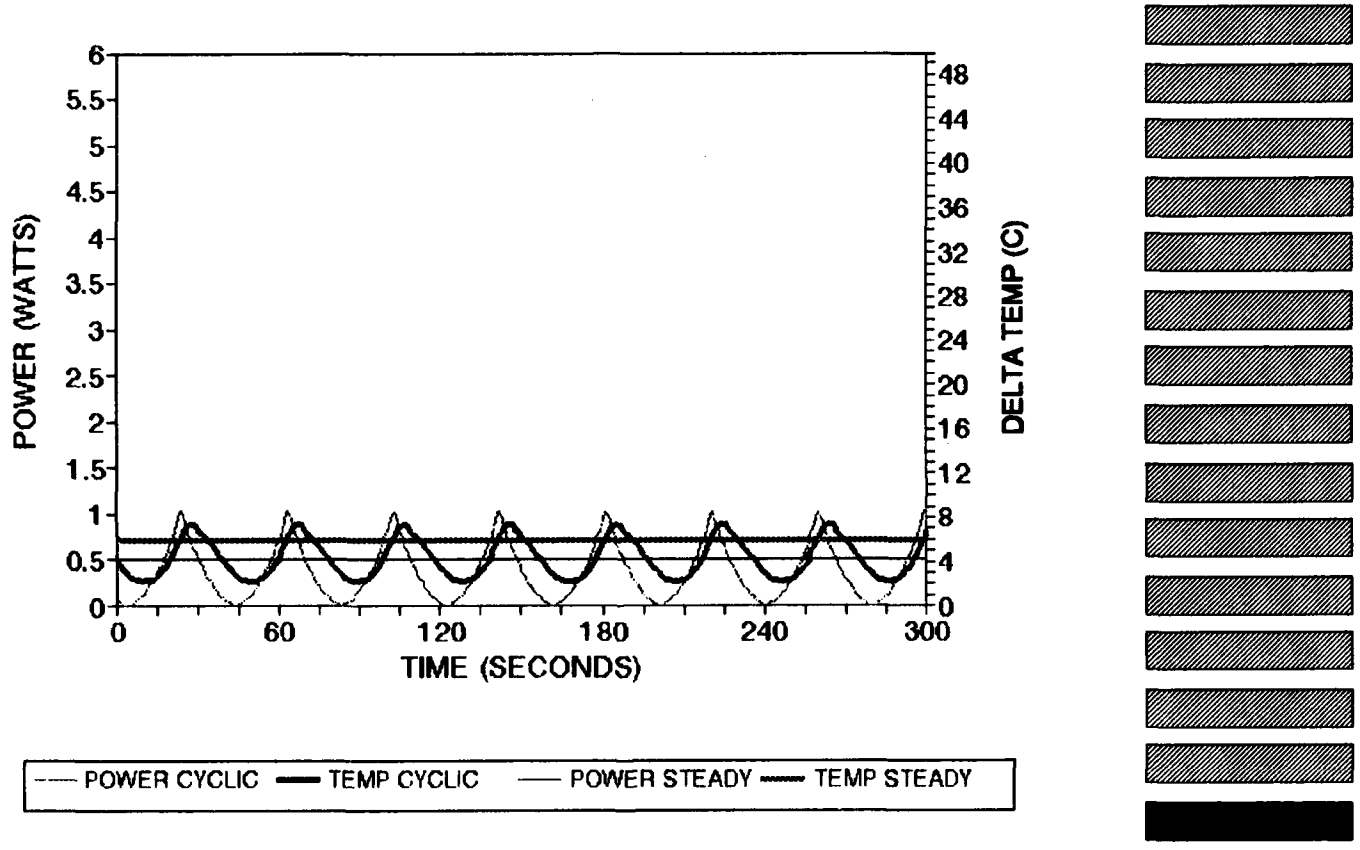

Figure DI. Time dependent transient power and delta temperature for triangular wave input, bottom heater, heater configuration A30, ambient temperature 19.4°C.

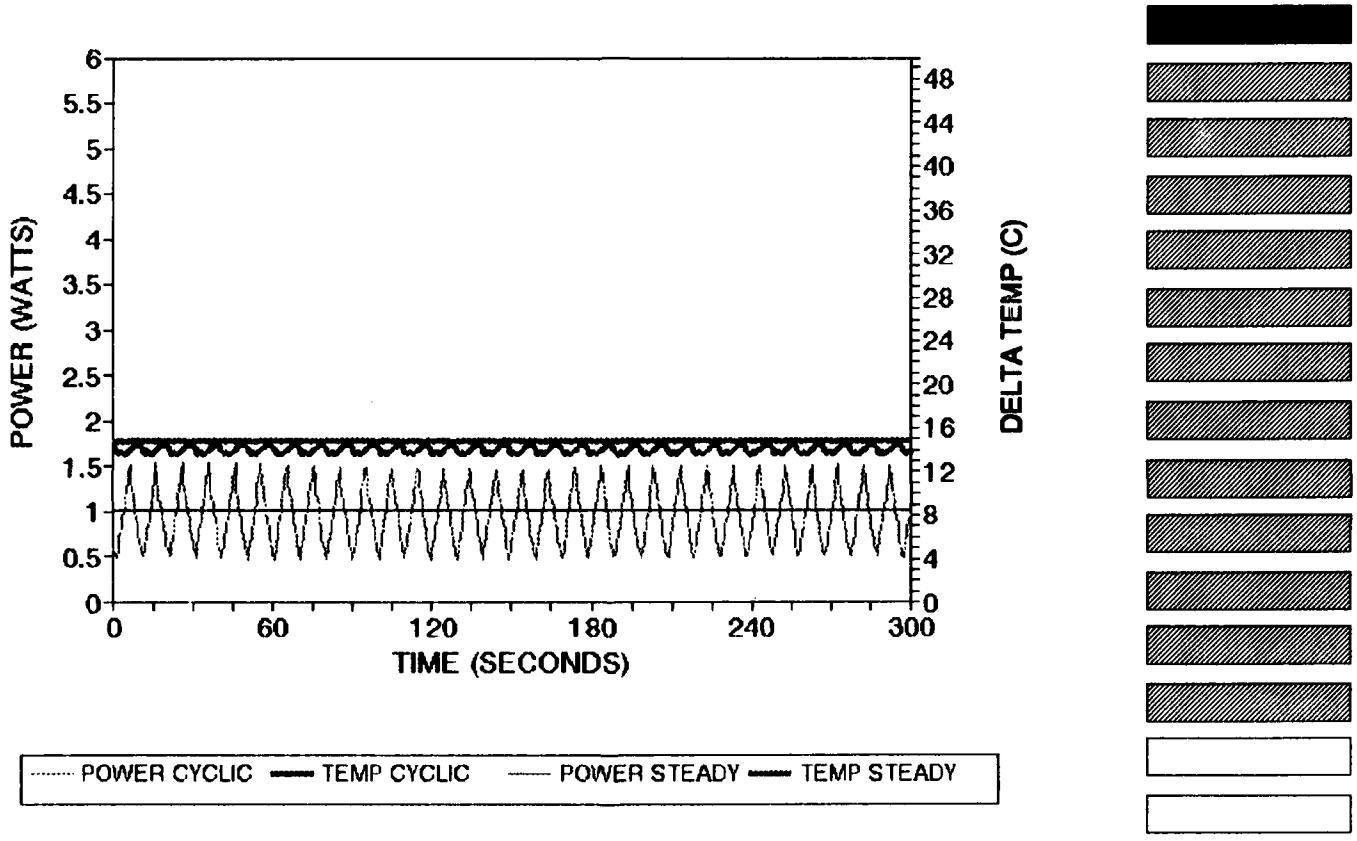

Figure EA. Time dependent transient power and delta temperature for triangular wave input, top heater, heater configuration B16, ambient temperature 20.4°C.

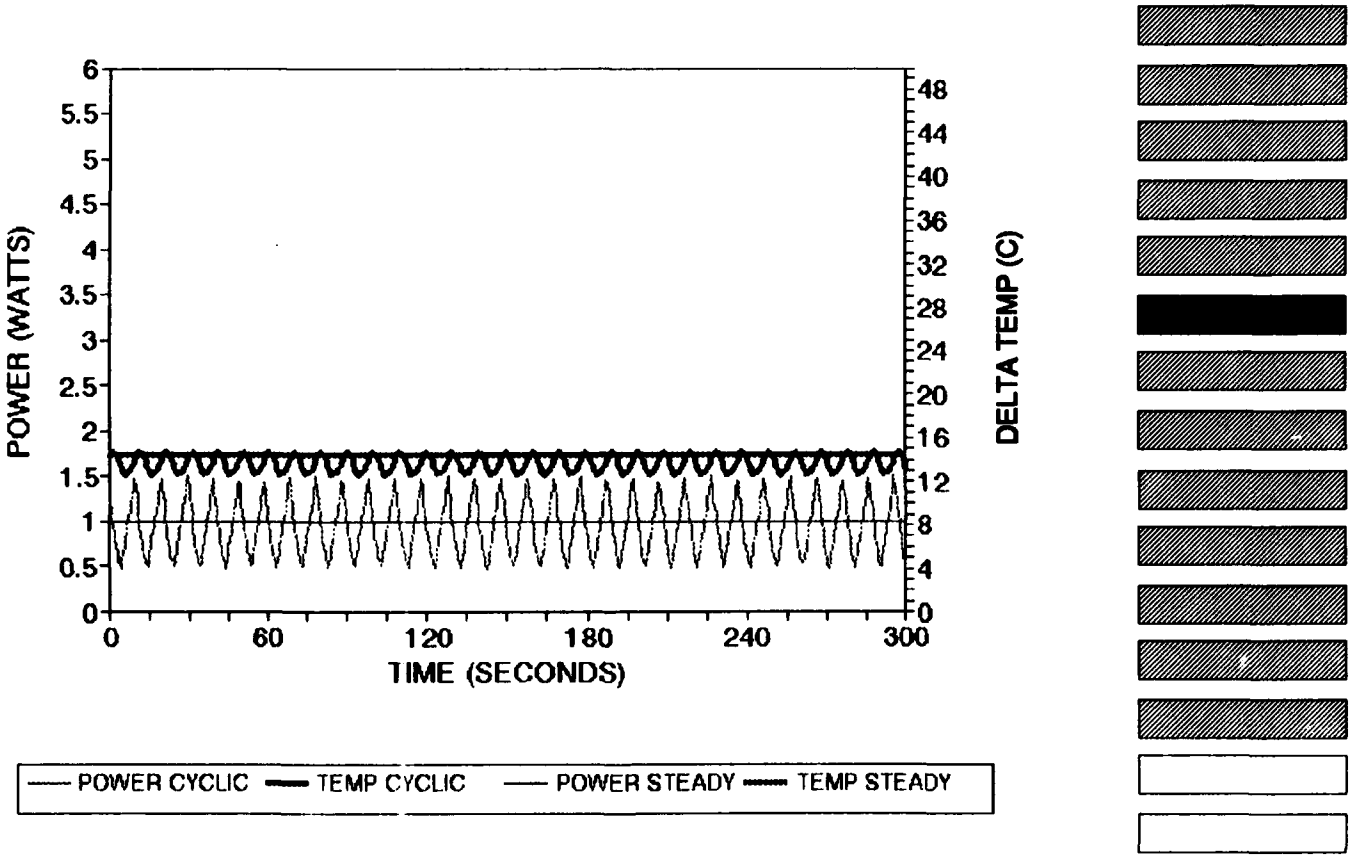

Figure EB. Time dependent transient power and delta temperature for triangular wave input, middle heater, heater configuration B21, ambient temperature 20.4°C.

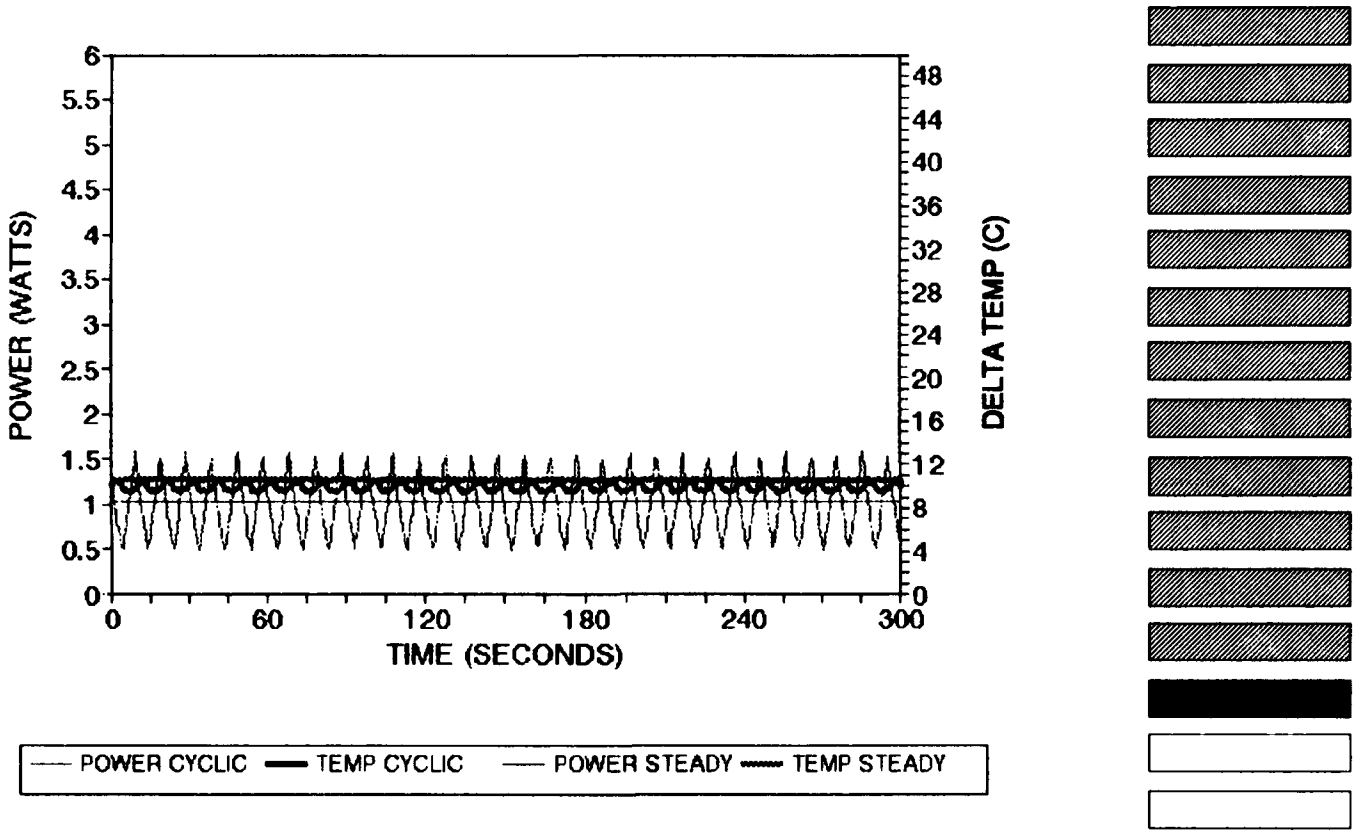

Figure EC. Time dependent transient power and delta temperature for triangular wave input, bottom heater, heater configuration B28, ambient temperature 20.4°C.

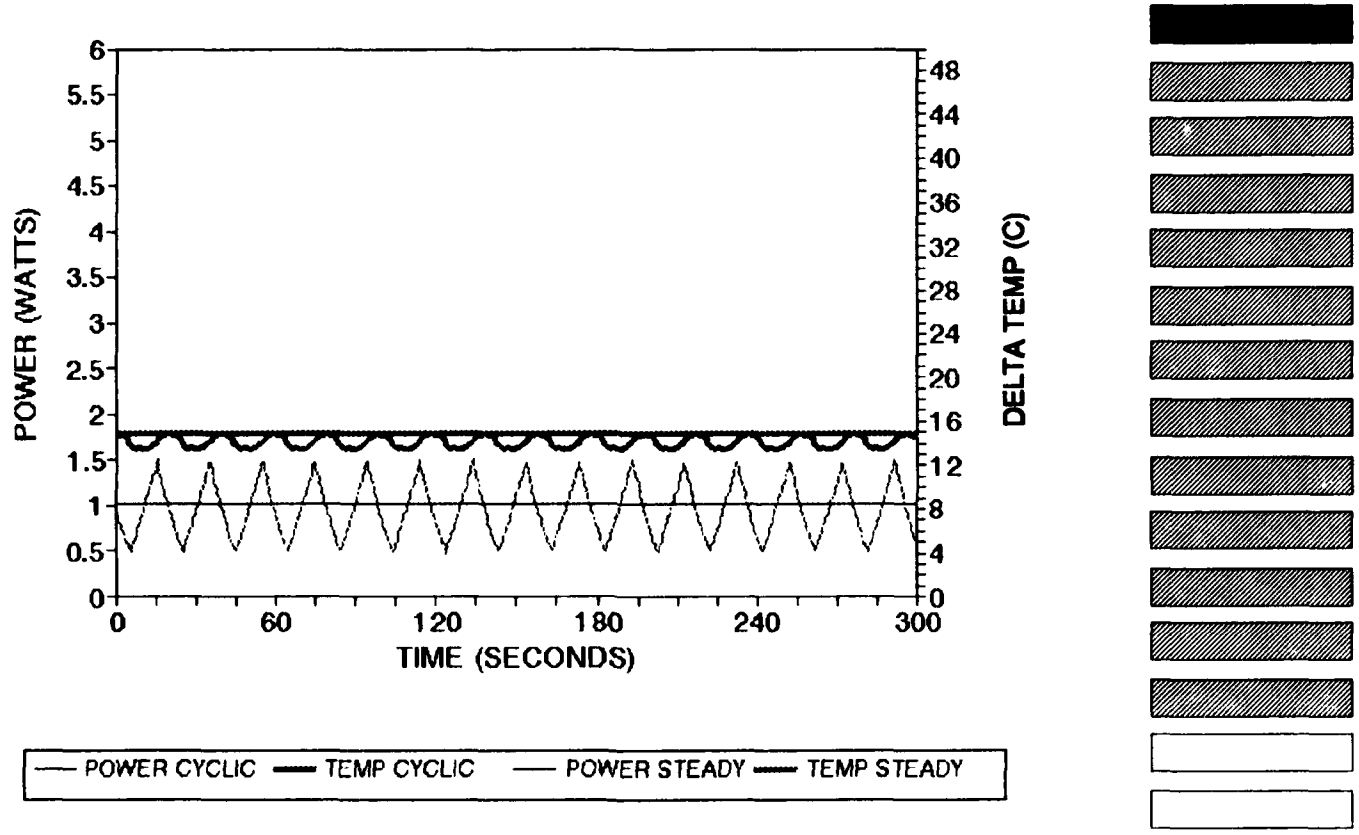

Figure ED. Time dependent transient power and delta temperature for triangular wave input, top heater, heater configuration B16, ambient temperature 20.4°C.

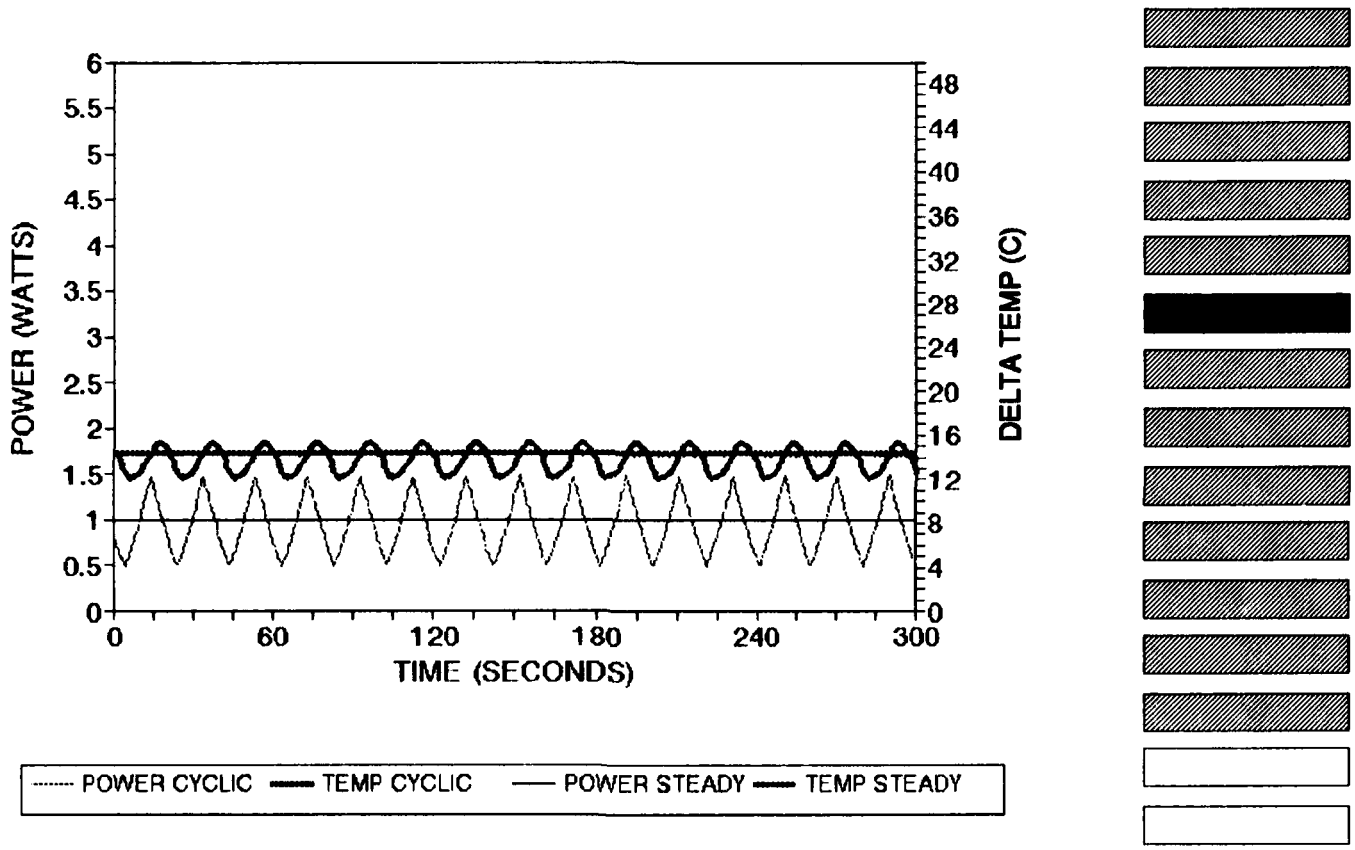

Figure EE. Time dependent transient power and delta temperature for triangular wave input, middle heater, heater configuration B21, ambient temperature 20.4°C.

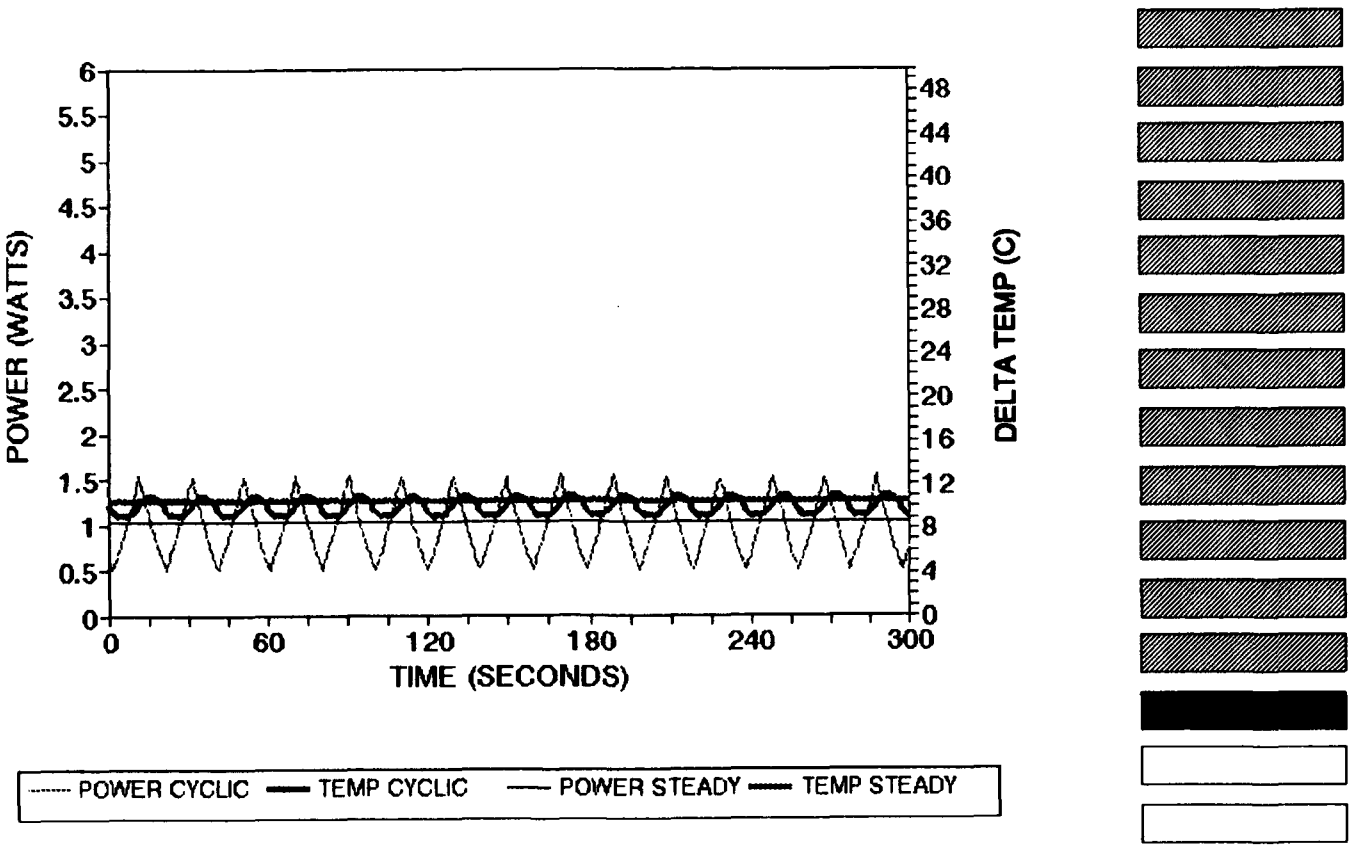

Figure EF. Time dependent transient power and delta temperature for triangular wave input, bottom heater, heater configuration B28, ambient temperature 20.4°C.

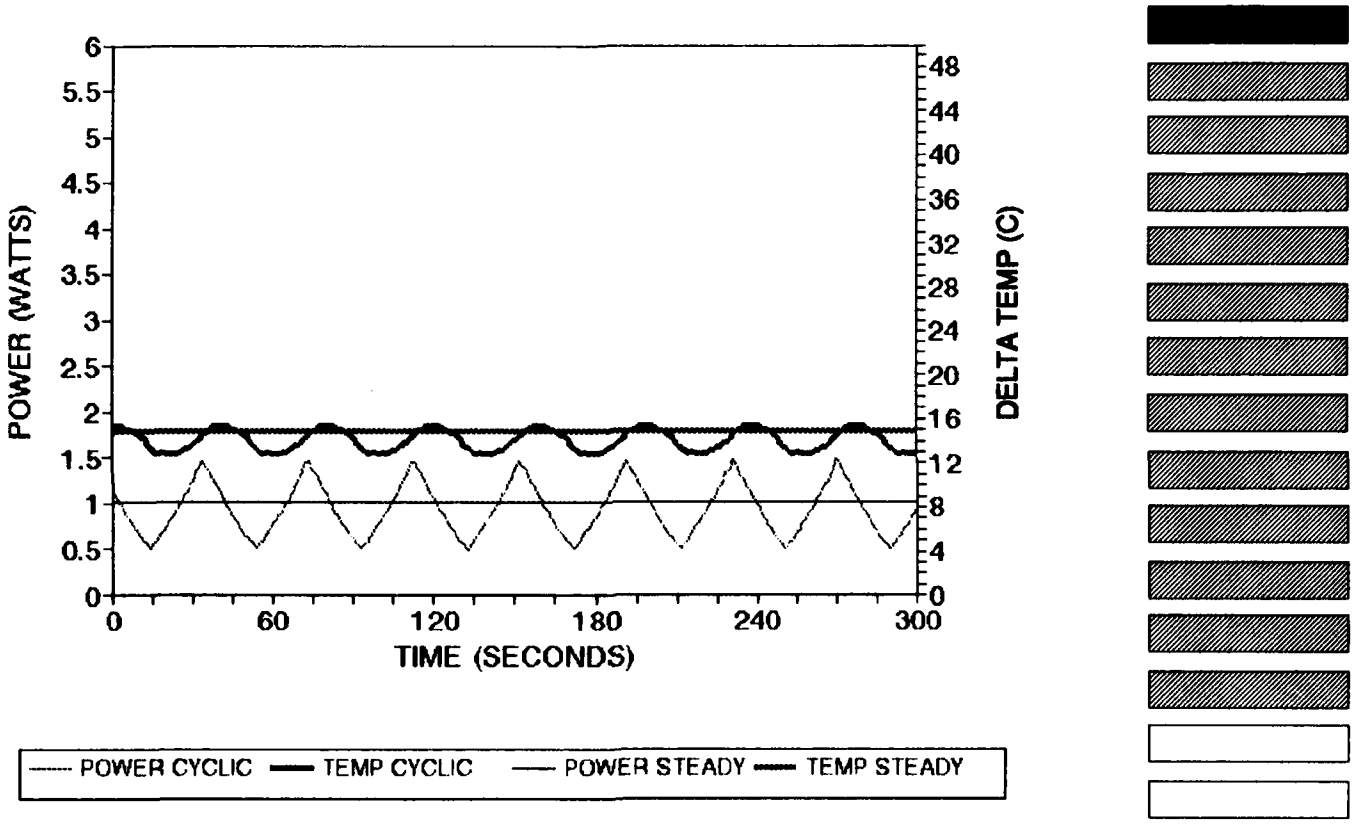

Figure EG. Time dependent transient power and delta temperature for triangular wave input, top heater, heater configuration B16, ambient temperature 20.4°C.

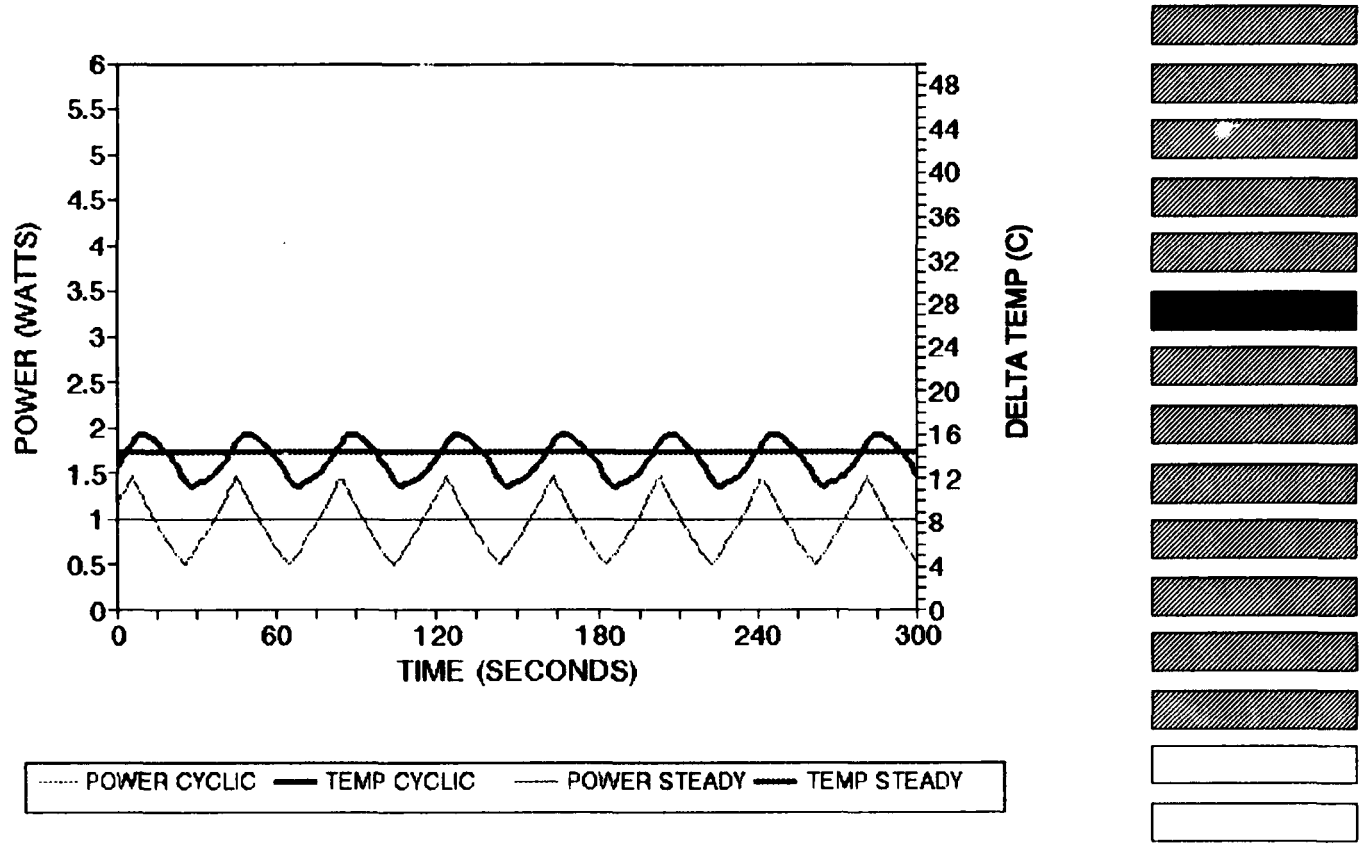

Figure EH. Time dependent transient power and delta temperature for triangular wave input, middle heater, heater configuration B21, ambient temperature 20.4°C.

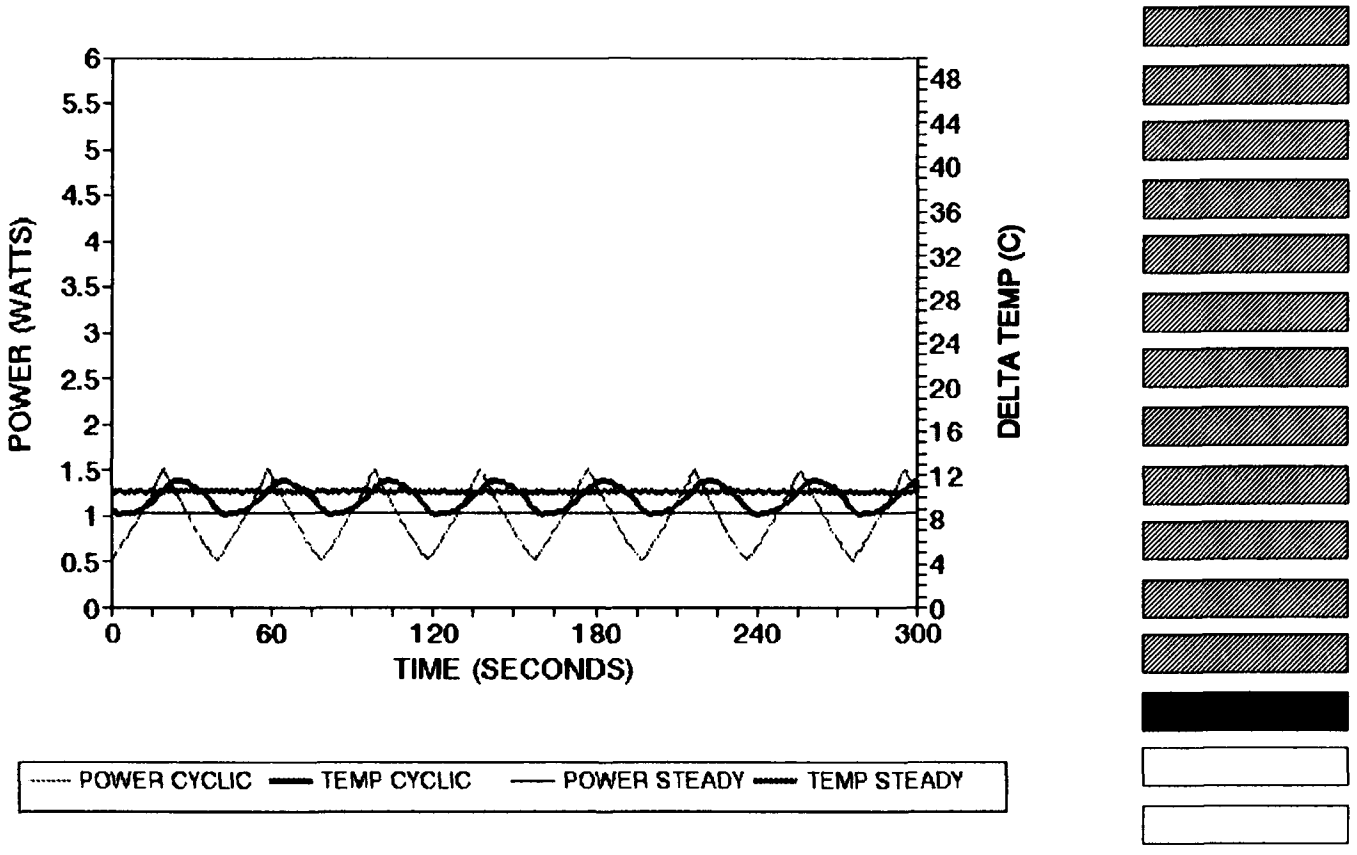

Figure EI. Time dependent transient power and delta temperature for triangular wave input, bottom heater, heater configuration B28, ambient temperature 20.4°C.

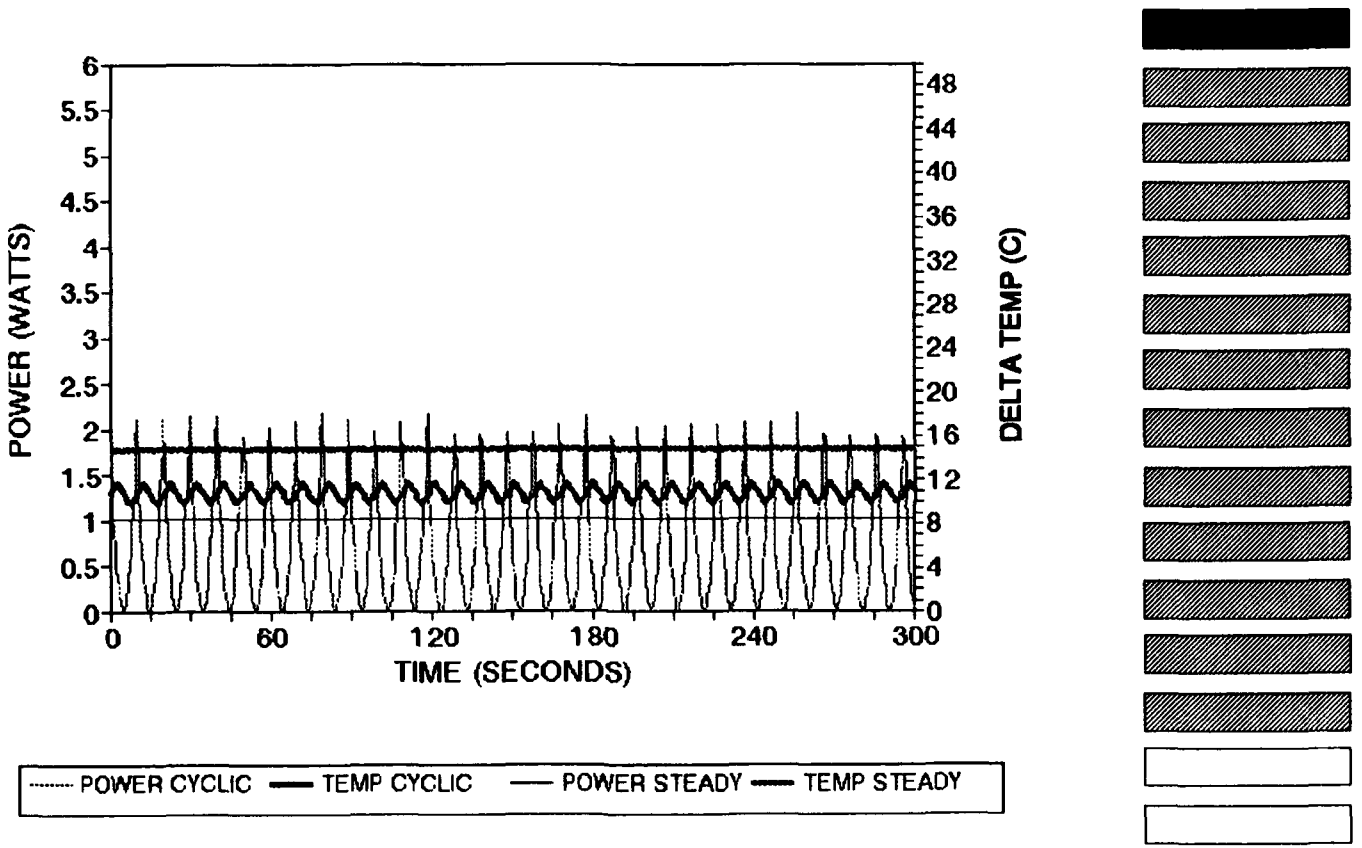

Figure FA. Time dependent transient power and delta temperature for triangular wave input, top heater, heater configuration B16, ambient temperature 20.3°C.

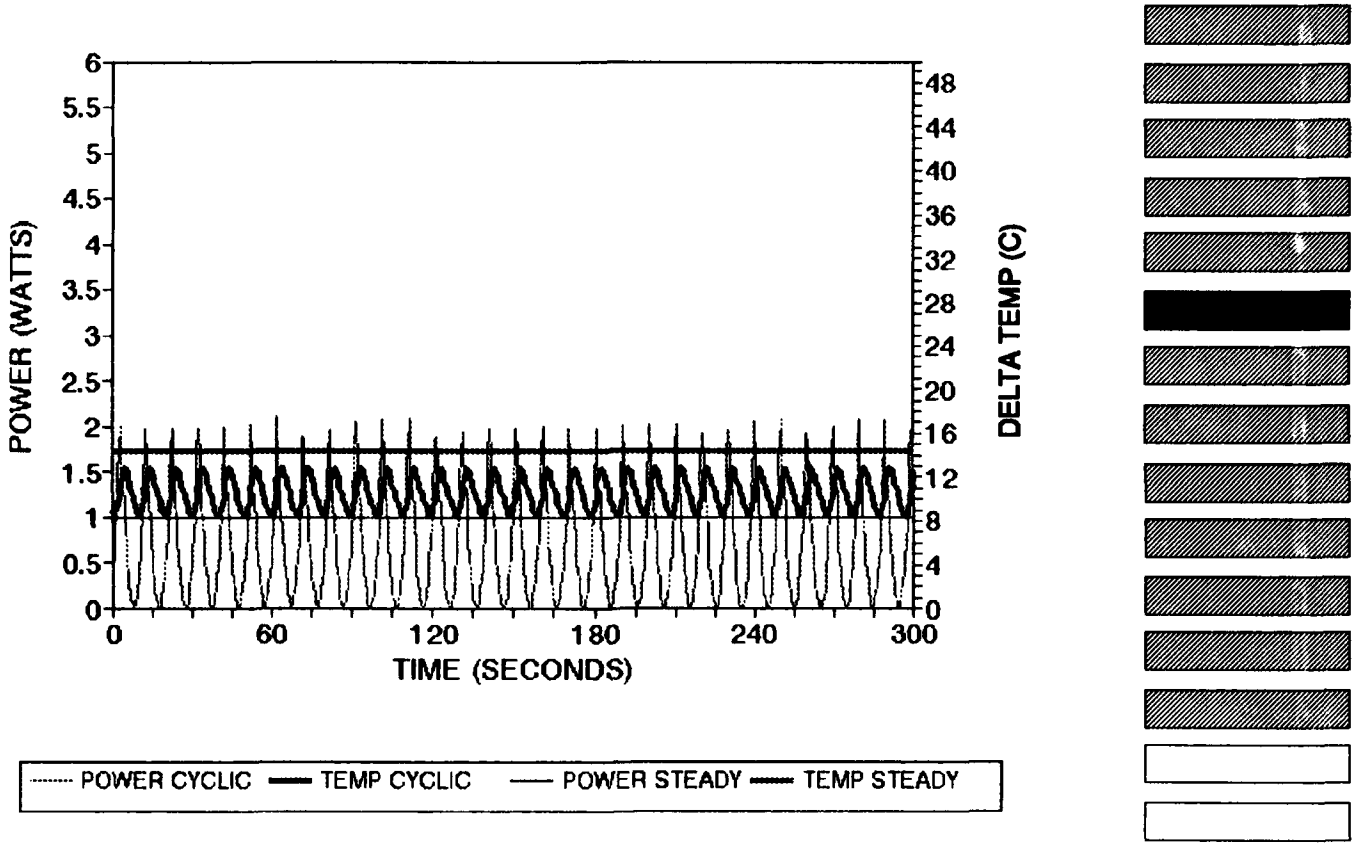

Figure FB. Time dependent transient power and delta temperature for triangular wave input, middle heater, heater configuration B21, ambient temperature 20.2°C.

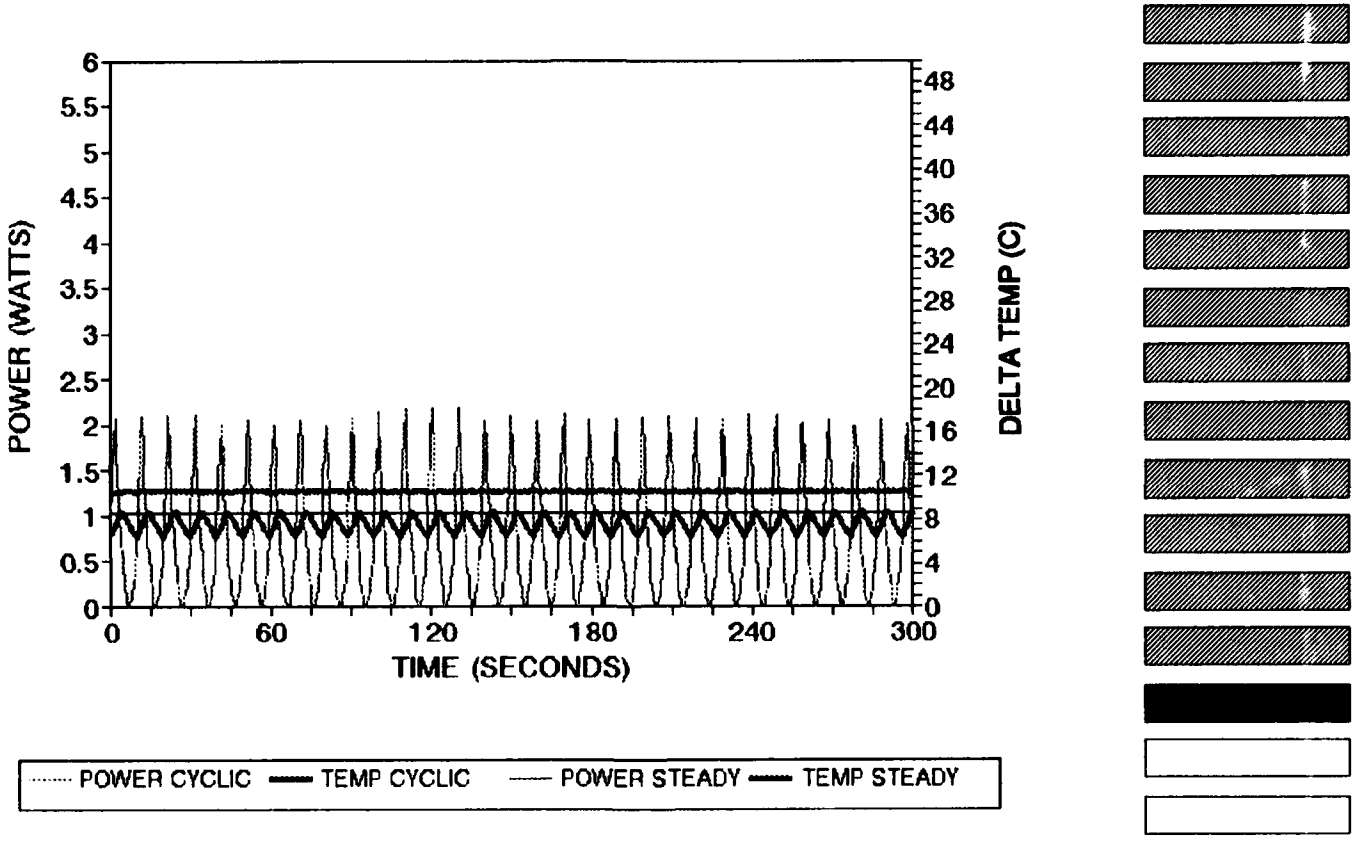

Figure FC. Time dependent transient power and delta temperature for triangular wave input, bottom heater, heater configuration B28, ambient temperature 20.3°C.

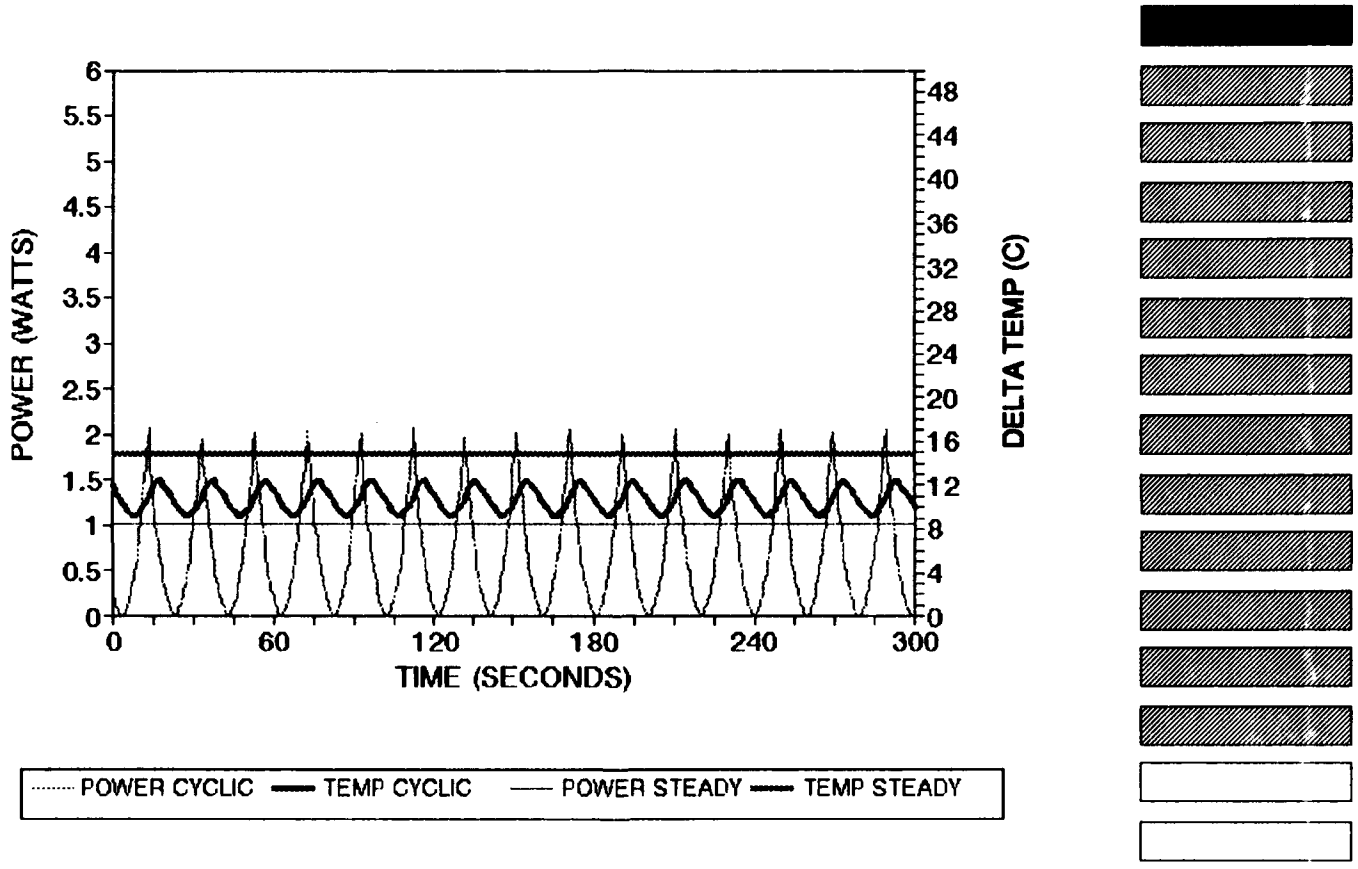

Figure FD. Time dependent transient power and delta temperature for triangular wave input, top heater, heater configuration B16, ambient temperature 20.4°C.

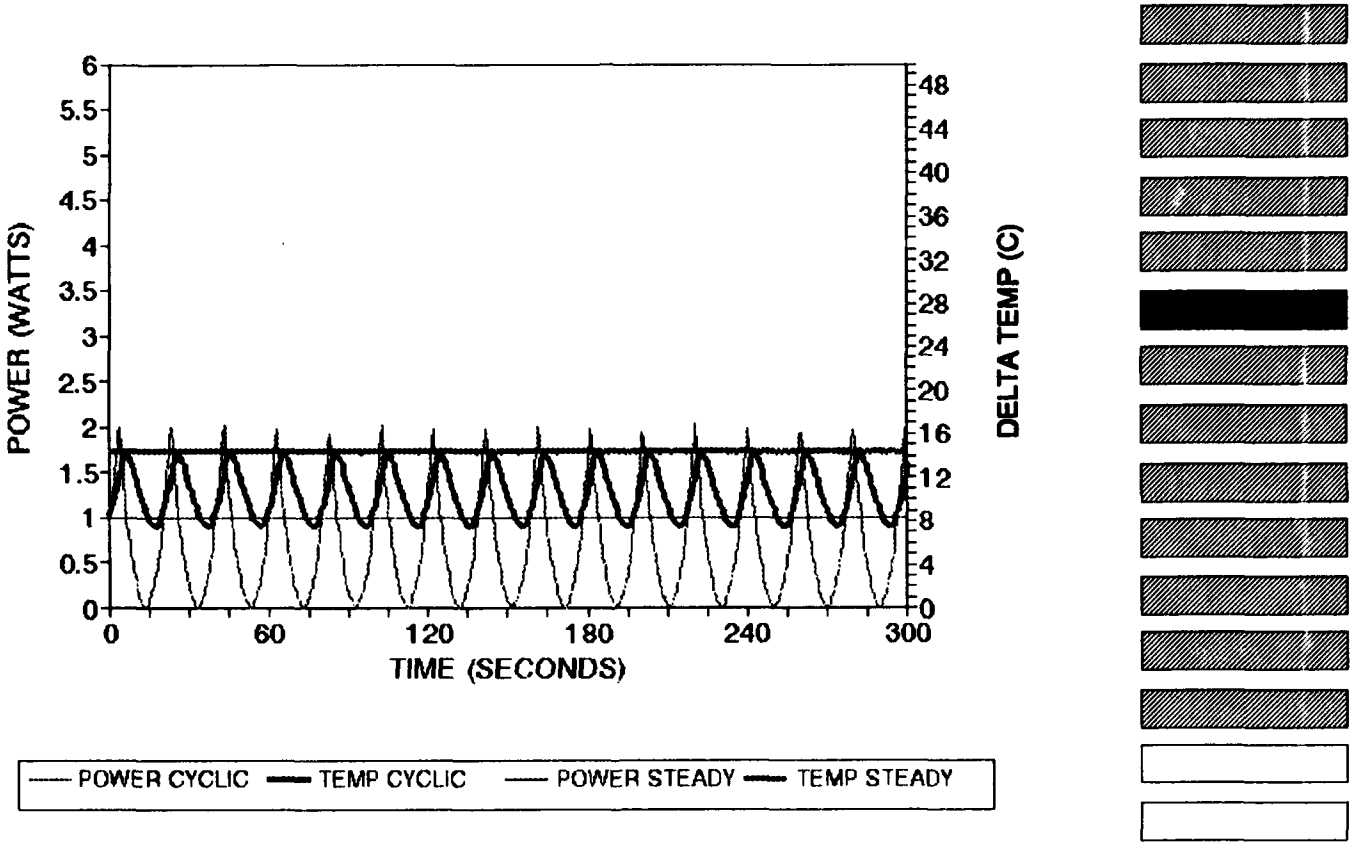

Figure FE. Time dependent transient power and delta temperature for triangular wave input, middle heater, heater configuration B21, ambient temperature 20.3°C.

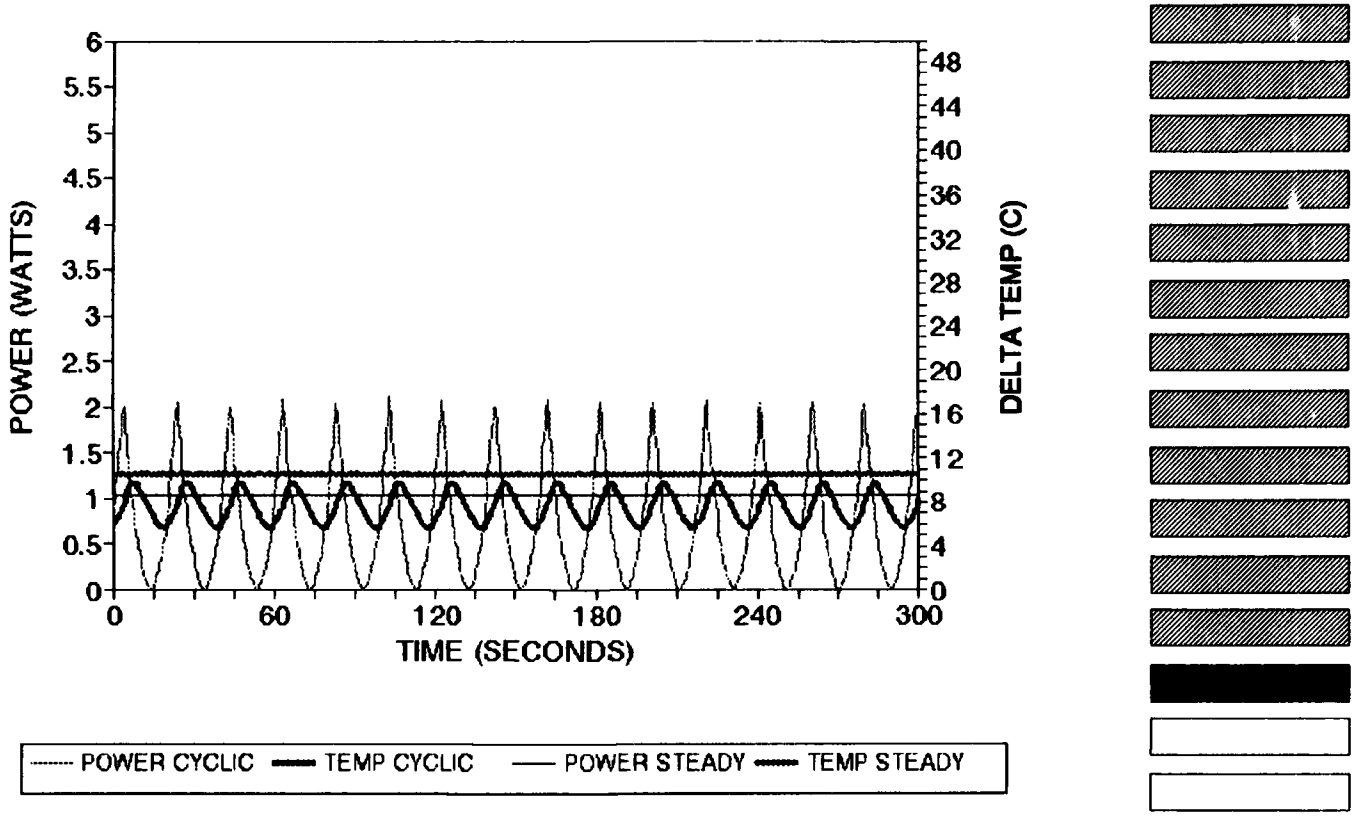

Figure FF. Time dependent transient power and delta temperature for triangular wave input, bottom heater, heater configuration B28, ambient temperature 20.3°C.

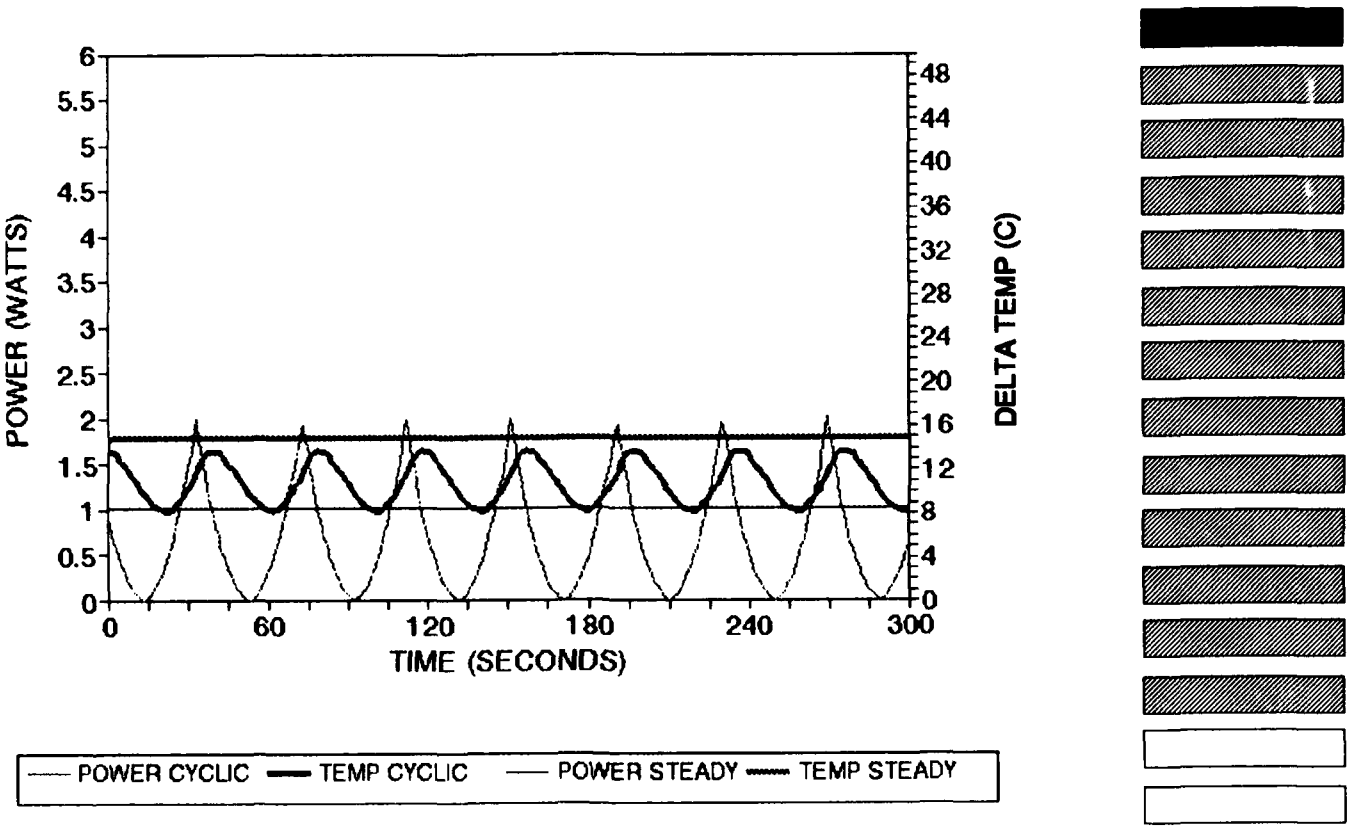

Figure FG. Time dependent transient power and delta temperature for triangular wave input, top heater, heater configuration B16, ambient temperature 20.3°C.

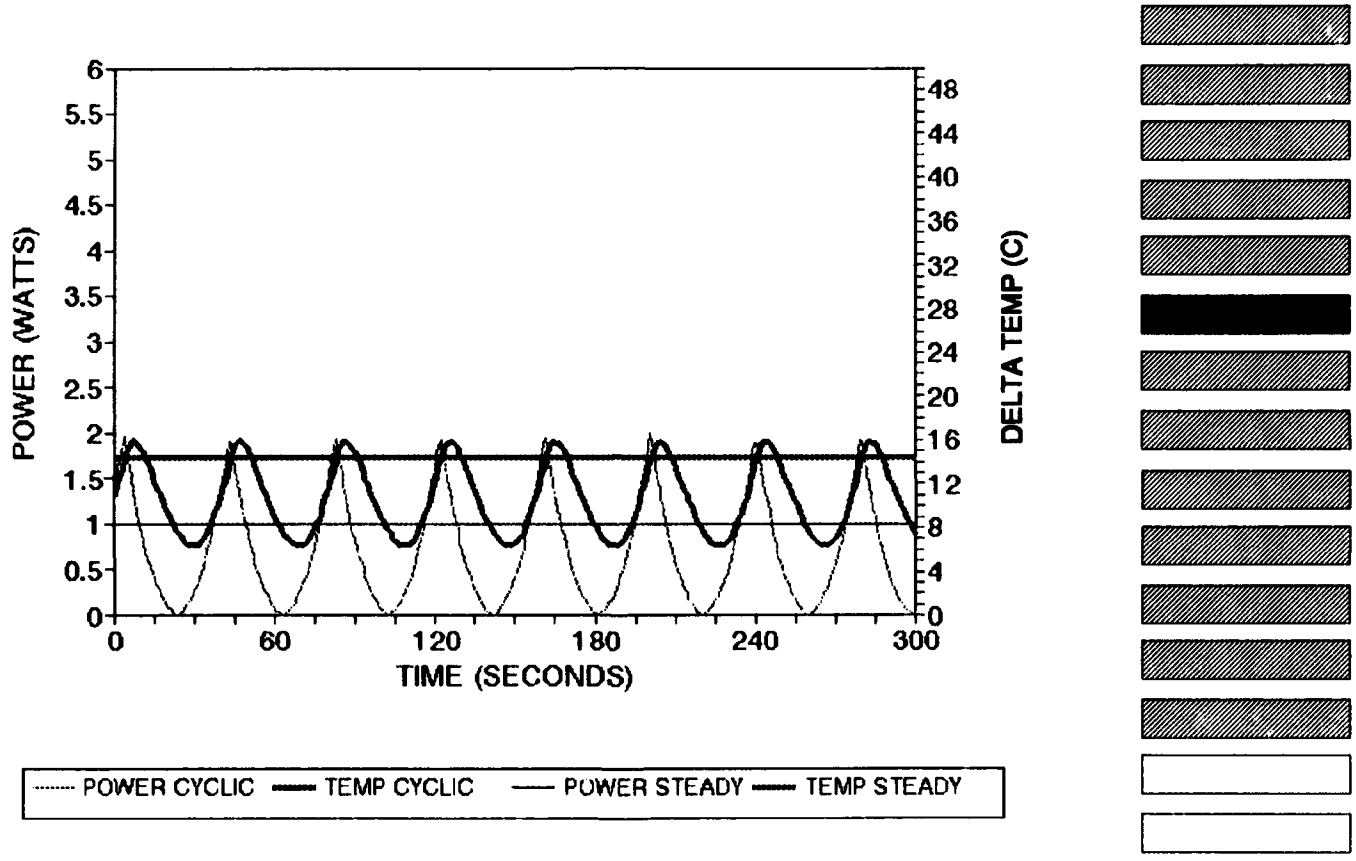

Figure FH. Time dependent transient power and delta temperature for triangular wave input, middle heater, heater configuration B21, ambient temperature 20.2°C.

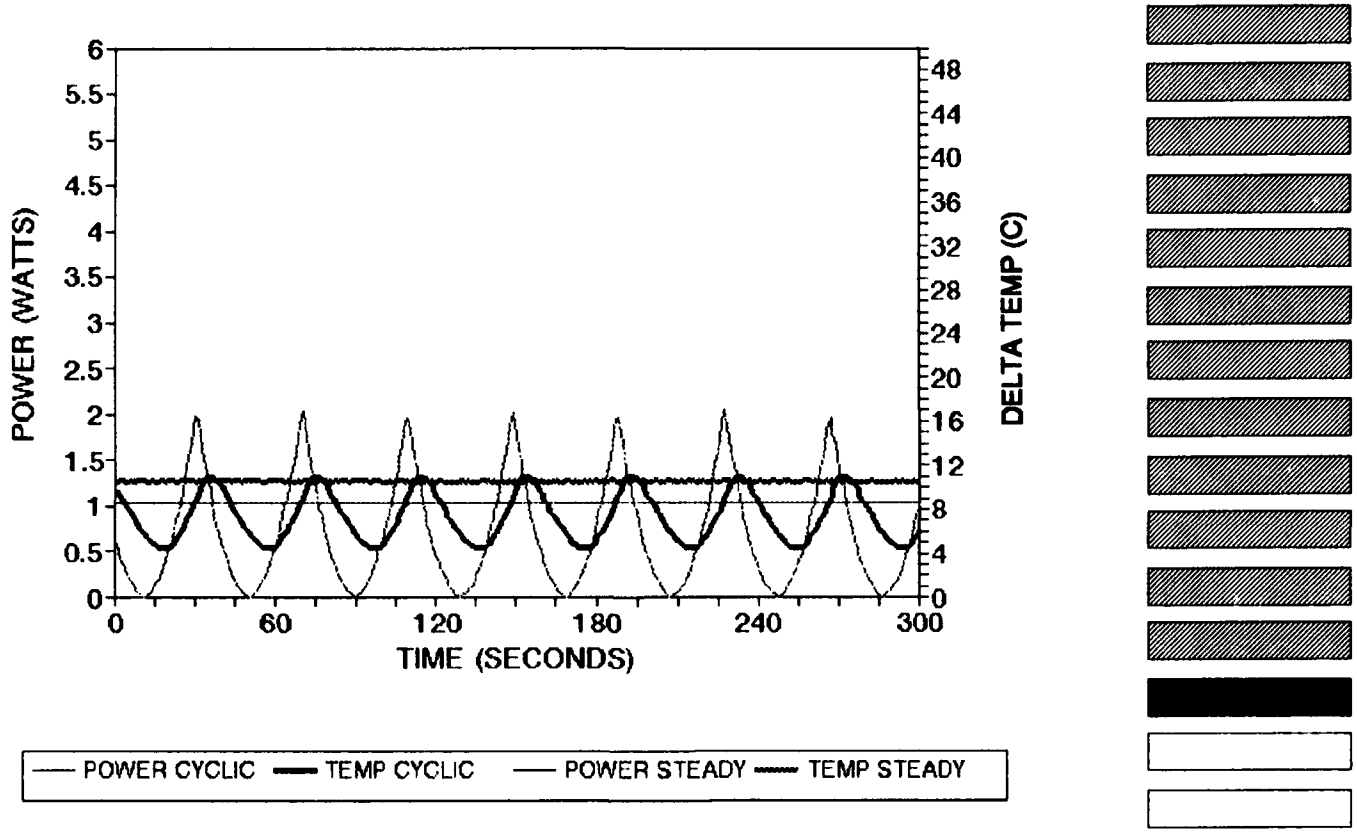

Figure FI. Time dependent transient power and delta temperature for triangular wave input, bottom heater, heater configuration B28, ambient temperature 20.4°C.

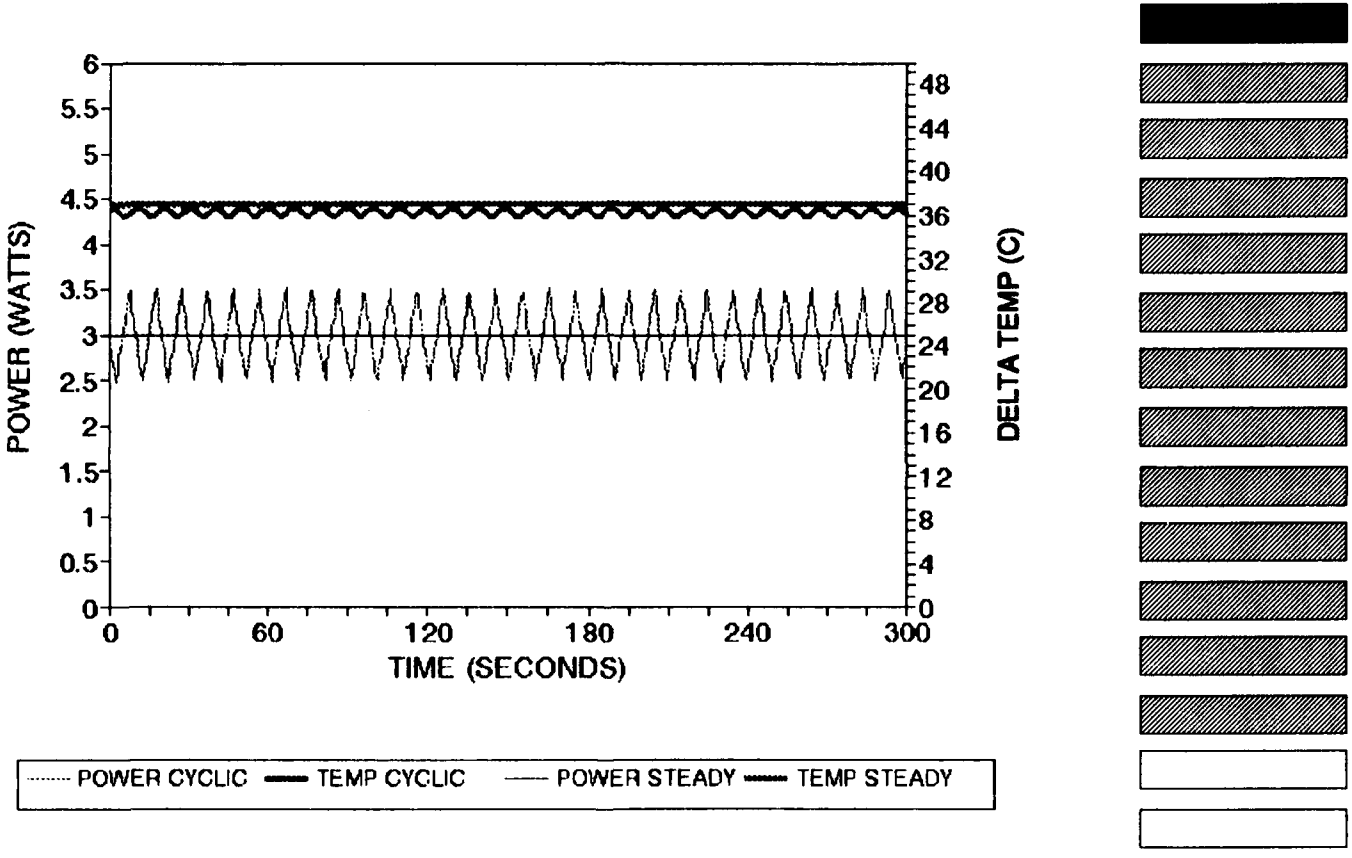

Figure GA. Time dependent transient power and delta temperature for triangular wave input, top heater, heater configuration B16, ambient temperature 19.8°C.

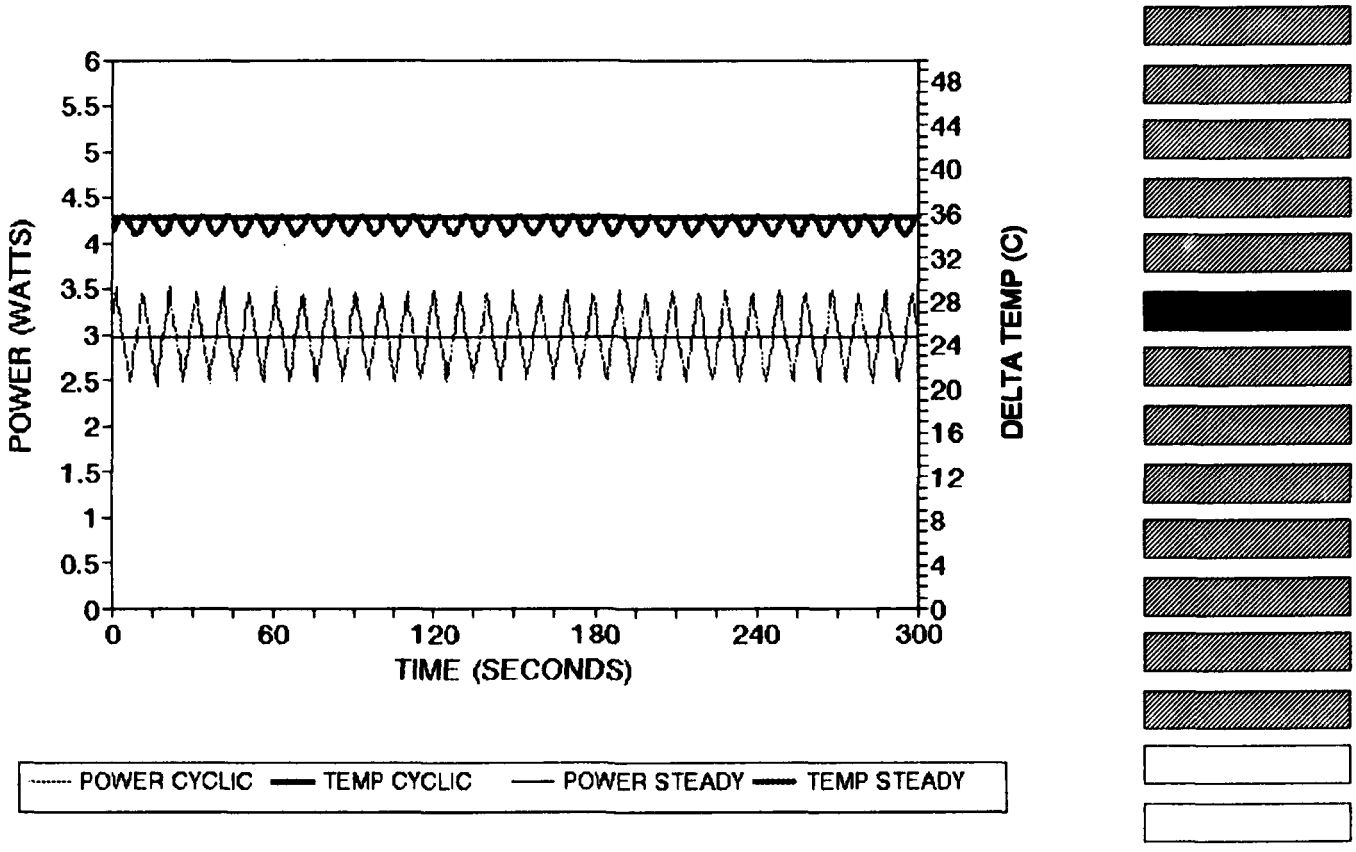

Figure GB. Time dependent transient power and delta temperature for triangular wave input, middle heater, heater configuration B21, ambient temperature 19.8°C.

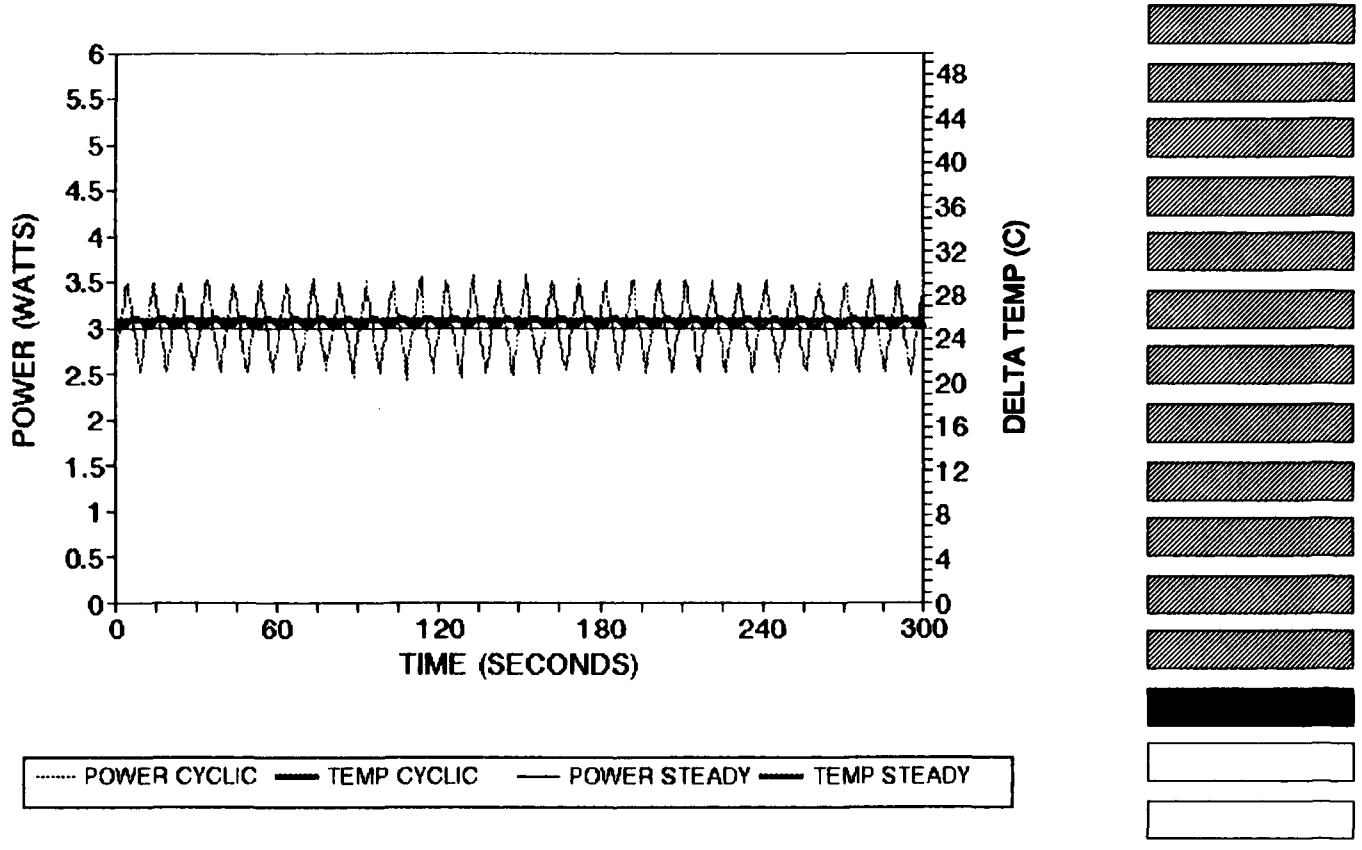

Figure GC. Time dependent transient power and delta temperature for triangular wave input, bottom heater, heater configuration B28, ambient temperature 19.8°C.

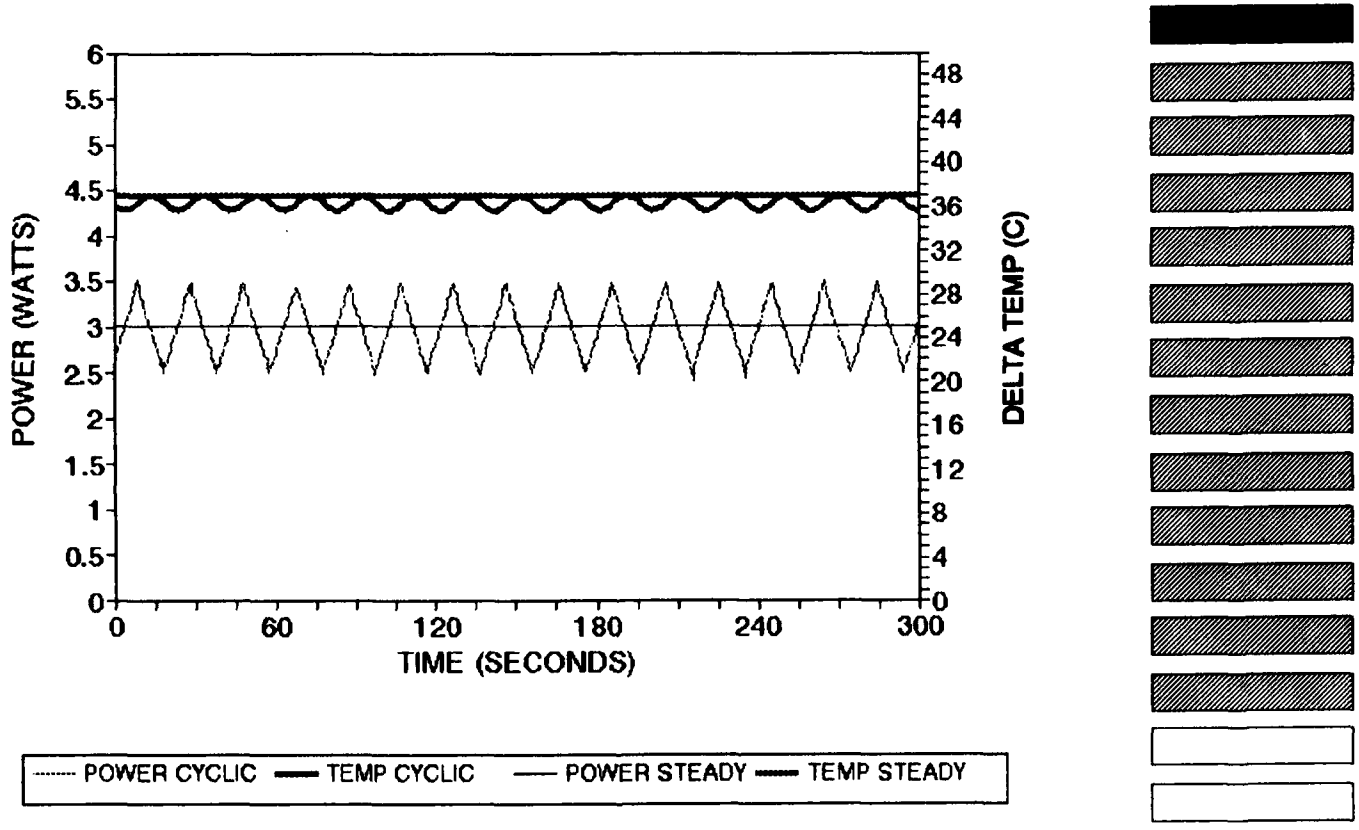

Figure GD. Time dependent transient power and delta temperature for triangular wave input, top heater, heater configuration B16, ambient temperature 19.8°C.

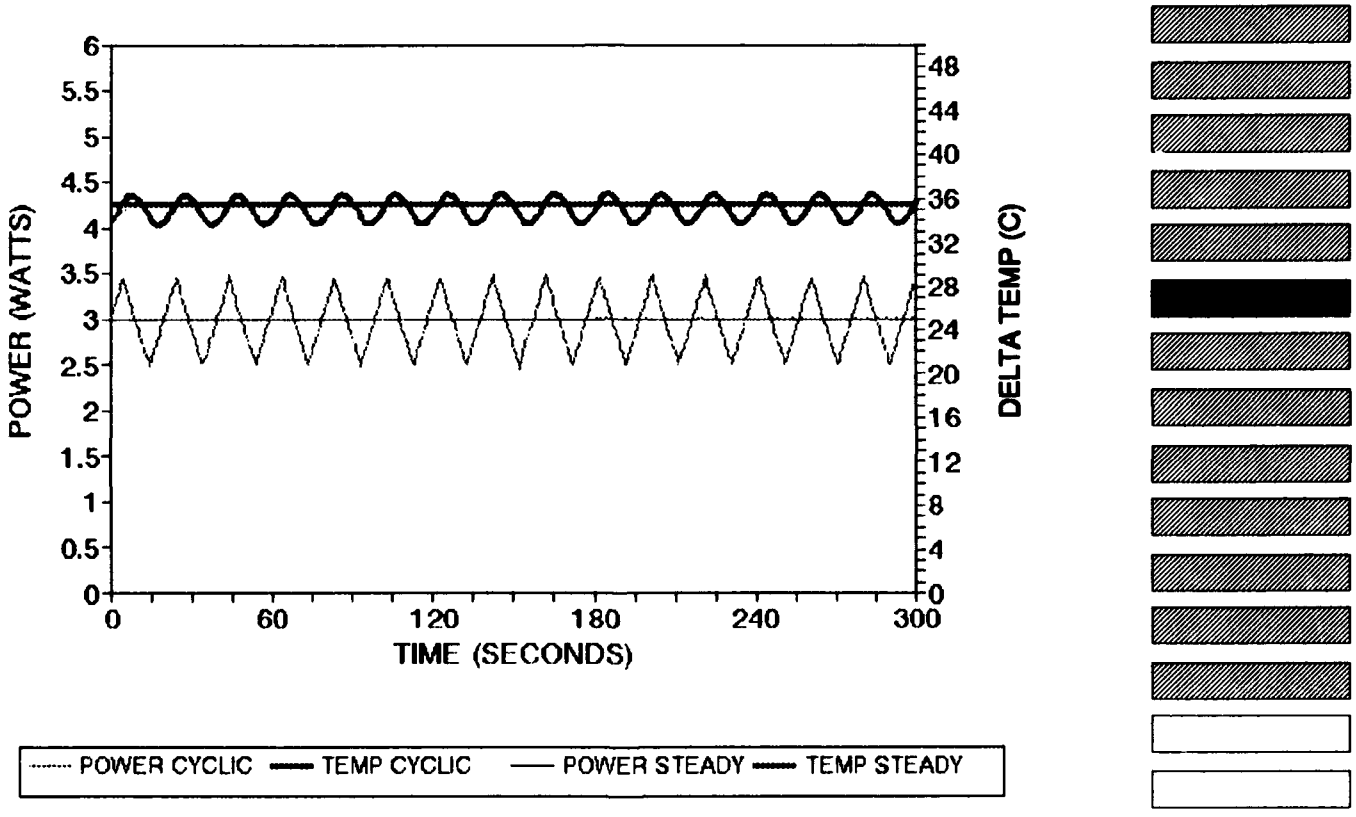

Figure GE. Time dependent transient power and delta temperature for triangular wave input, middle heater, heater configuration B21, ambient temperature 19.8°C.

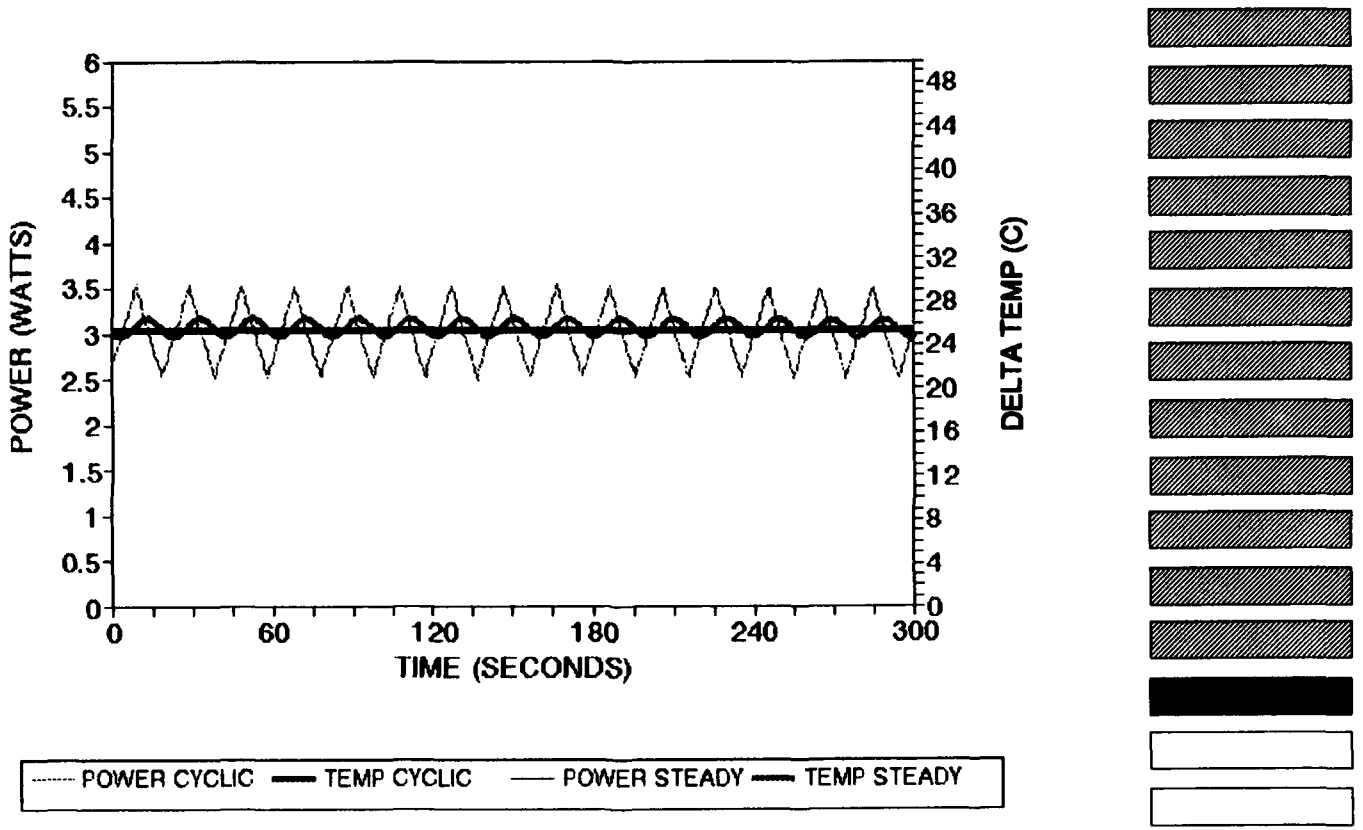

Figure GF. Time dependent transient power and delta temperature for triangular wave input, bottom heater, heater configuration B28, ambient temperature 19.8°C.

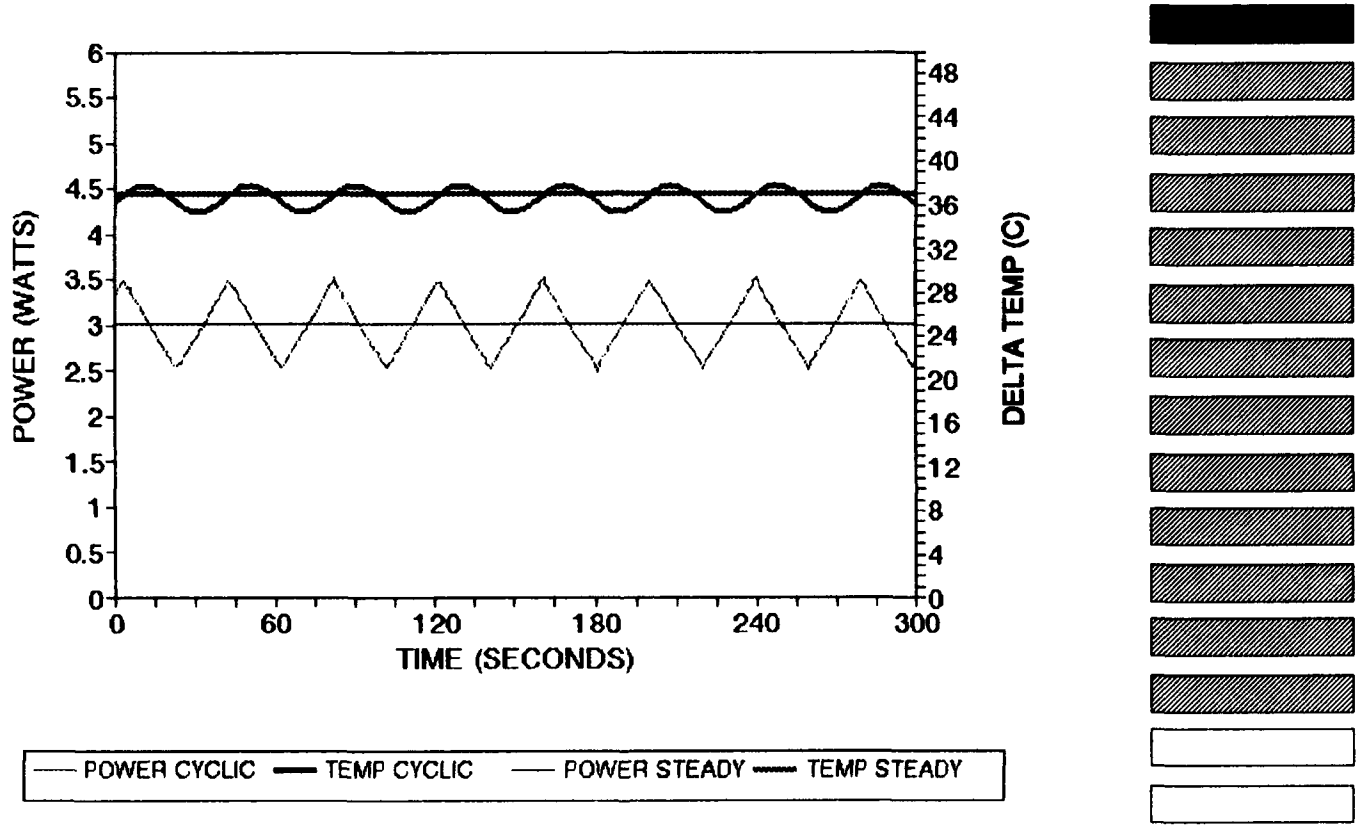

Figure GG. Time dependent transient power and delta temperature for triangular wave input, top heater, heater configuration B16, ambient temperature 19.8°C.

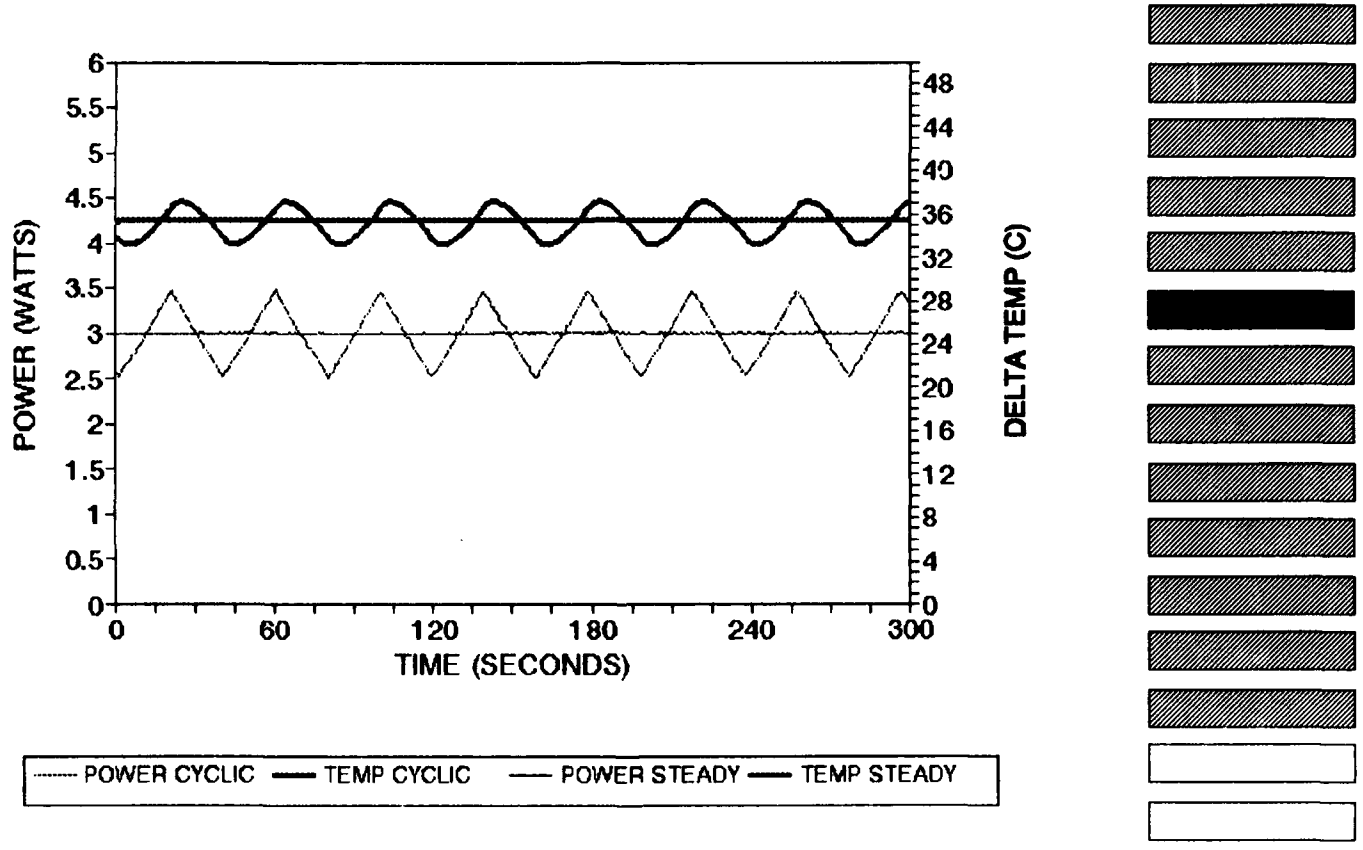

Figure GH. Time dependent transient power and delta temperature for triangular wave input, middle heater, heater configuration B21, ambient temperature 19.8°C.

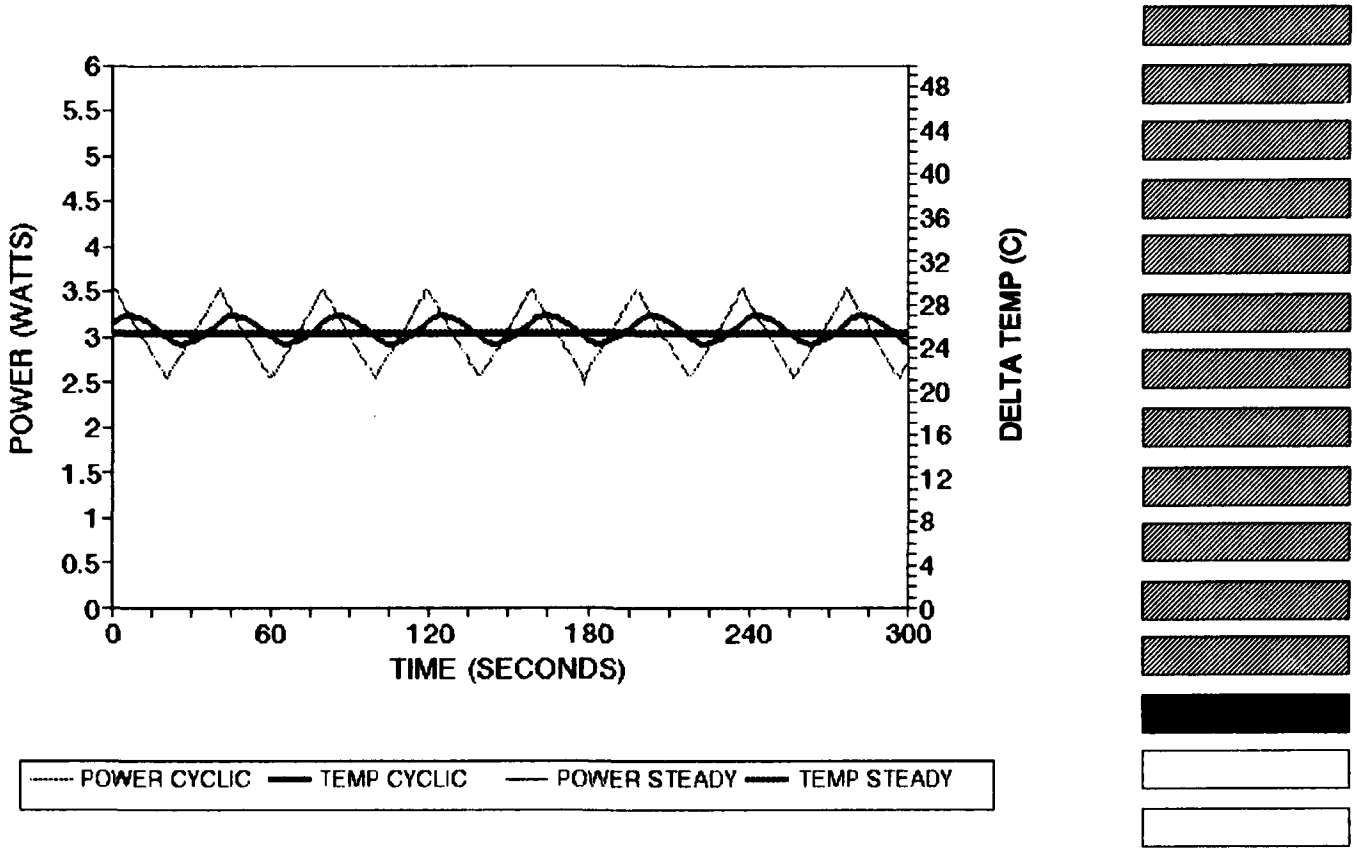

Figure GI. Time dependent transient power and delta temperature for triangular wave input, bottom heater, heater configuration B28, ambient temperature 19.8°C.

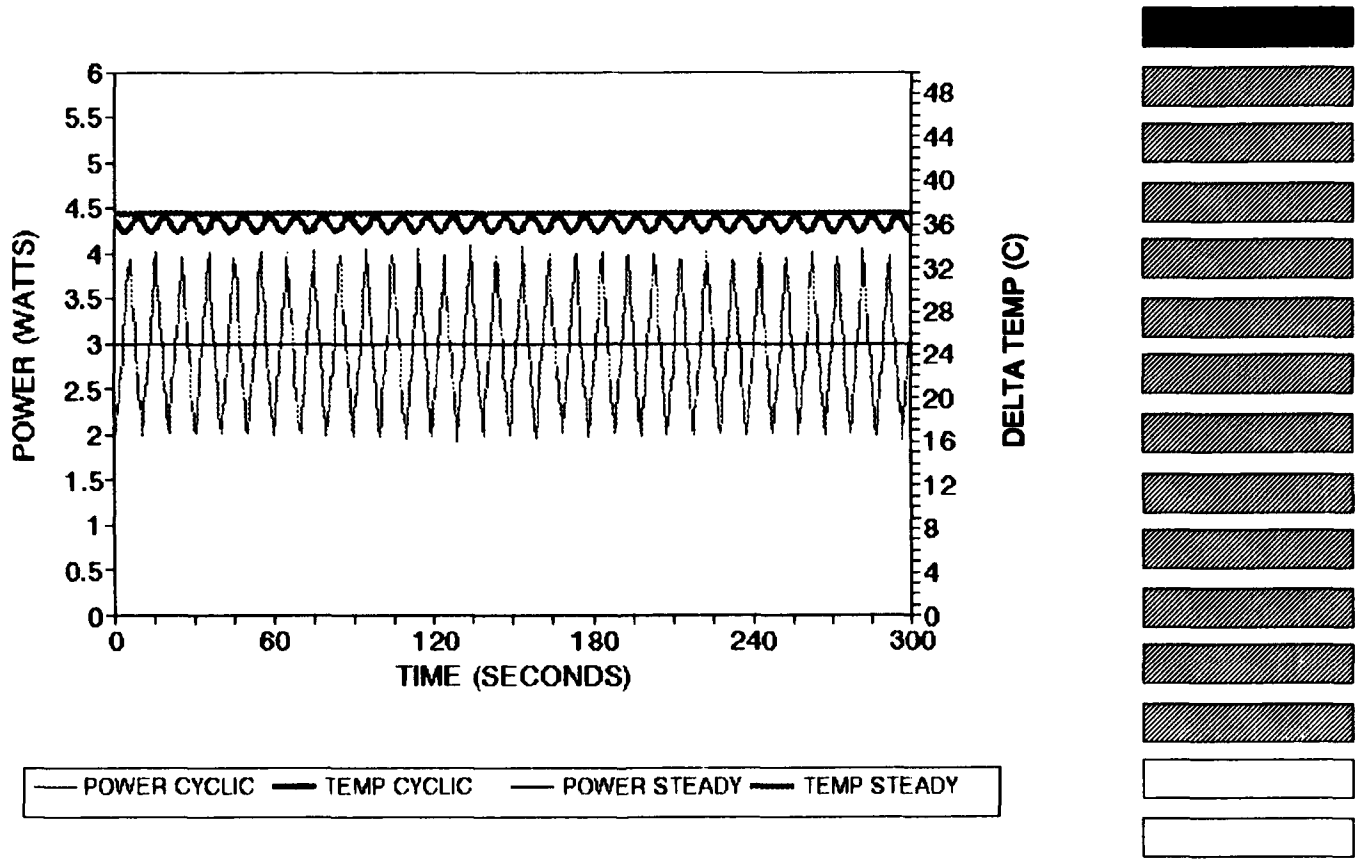

Figure HA. Time dependent transient power and delta temperature for triangular wave input, top heater, heater configuration B16, ambient temperature 19.8°C.

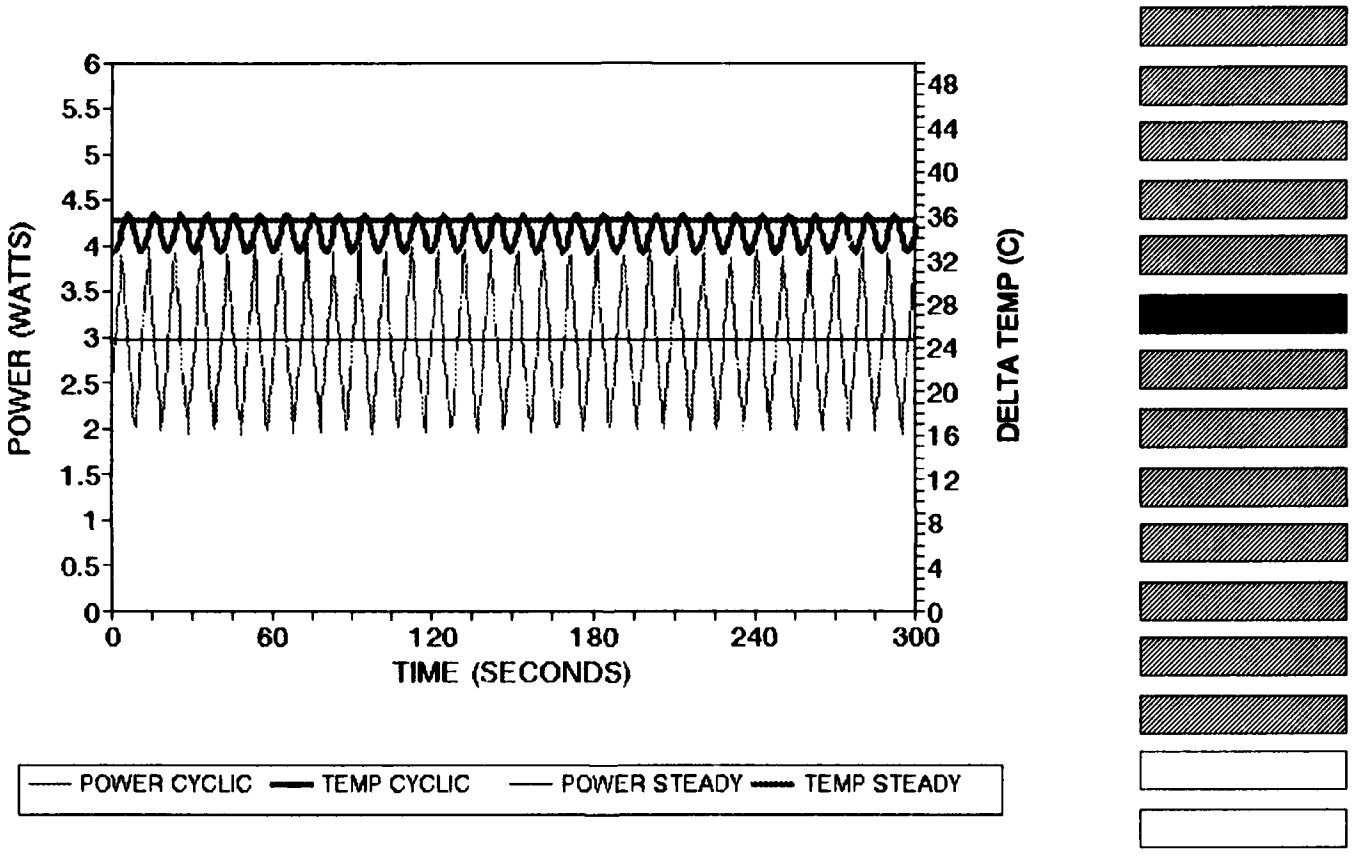

Figure HB. Time dependent transient power and delta temperature for triangular wave input, middle, heater, heater configuration B21, ambient temperature 19.8°C.

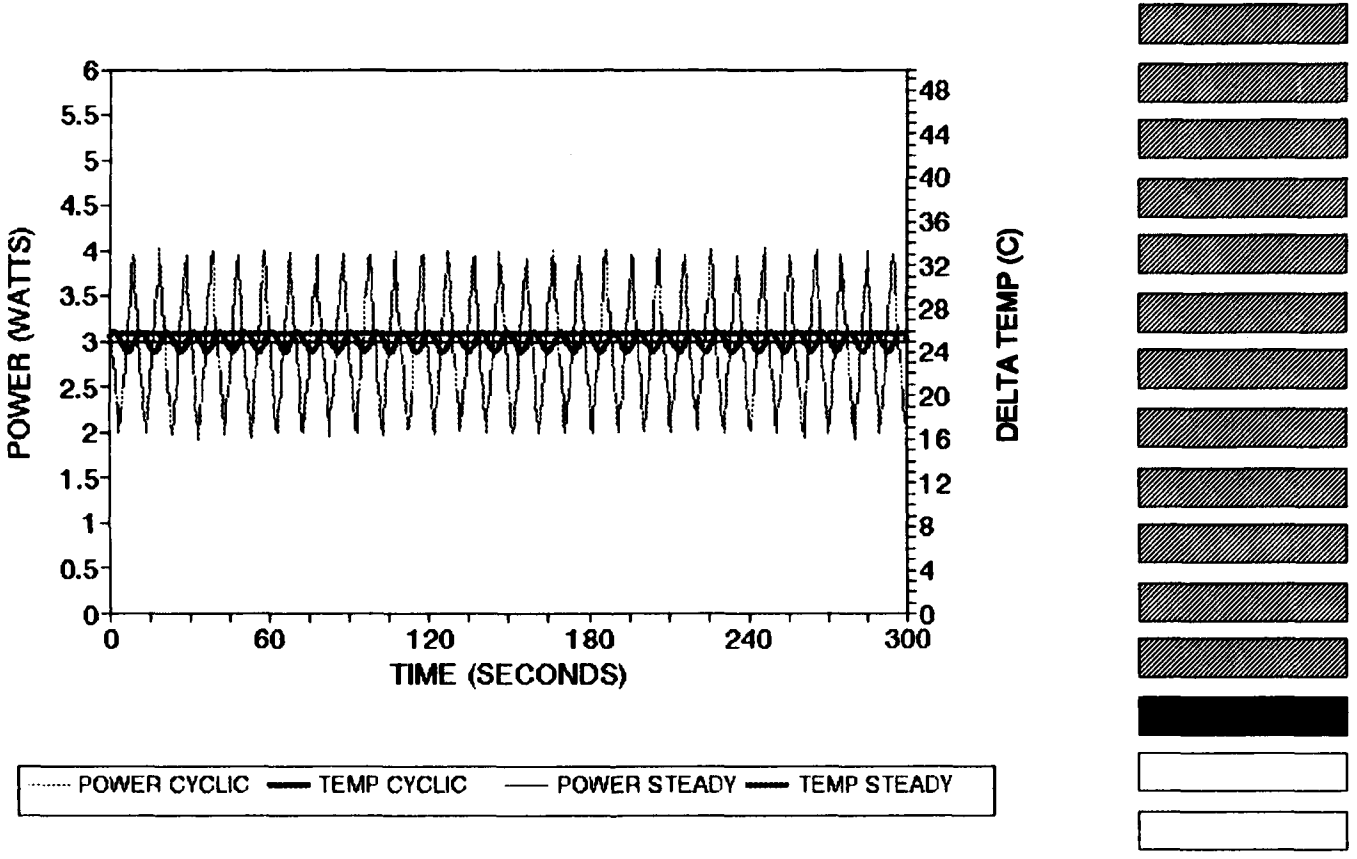

Figure HC. Time dependent transient power and delta temperature for triangular wave input, bottom heater, heater configuration B28, ambient temperature 19.8°C.

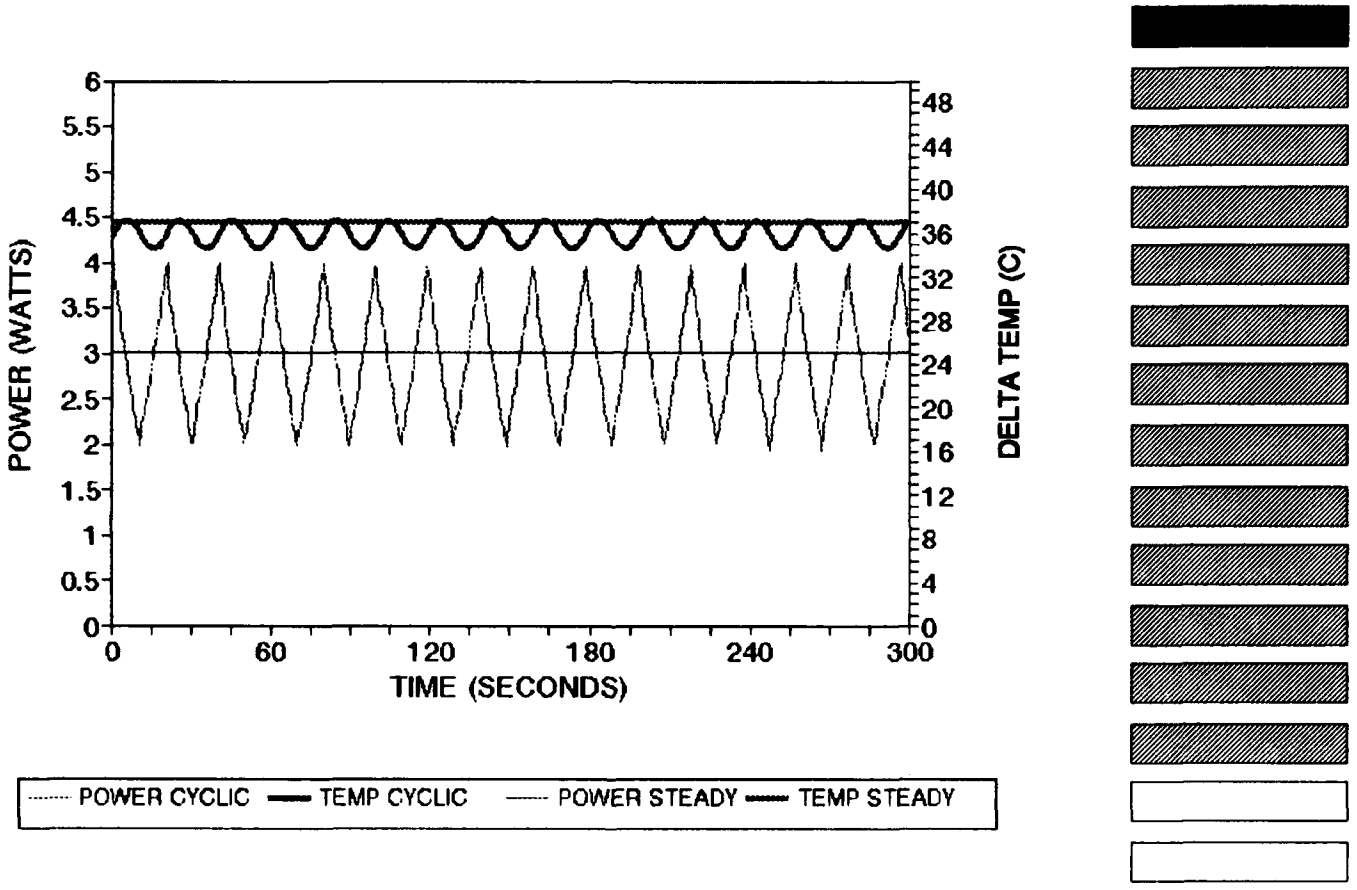

Figure HD. Time dependent transient power and delta temperature for triangular wave input, top heater, heater configuration B16, ambient temperature 19.8°C.

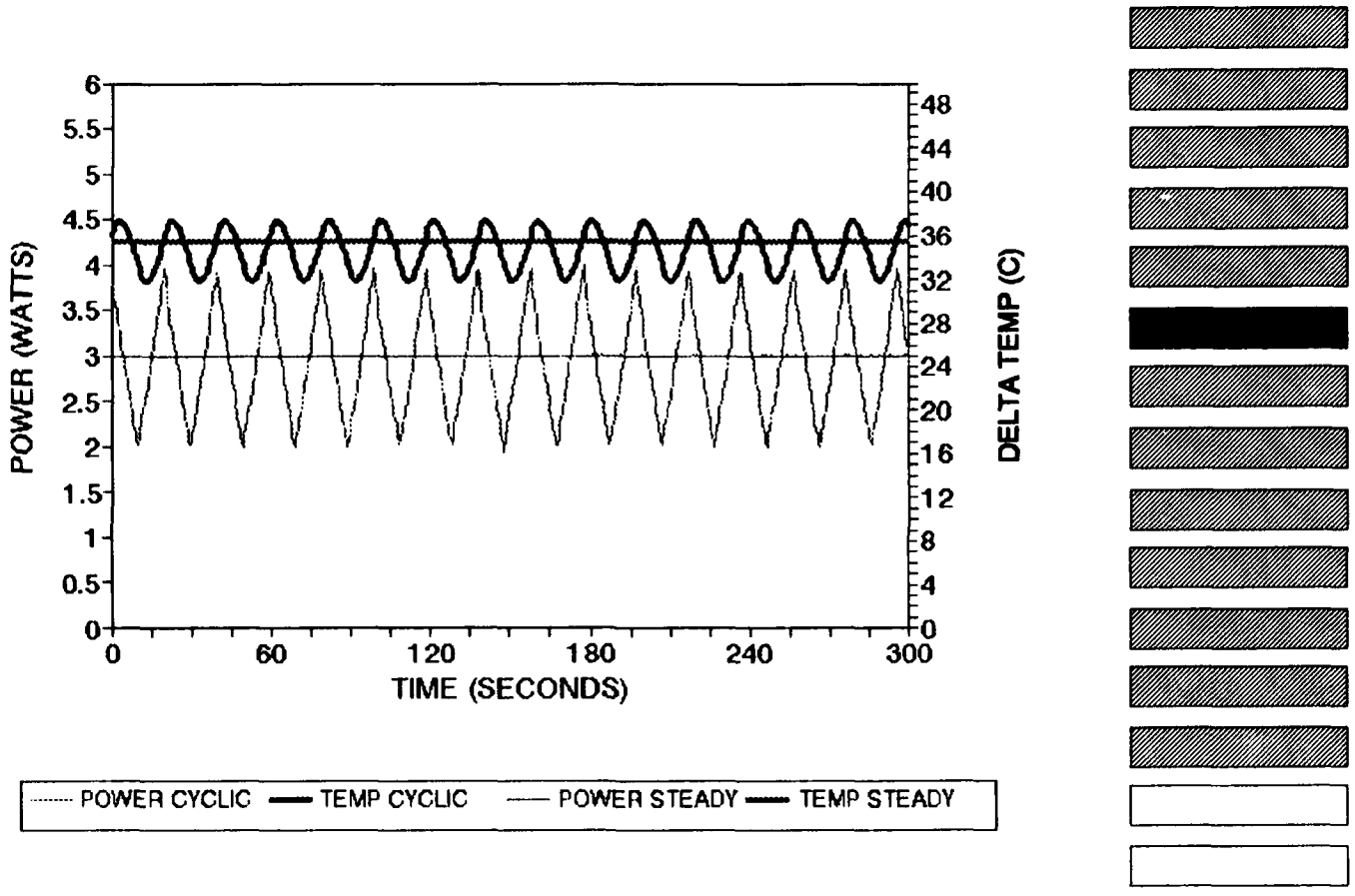

Figure HE. Time dependent transient power and delta temperature for triangular wave input, middle heater, heater configuration B21, ambient temperature 19.9°C.

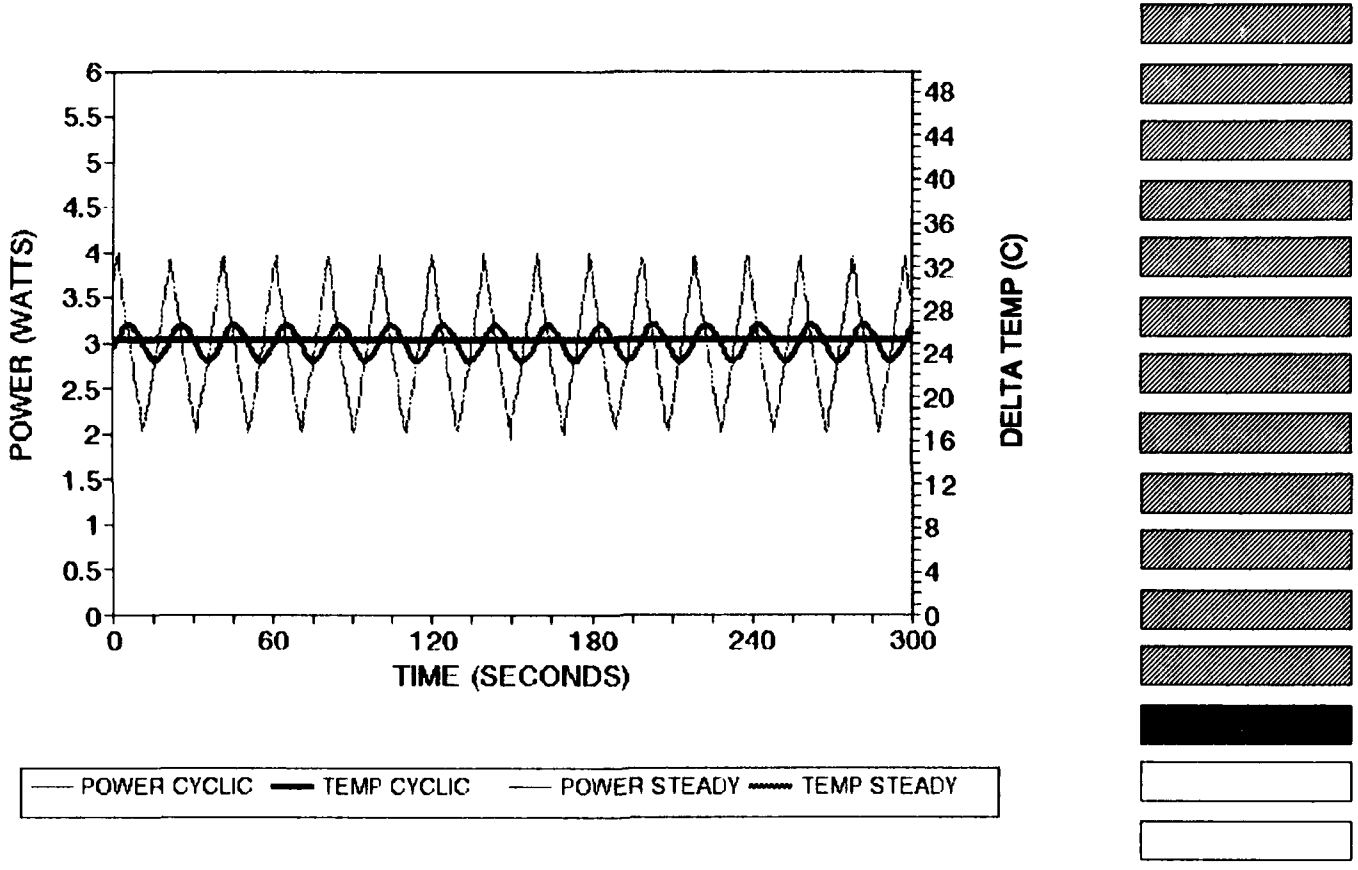

Figure HF. Time dependent transient power and delta temperature for triangular wave input, bottom heater, heater configuration B28, ambient temperature 19.9°C.

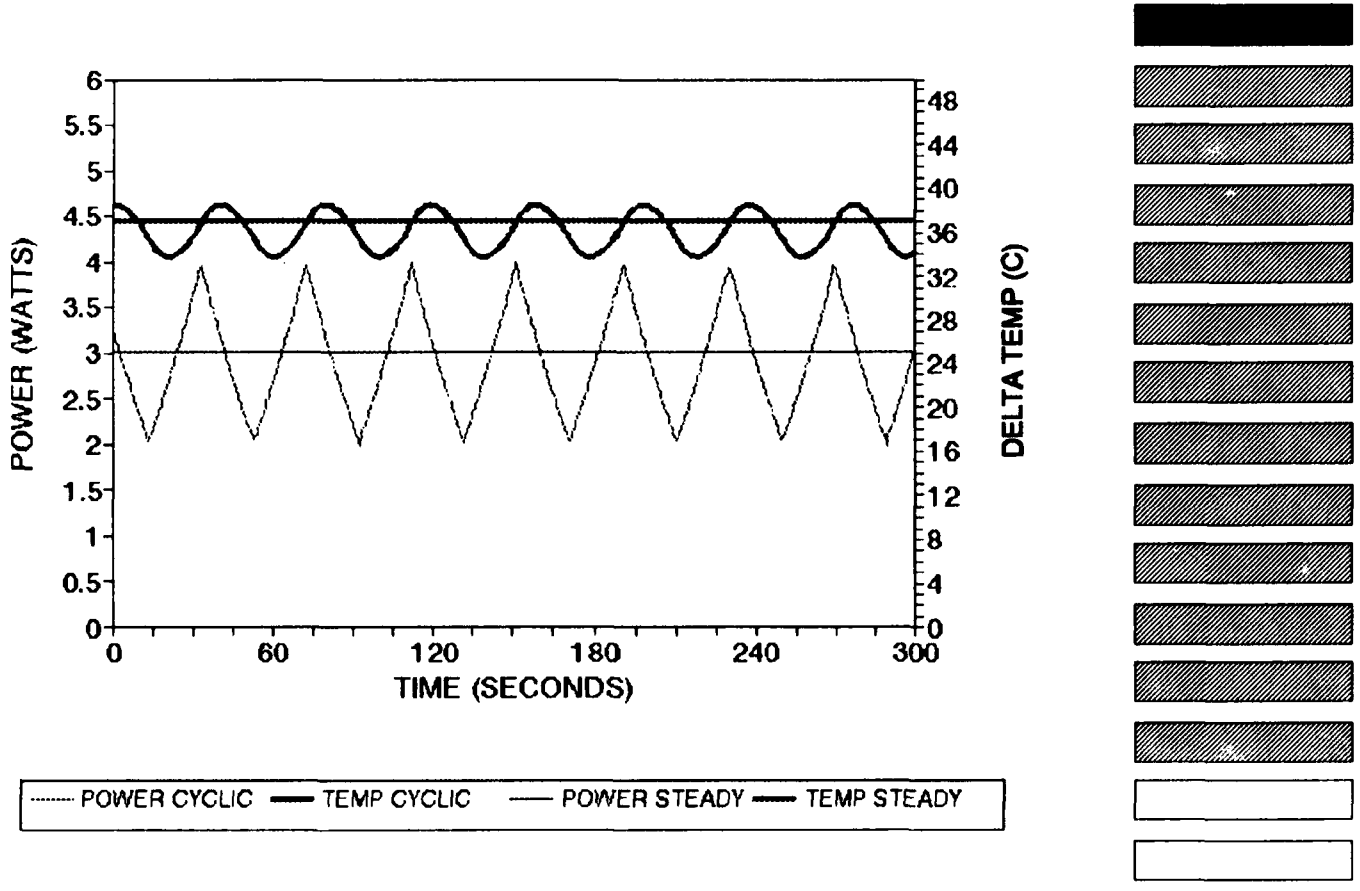

Figure HG. Time dependent transient power and delta temperature for triangular wave input, top heater, heater configuration B16, ambient temperature 19.9°C.

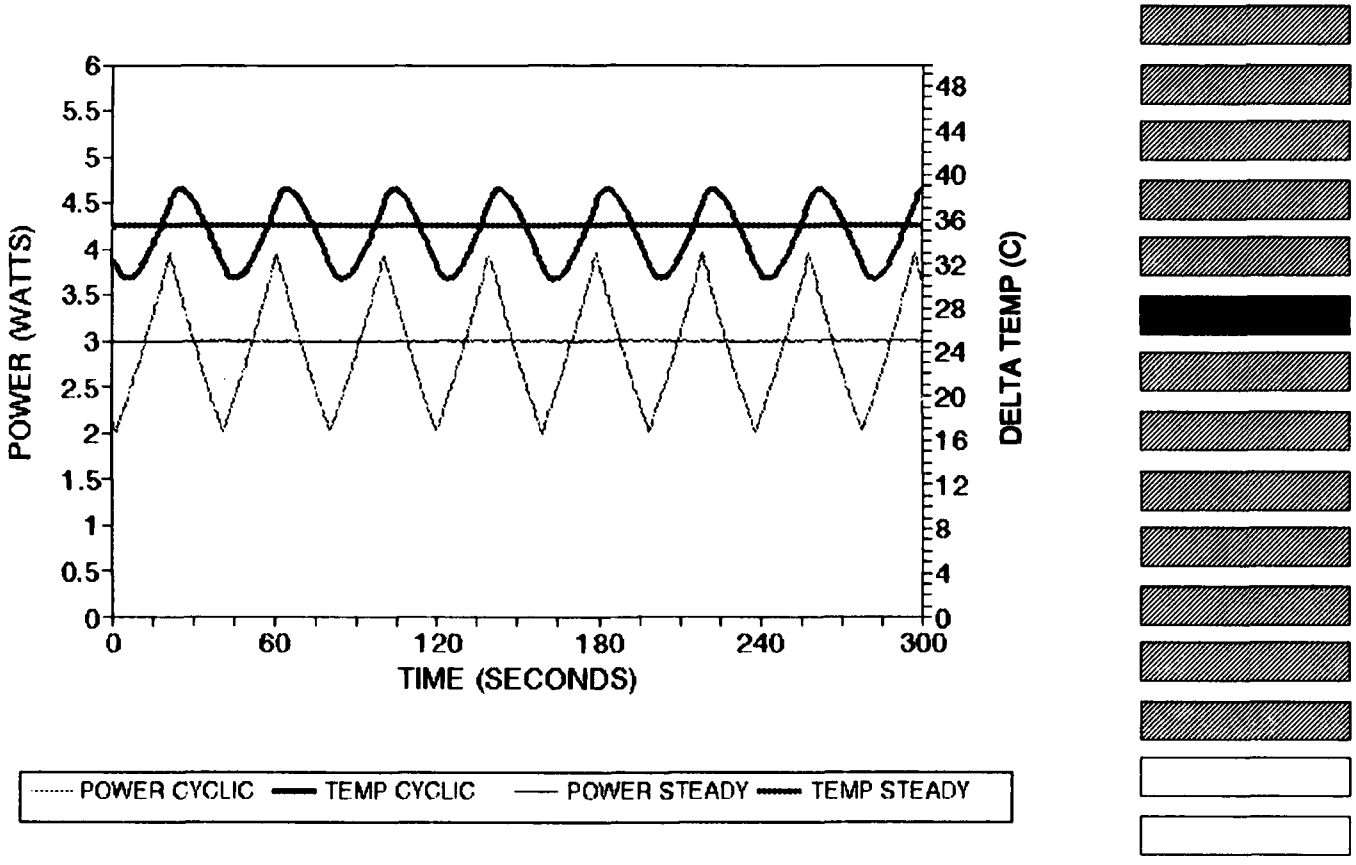

Figure HH. Time dependent transient power and delta temperature for triangular wave input, middle heater, heater configuration B21, ambient temperature 19.9°C.

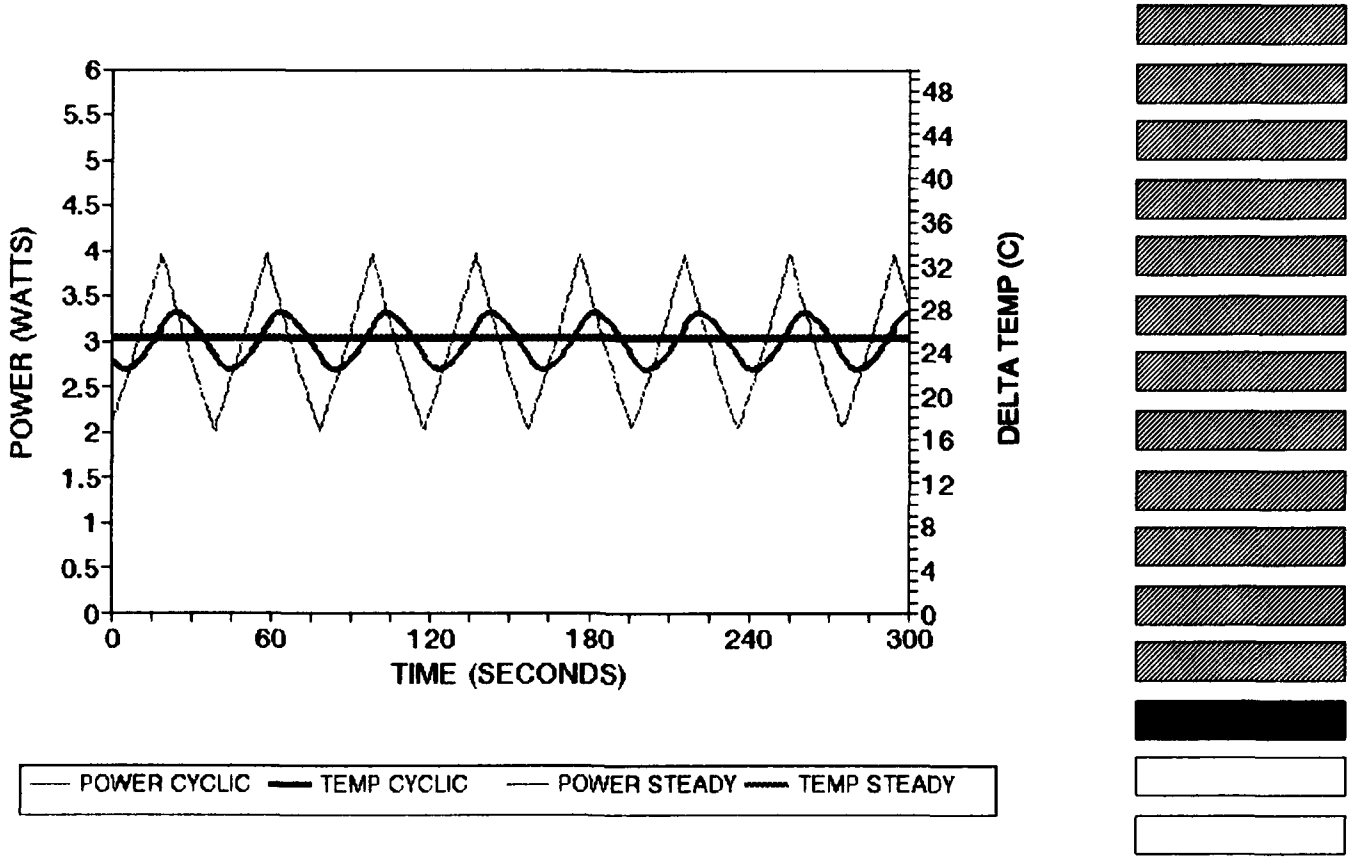

Figure HI. Time dependent transient power and delta temperature for triangular wave input, bottom heater, heater configuration B28, ambient temperature 19.9°C.

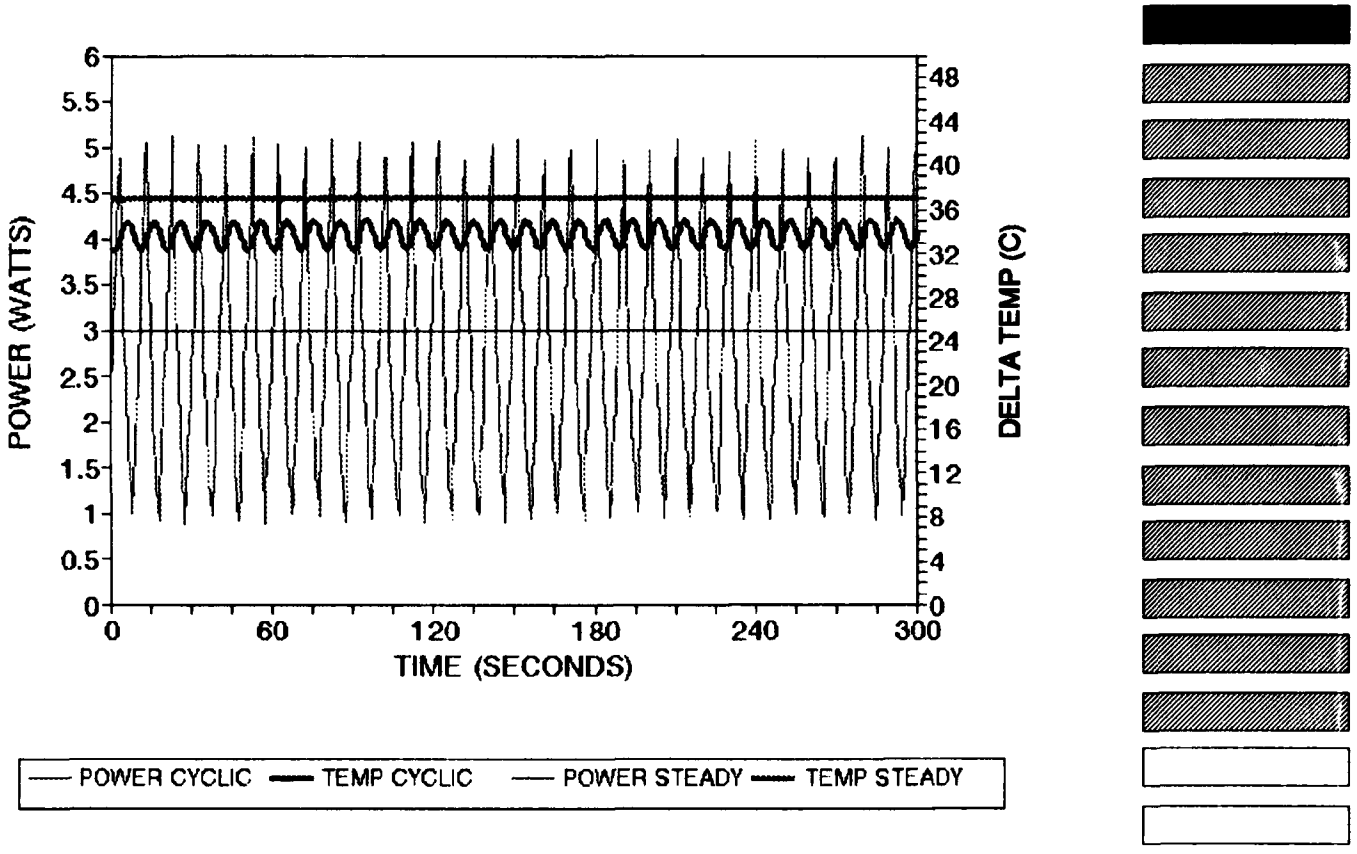

Figure IA. Time dependent transient power and delta temperature for triangular wave input, top heater, heater configuration B21, ambient temperature 18.1°C.

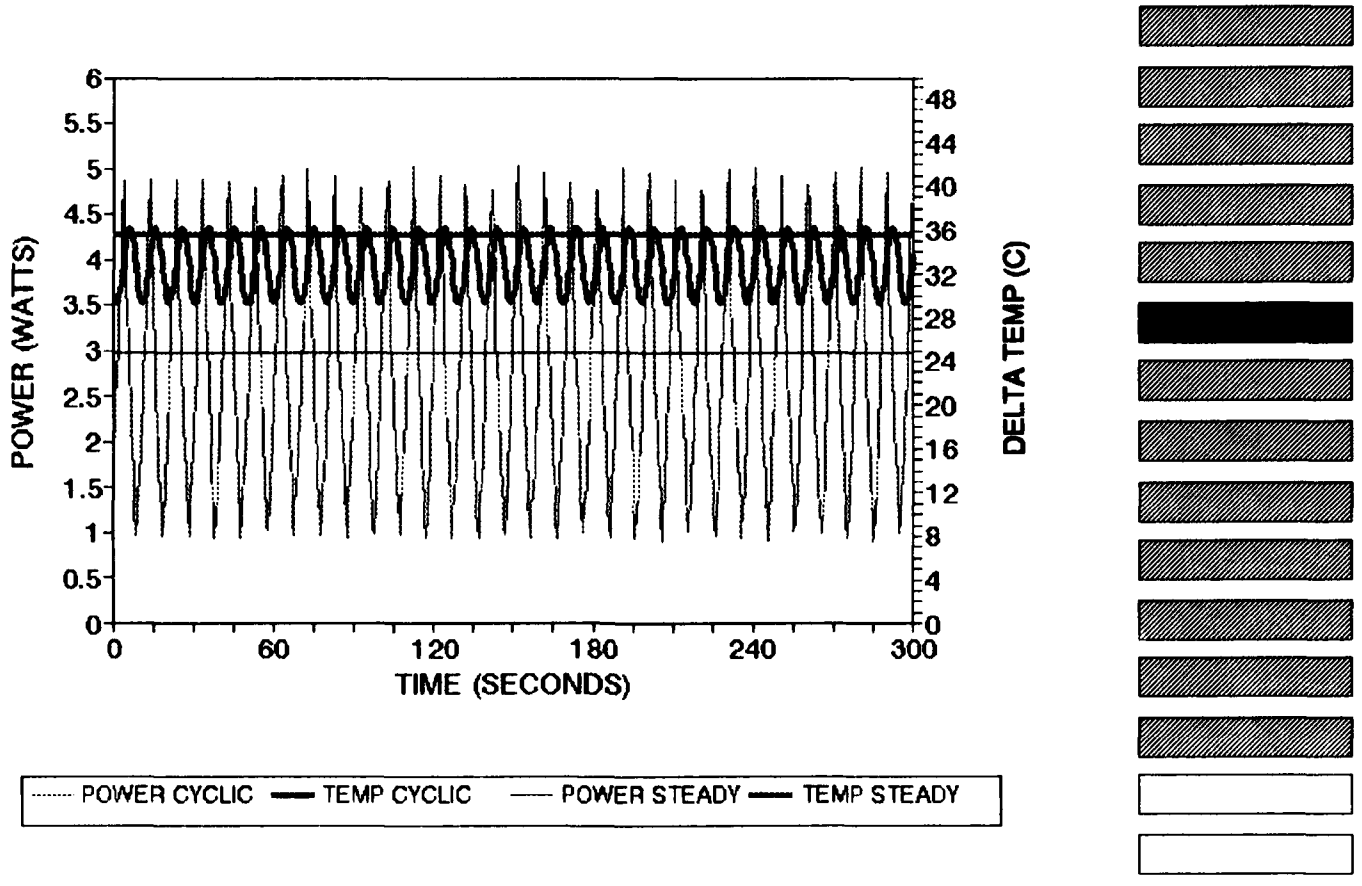

Figure IB. Time dependent transient power and delta temperature for triangular wave input, middle heater, heater configuration B21, ambient temperature 18.1°C.

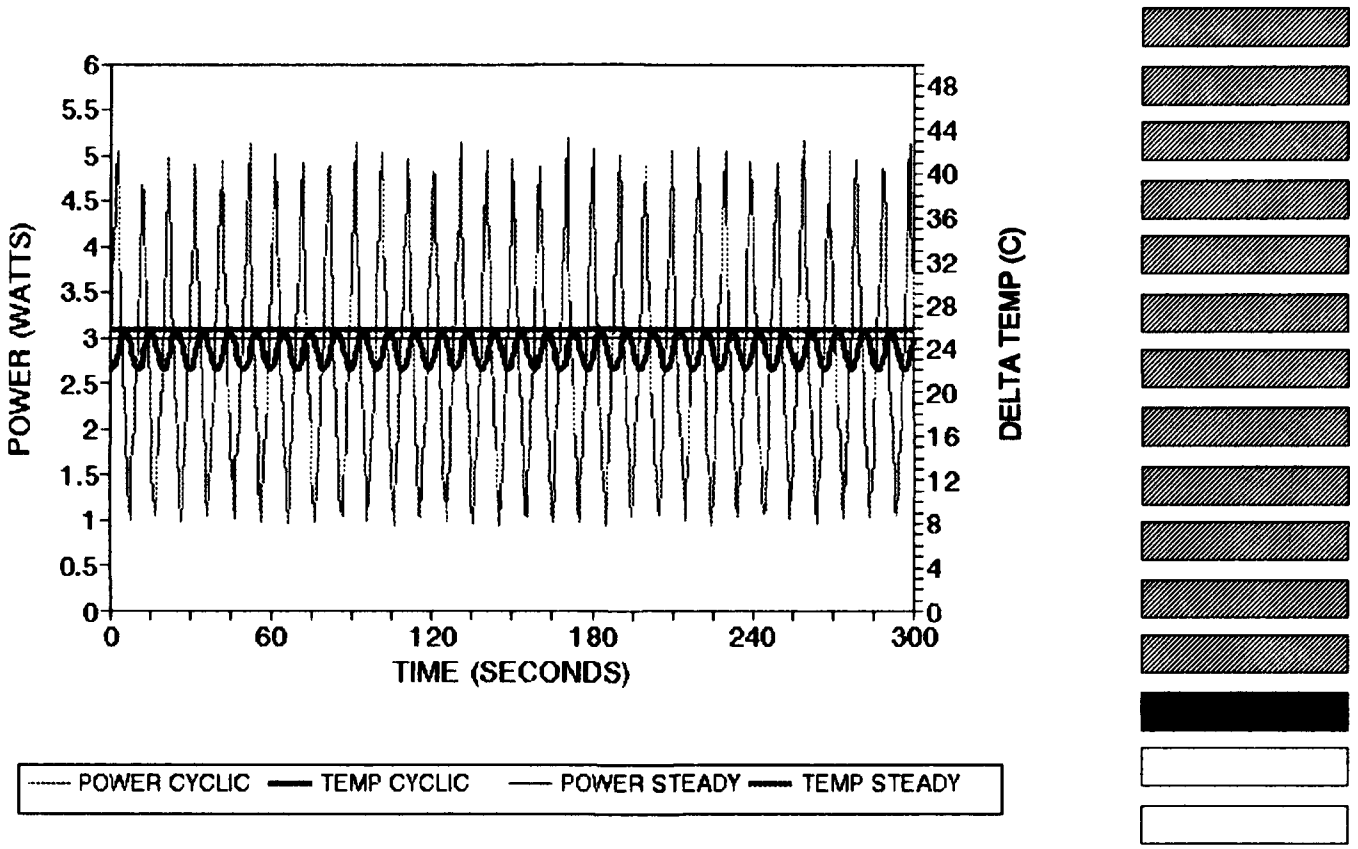

Figure IC. Time dependent transient power and delta temperature for triangular wave input, bottom heater, heater configuration B28, ambient temperature 18.1°C.

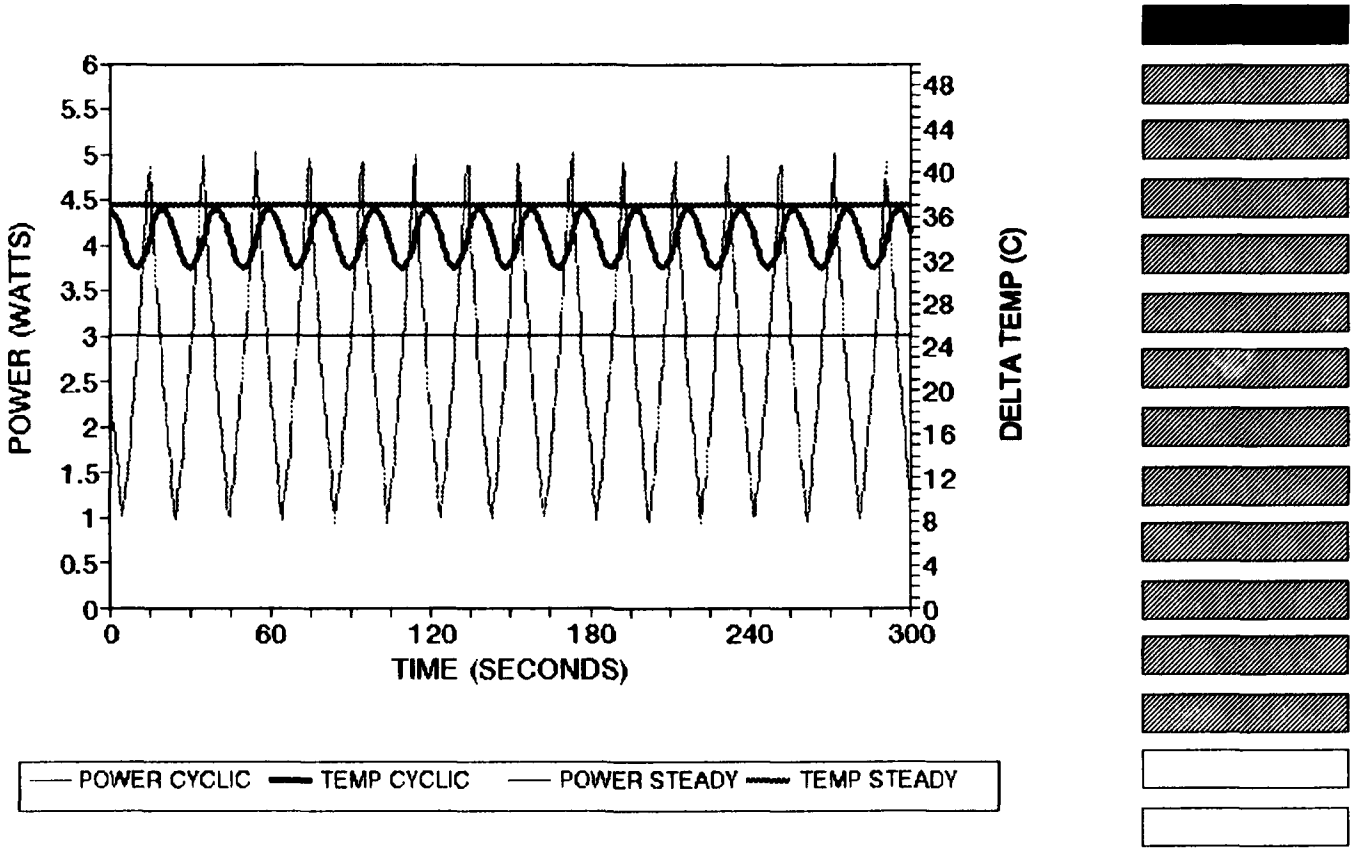

Figure ID. Time dependent transient power and delta temperature for triangular wave input, top heater, heater configuration B16, ambient temperature 19.6°C.

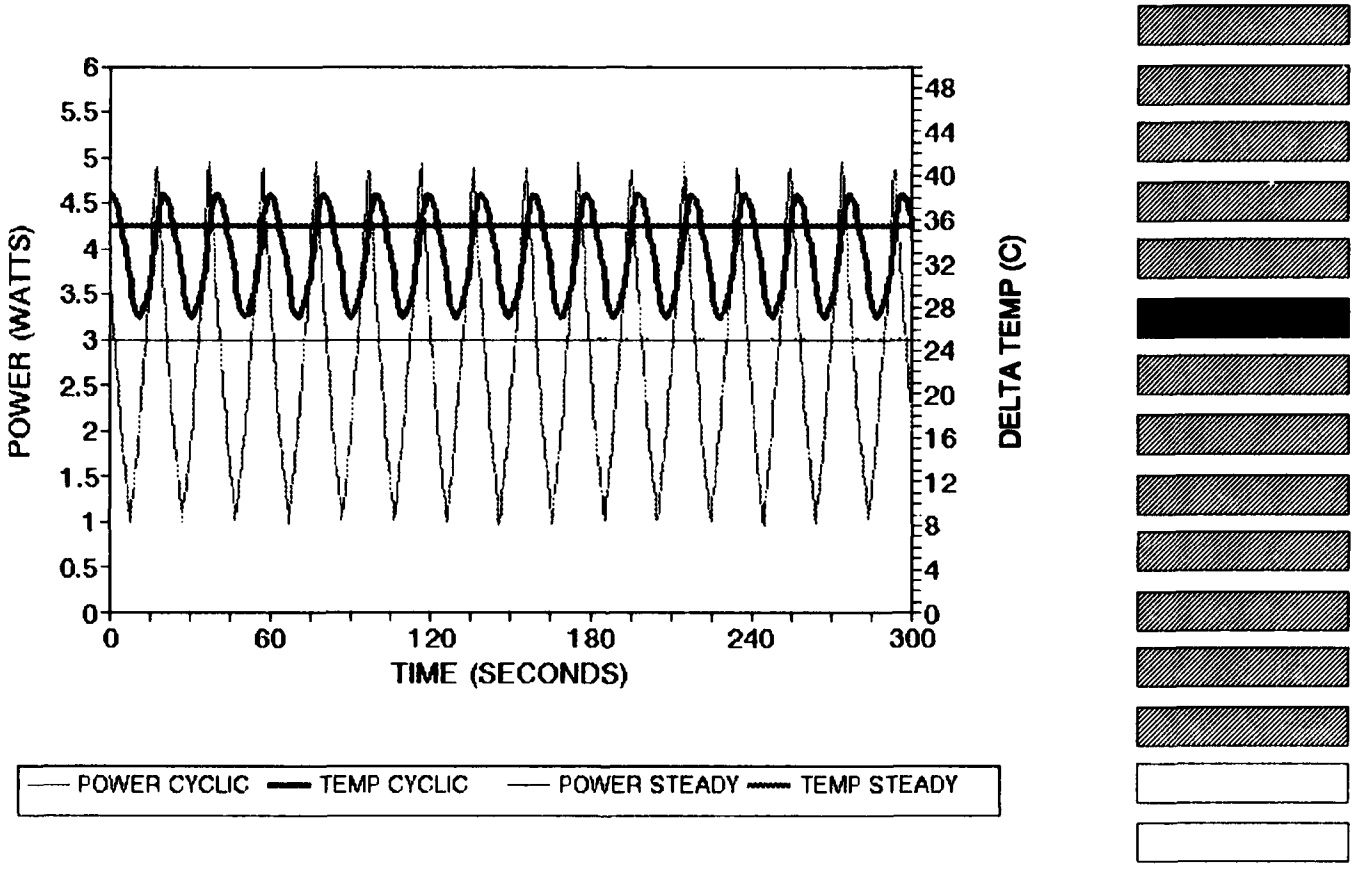

Figure IE. Time dependent transient power and delta temperature for triangular wave input, middle heater, heater configuration B21, ambient temperature 19.6°C.

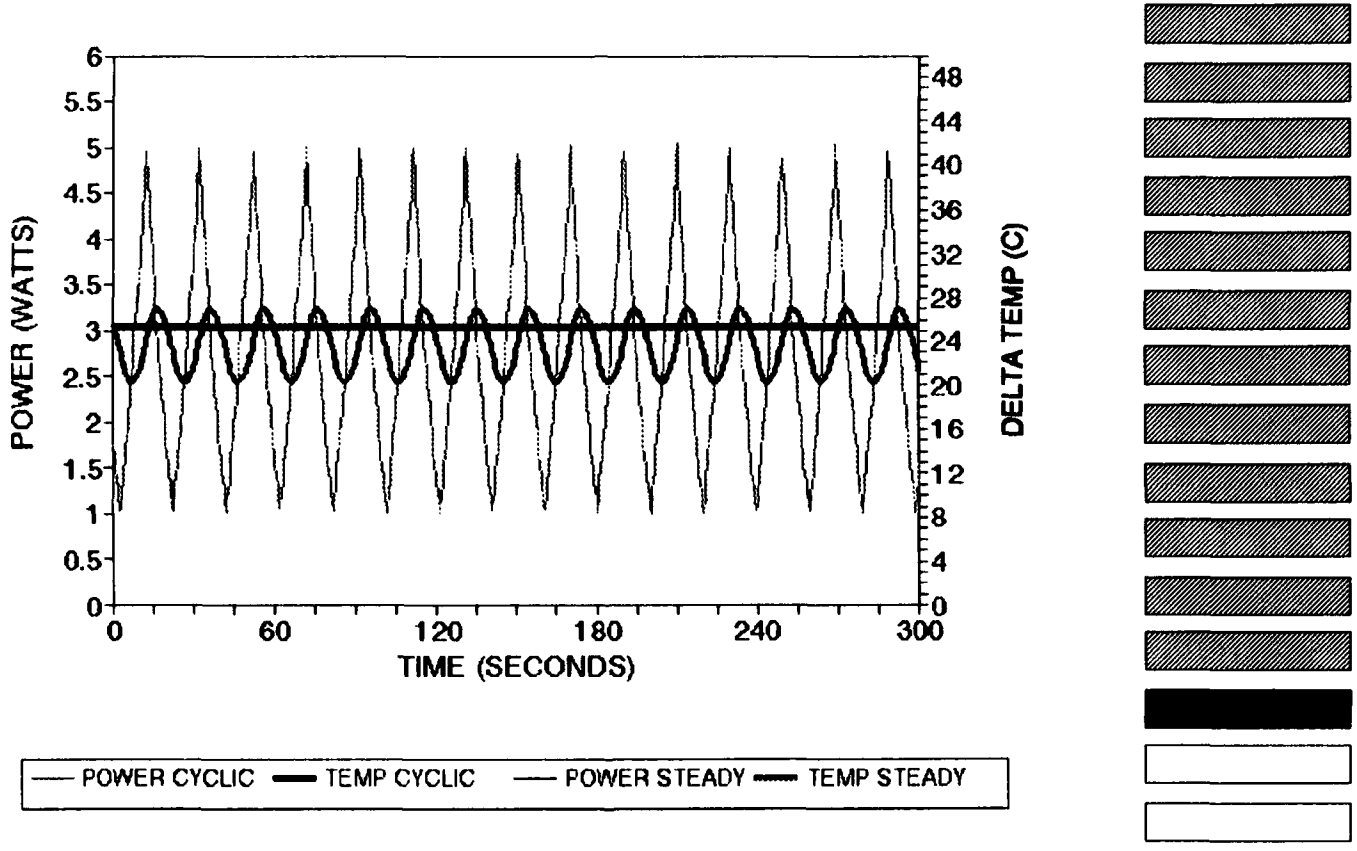

Figure IF. Time dependent transient power and delta temperature for triangular wave input, bottom heater, heater configuration B28, ambient temperature 19.6°C.

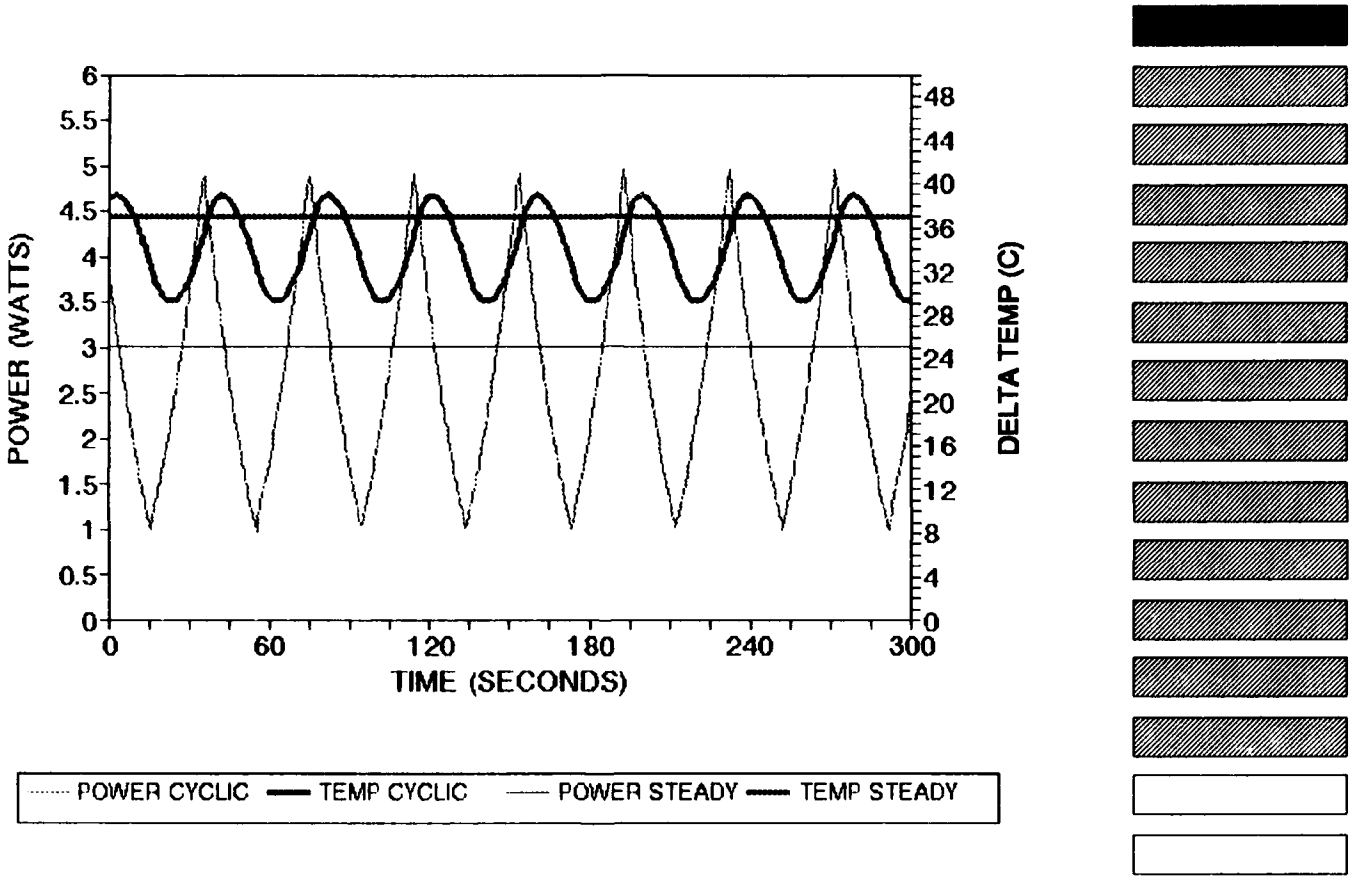

Figure IG. Time dependent transient power and delta temperature for triangular wave input, top heater, heater configuration B16, ambient temperature 20.0°C.

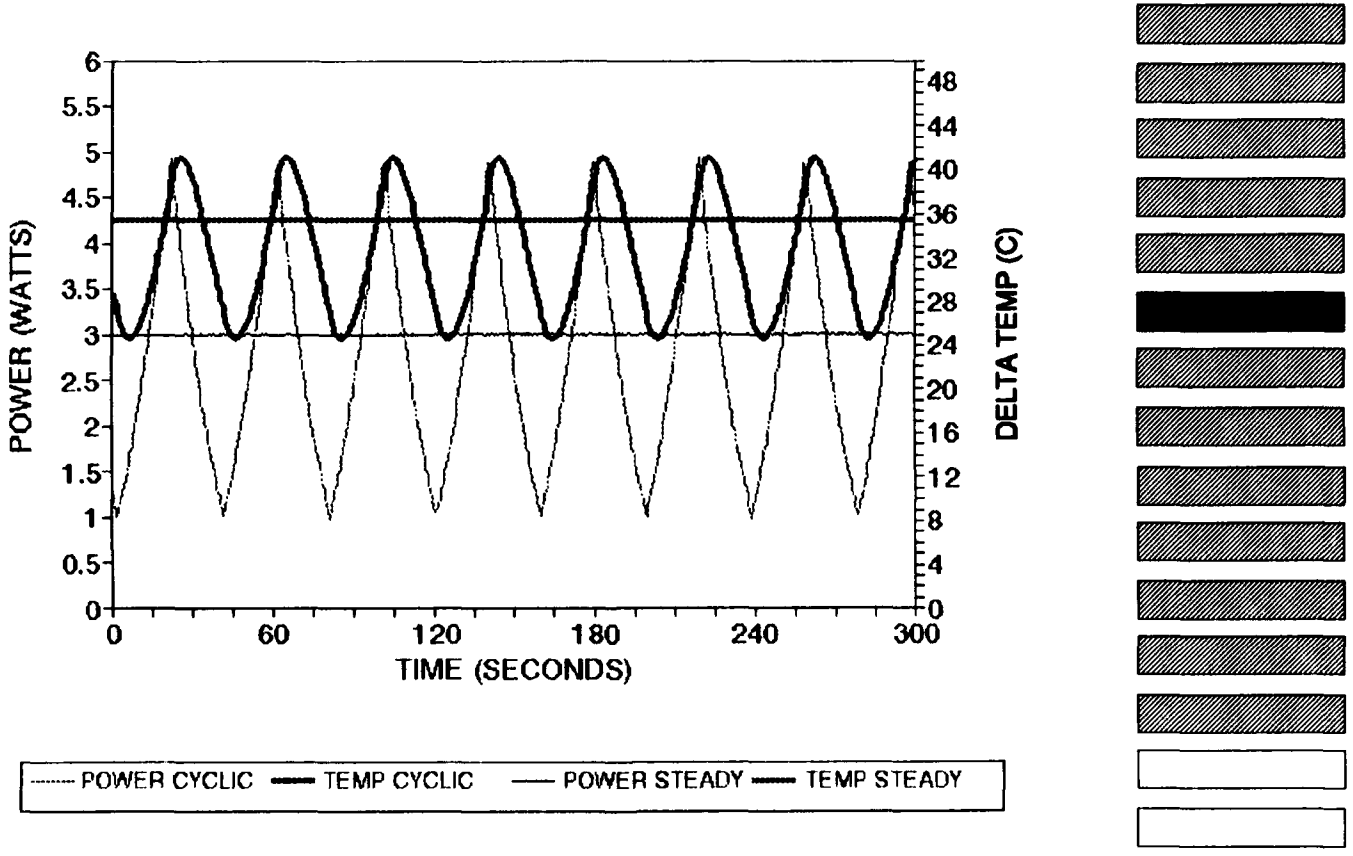

Figure IH. Time dependent transient power and delta temperature for triangular wave input, middle heater, heater configuration B21, ambient temperature 20.0°C.

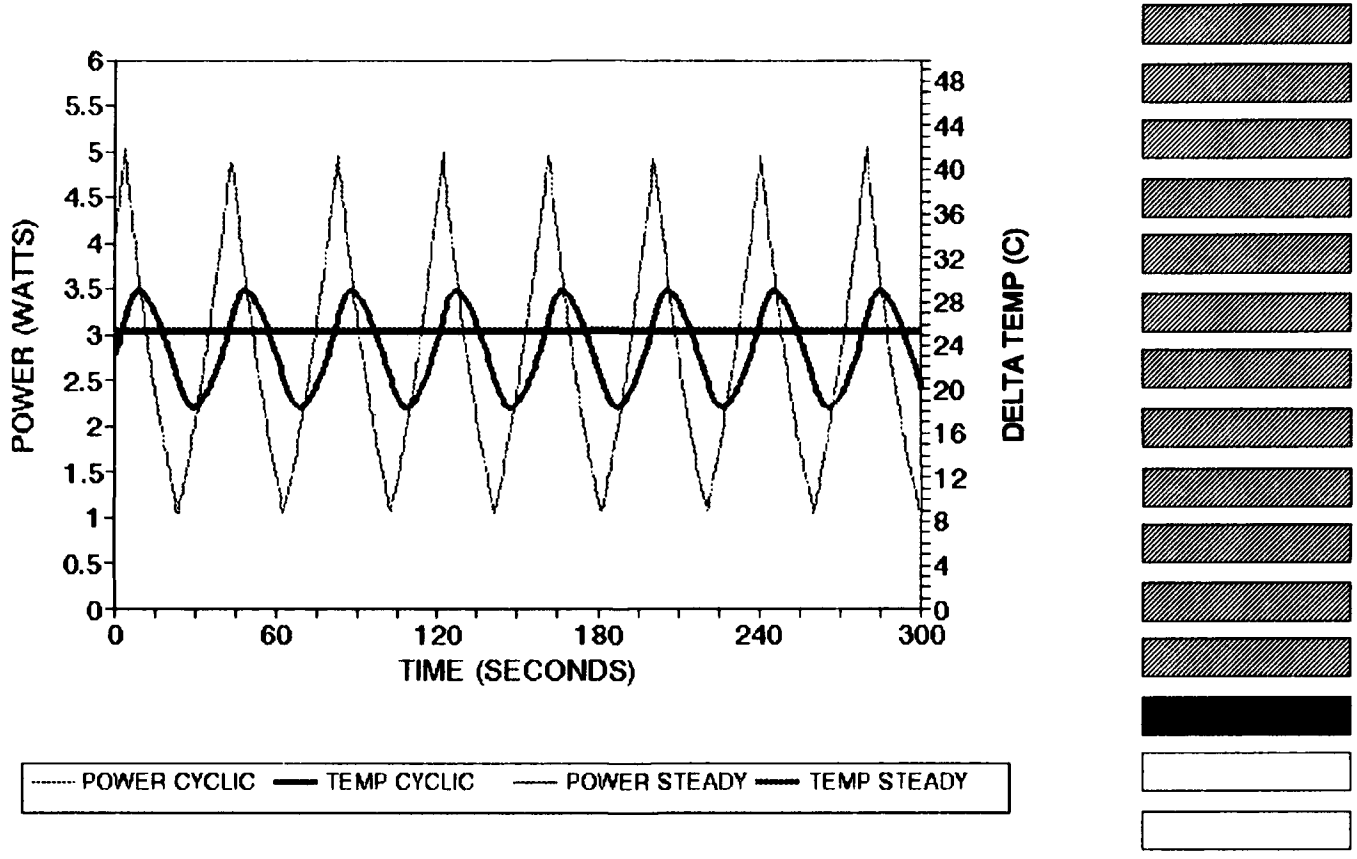

Figure II. Time dependent transient power and delta temperature for triangular wave input, bottom heater, heater configuration B28, ambient temperature 20.0°C.

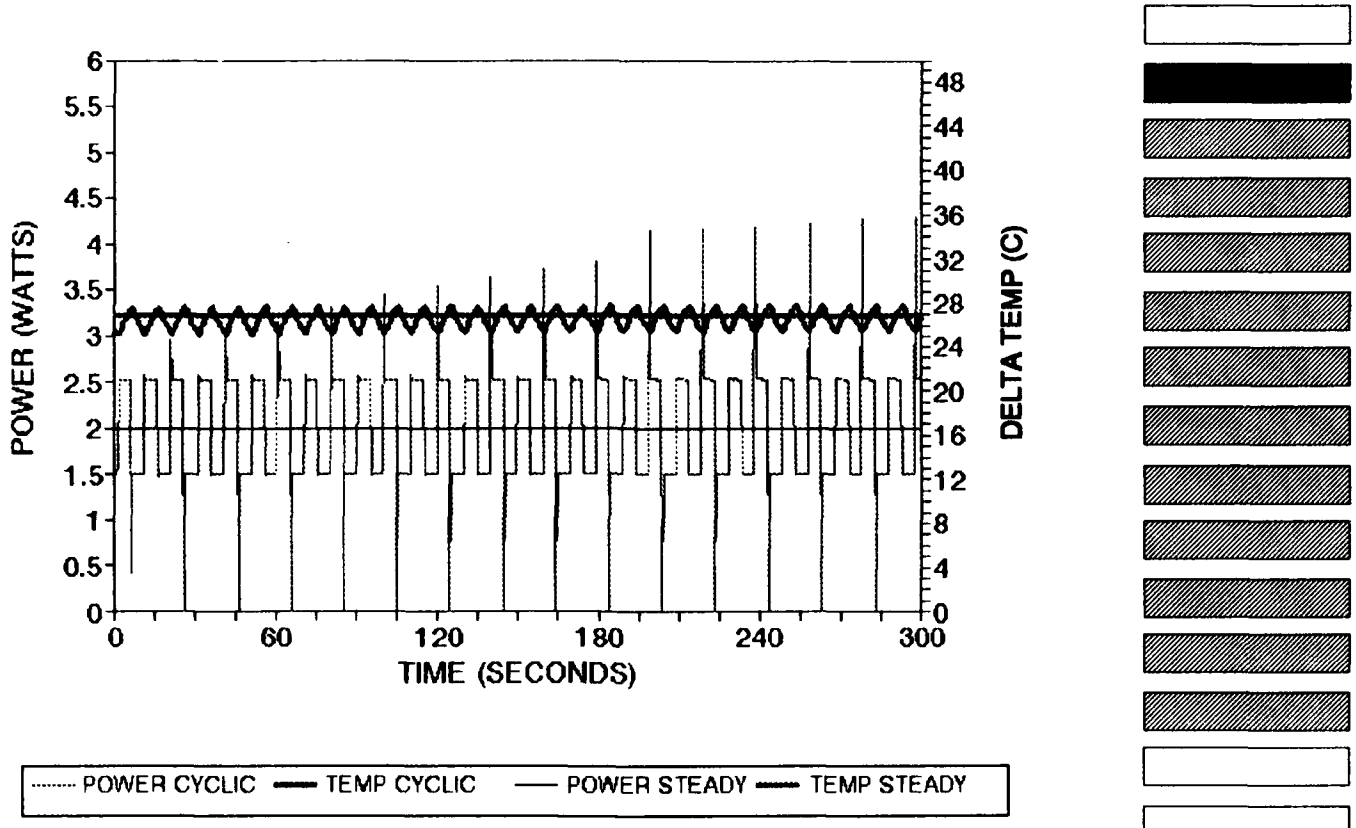

Figure JA. Time dependent transient power and delta temperature for square wave input, top heater, heater configuration C17, ambient temperature 17.3°C.

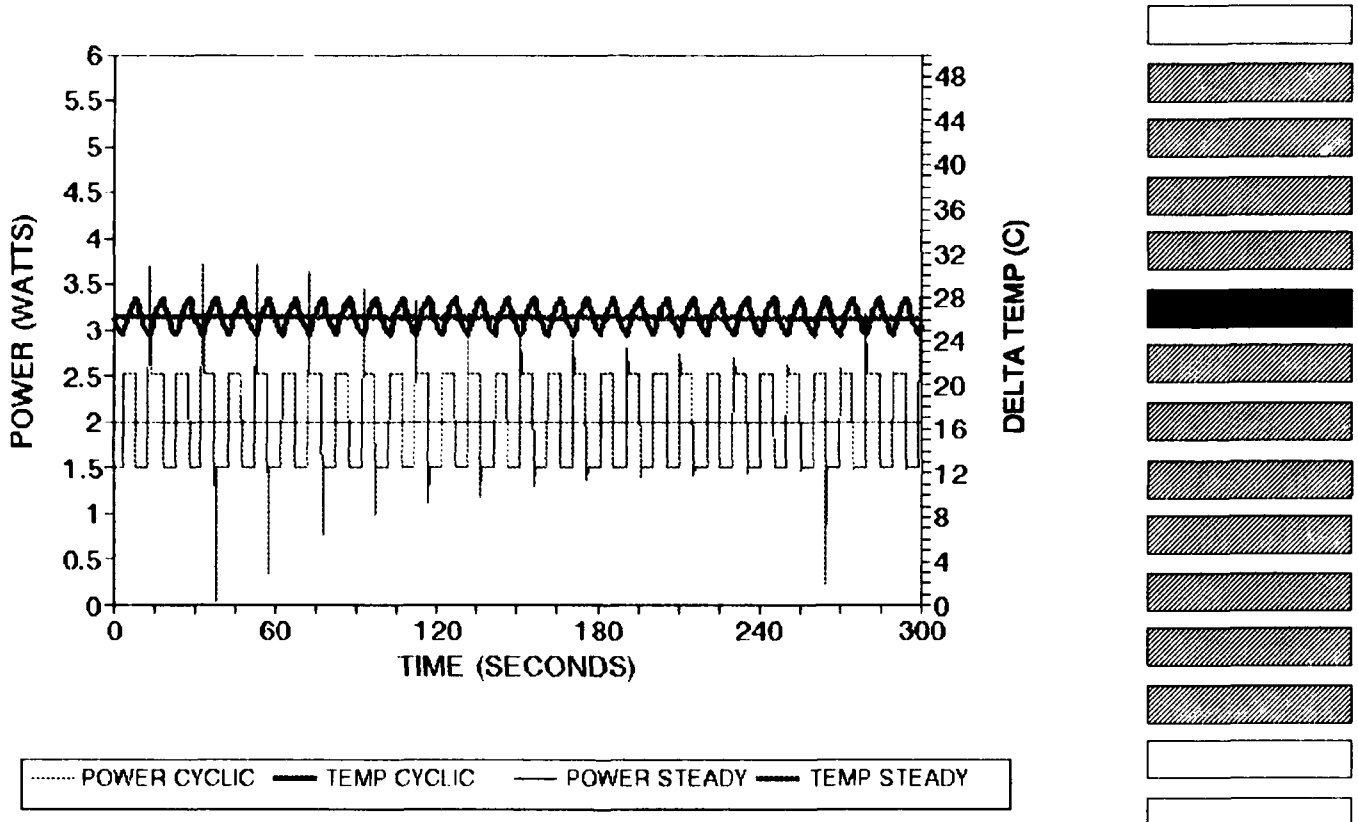

Figure JB. Time dependent transient power and delta temperature for square wave input, middle heater, heater configuration C21, ambient temperature 17.3°C.

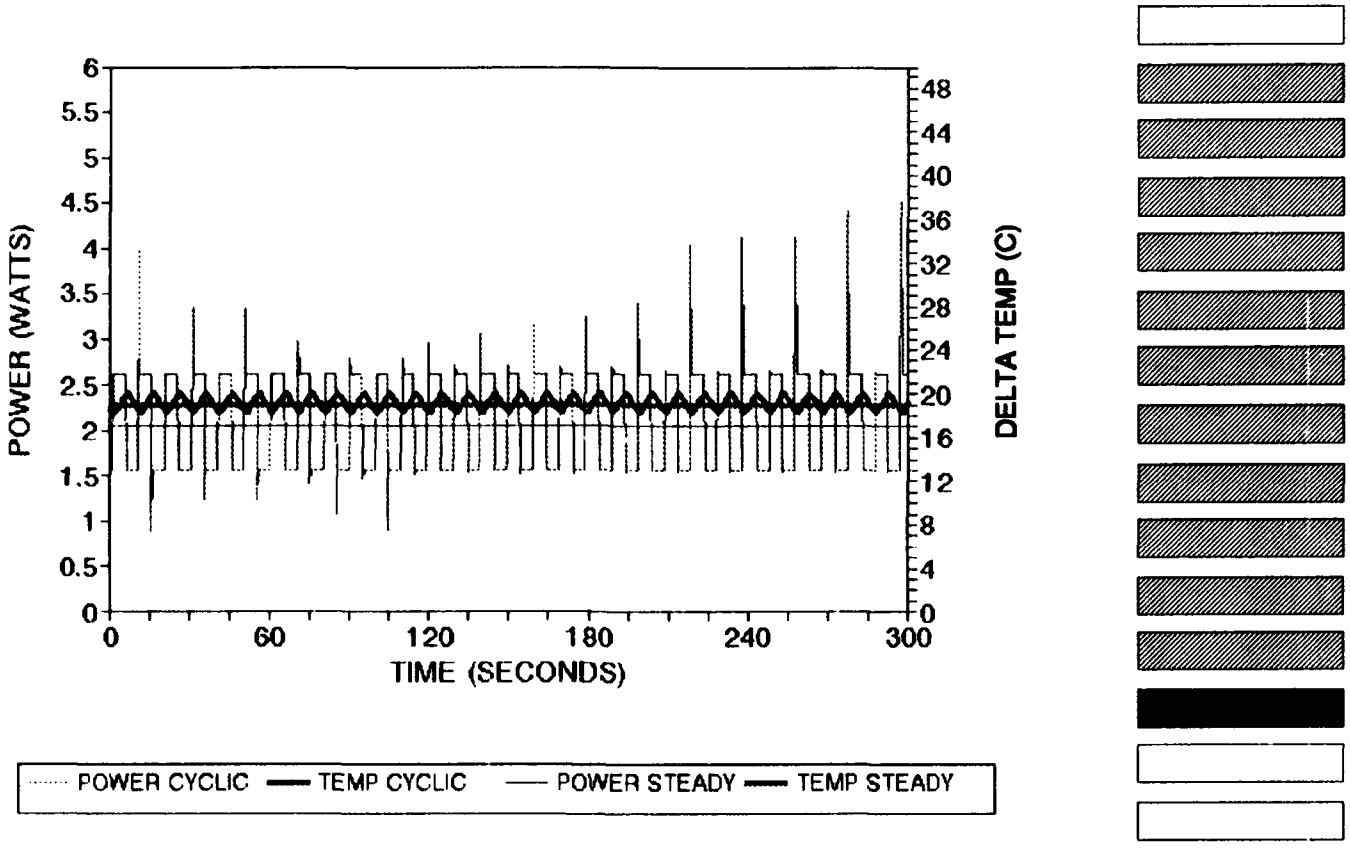

Figure JC. Time dependent transient power and delta temperature for square wave input, bottom heater, heater configuration C28, ambient temperature 17.3°C.

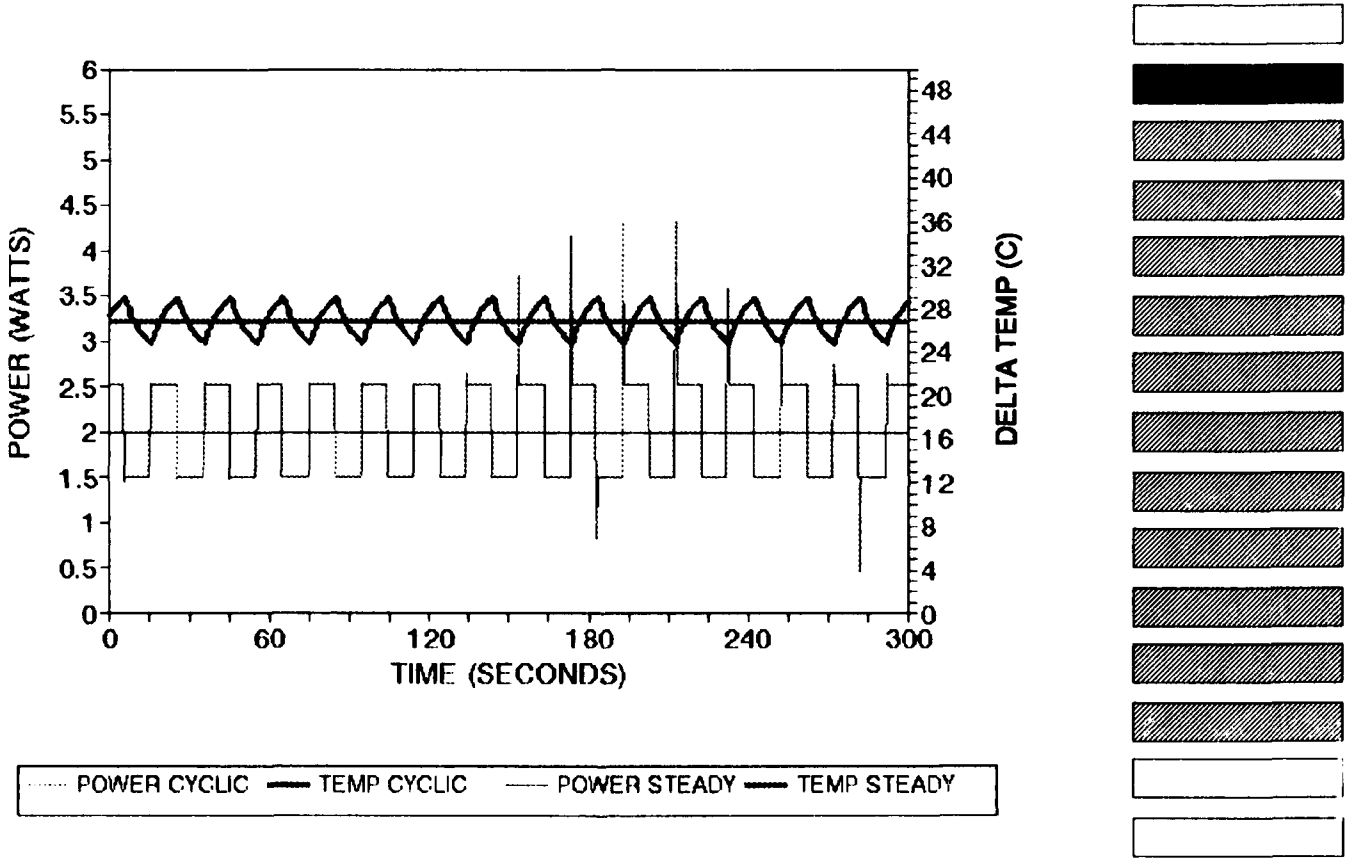

Figure JD. Time dependent transient power and delta temperature for square wave input, top heater, heater configuration C17, ambient temperature 17.3°C.

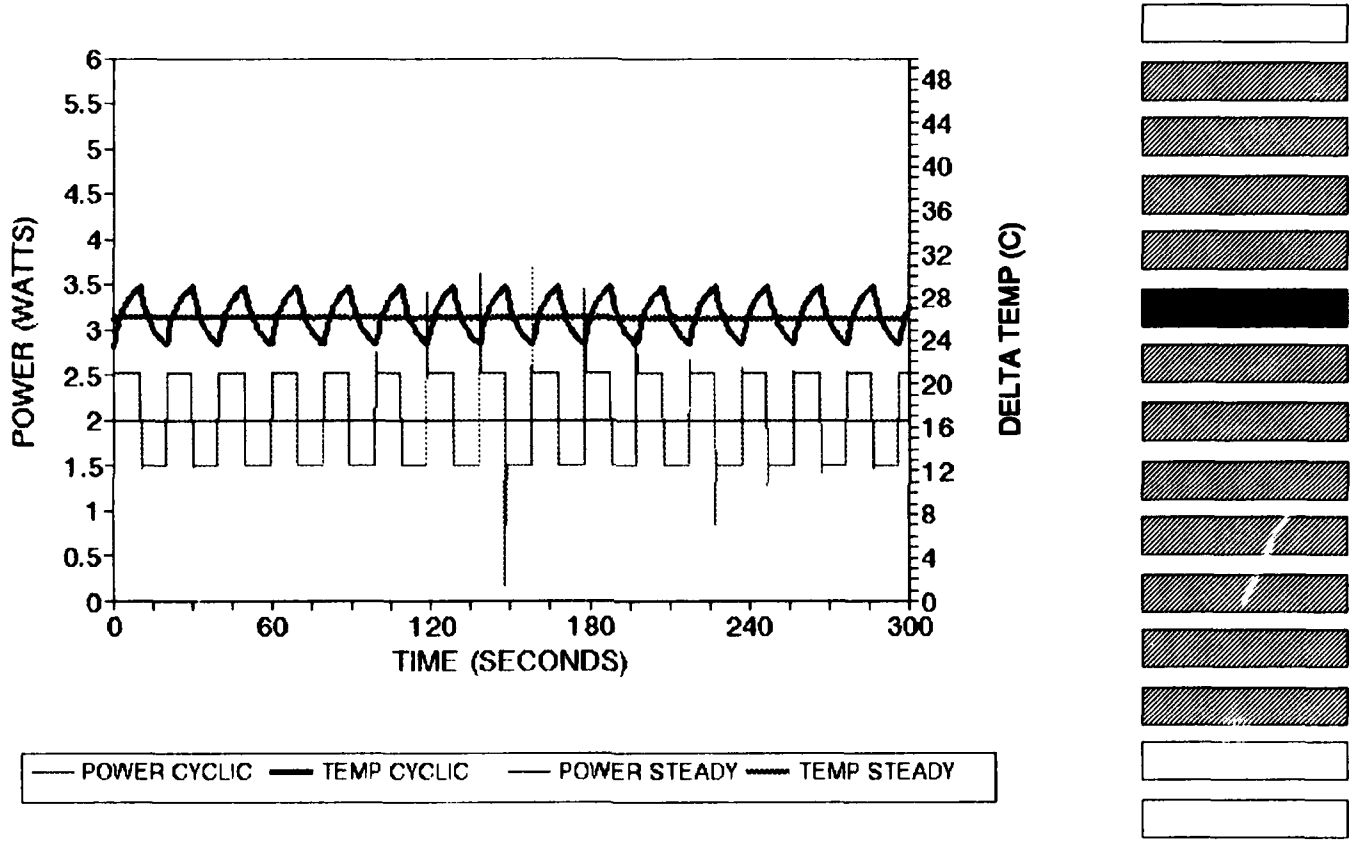

Figure JE. Time dependent transient power and delta temperature for square wave input, middle heater, heater configuration C21, ambient temperature 17.3°C.

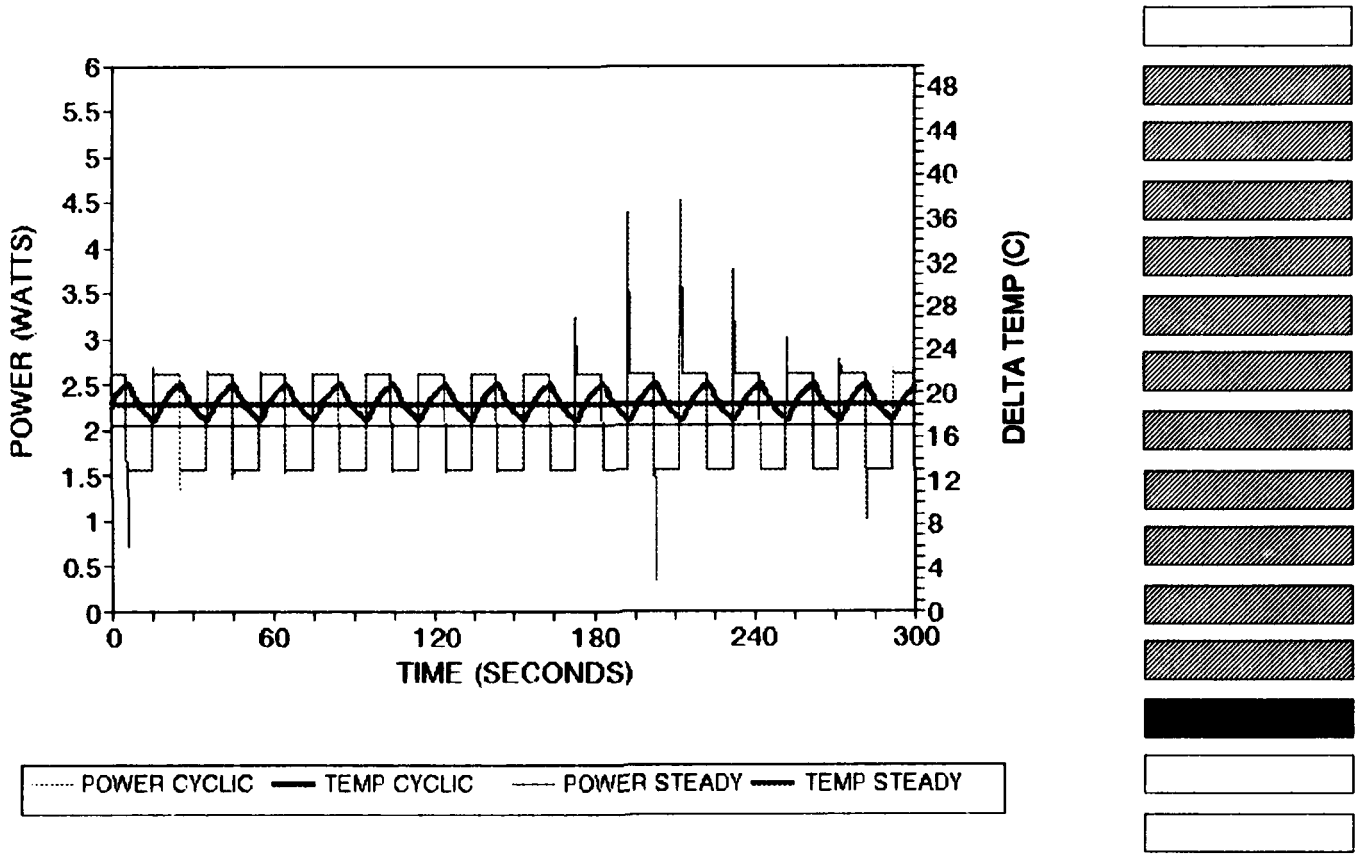

Figure JF. Time dependent transient power and delta temperature for square wave input, bottom heater, heater configuration C28, ambient temperature 17.3°C.

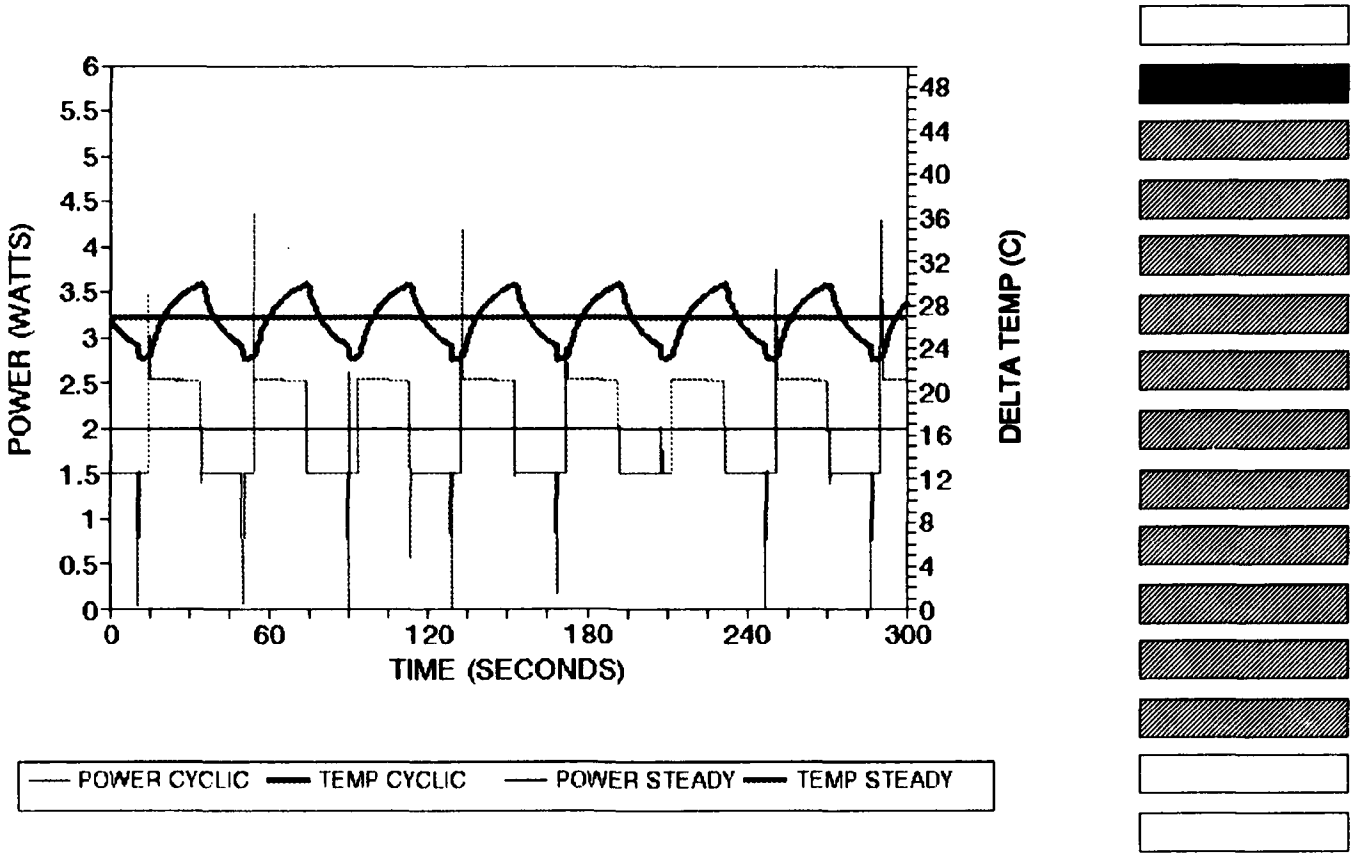

Figure JG. Time dependent transient power and delta temperature for square wave input, top heater, heater configuration C17, ambient temperature 17.3°C.

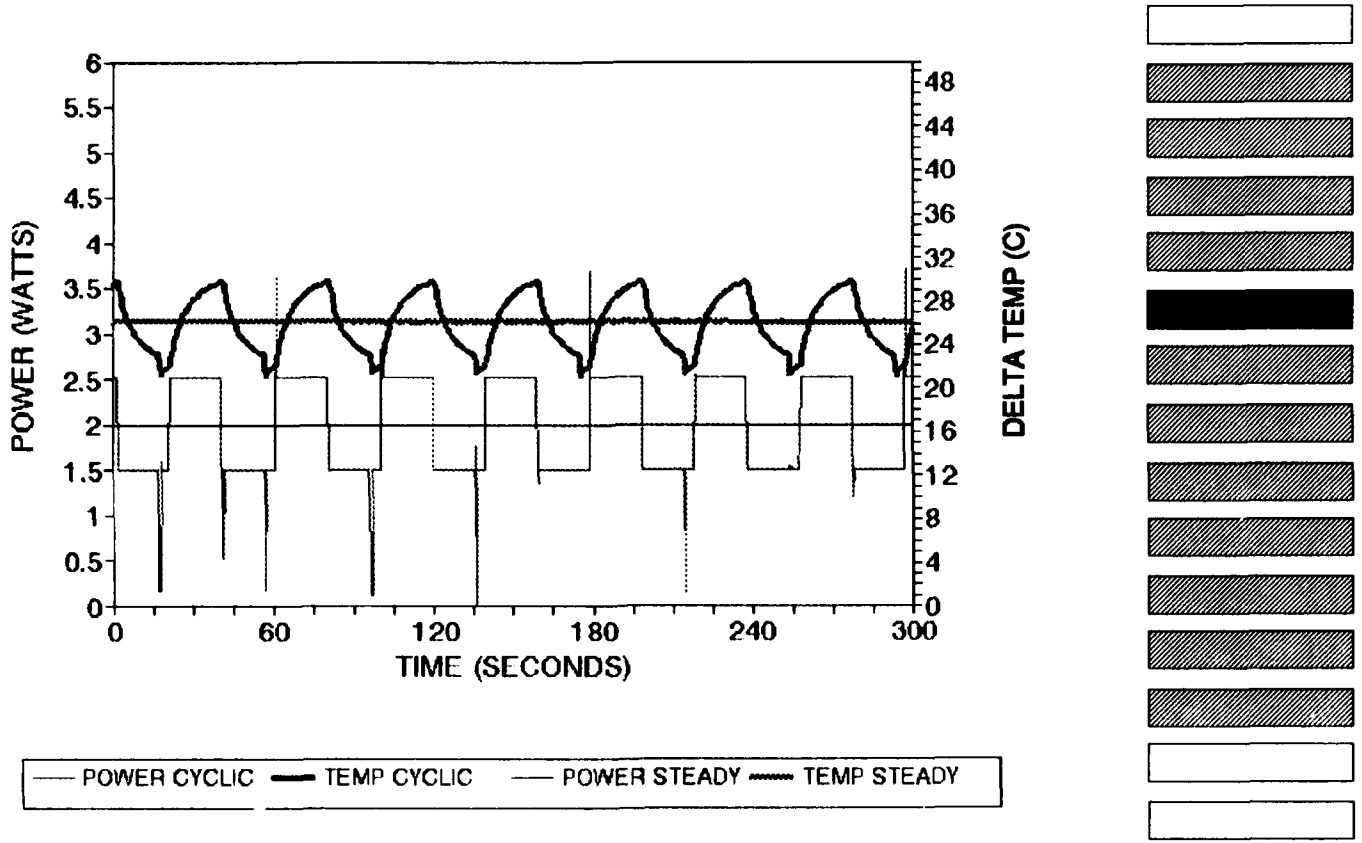

Figure JH. Time dependent transient power and delta temperature for square wave input, middle heater, heater configuration C21, ambient temperature 17.3°C.

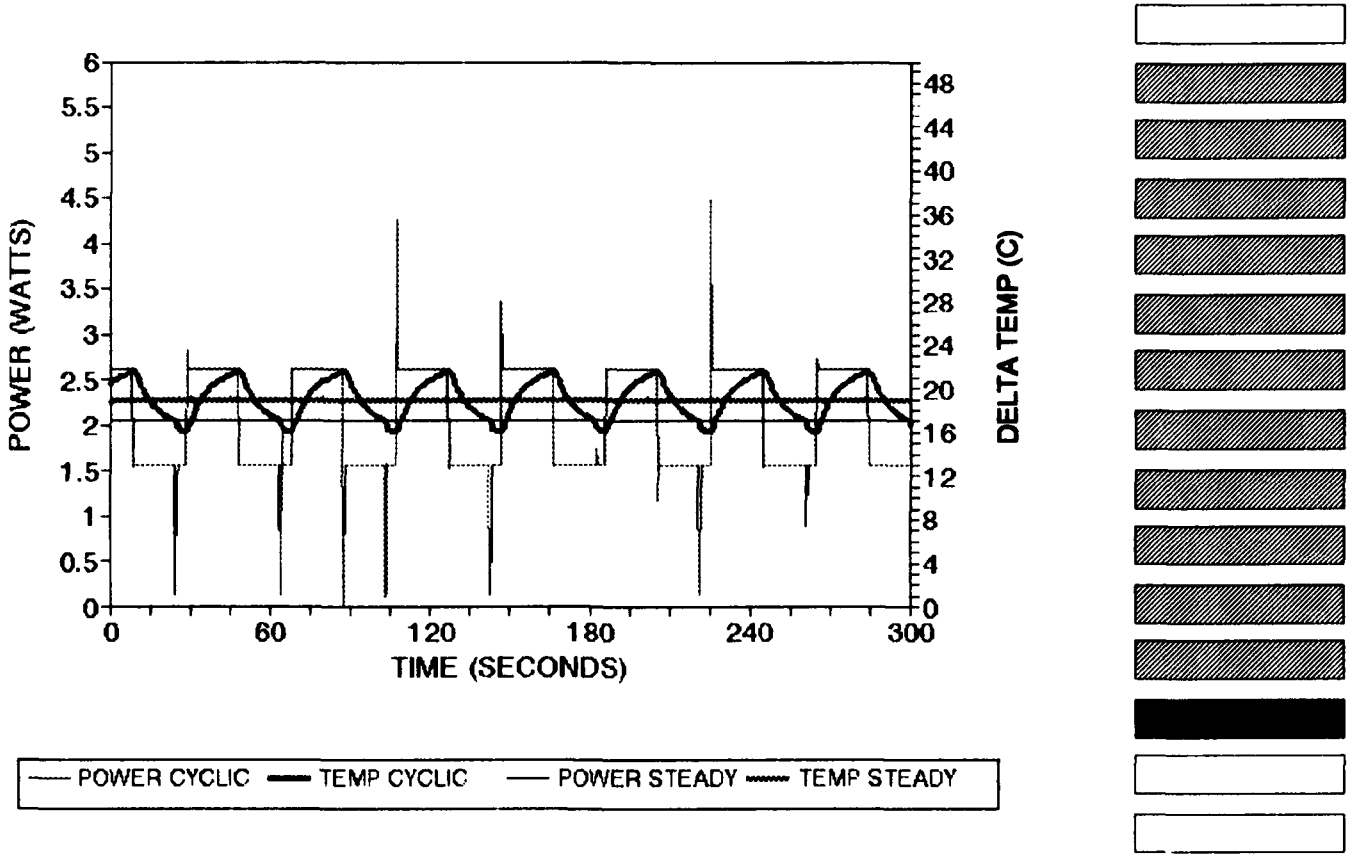

Figure JI. Time dependent transient power and delta temperature for square wave input, bottom heater, heater configuration C28, ambient temperature 17.3°C.

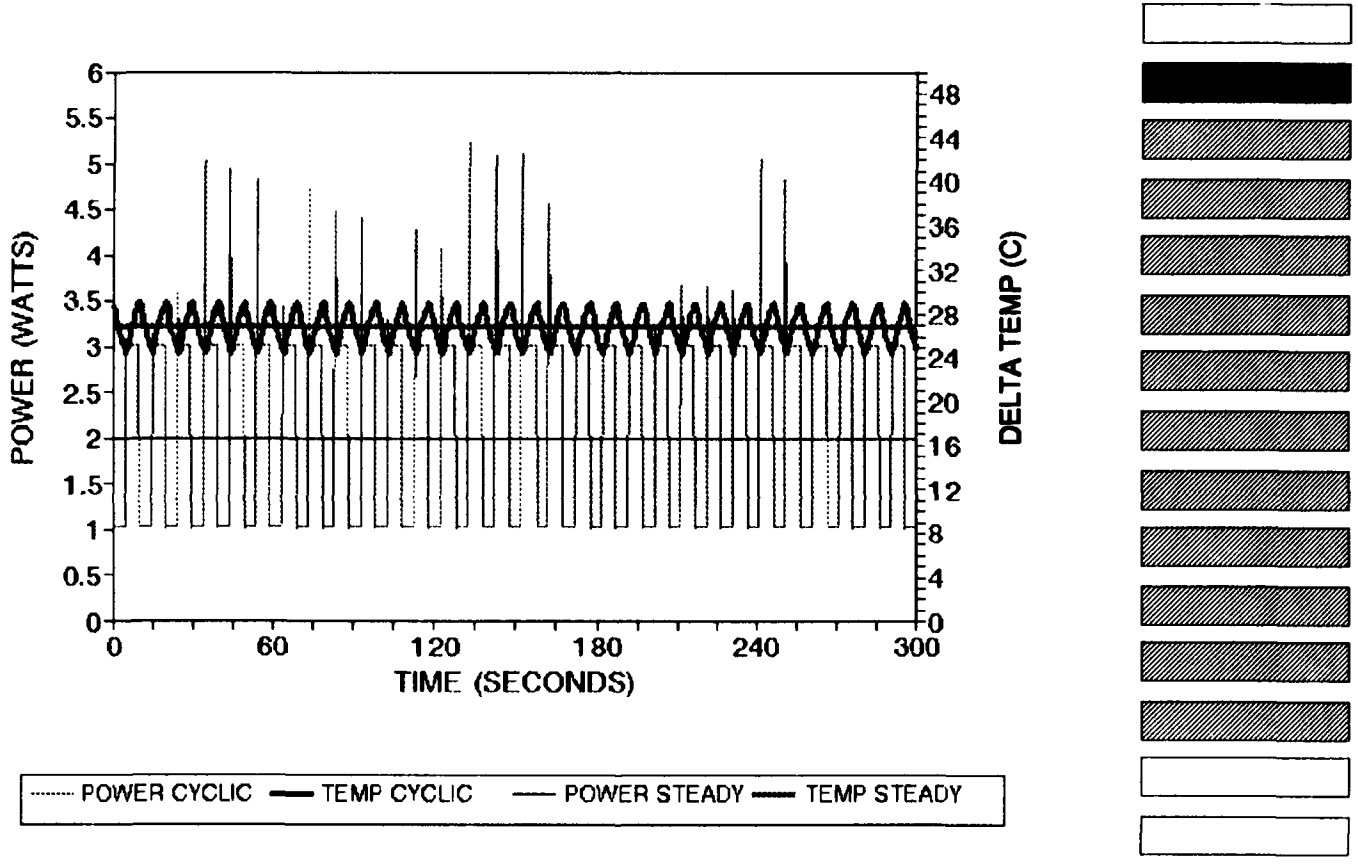

Figure KA. Time dependent transient power and delta temperature for square wave input, top heater, heater configuration C17, ambient temperature 17.3°C.

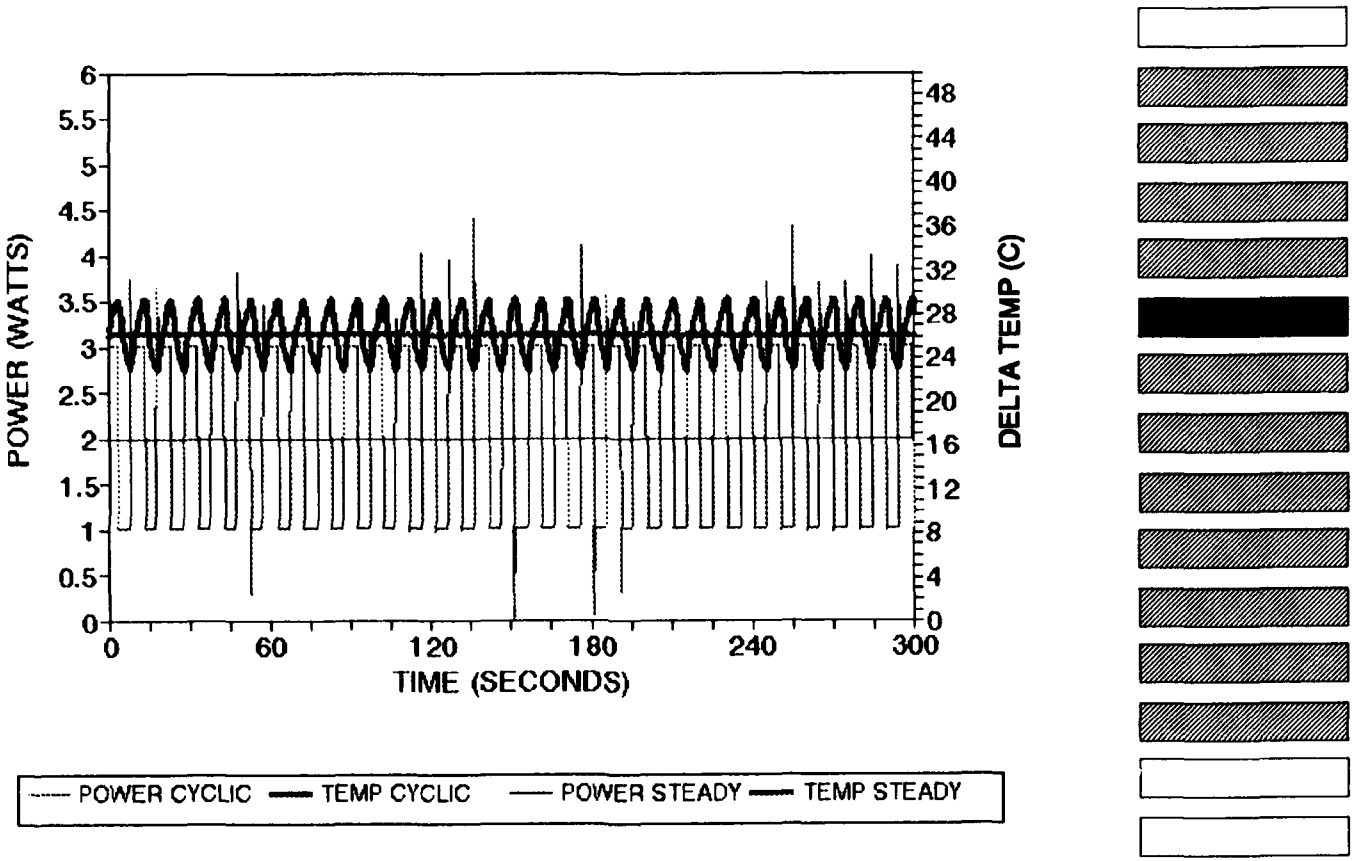

Figure KB. Time dependent transient power and delta temperature for square wave input, middle heater, heater configuration C21, ambient temperature 17.3°C.

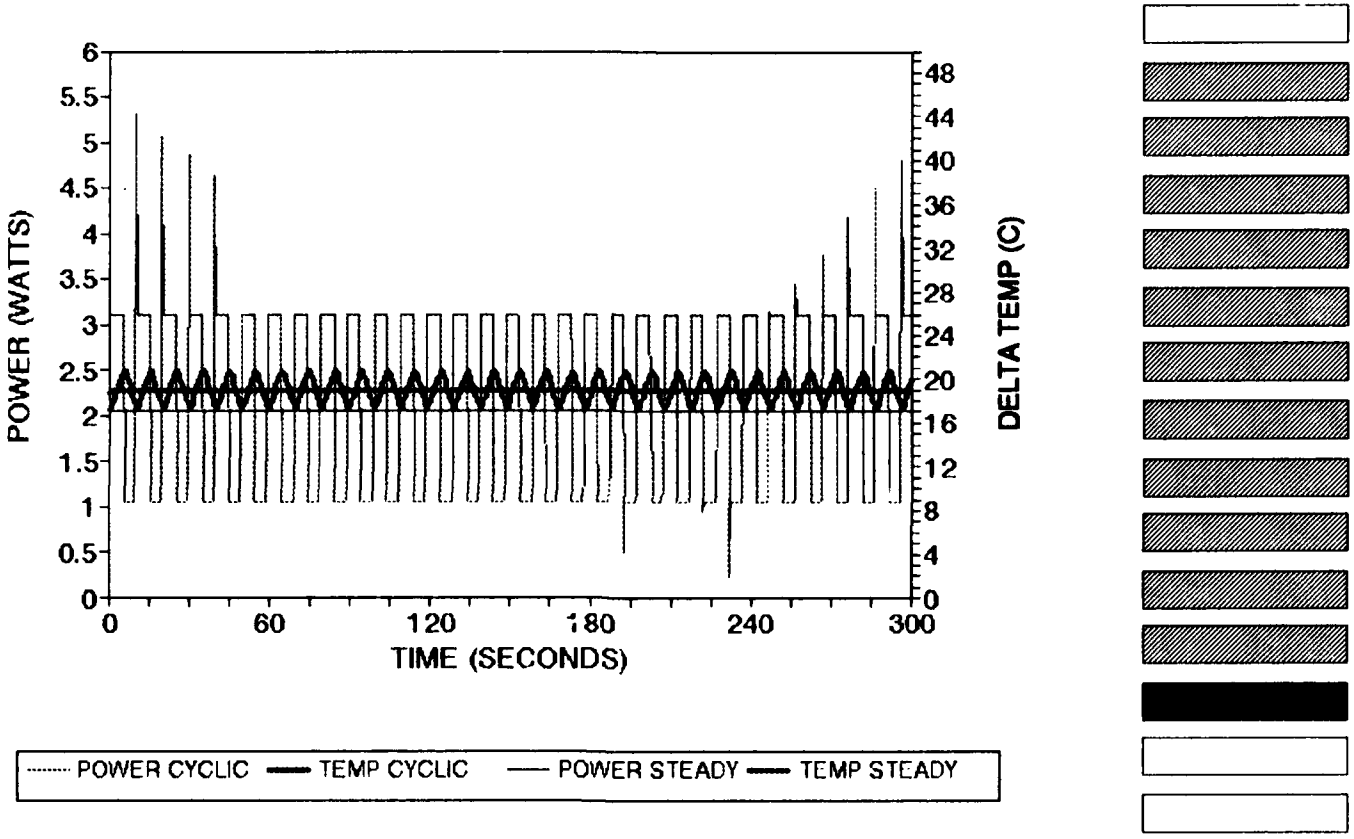

Figure KC. Time dependent transient power and delta temperature for square wave input, bottom heater, heater configuration C28, ambient temperature 17.3°C.

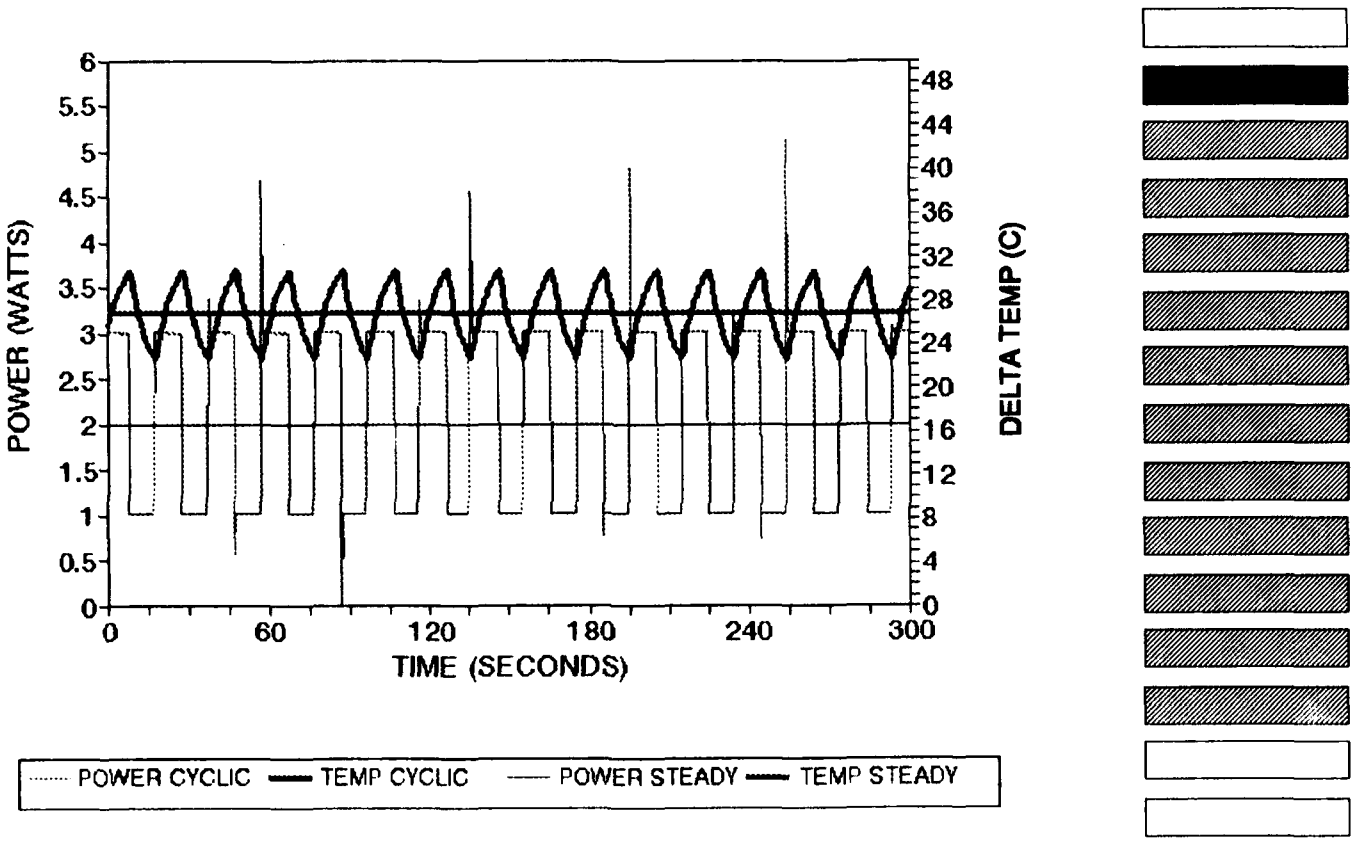

Figure KD. Time dependent transient power and delta temperature for square wave input, top heater, heater configuration C17, ambient temperature 17.3°C.

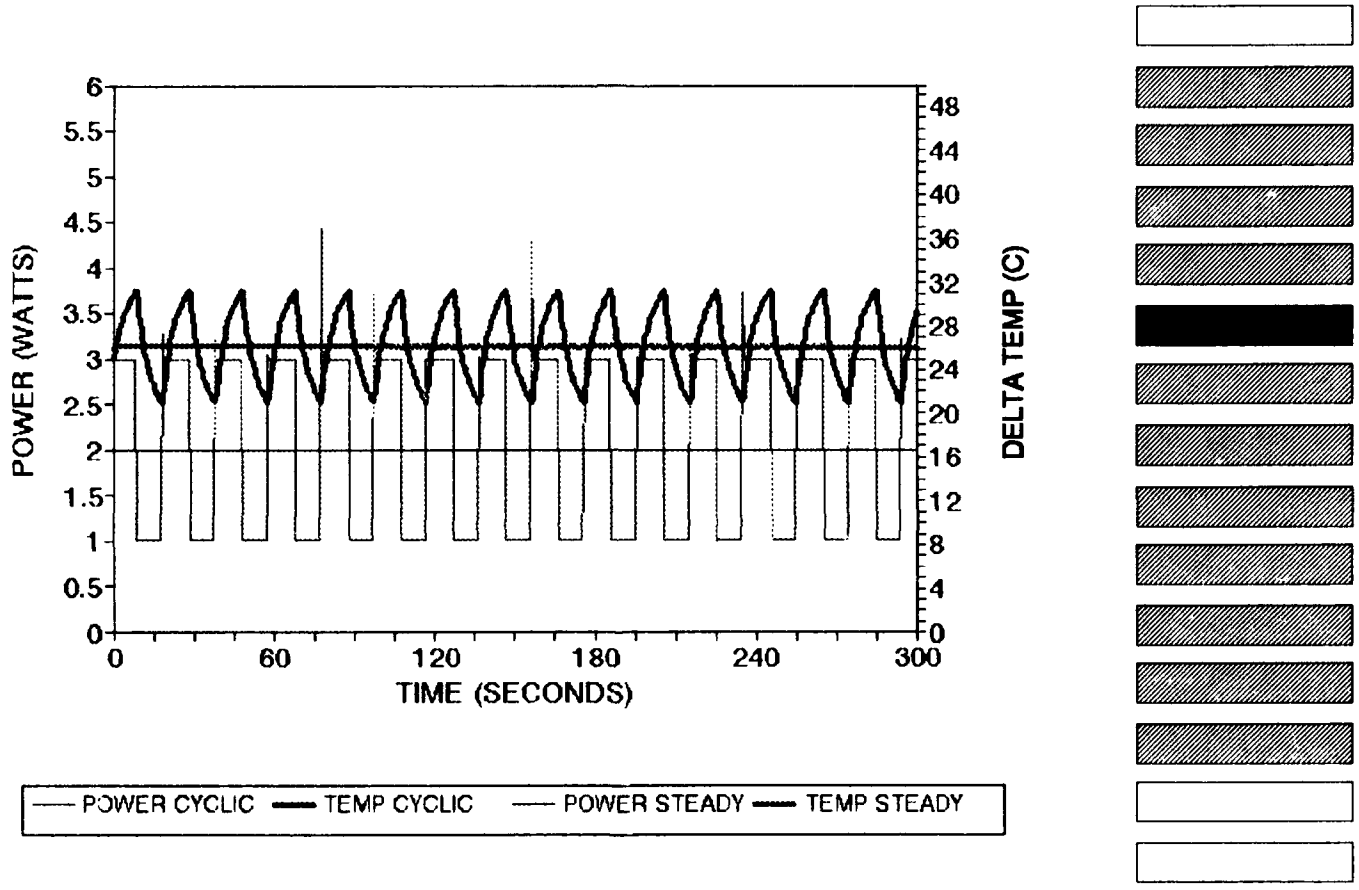

Figure KE. Time dependent transient power and delta temperature for square wave input, middle heater, heater configuration C21, ambient temperature 17.3°C.

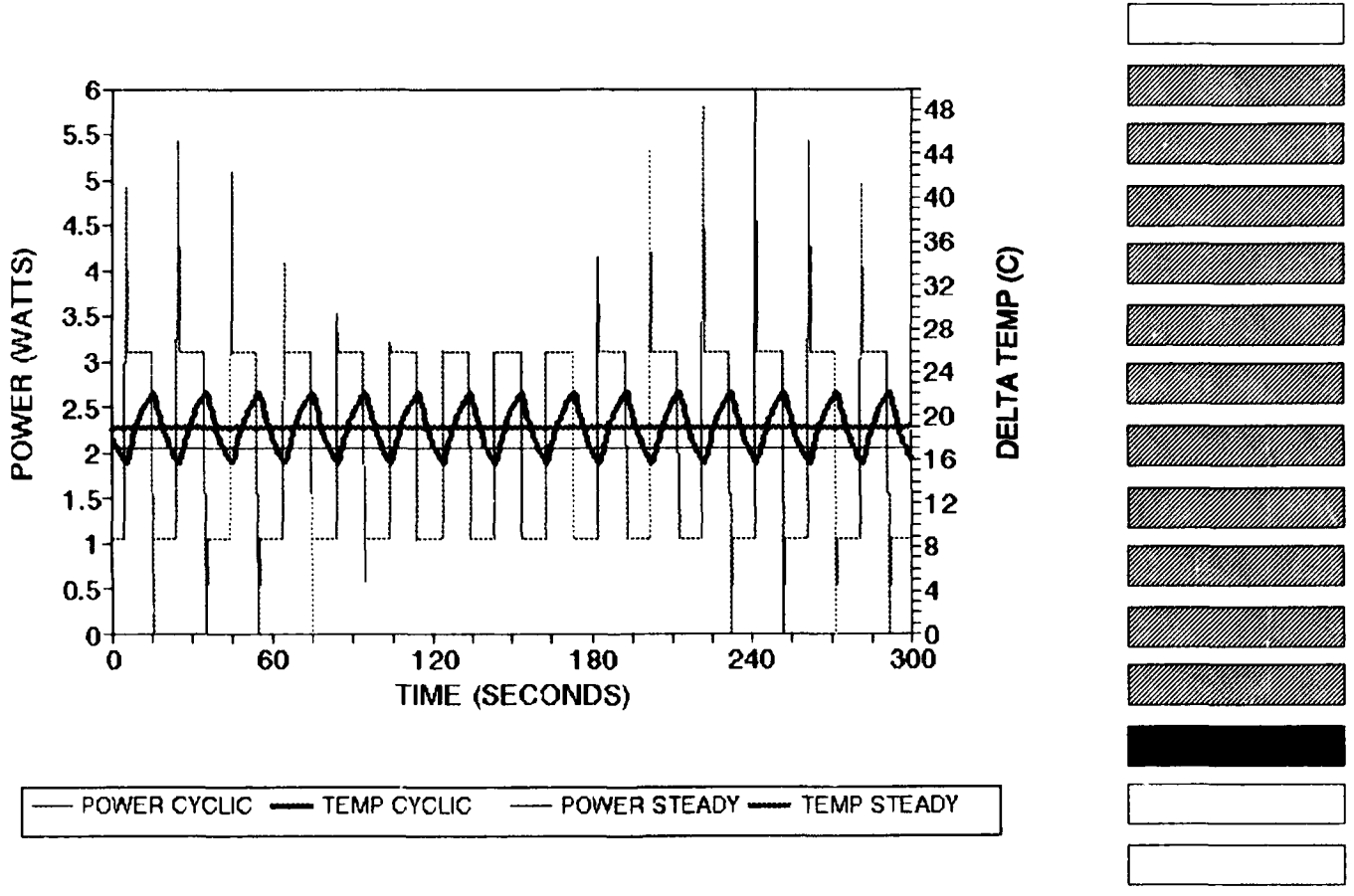

Figure KF. Time dependent transient power and delta temperature for square wave input, bottom heater, heater configuration C28, ambient temperature 17.3°C.

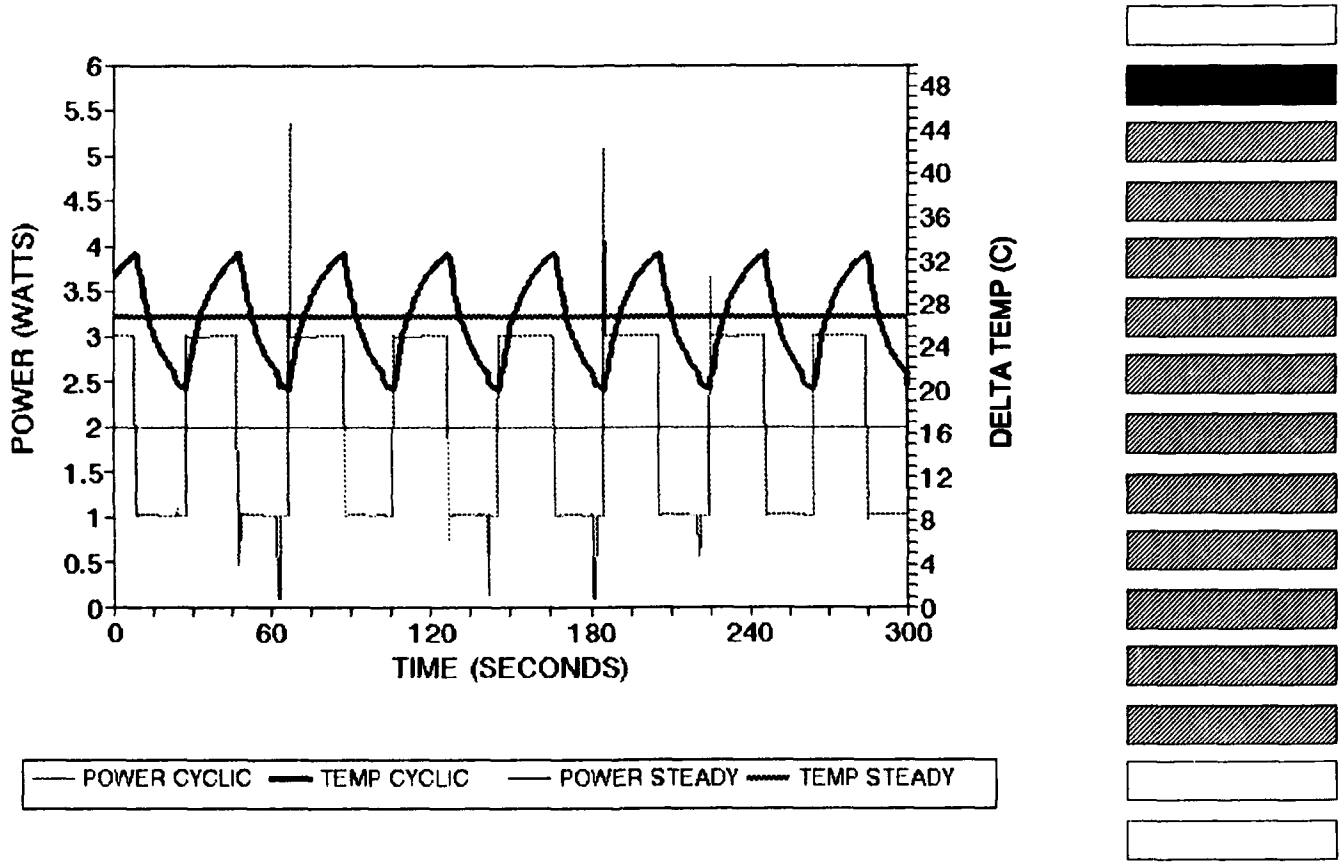

Figure KG. Time dependent transient power and delta temperature for square wave input, top heater, heater configuration C17, ambient temperature 17.4°C.

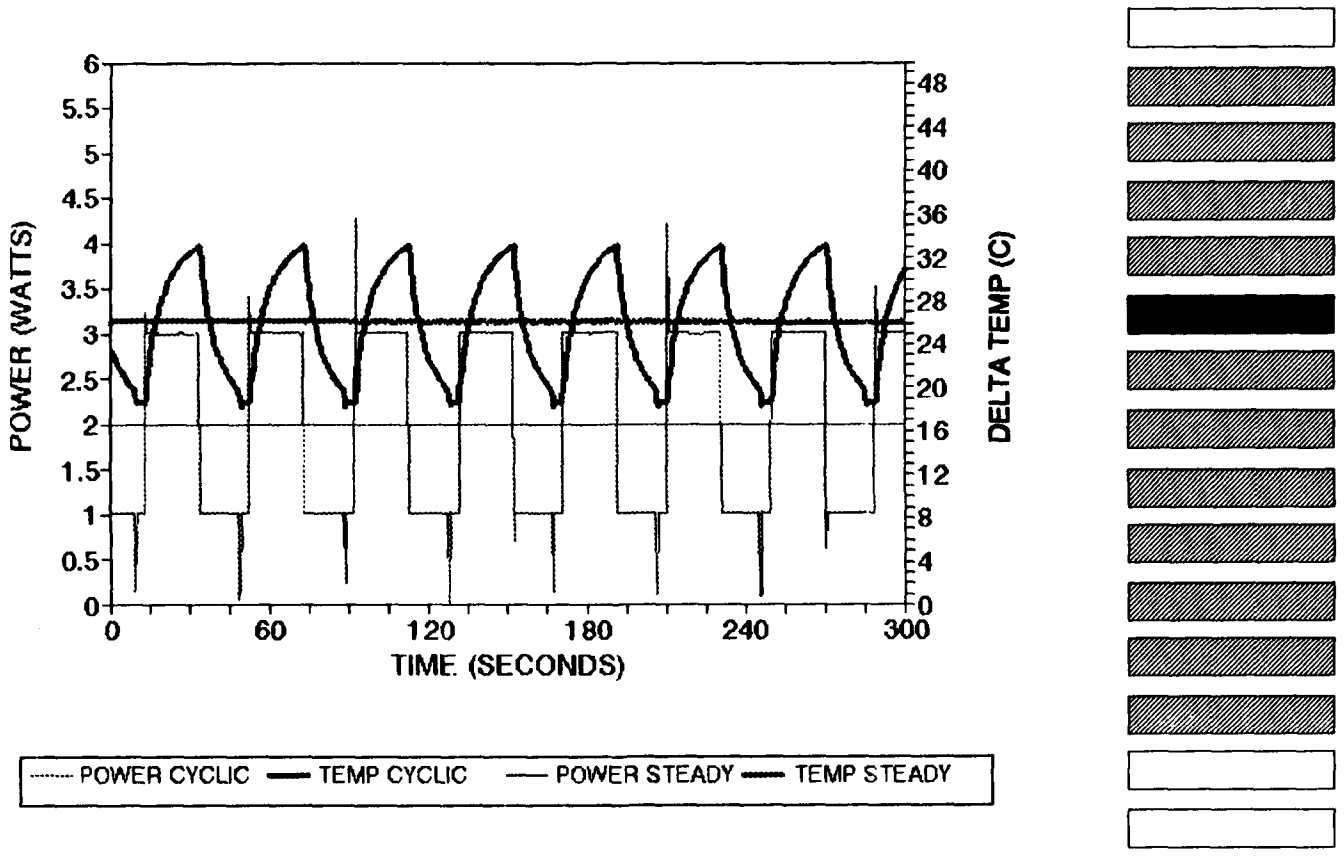

Figure KH. Time dependent transient power and delta temperature for square wave input, middle heater, heater configuration C21, ambient temperature 17.4°C.

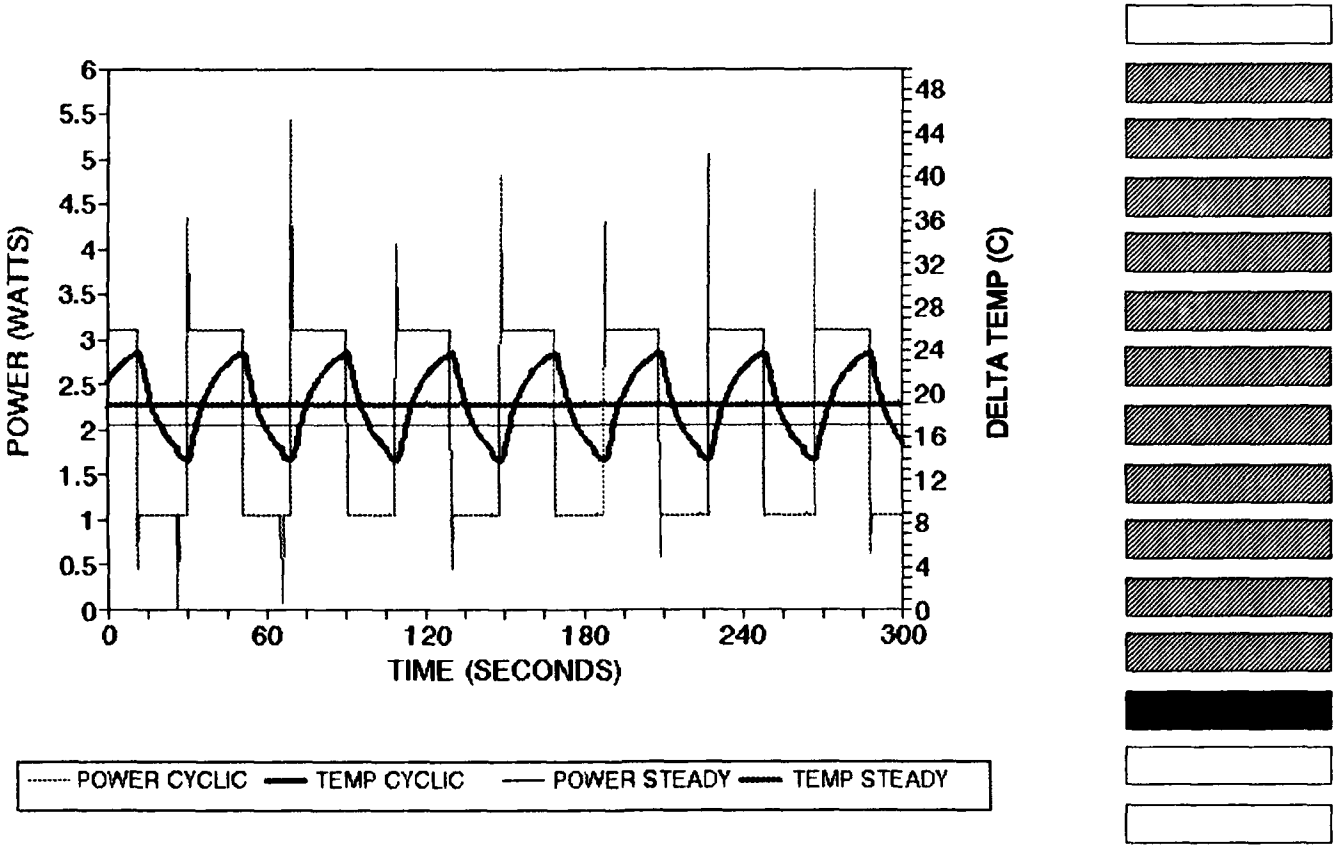

Figure KI. Time dependent transient power and delta temperature for square wave input, bottom heater, heater configuration C28, ambient temperature 17.3°C.

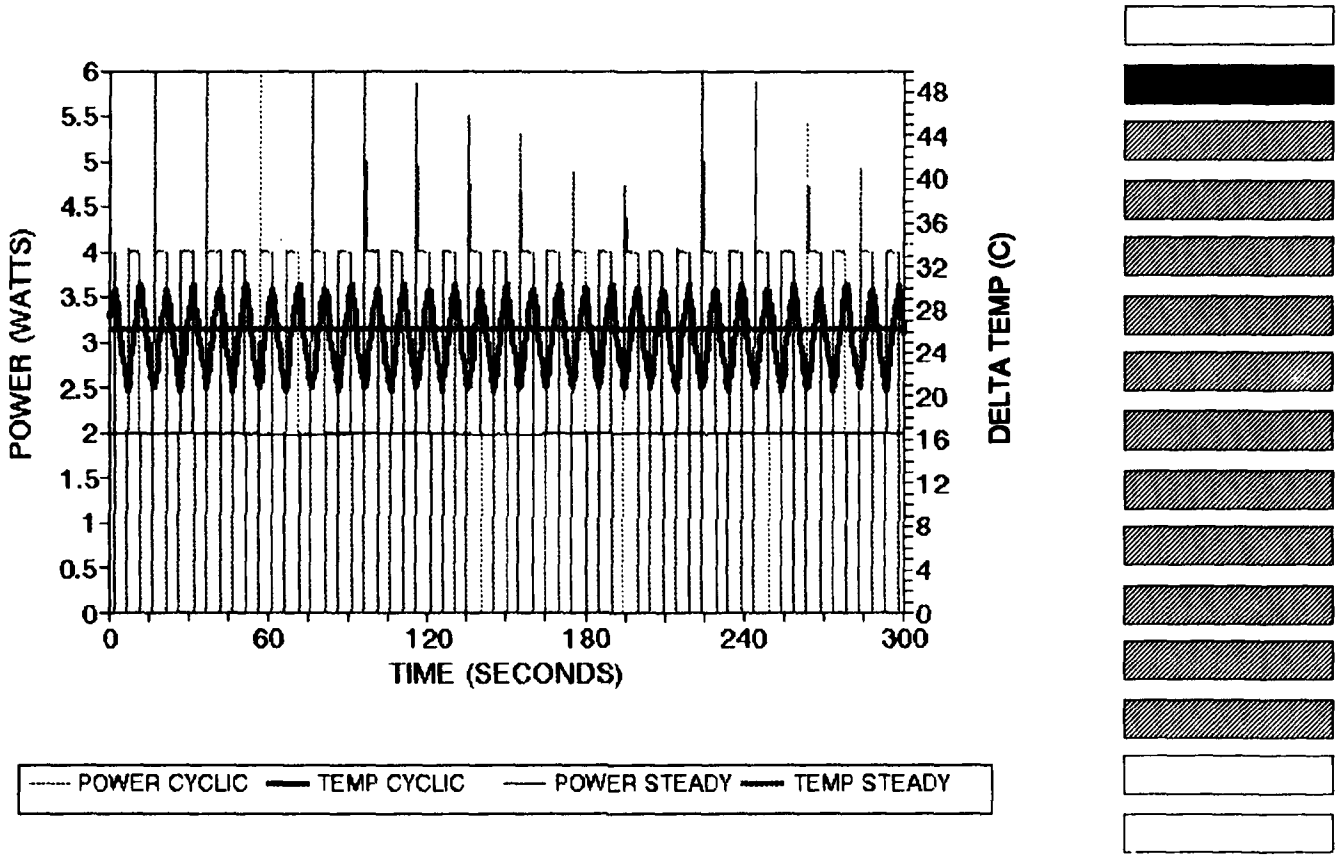

Figure LA. Time dependent transient power and delta temperature for square wave input, top heater, heater configuration C17, ambient temperature 19.6°C.

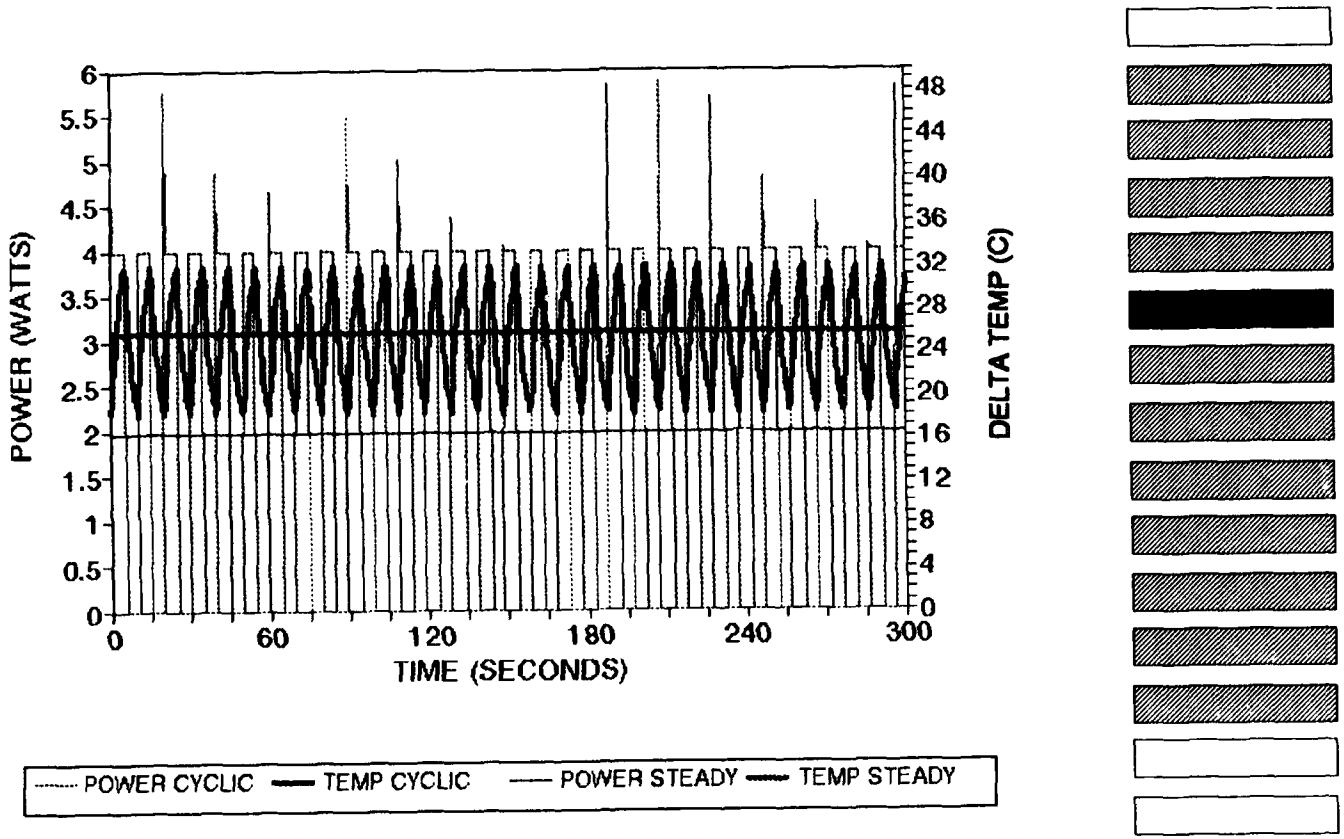

Figure LB. Time dependent transient power and delta temperature for square wave input, middle heater, heater configuration C21, ambient temperature 19.6°C.

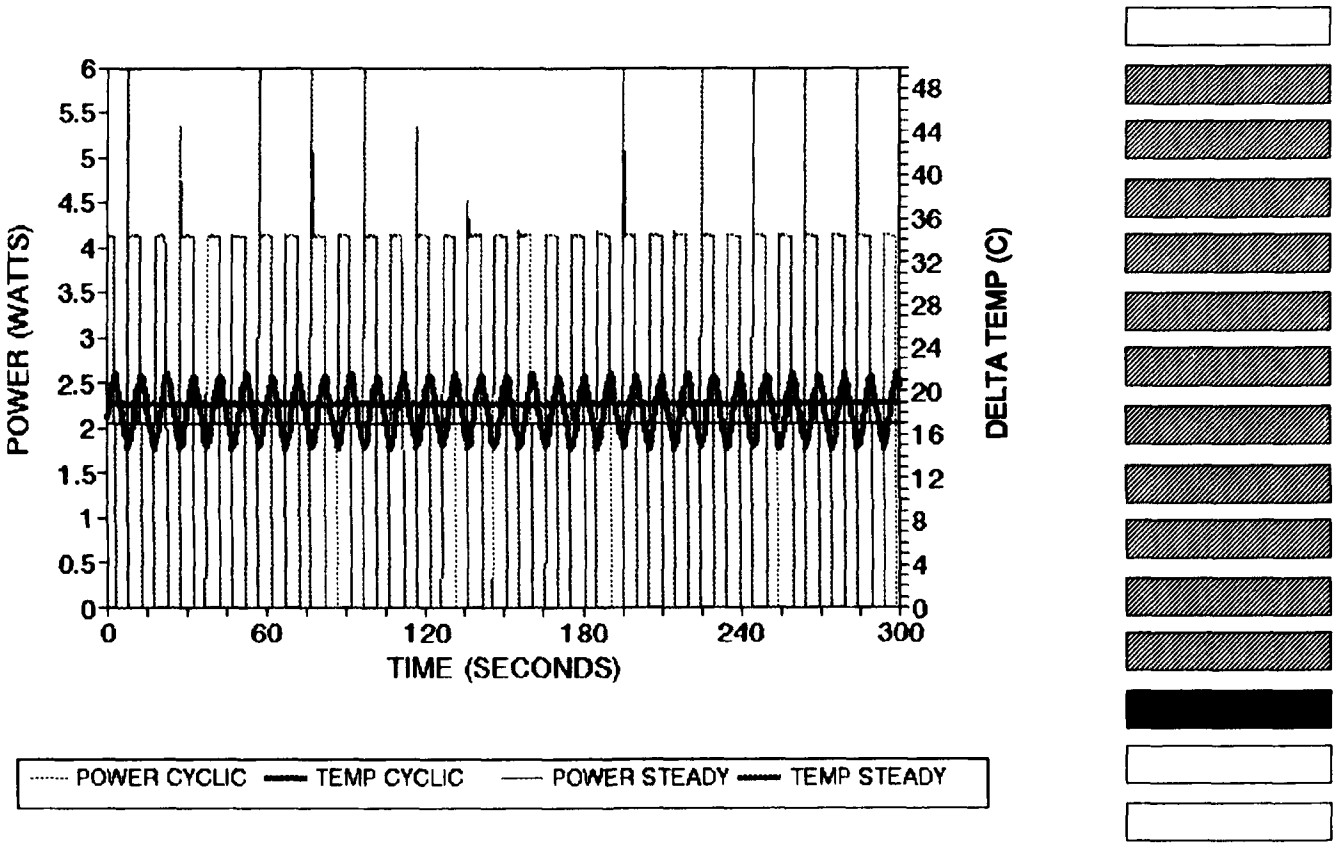

Figure LC. Time dependent transient power and delta temperature for square wave input, bottom heater, heater configuration C28, ambient temperature 19.6°C.

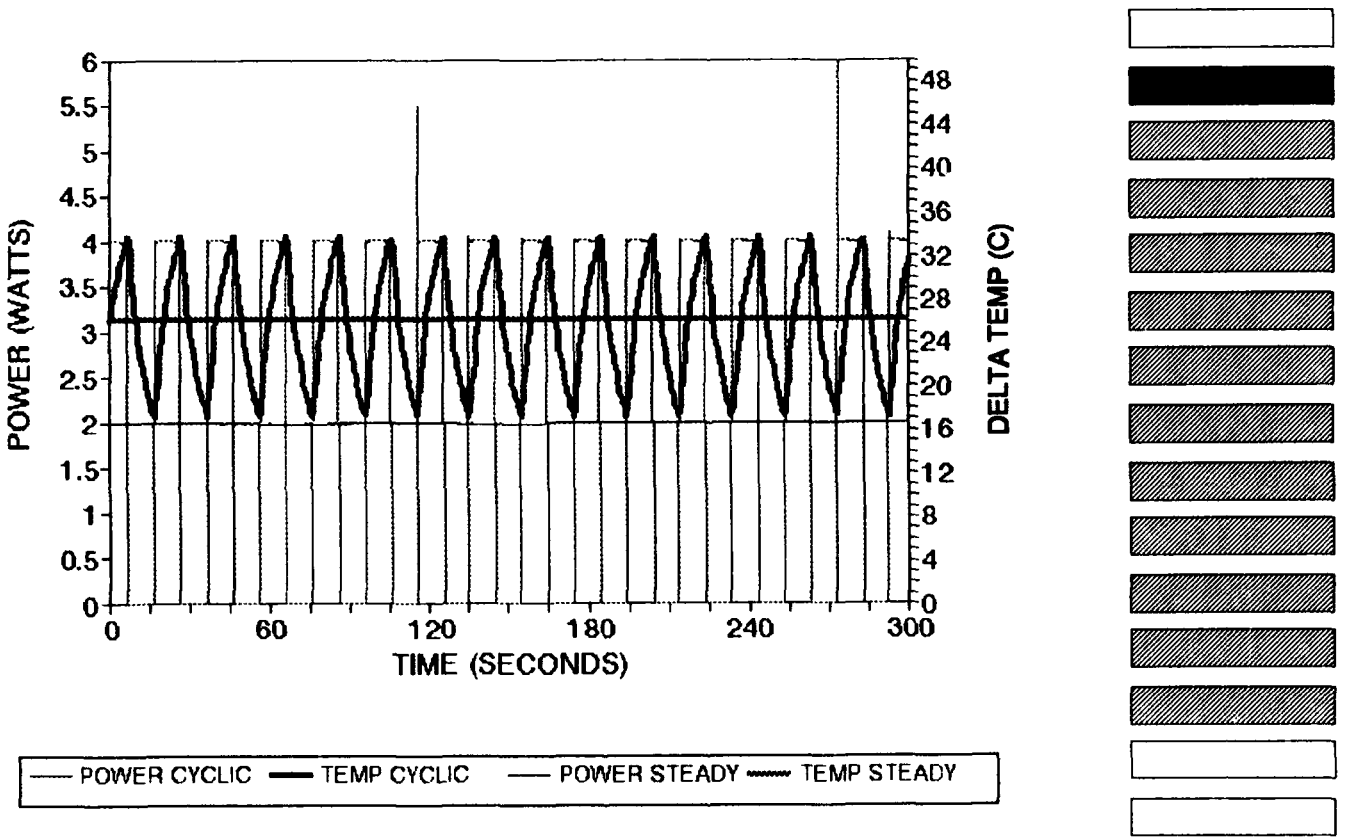

Figure LD. Time dependent transient power and delta temperature for square wave input, top heater, heater configuration C17, ambient temperature 19.6°C.

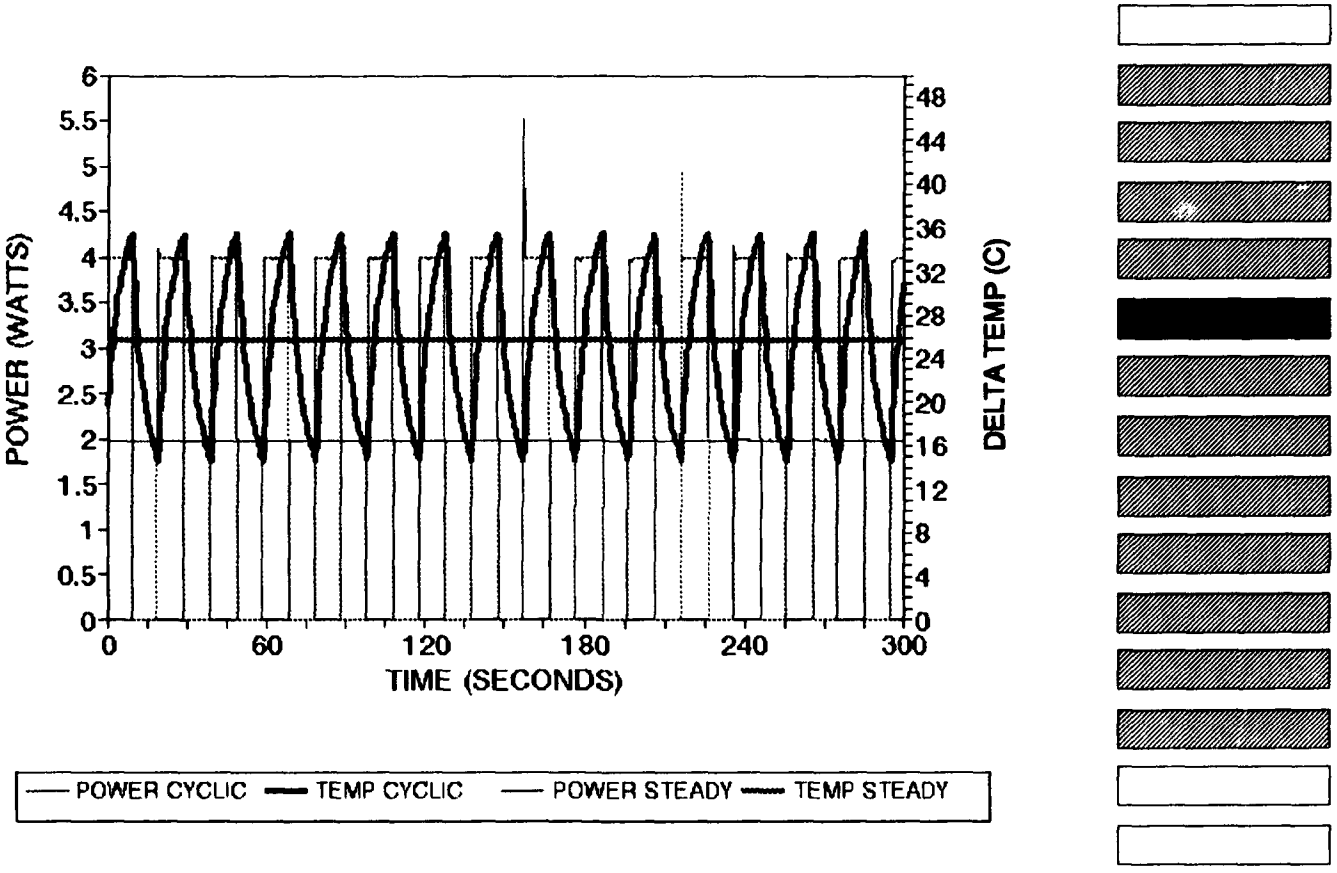

Figure LE. Time dependent transient power and delta temperature for square wave input, middle heater, heater configuration C21, ambient temperature 19.6°C.

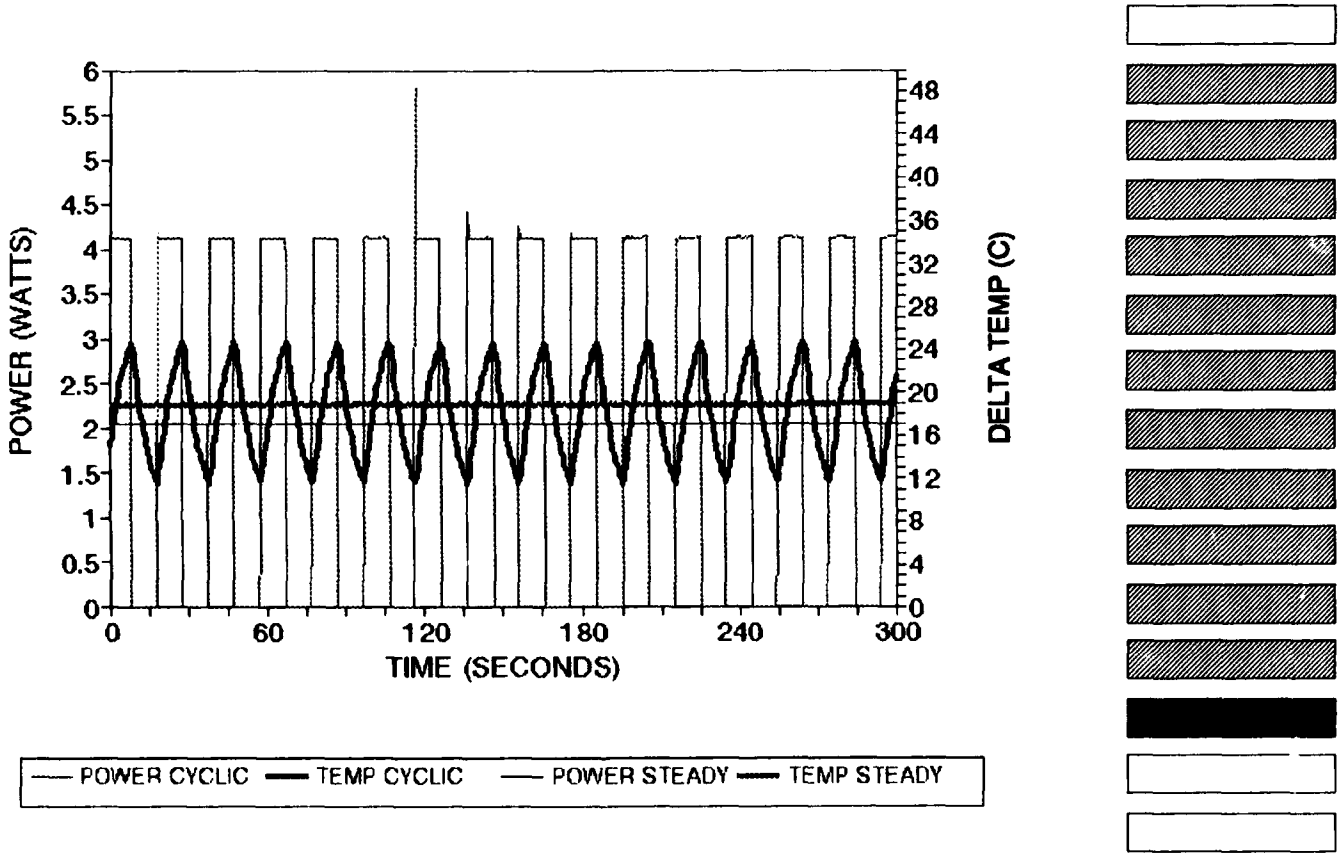

Figure LF. Time dependent transient power and delta temperature for square wave input, bottom heater, heater configuration C28, ambient temperature 19.6°C.

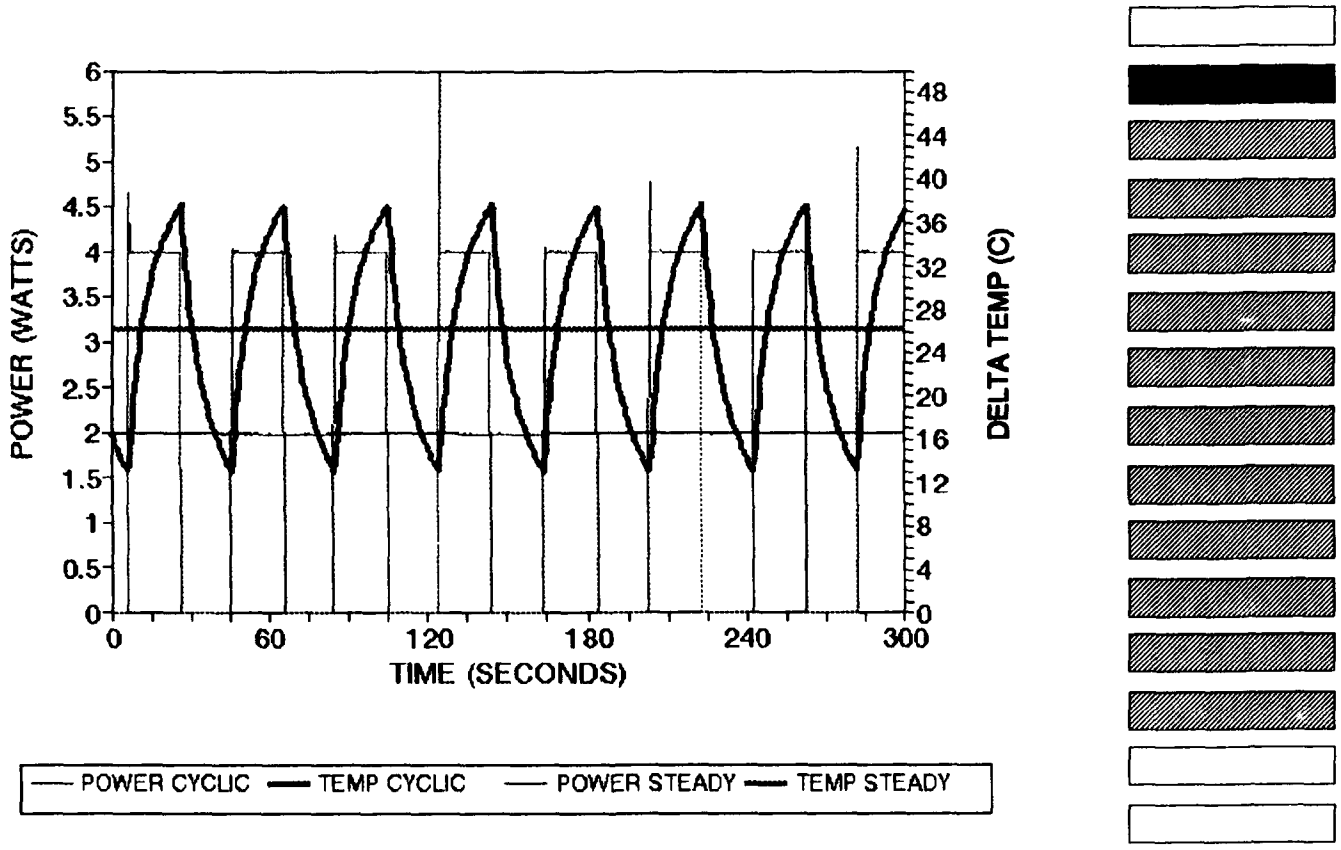

Figure LG. Time dependent transient power and delta temperature for square wave input, top heater, heater configuration C17, ambient temperature 19.6°C.

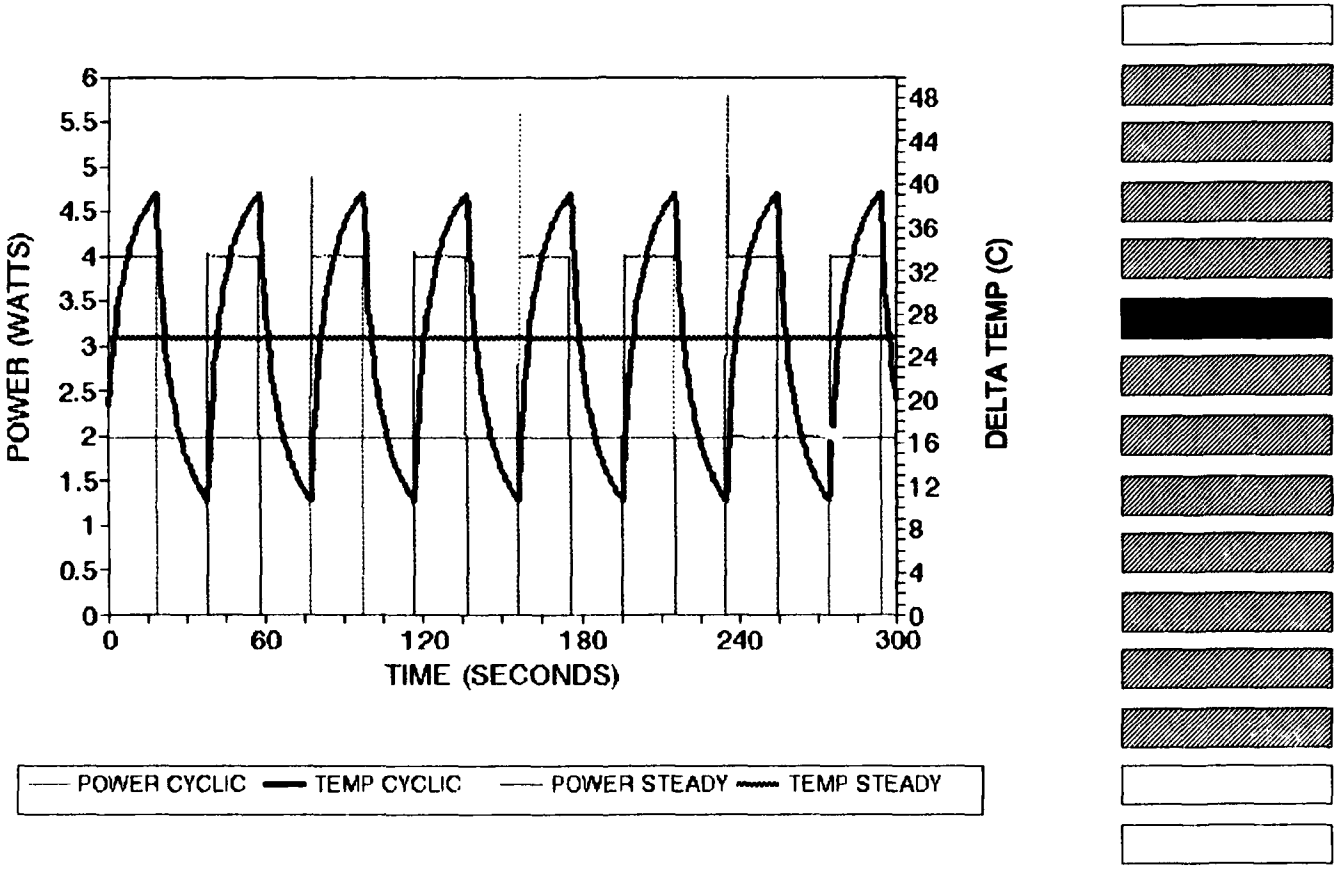

Figure LH. Time dependent transient power and delta temperature for square wave input, middle heater, heater configuration C21, ambient temperature 19.6°C.

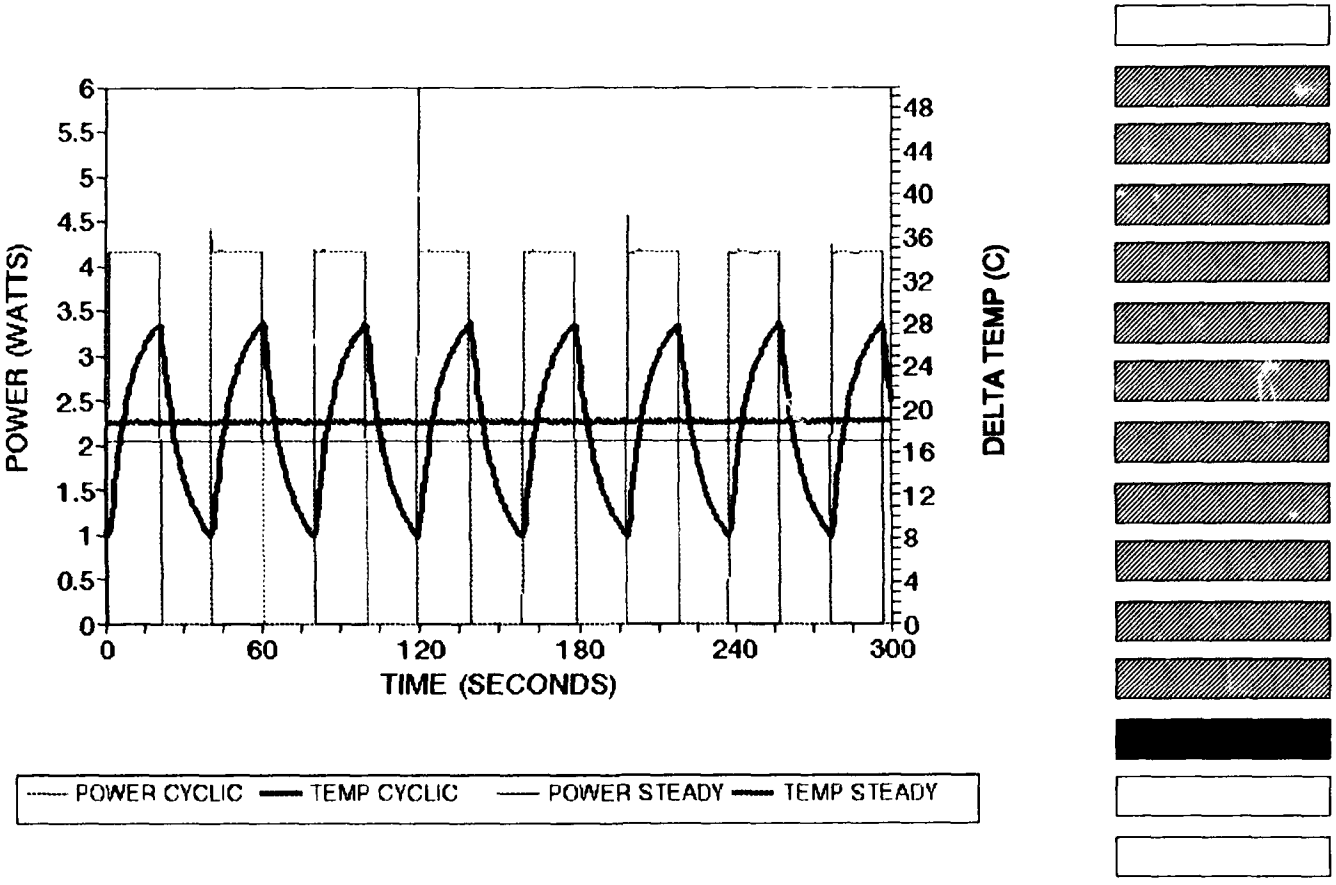

Figure LI. Time dependent transient power and delta temperature for square wave input, bottom heater, heater configuration C28, ambient temperature 19.6°C.

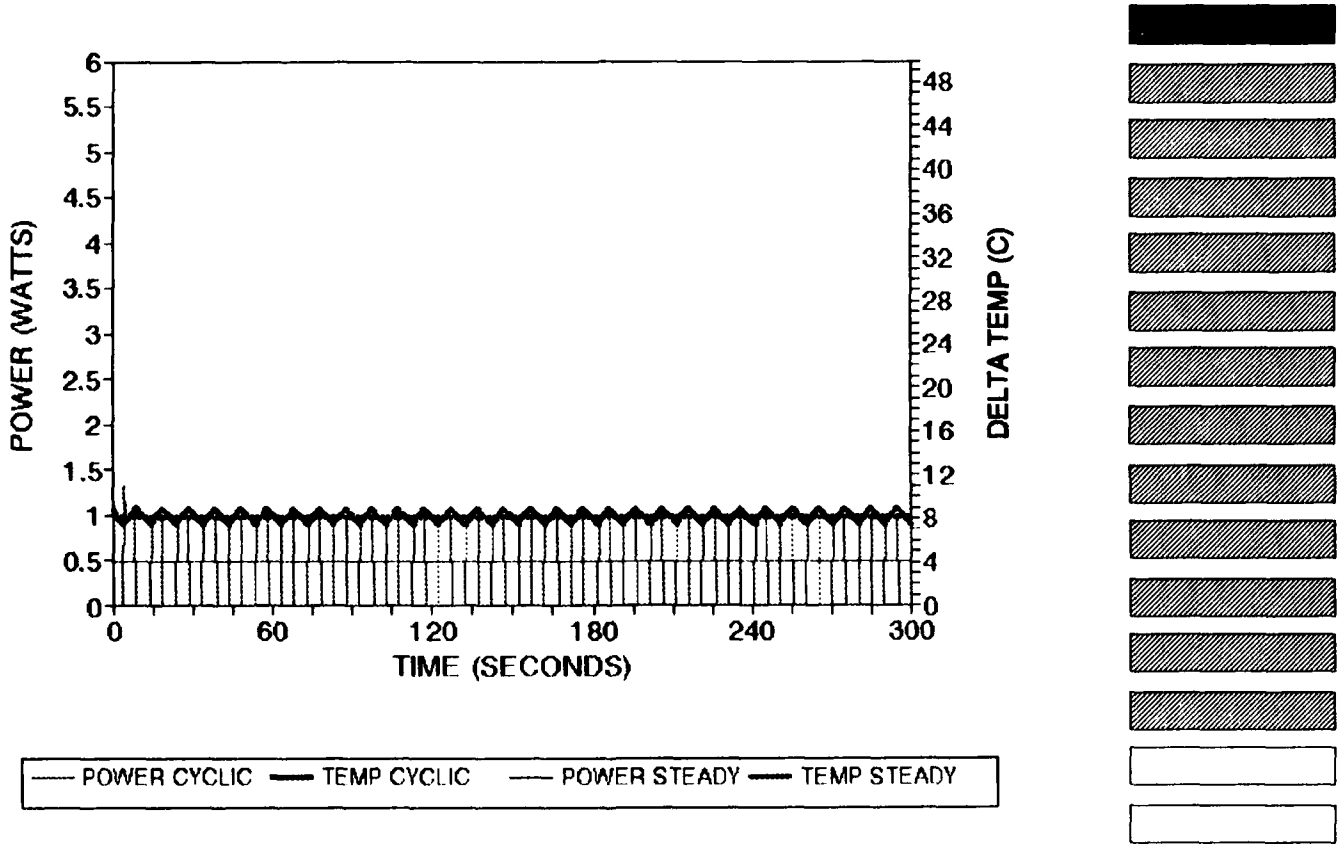

Figure MA. Time dependent transient power and delta temperature for square wave input, top heater, heater configuration B16, ambient temperature 18.1°C.

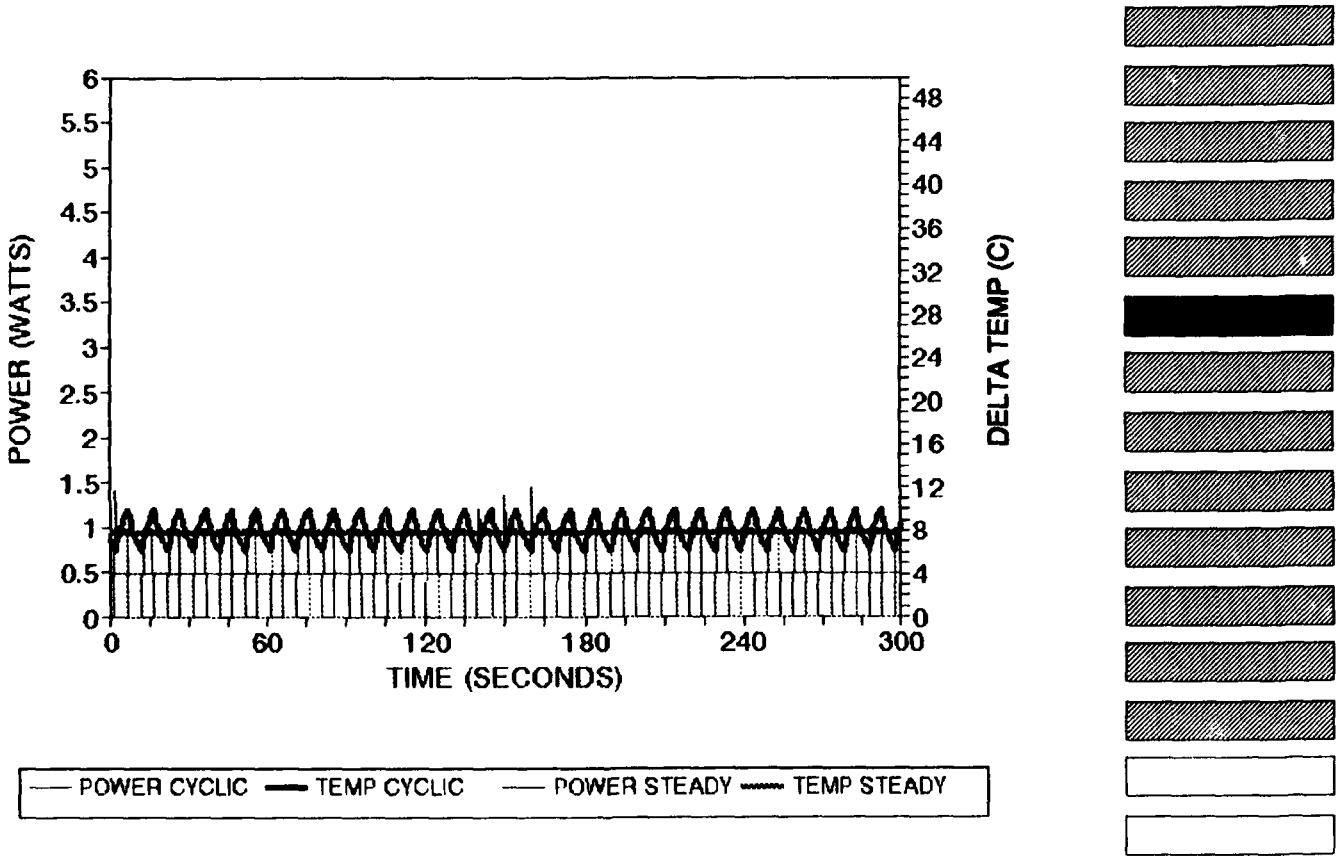

Figure MB. Time dependent transient power and delta temperature for square wave input, middle heater, heater configuration B21, ambient temperature 18.1°C.

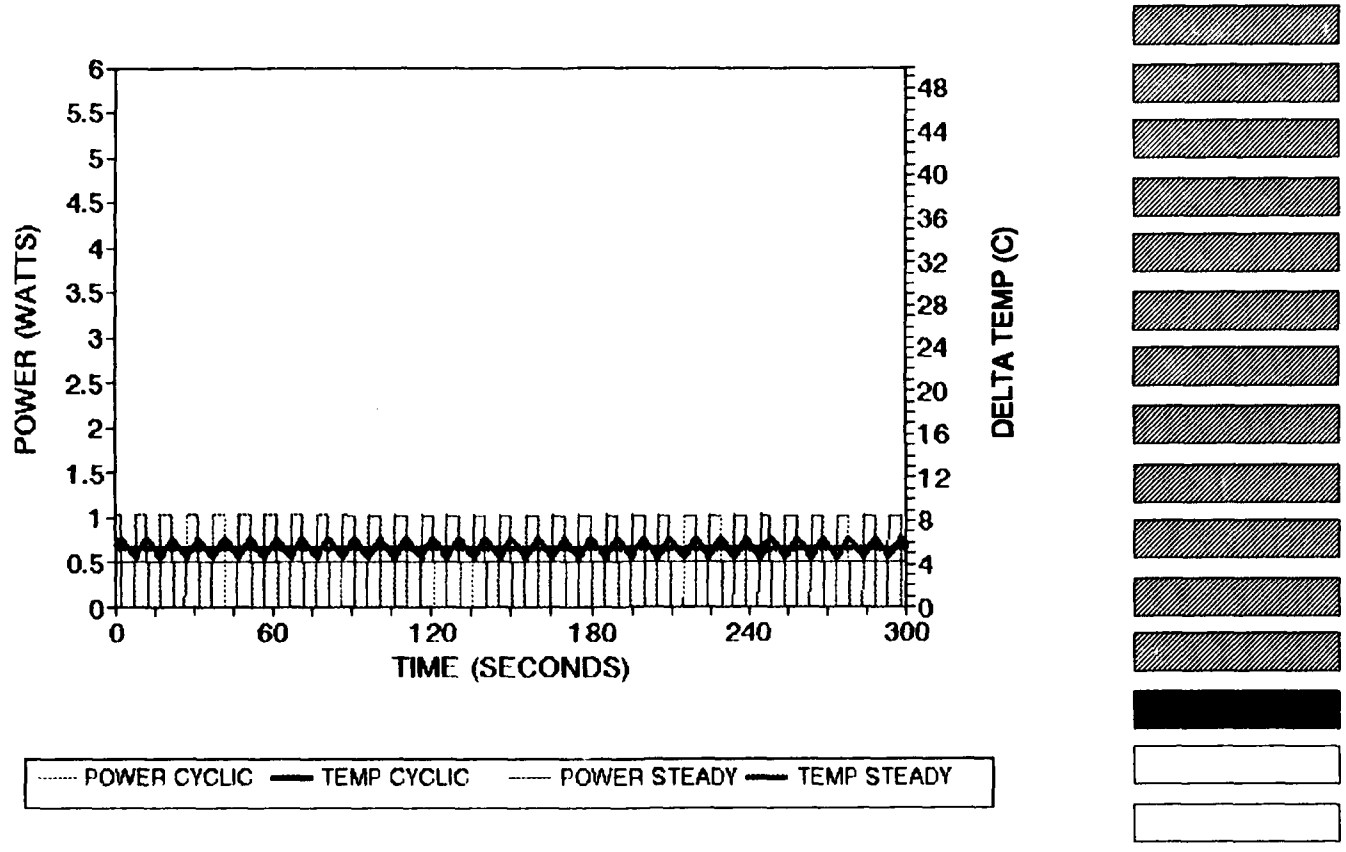

Figure MC. Time dependent transient power and delta temperature for square wave input, bottom heater, heater configuration B28, ambient temperature 18.1°C.

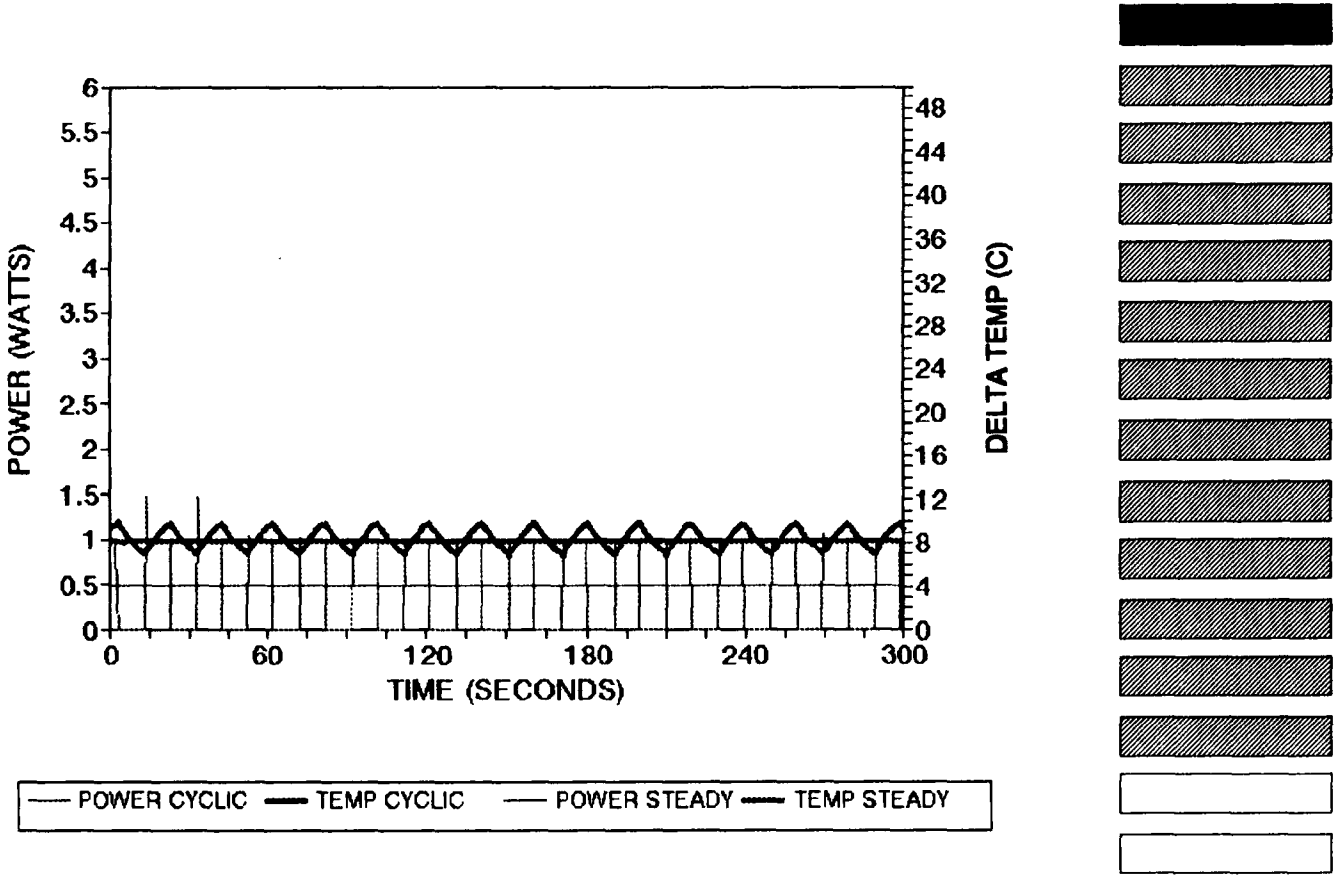

Figure MD. Time dependent transient power and delta temperature for square wave input, top heater, heater configuration B16, ambient temperature 18.1°C.

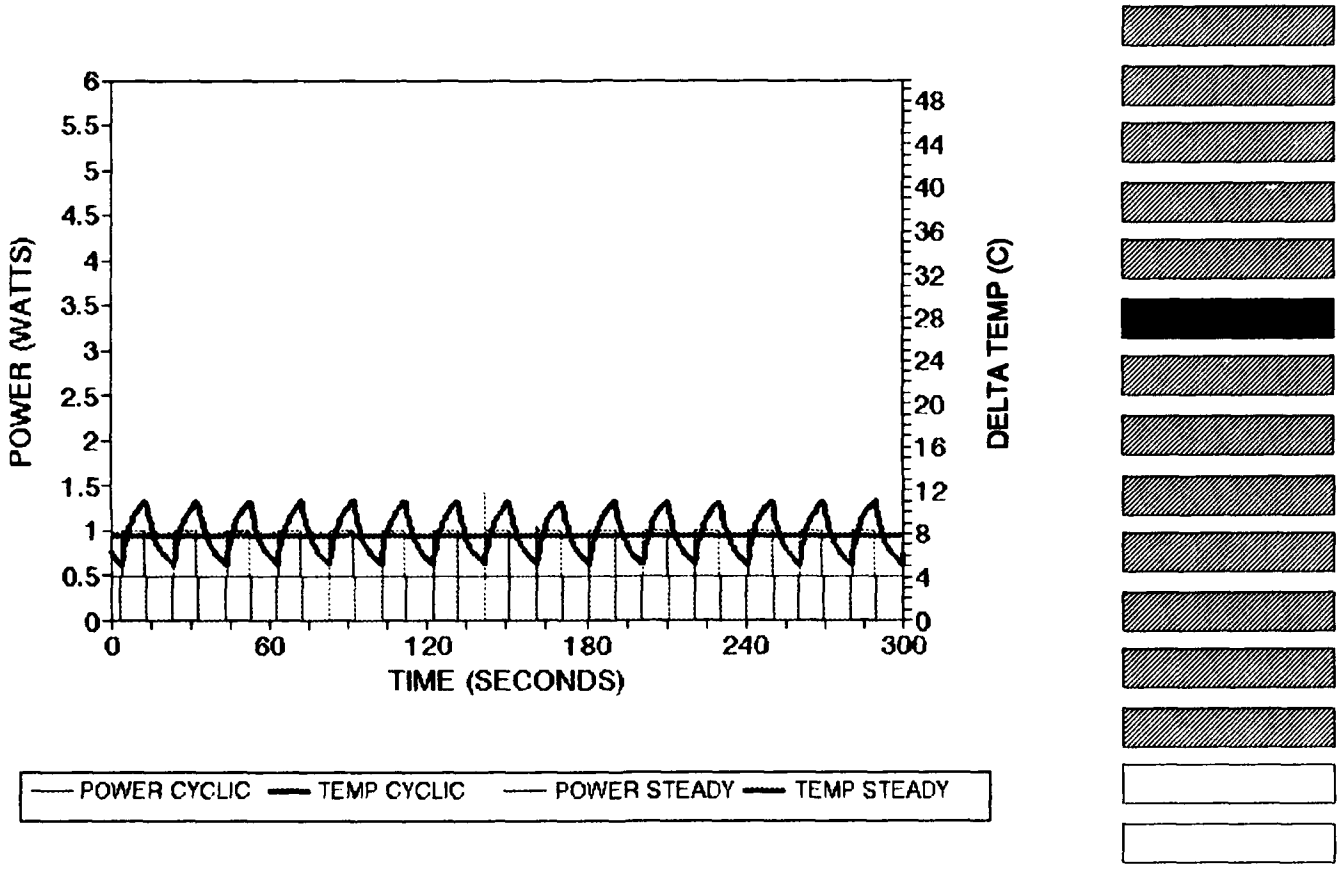

Figure ME. Time dependent transient power and delta temperature for square wave input, middle heater, heater configuration B21, ambient temperature 18.2°C.

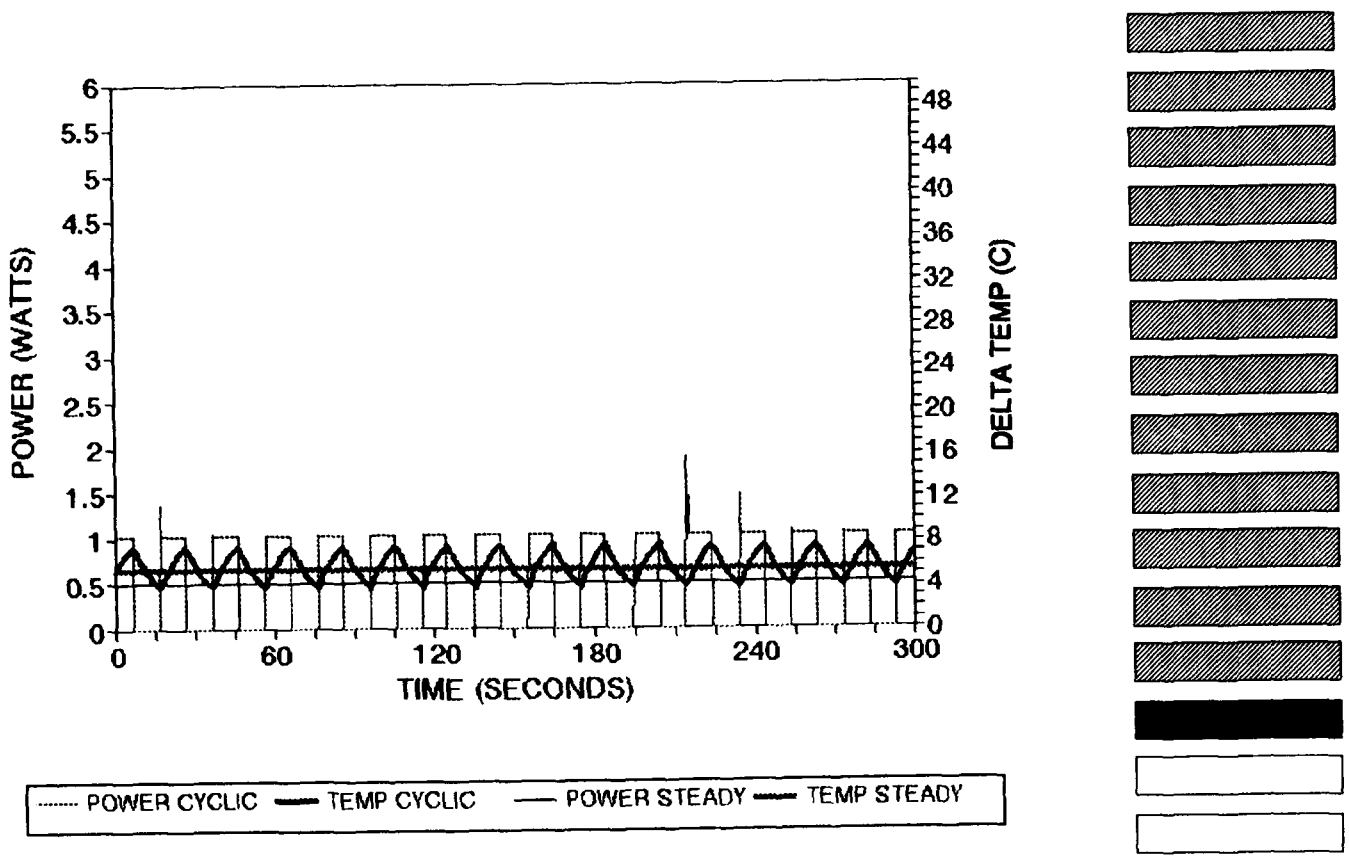

Figure MF. Time dependent transient power and delta temperature for square wave input, bottom heater, heater configuration B28, ambient temperature 18.0°C.

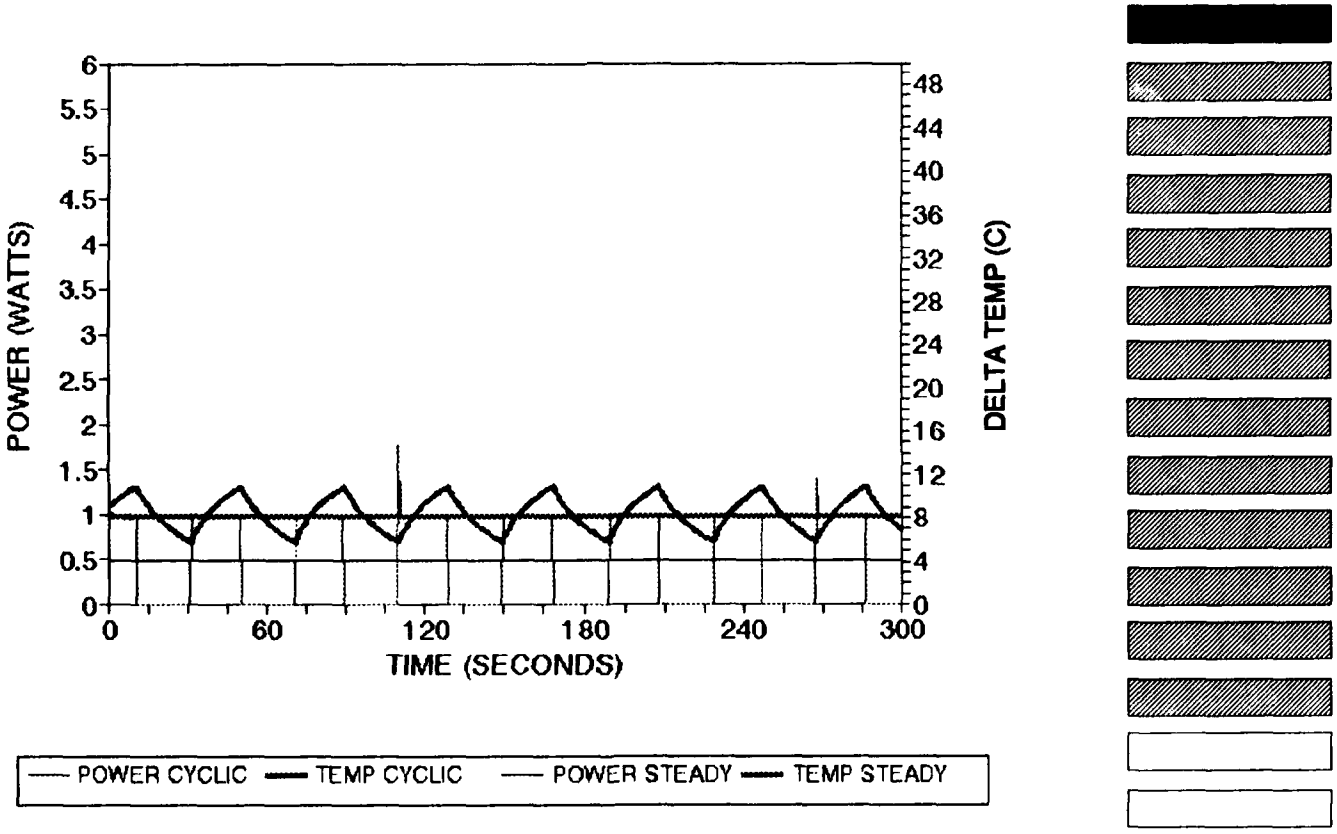

Figure MG. Time dependent transient power and delta temperature for square wave input, top heater, heater configuration B16, ambient temperature 18.2°C.

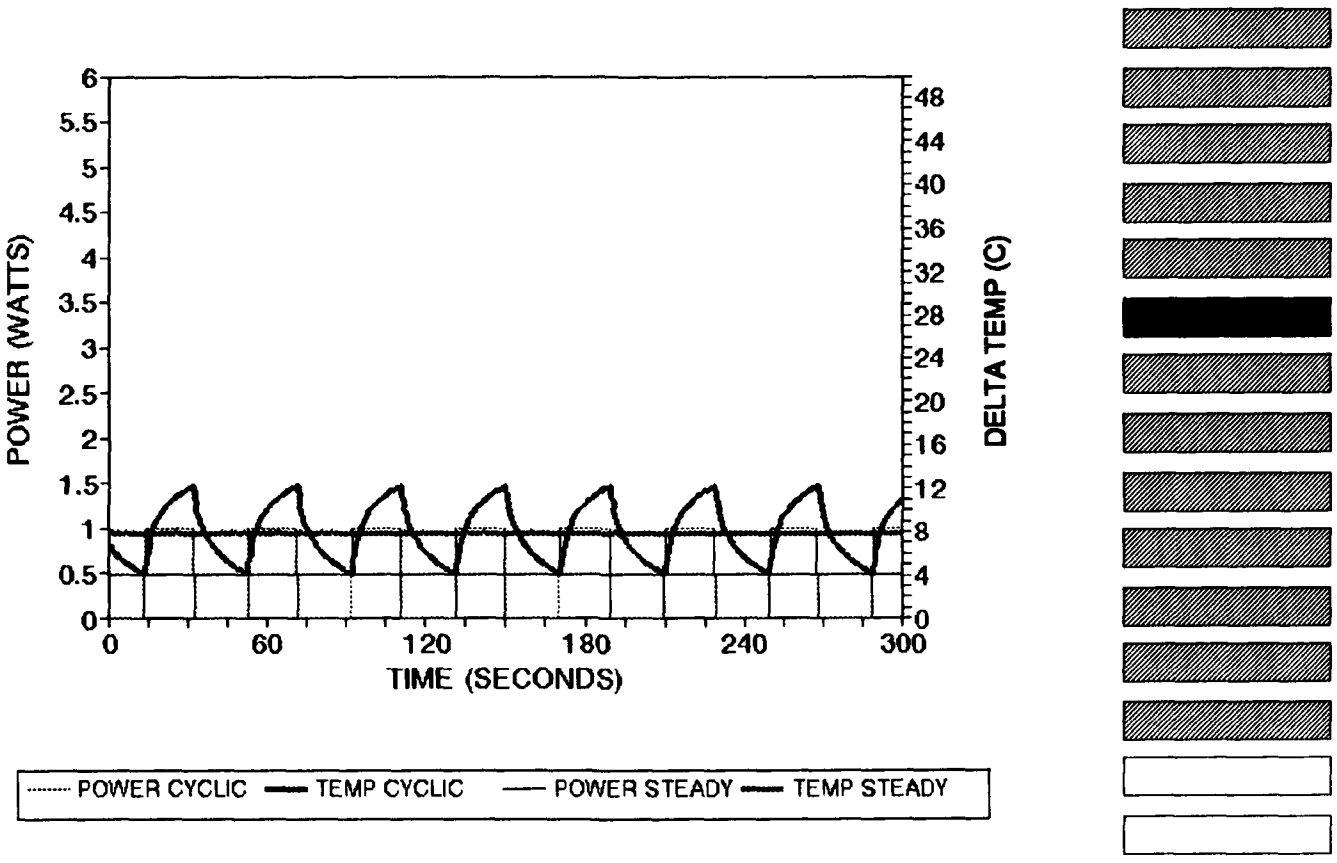

Figure MH. Time dependent transient power and delta temperature for square wave input, middle heater, heater configuration B21, ambient temperature 18.2°C.

Figure MI. Time dependent transient power and delta temperature for square wave input, bottom heater, heater configuration B28, ambient temperature 18.2°C.

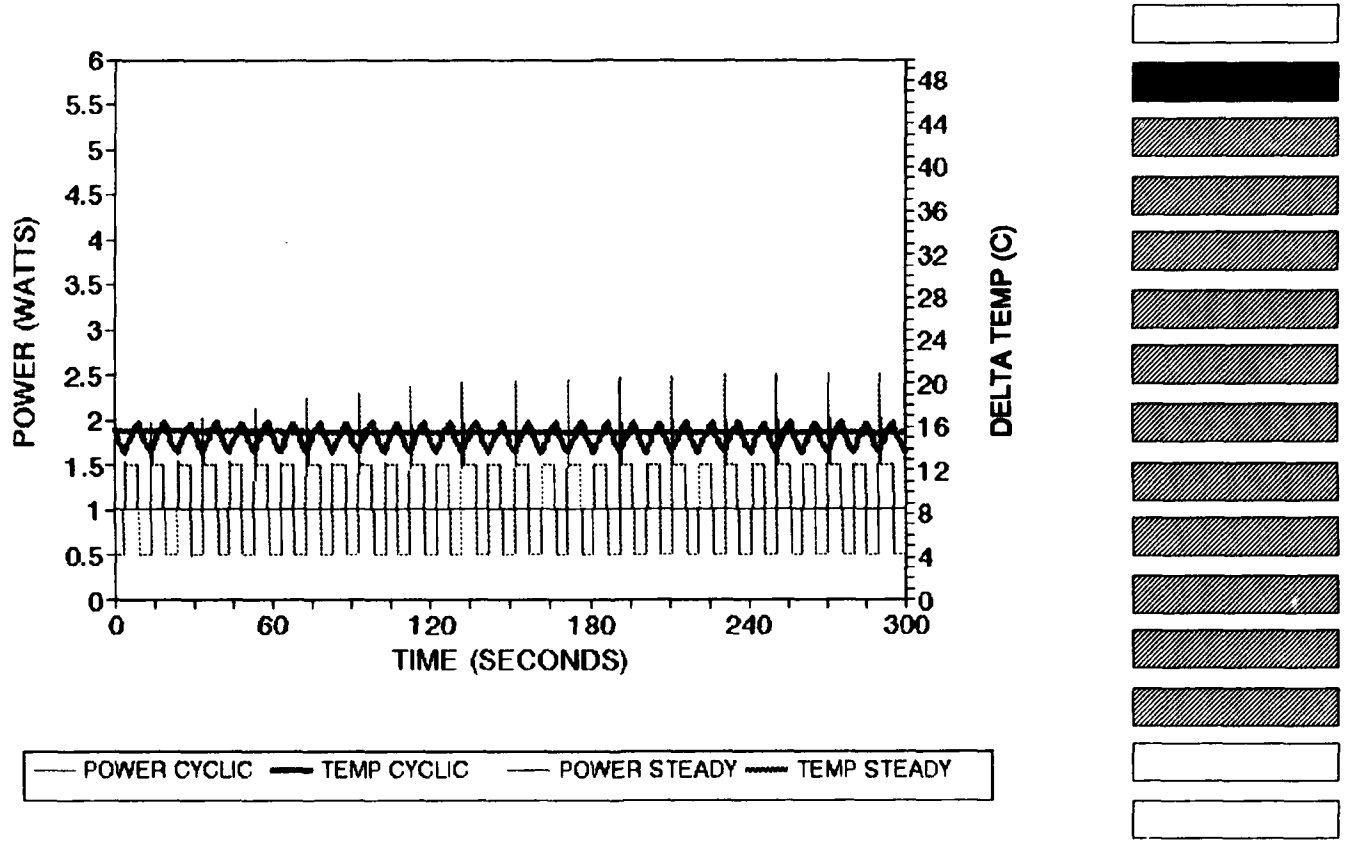

Figure NA. Time dependent transient power and delta temperature for square wave input, top heater, heater configuration C17, ambient temperature 17.3°C.

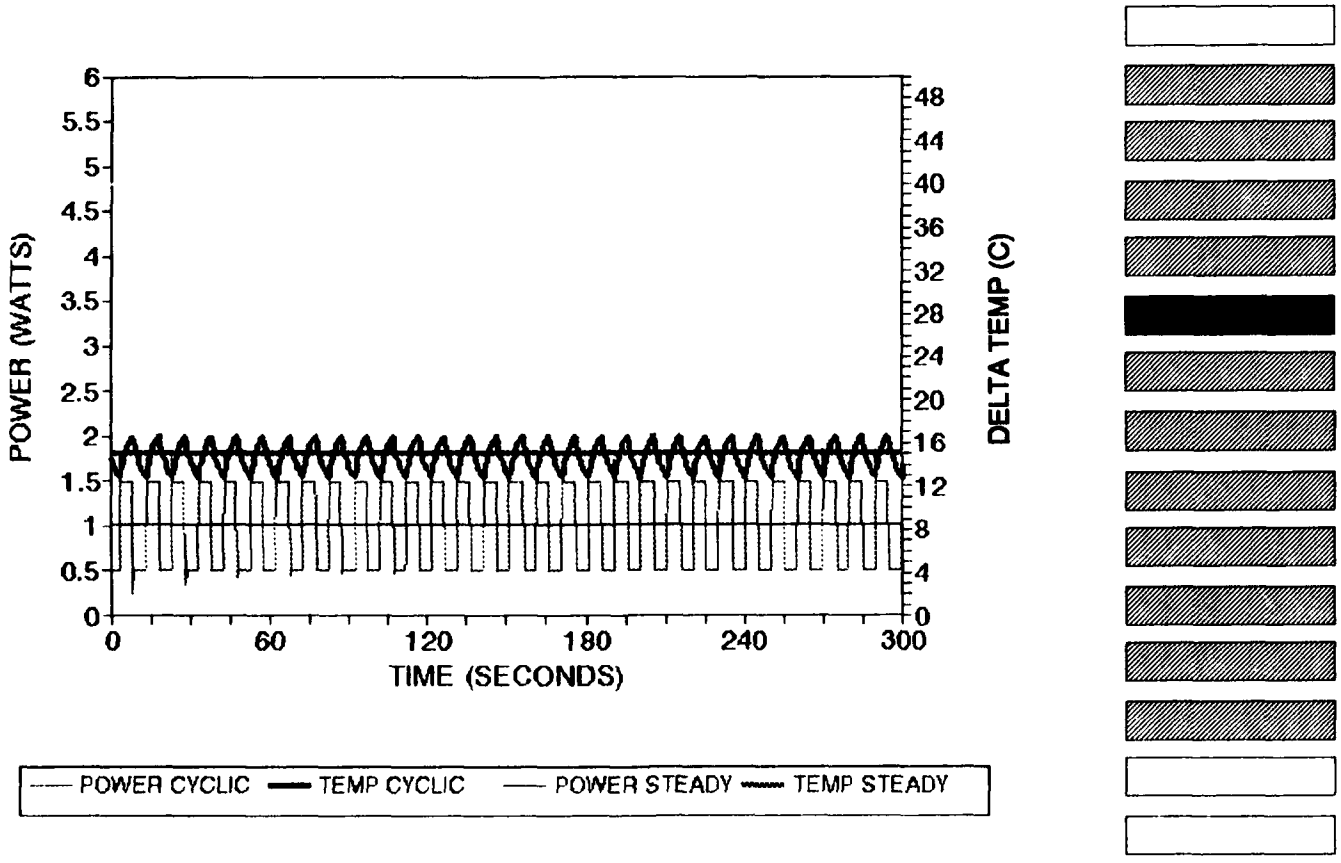

Figure NB. Time dependent transient power and delta temperature for square wave input, middle heater, heater configuration C21, ambient temperature 17.3°C.

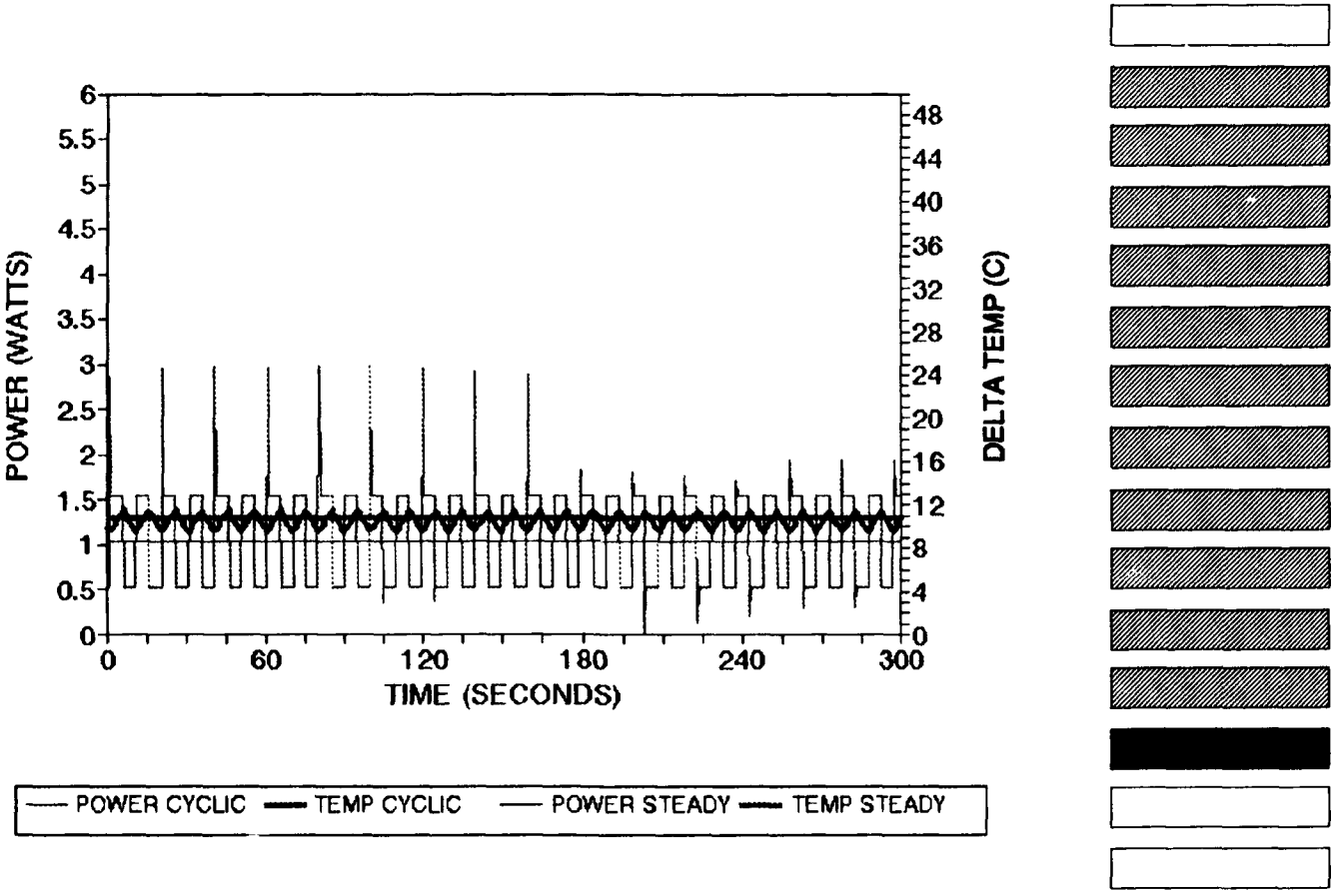

Figure NC. Time dependent transient power and delta temperature for square wave input, bottom heater, heater configuration C28, ambient temperature 17.3°C.

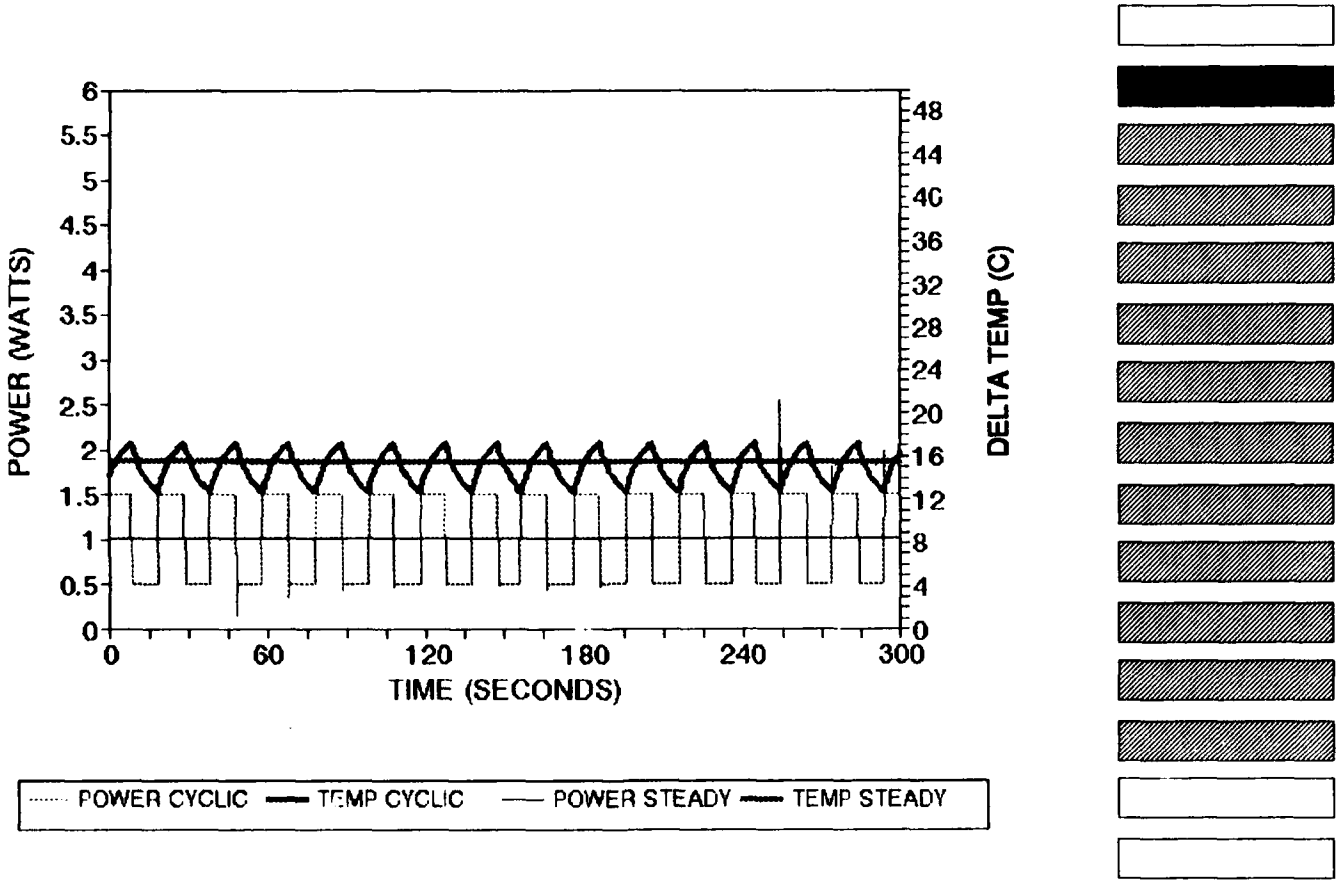

Figure ND. Time dependent transient power and delta temperature for square wave input, top heater, heater configuration C17, ambient temperature 17.4°C.

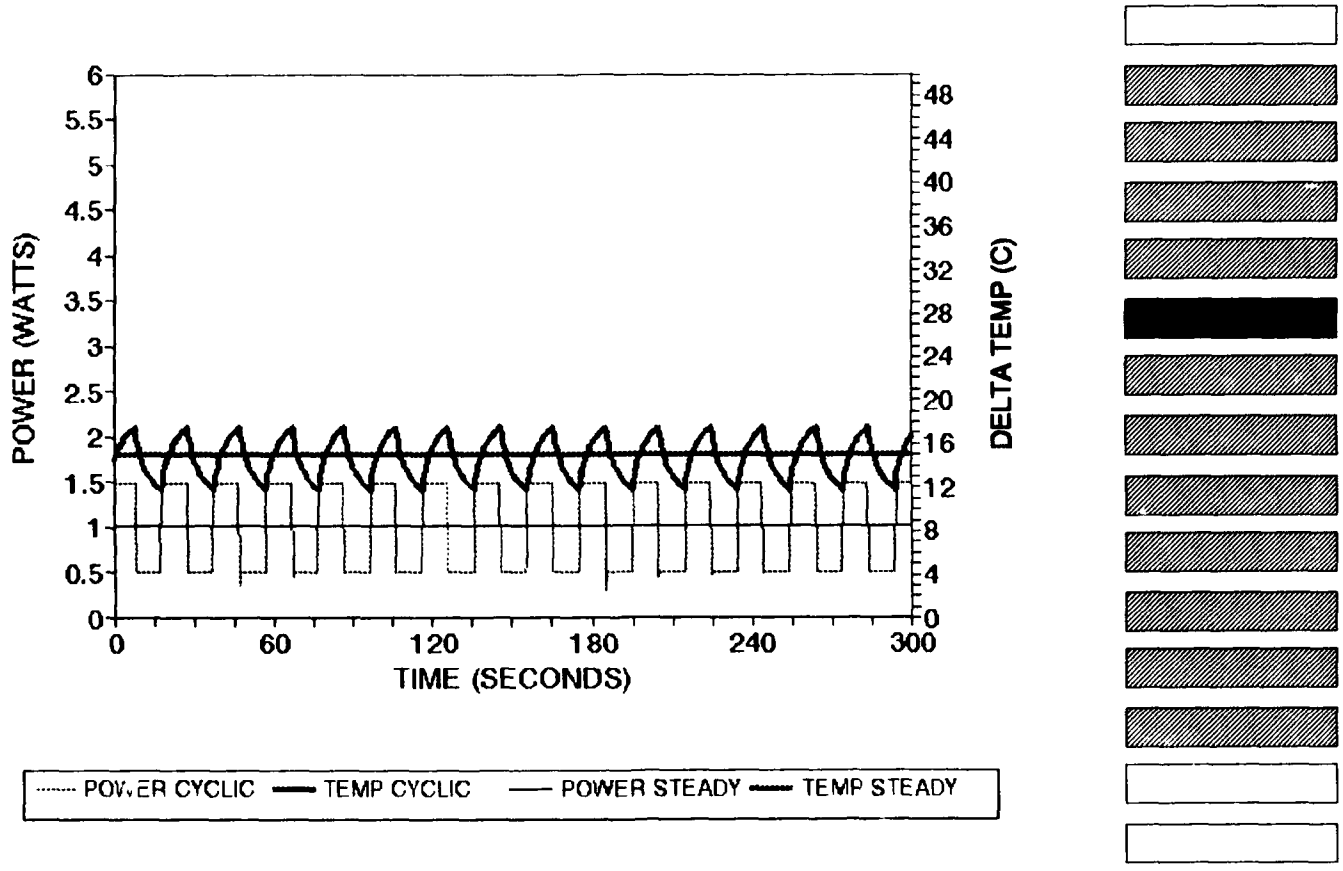

Figure NE. Time dependent transient power and delta temperature for square wave input, middle heater, heater configuration C21, ambient temperature 17.4°C.

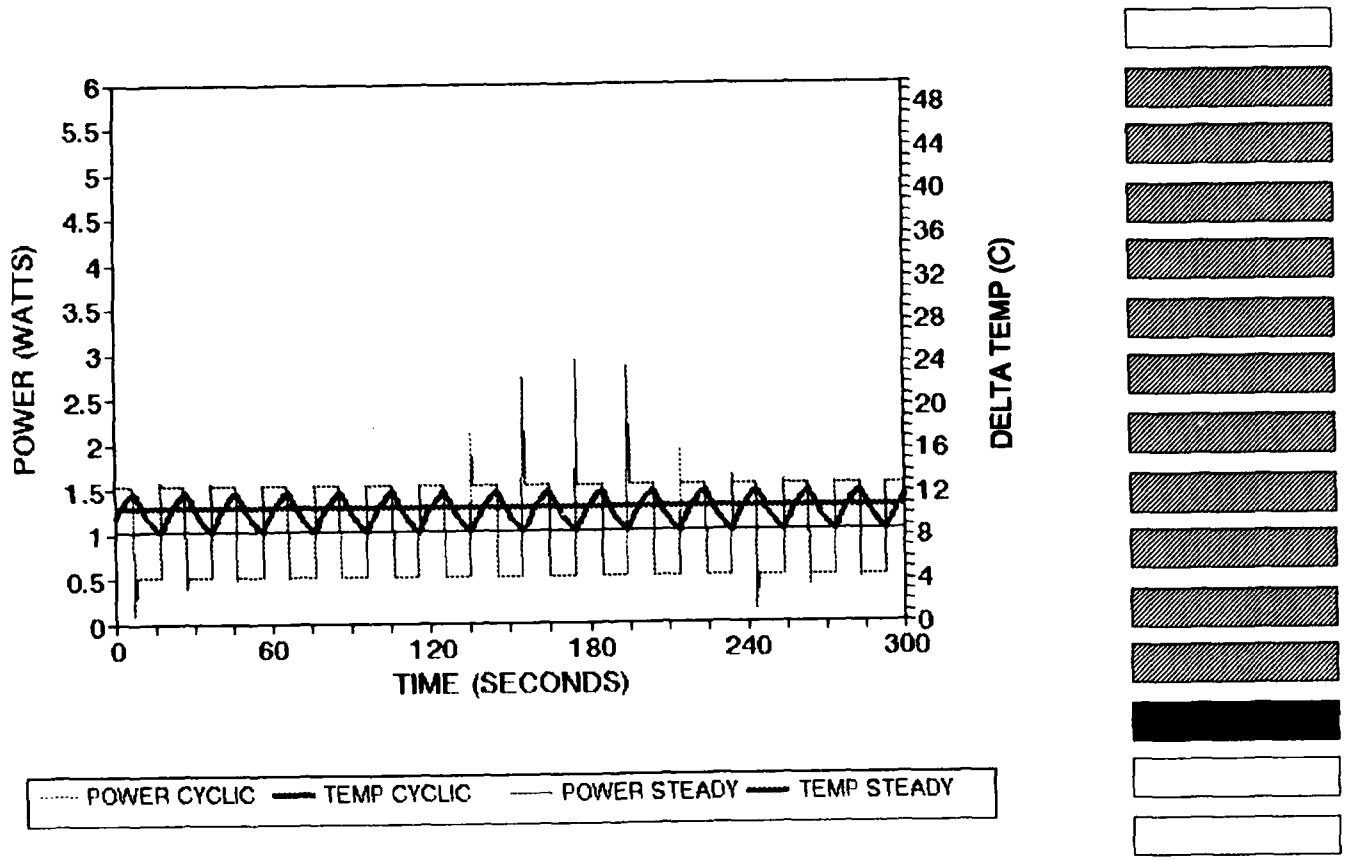

Figure NF. Time dependent transient power and delta temperature for square wave input, bottom heater, heater configuration C28, ambient temperature 17.4°C.

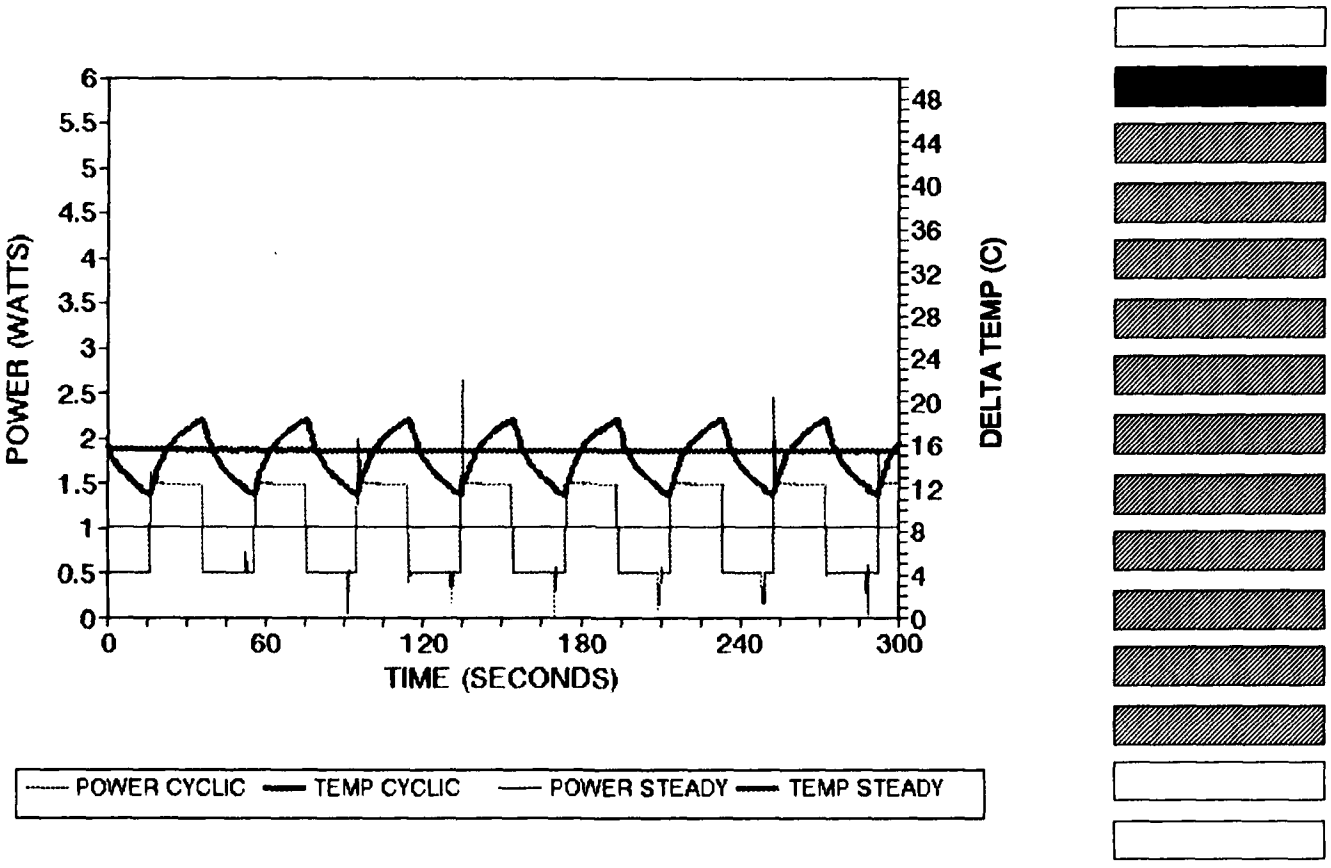

Figure NG. Time dependent transient power and delta temperature for square wave input, top heater, heater configuration C17, ambient temperature 17.4°C.

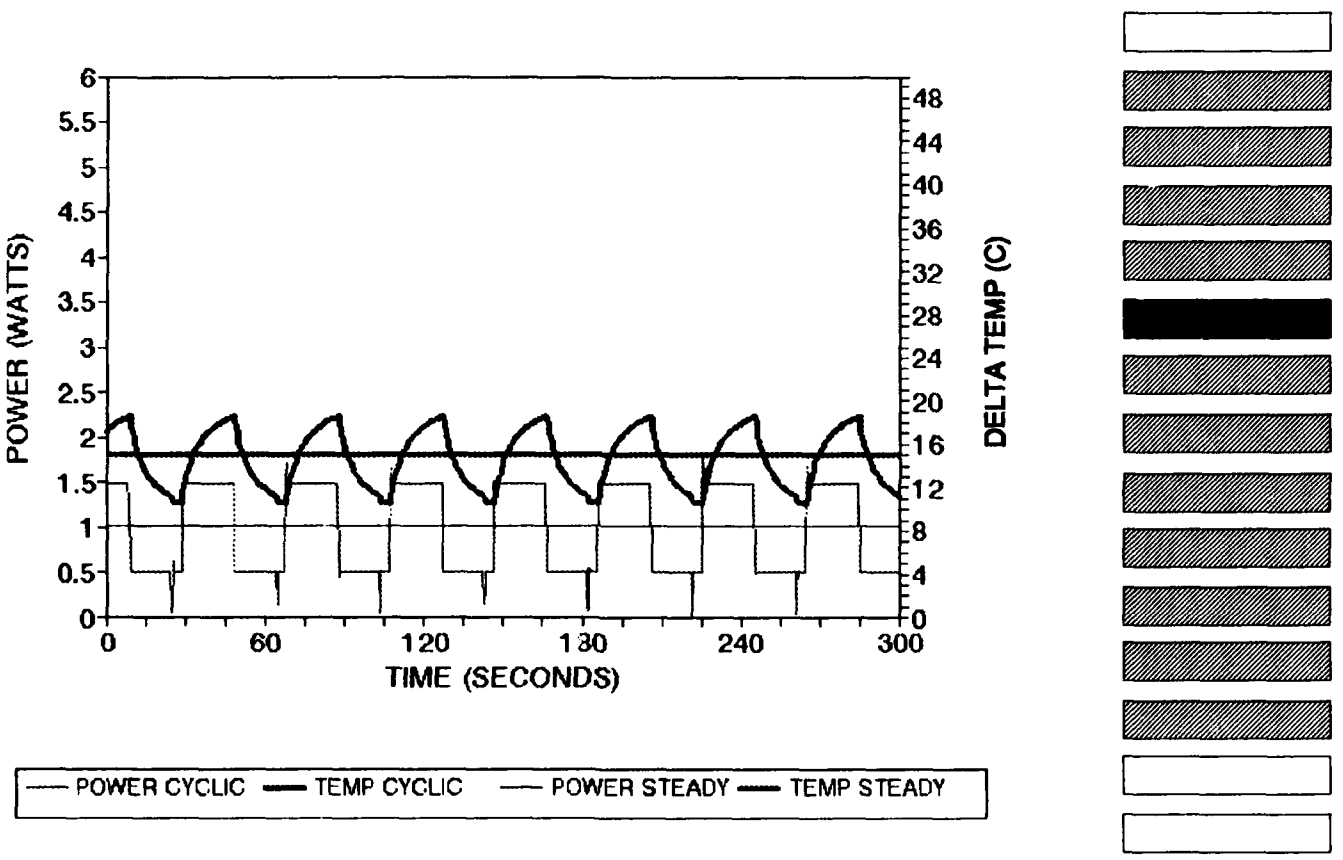

Figure NH. Time dependent transient power and delta temperature for square wave input, middle heater, heater configuration C21, ambient temperature 17.3°C.

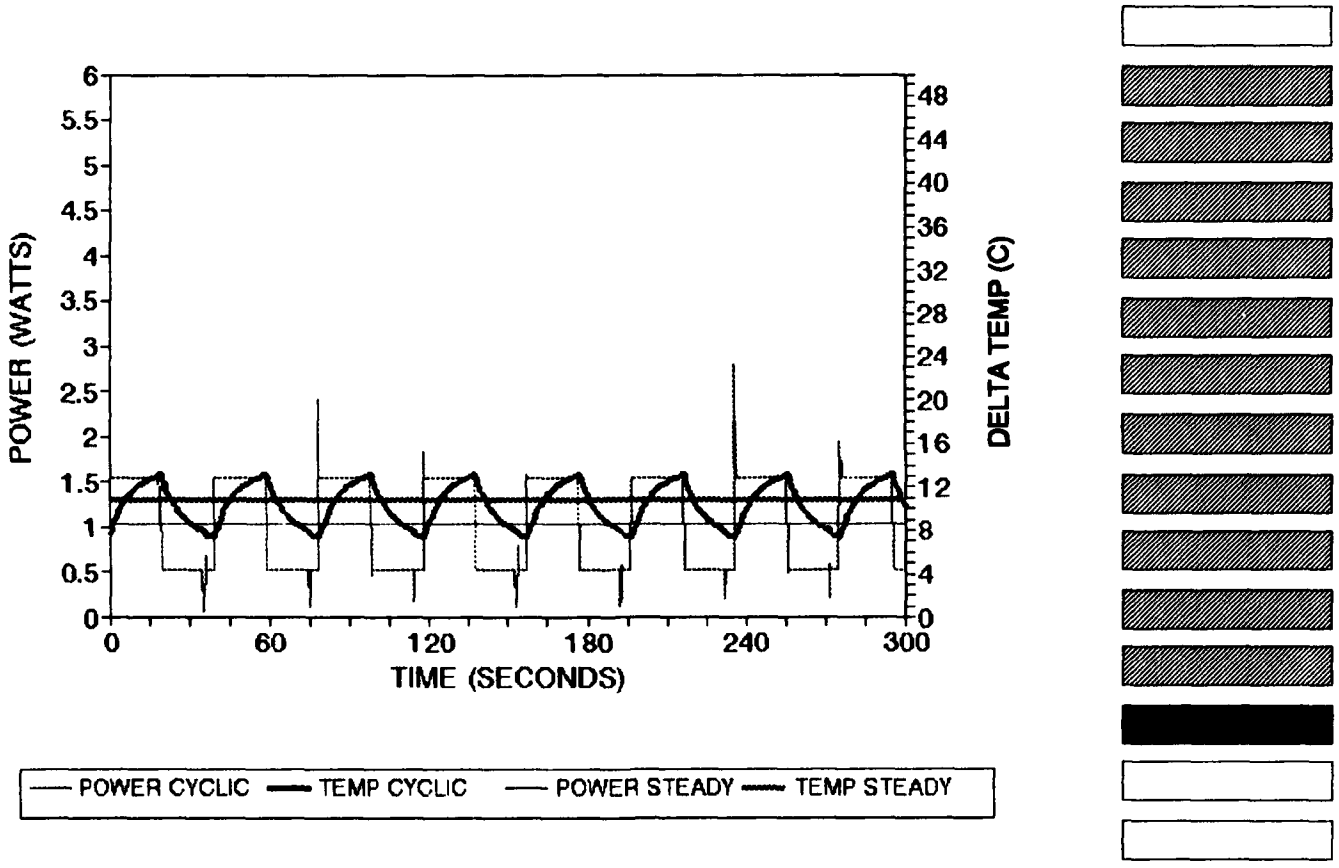

Figure NI. Time dependent transient power and delta temperature for square wave input, bottom heater, heater configuration C28, ambient temperature 17.4°C.

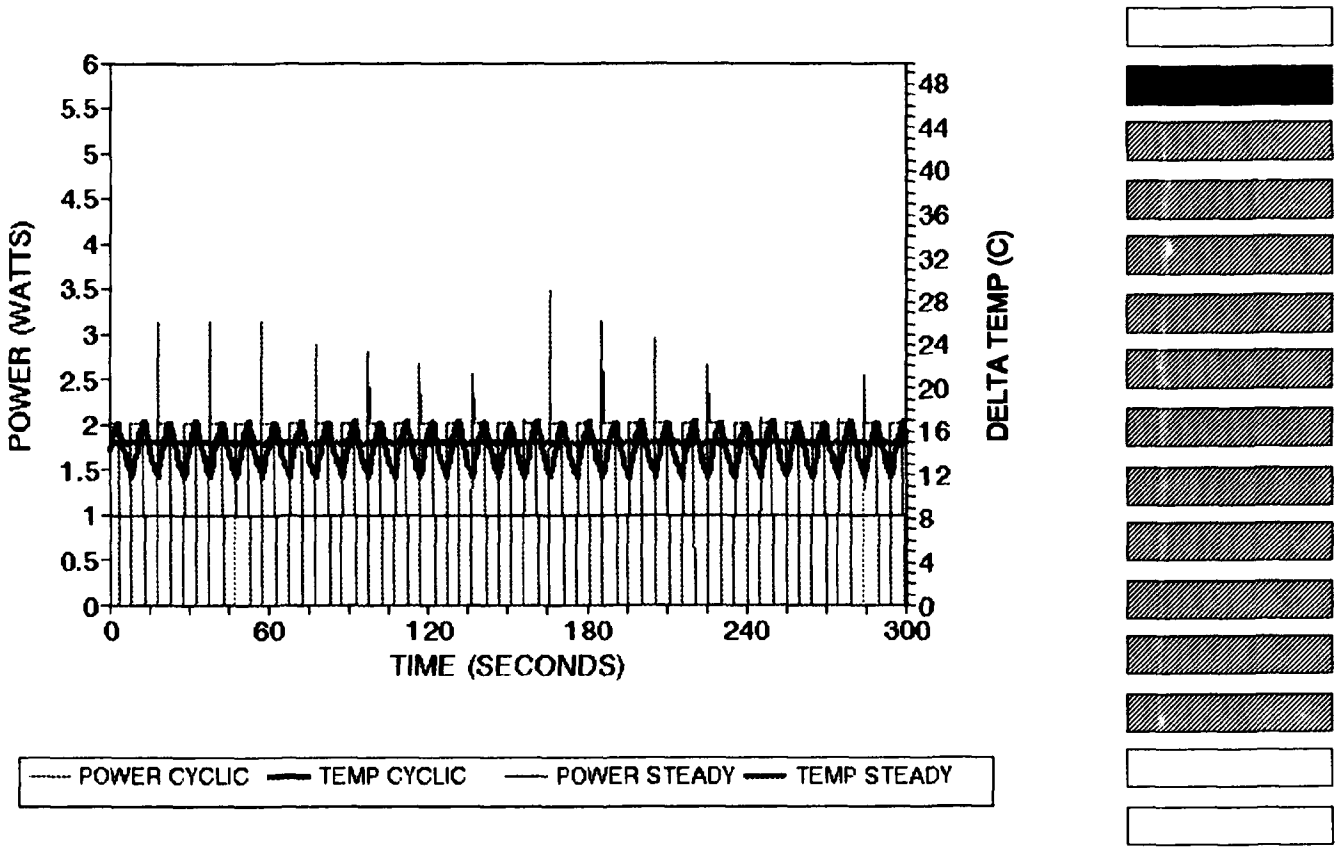

Figure OA. Time dependent transient power and delta temperature for square wave input, top heater, heater configuration C17, ambient temperature 20.7°C.

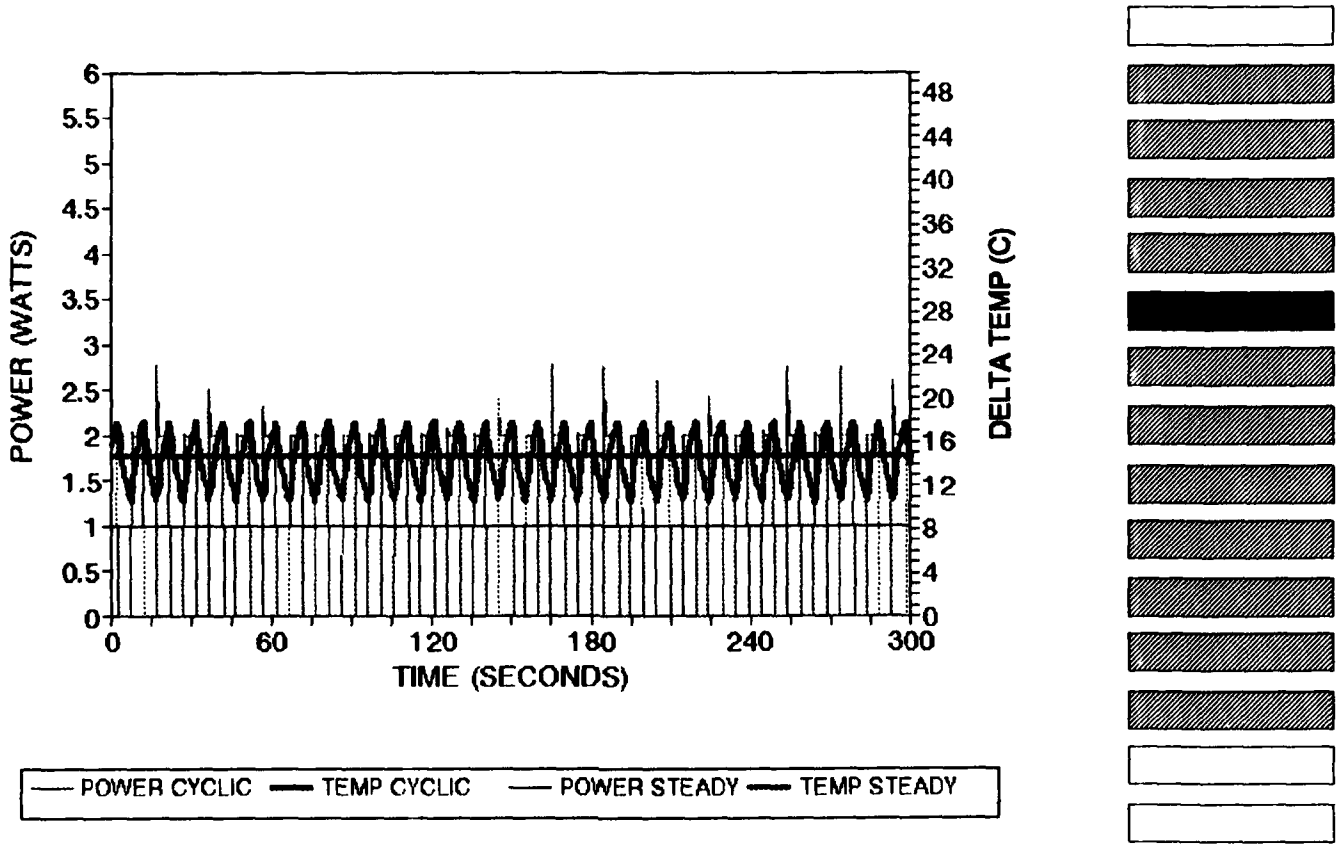

Figure 0B. Time dependent transient power and delta temperature for square wave input, middle heater, heater configuration C21, ambient temperature 20.7°C.

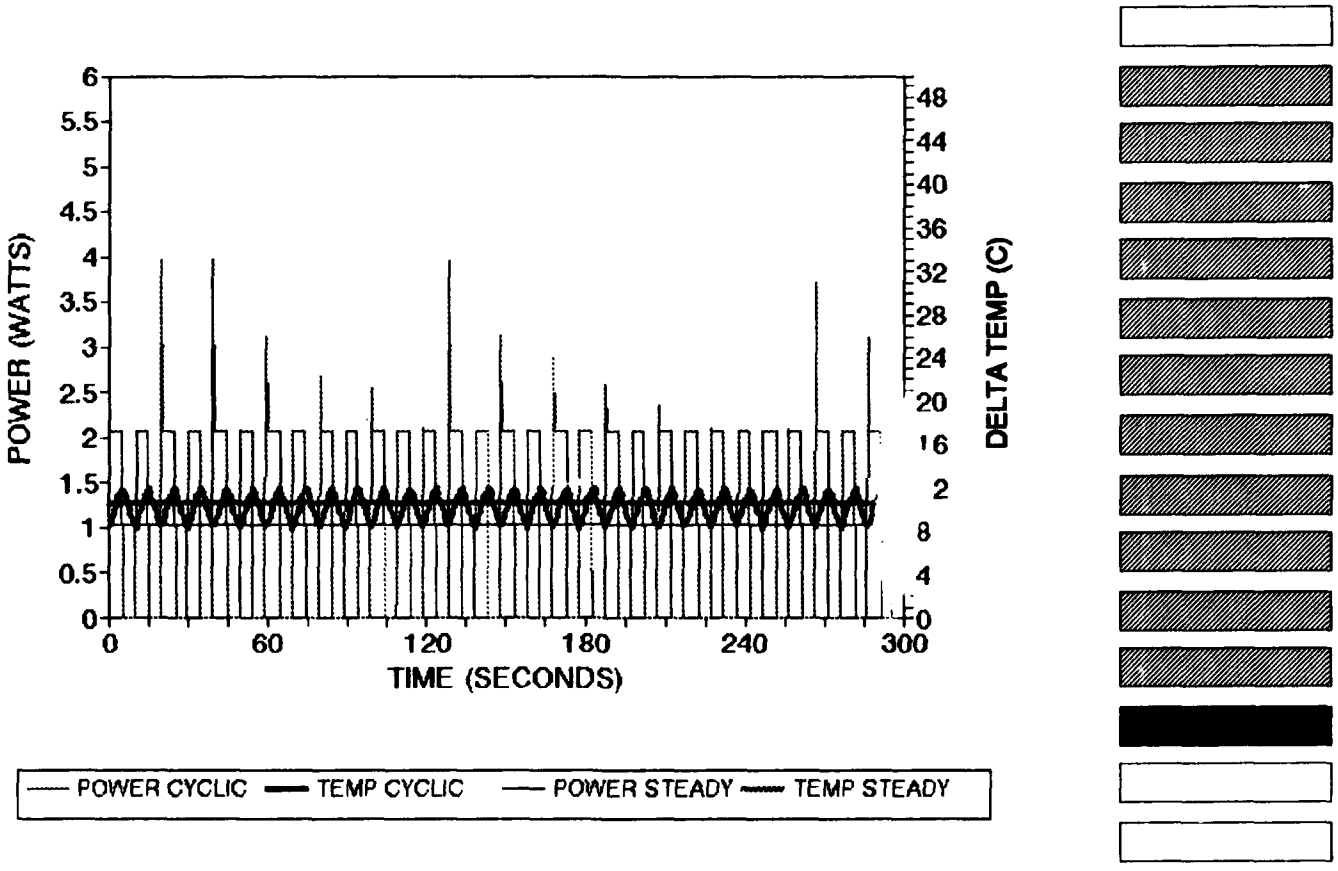

Figure OC. Time dependent transient power and delta temperature for square wave input, bottom heater, heater configuration C28, ambient temperature 20.7°C.

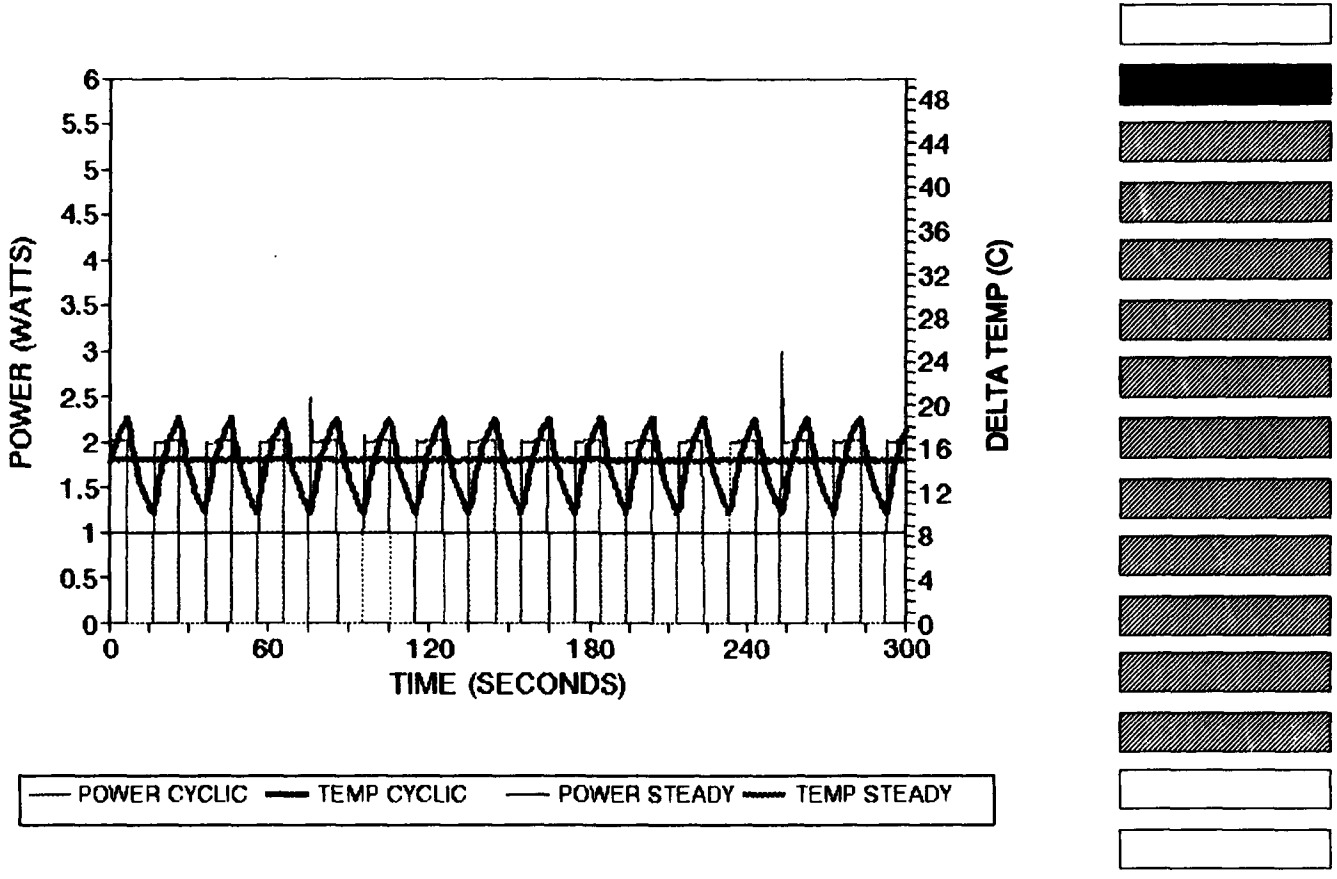

Figure OD. Time dependent transient power and delta temperature for square wave input, top heater, heater configuration C17, ambient temperature 20.7°C.

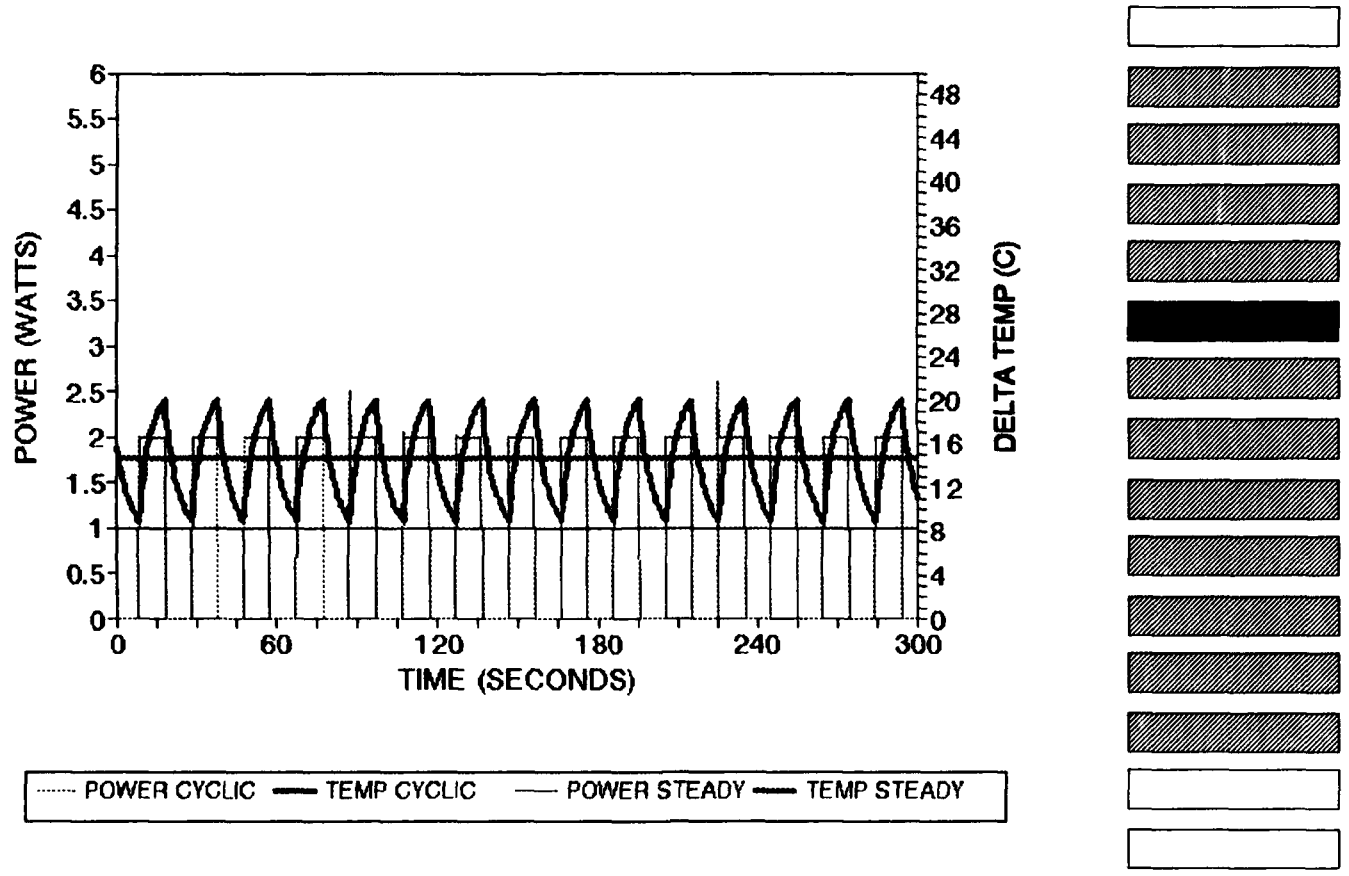

Figure OE. Time dependent transient power and delta temperature for square wave input, middle heater, heater configuration C21, ambient temperature 20.4°C.

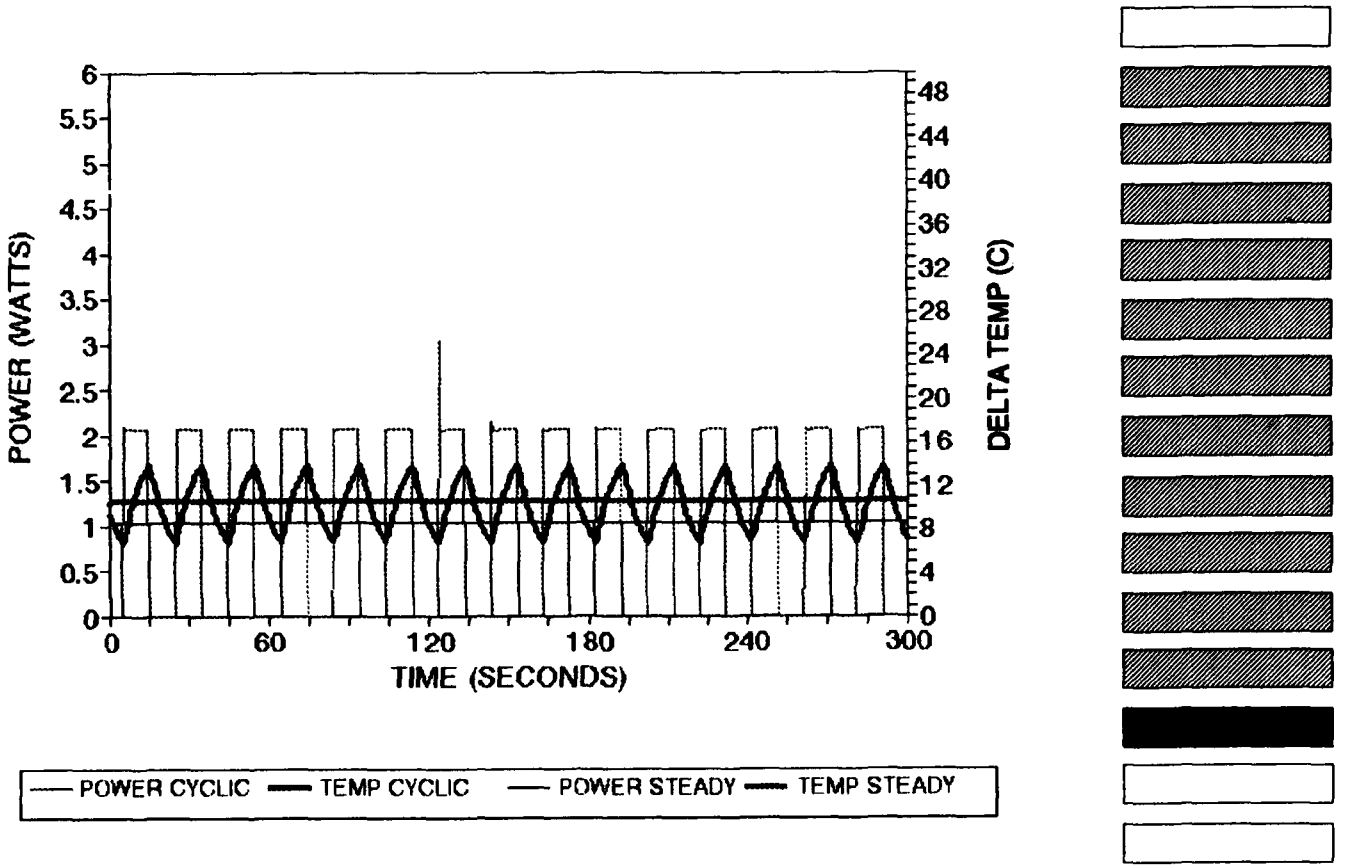

Figure OF. Time dependent transient power and delta temperature for square wave input, bottom heater, heater configuration C28, ambient temperature 20.4°C.

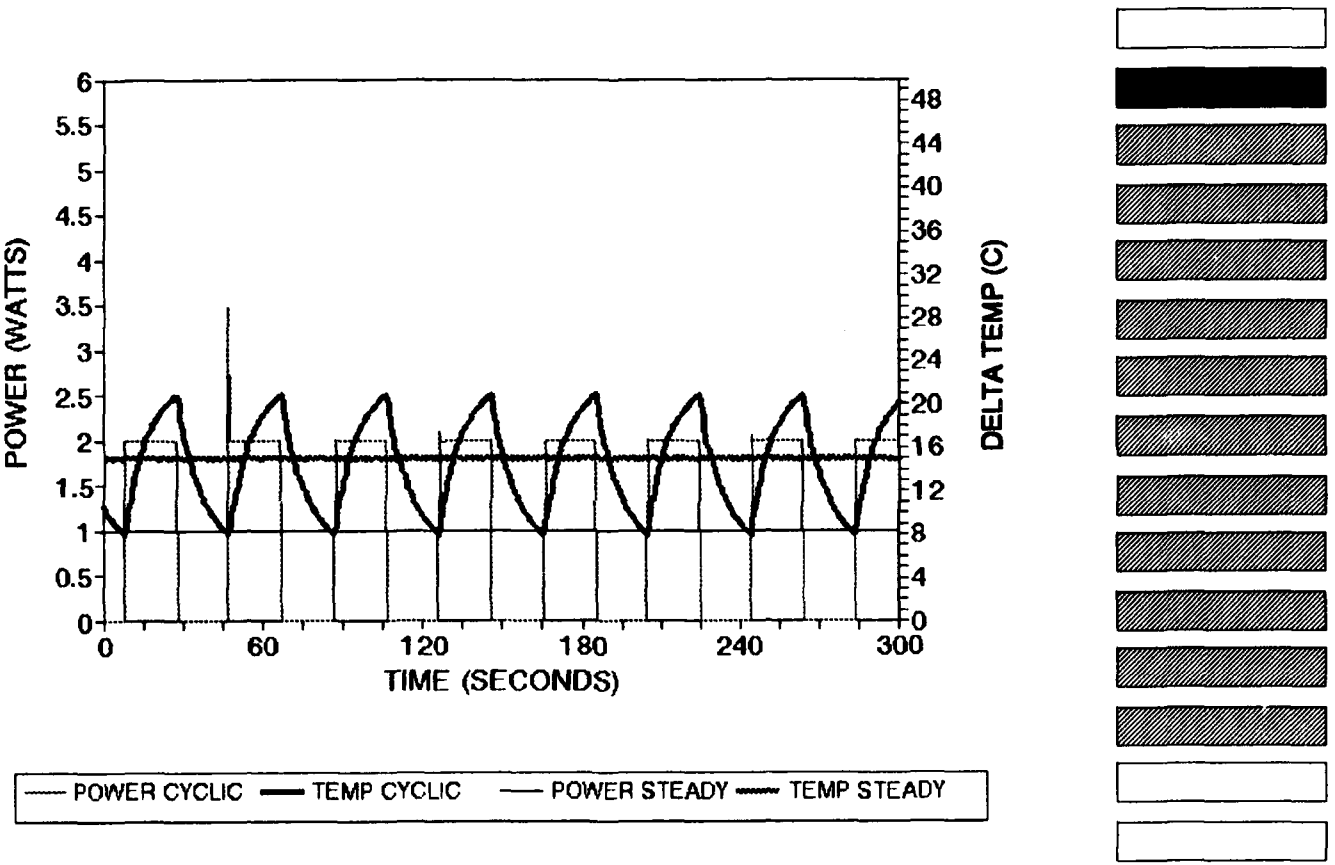

Figure OG. Time dependent transient power and delta temperature for square wave input, top heater, heater configuration C17, ambient temperature 20.6°C.

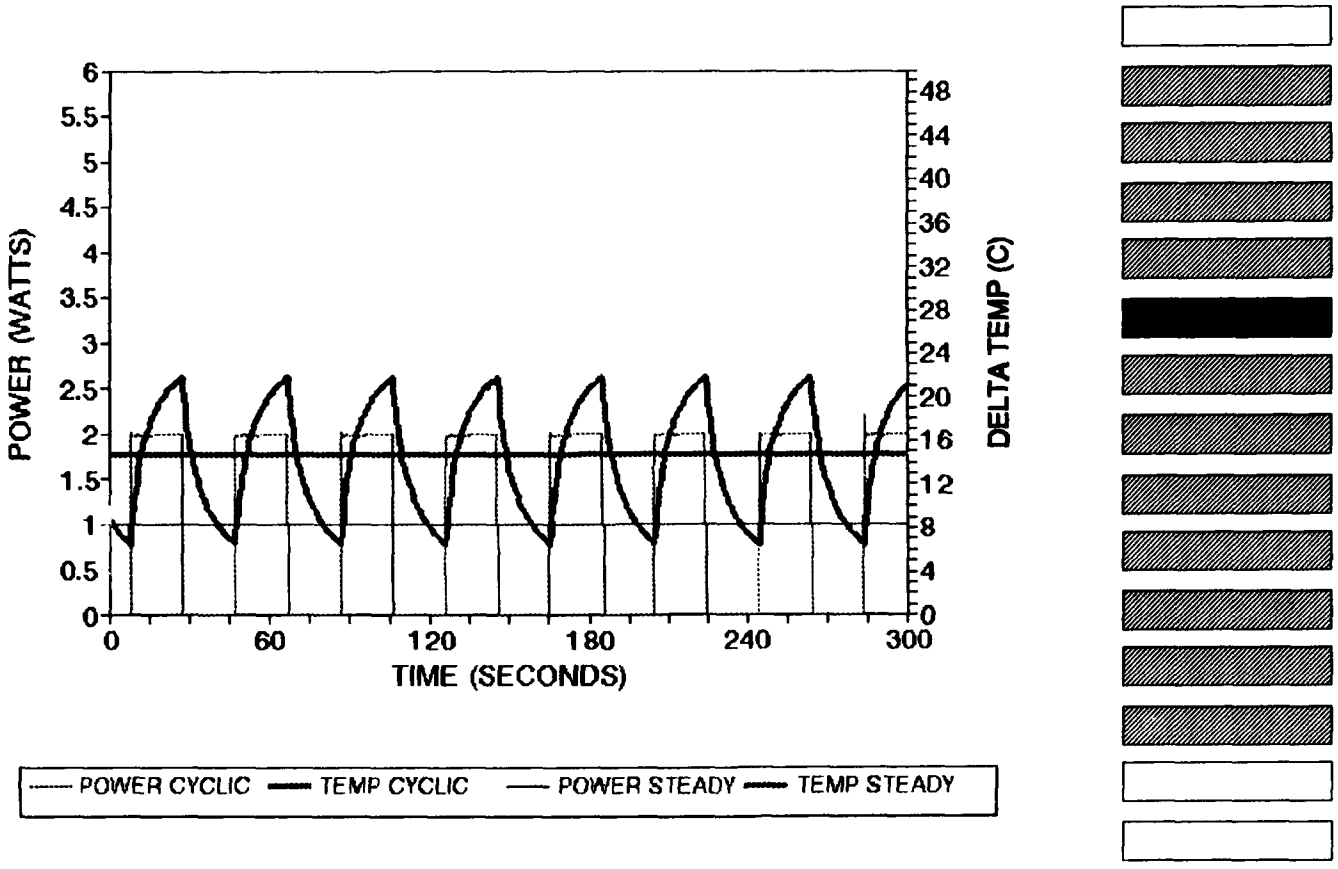

Figure OH. Time dependent transient power and delta temperature for square wave input, middle heater, heater configuration C21, ambient temperature 20.6°C.

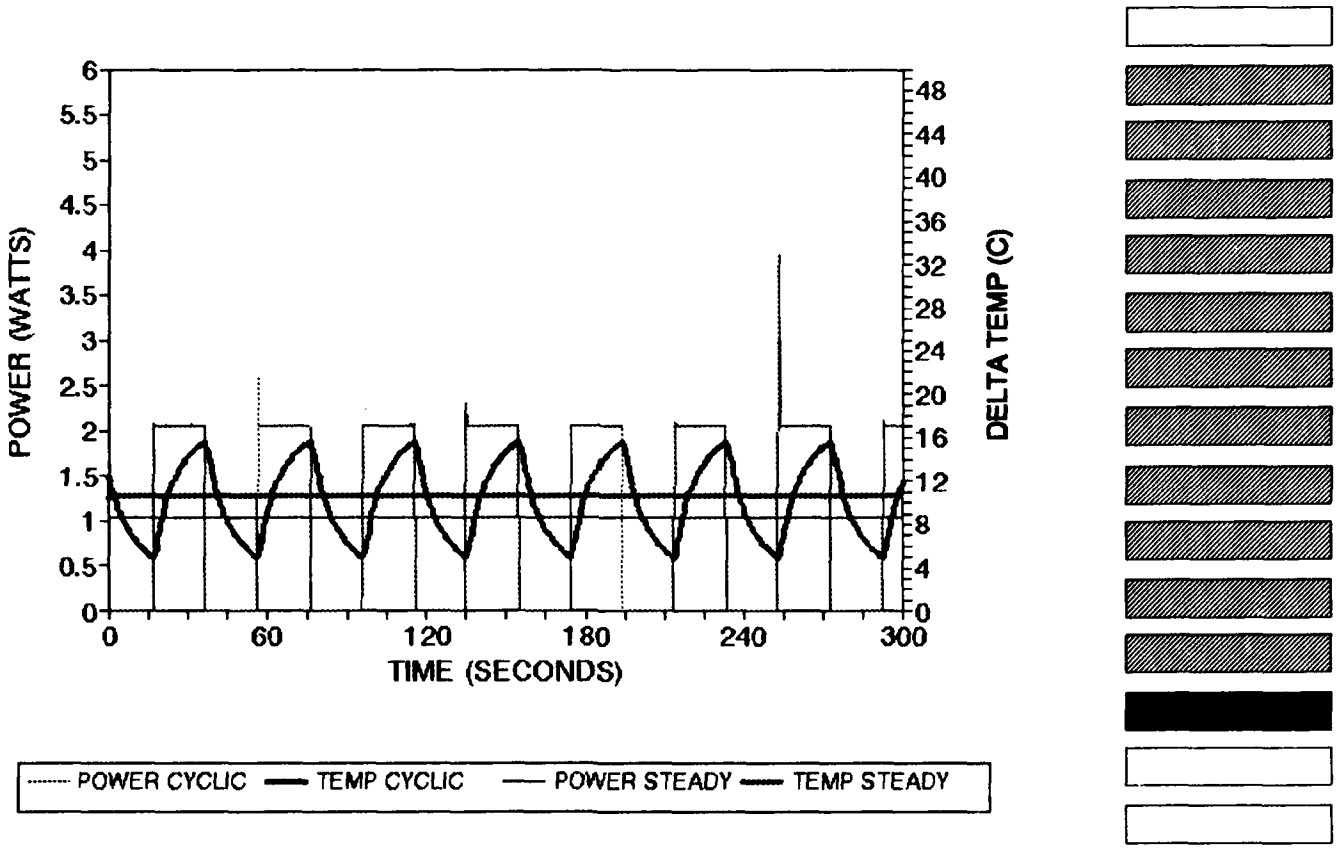

Figure OI. Time dependent transient power and delta temperature for square wave input, bottom heater, heater configuration C28, ambient temperature 20.4°C.

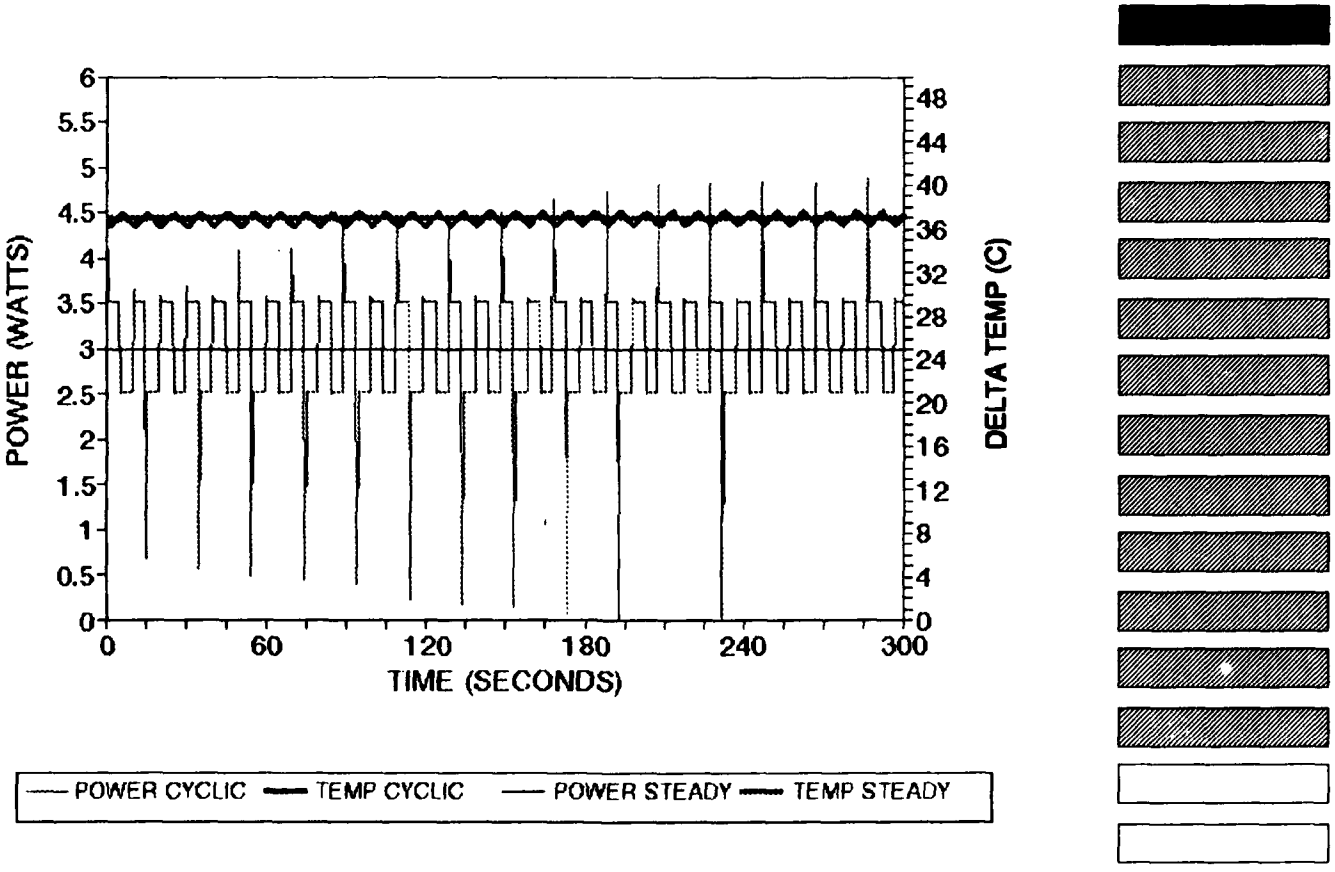

Figure PA. Time dependent transient power and delta temperature for square wave input, top heater, heater configuration B16, ambient temperature 17.5°C.

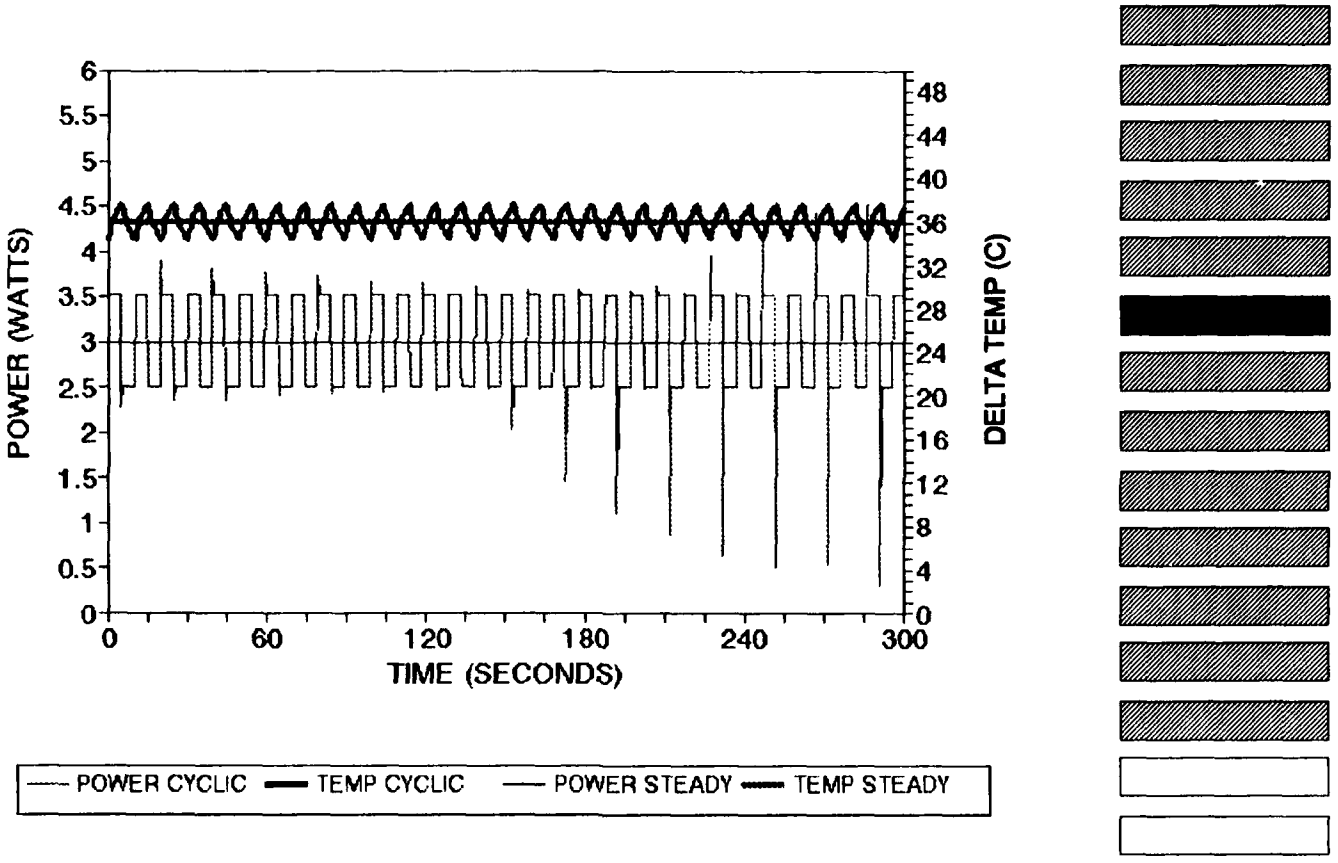

Figure PB. Time dependent transient power and delta temperature for square wave input, middle heater, heater configuration B21, ambient temperature 17.5°C.

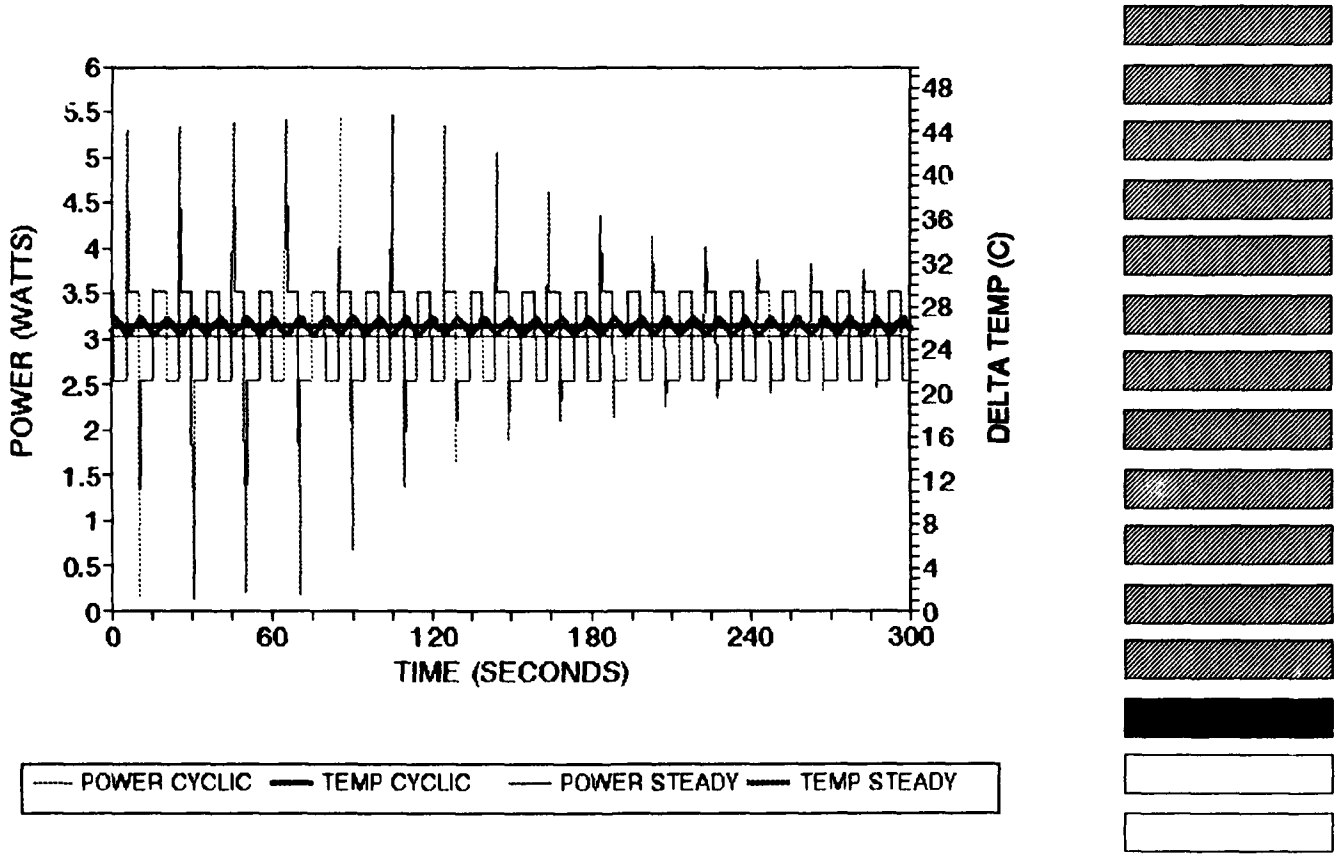

Figure PC. Time dependent transient power and delta temperature for square wave input, bottom heater, heater configuration B28, ambient temperature 17.5°C.

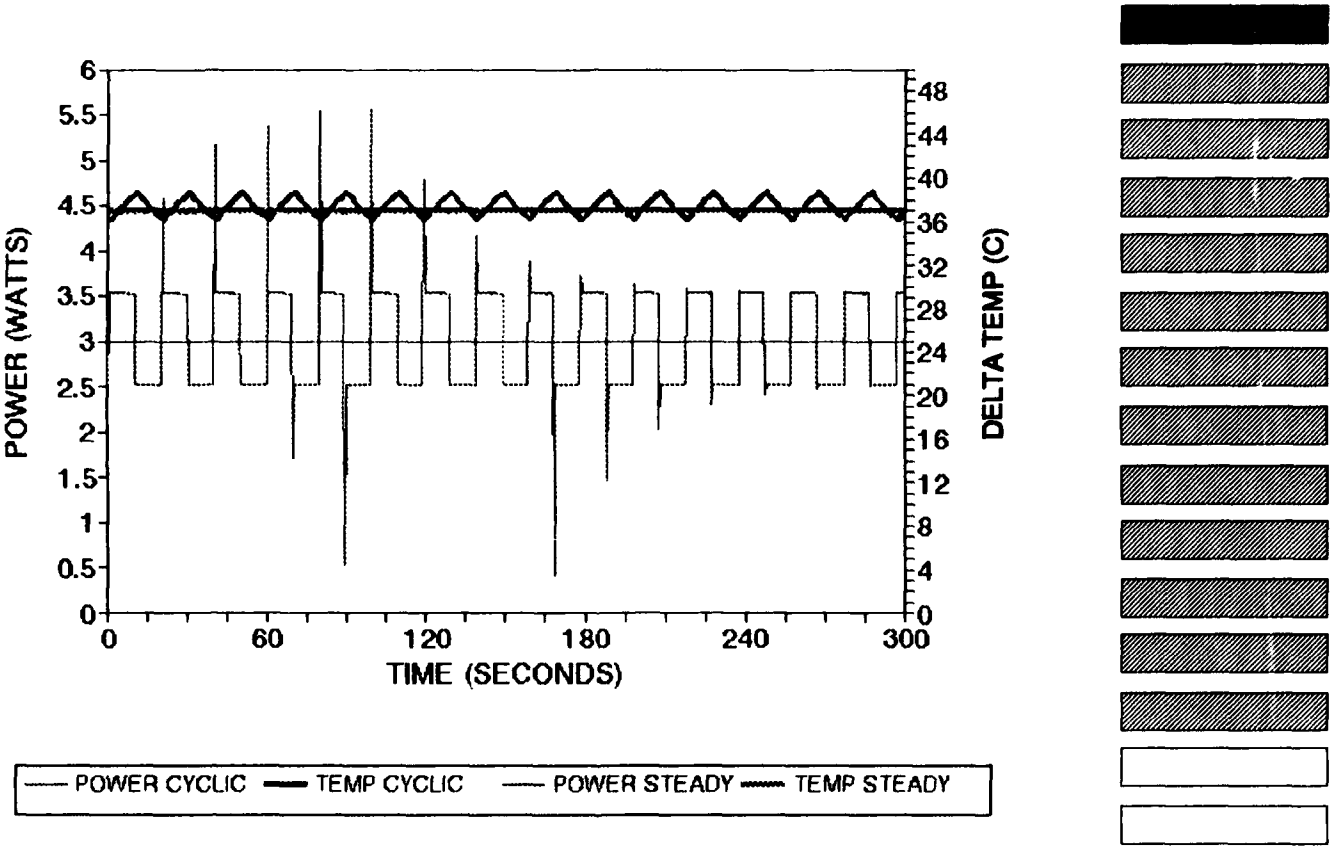

Figure PD. Time dependent transient power and delta temperature for square wave input, top heater, heater configuration B16, ambient temperature 17.5°C.

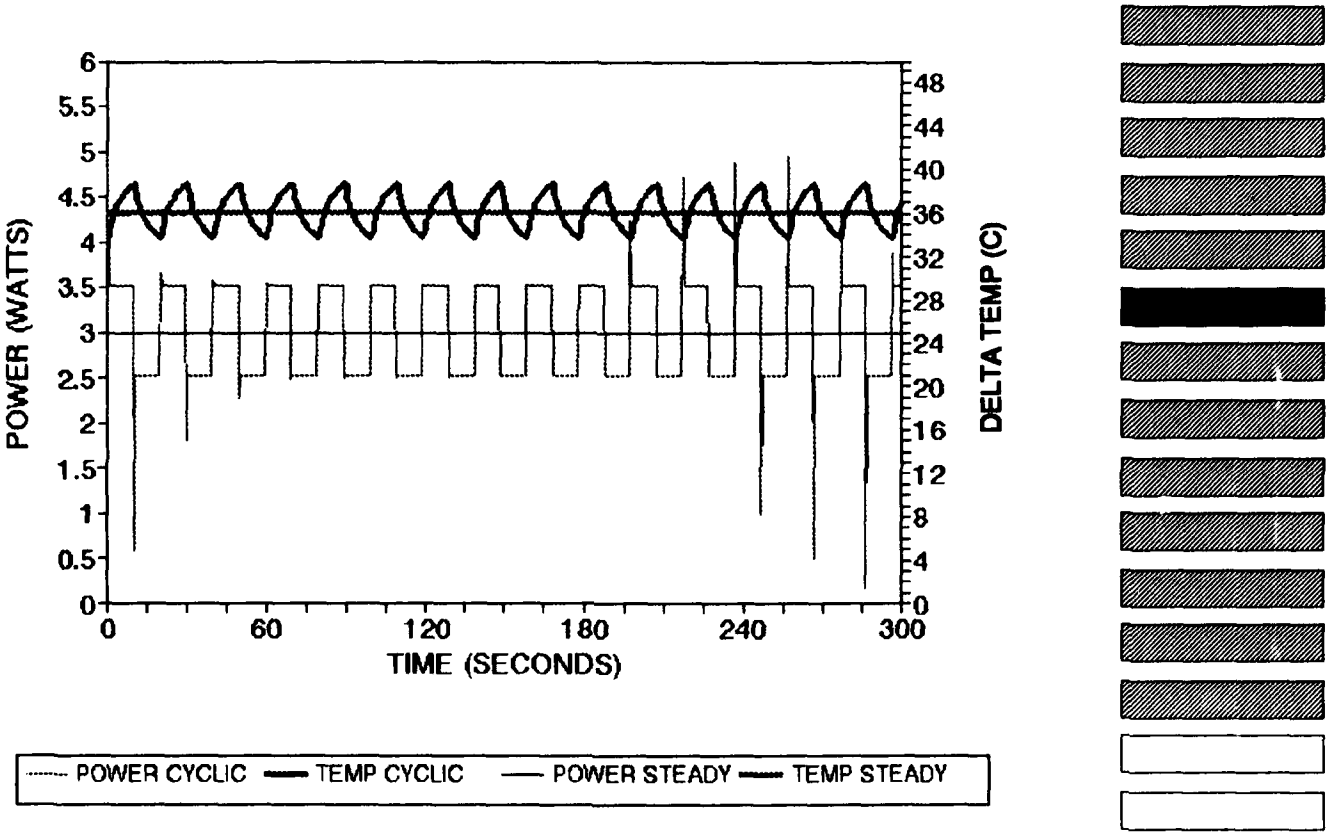

Figure PE. Time dependent transient power and delta temperature for square wave input, middle heater, heater configuration B21, ambient temperature 17.5°C.

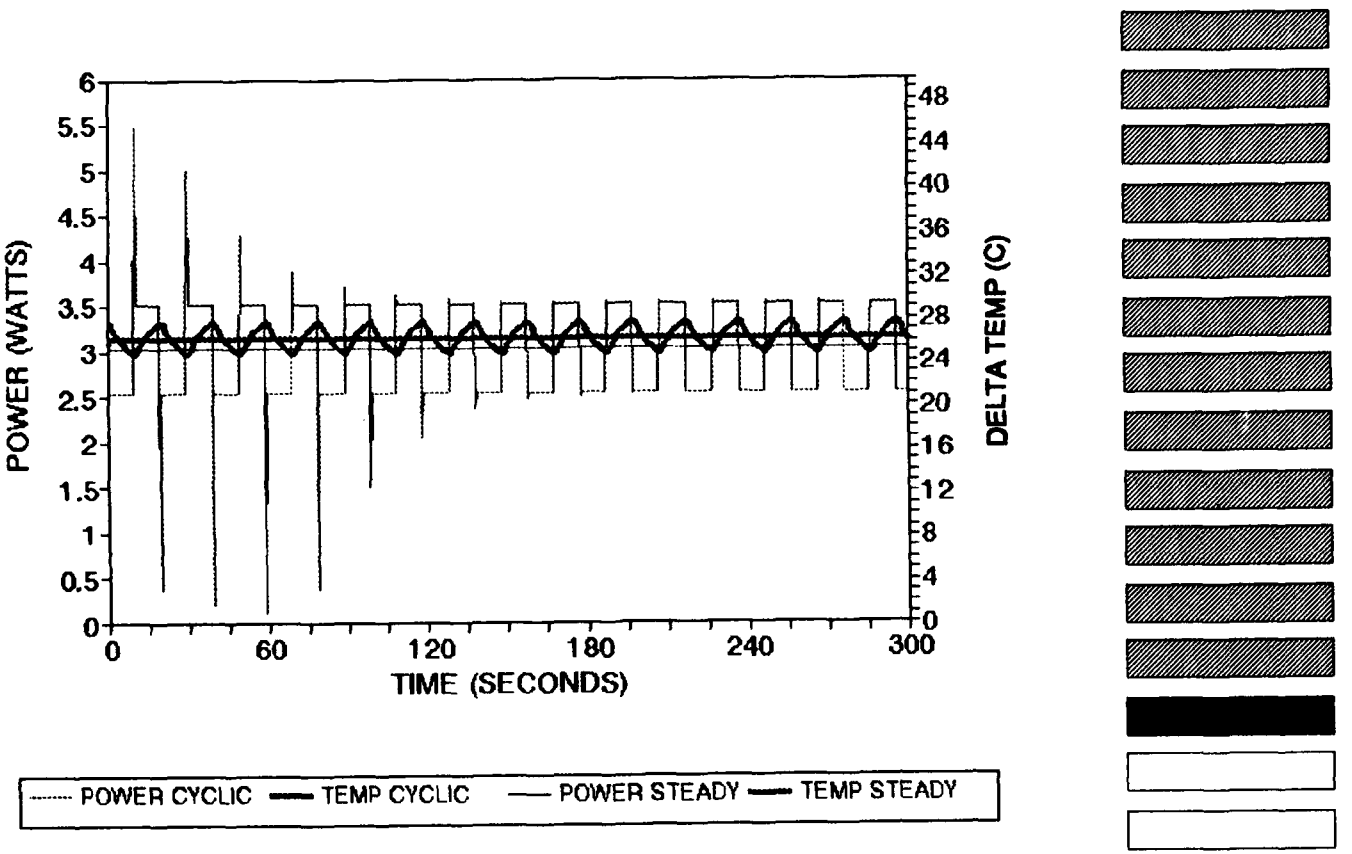

Figure PF. Time dependent transient power and delta temperature for square wave input, bottom heater, heater configuration B28, ambient temperature 17.5°C.

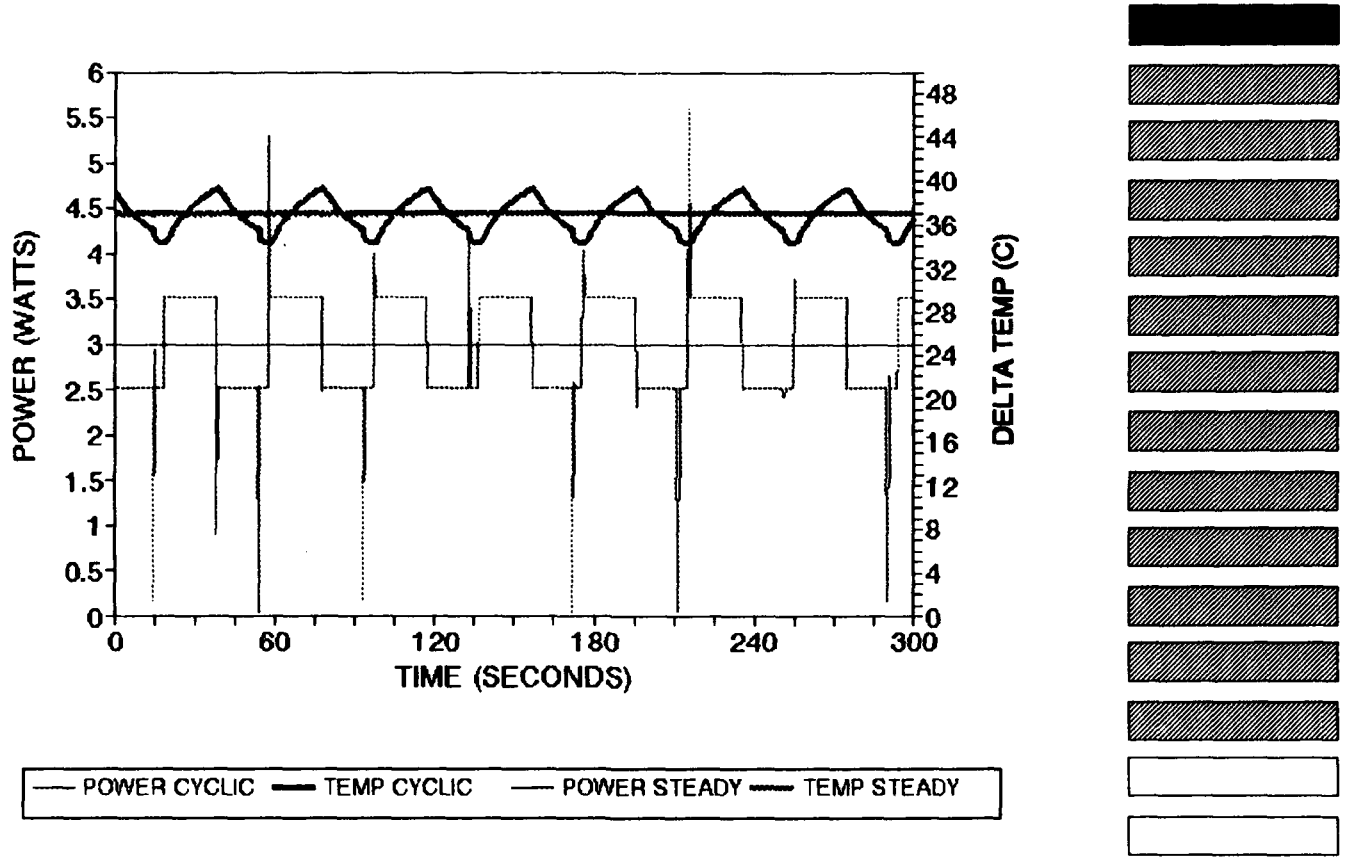

Figure PG. Time dependent transient power and delta temperature for square wave input, top heater, heater configuration B16, ambient temperature 17.5°C.

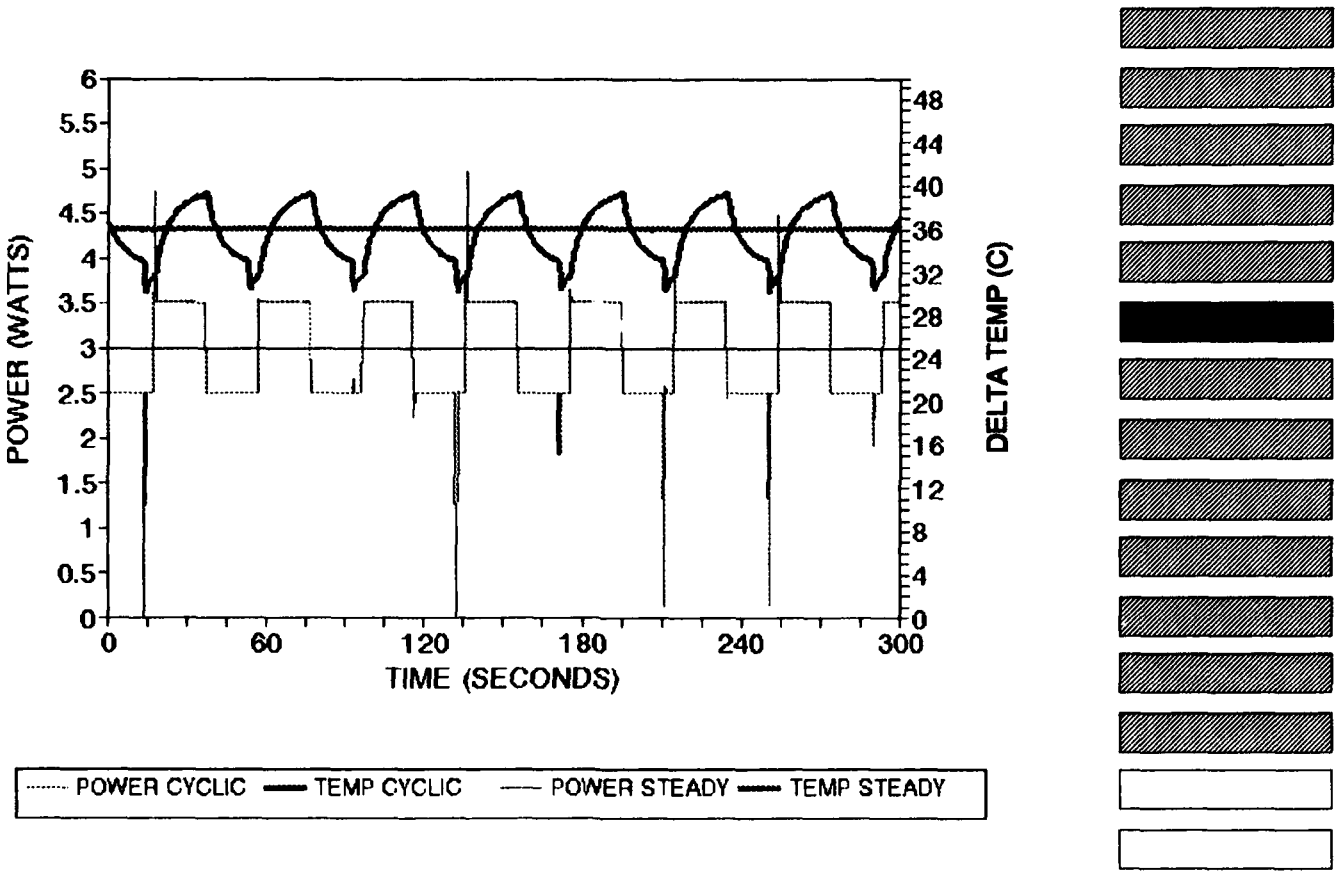

Figure PH. Time dependent transient power and delta temperature for square wave input, middle heater, heater configuration B21, ambient temperature 17.5°C.

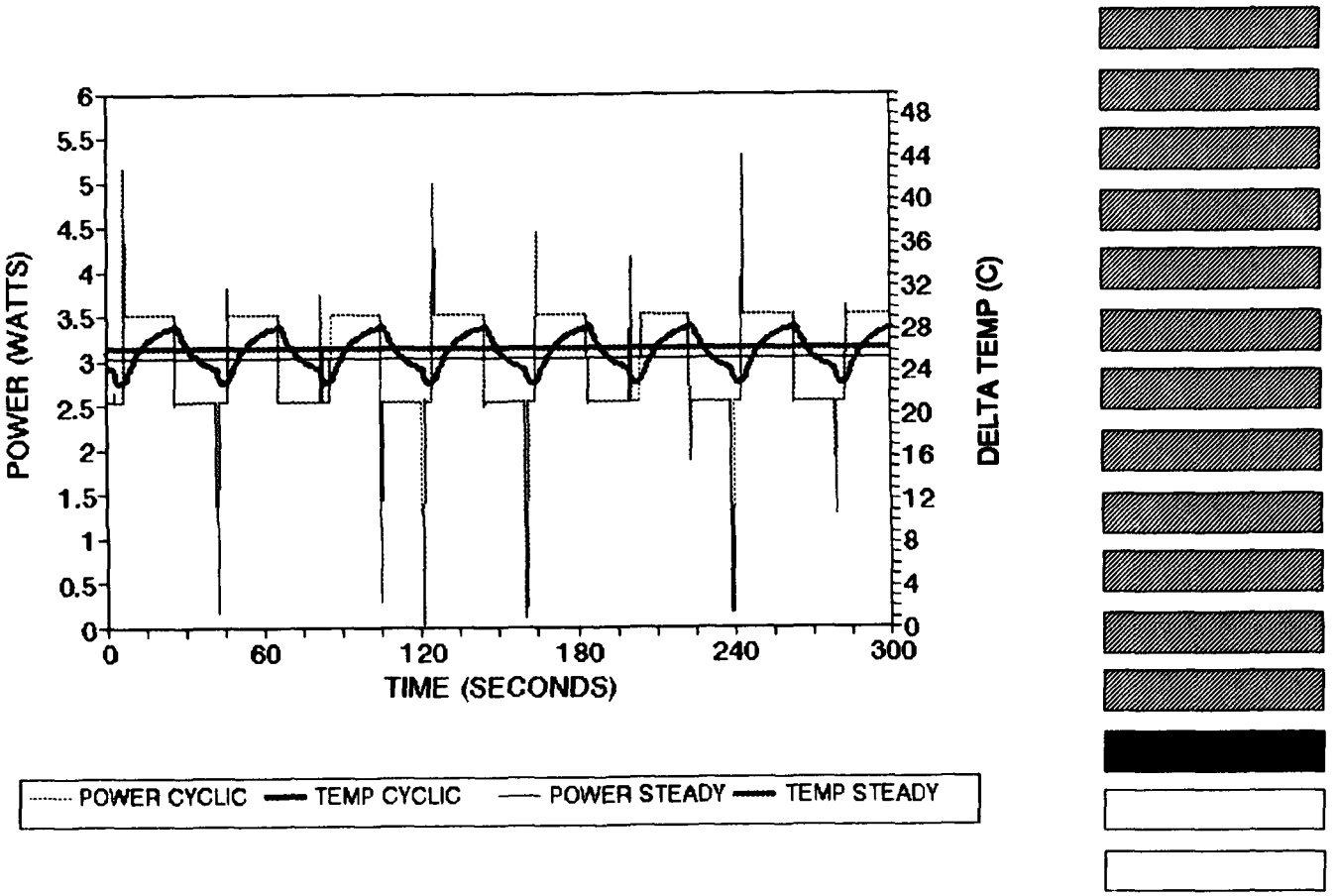

Figure PI. Time dependent transient power and delta temperature for square wave input, bottom heater, heater configuration B28, ambient temperature 17.5°C.

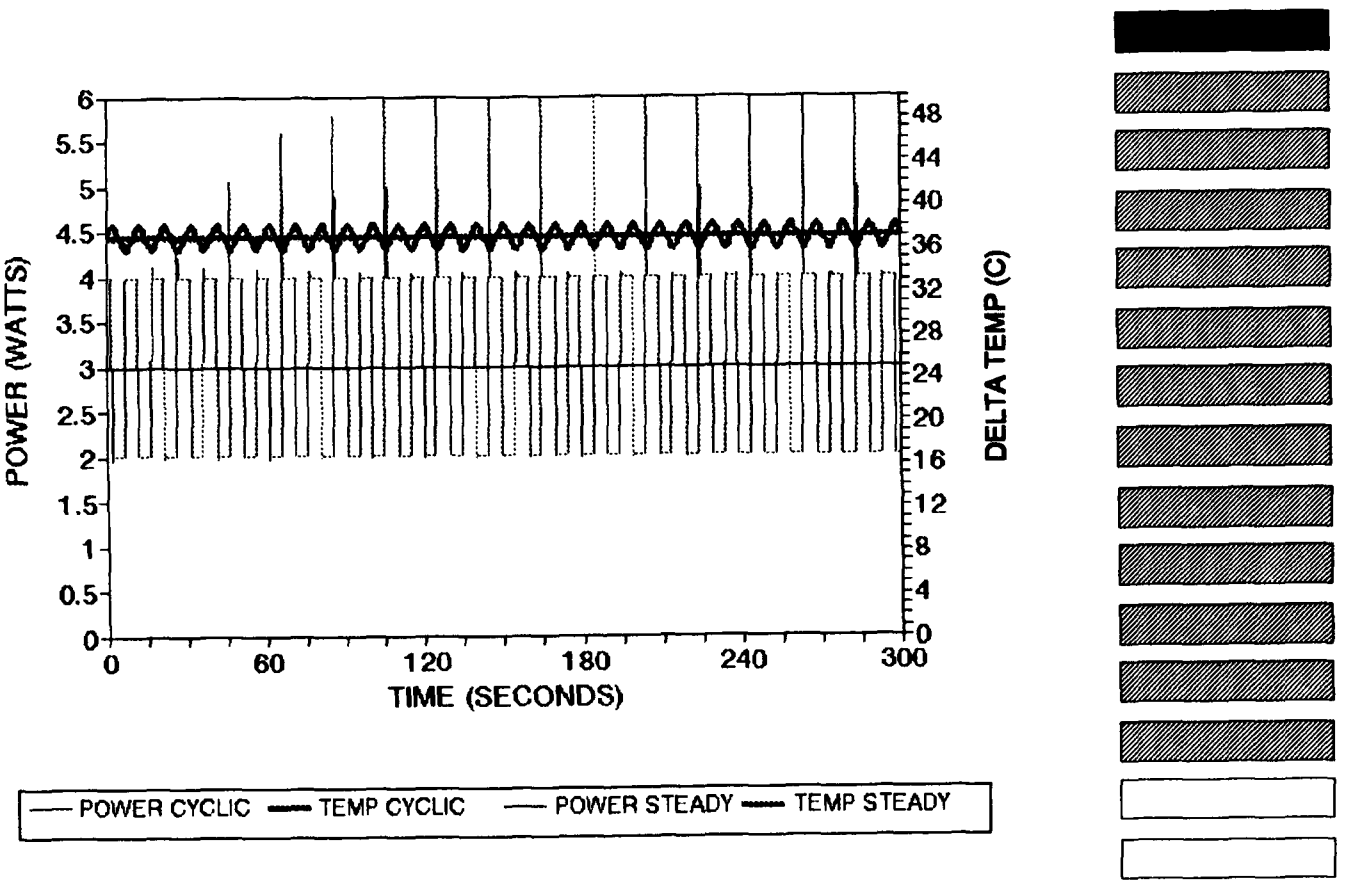

Figure QA. Time dependent transient power and delta temperature for square wave input, top heater, heater configuration B16, ambient temperature 17.5°C.

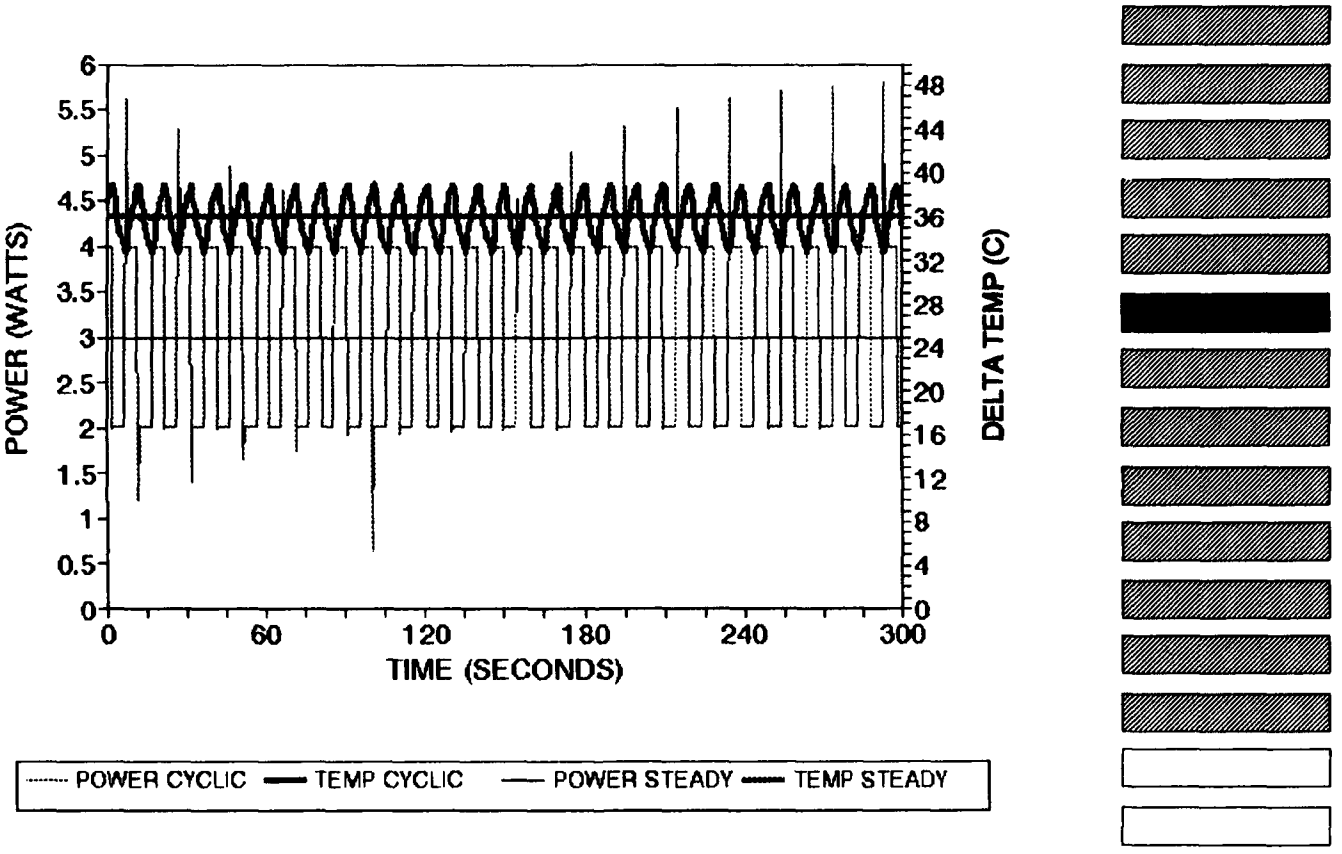

Figure QB. Time dependent transient power and delta temperature for square wave input, middle heater, heater configuration B21, ambient temperature 17.5°C.

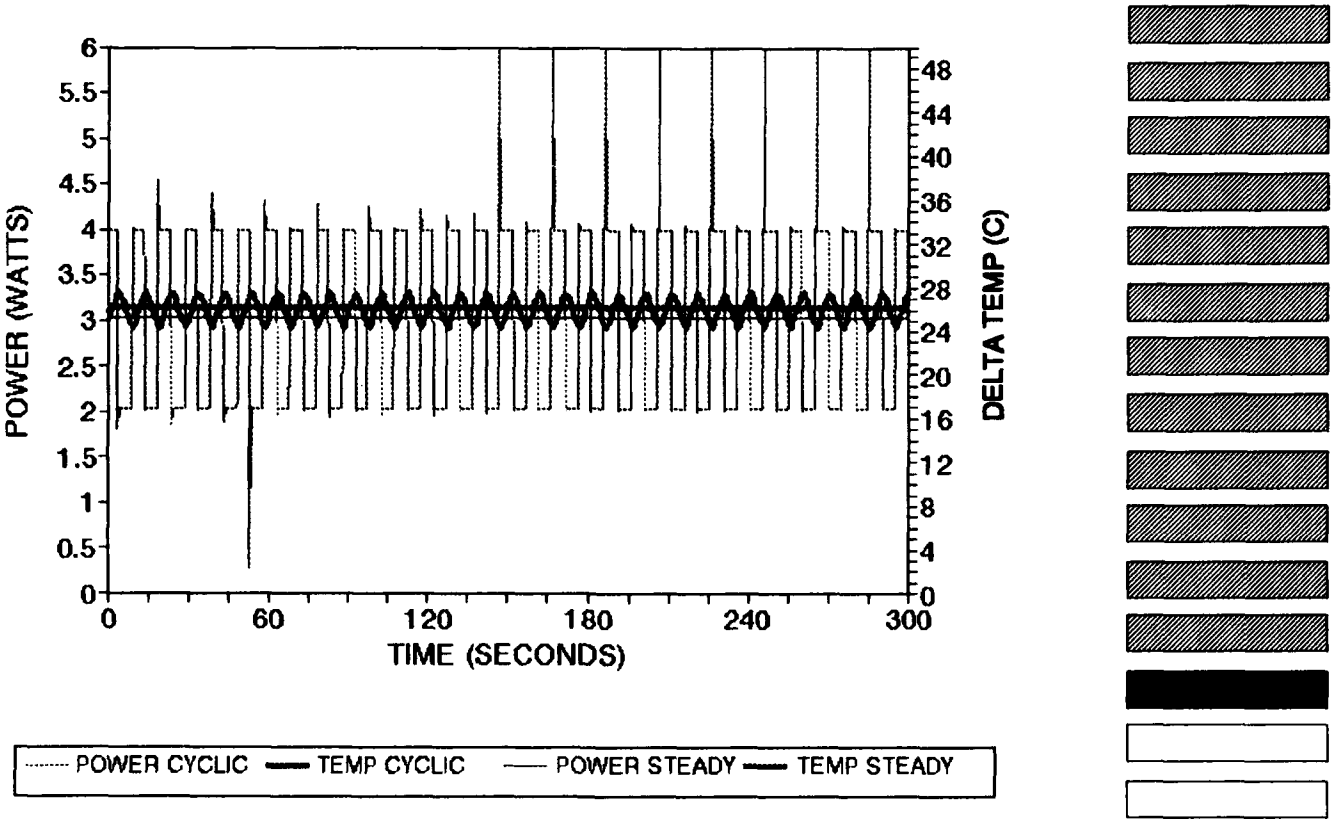

Figure QC. Time dependent transient power and delta temperature for square wave input, bottom heater, heater configuration B28, ambient temperature 17.5°C.

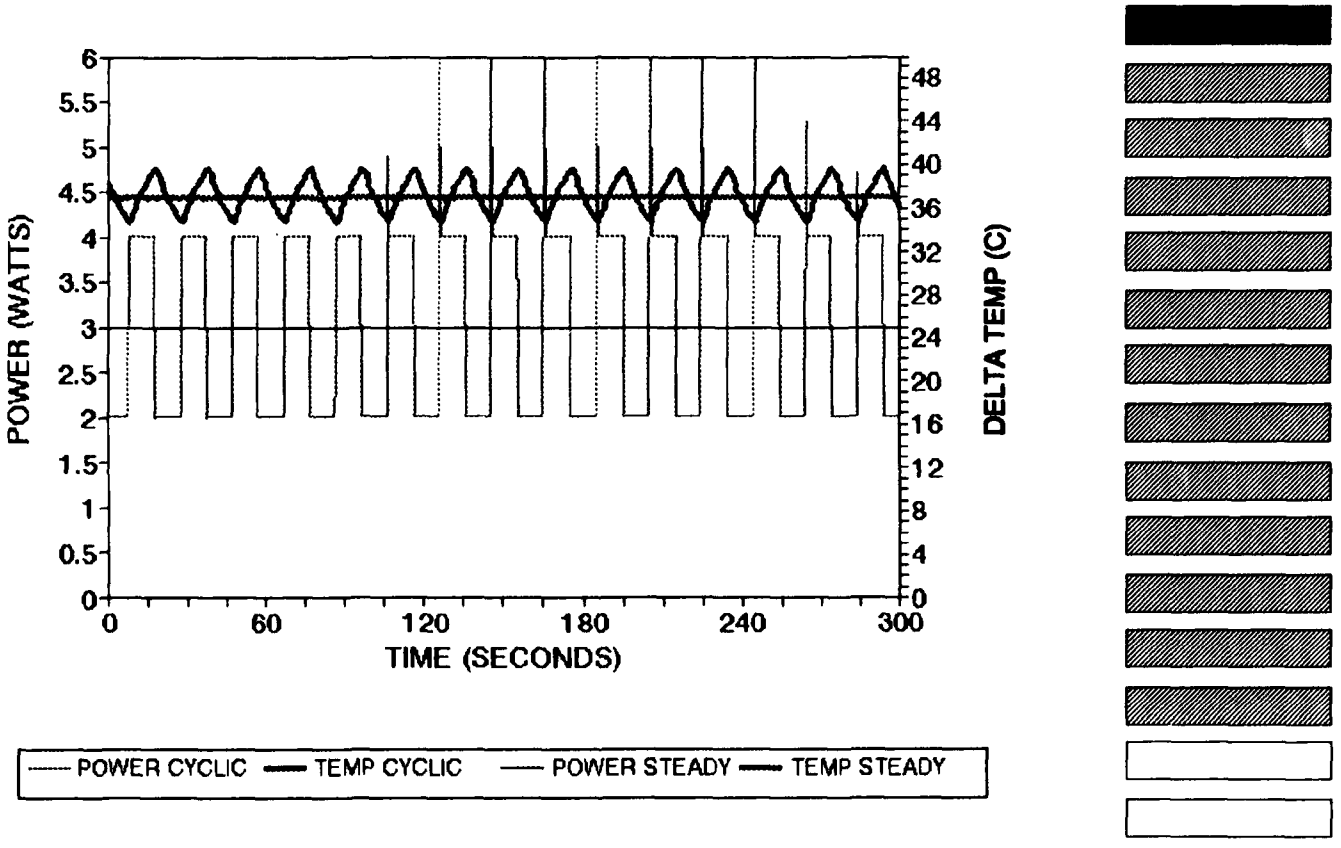

Figure QD. Time dependent transient power and delta temperature for square wave input, top heater, heater configuration B16, ambient temperature 17.5°C.

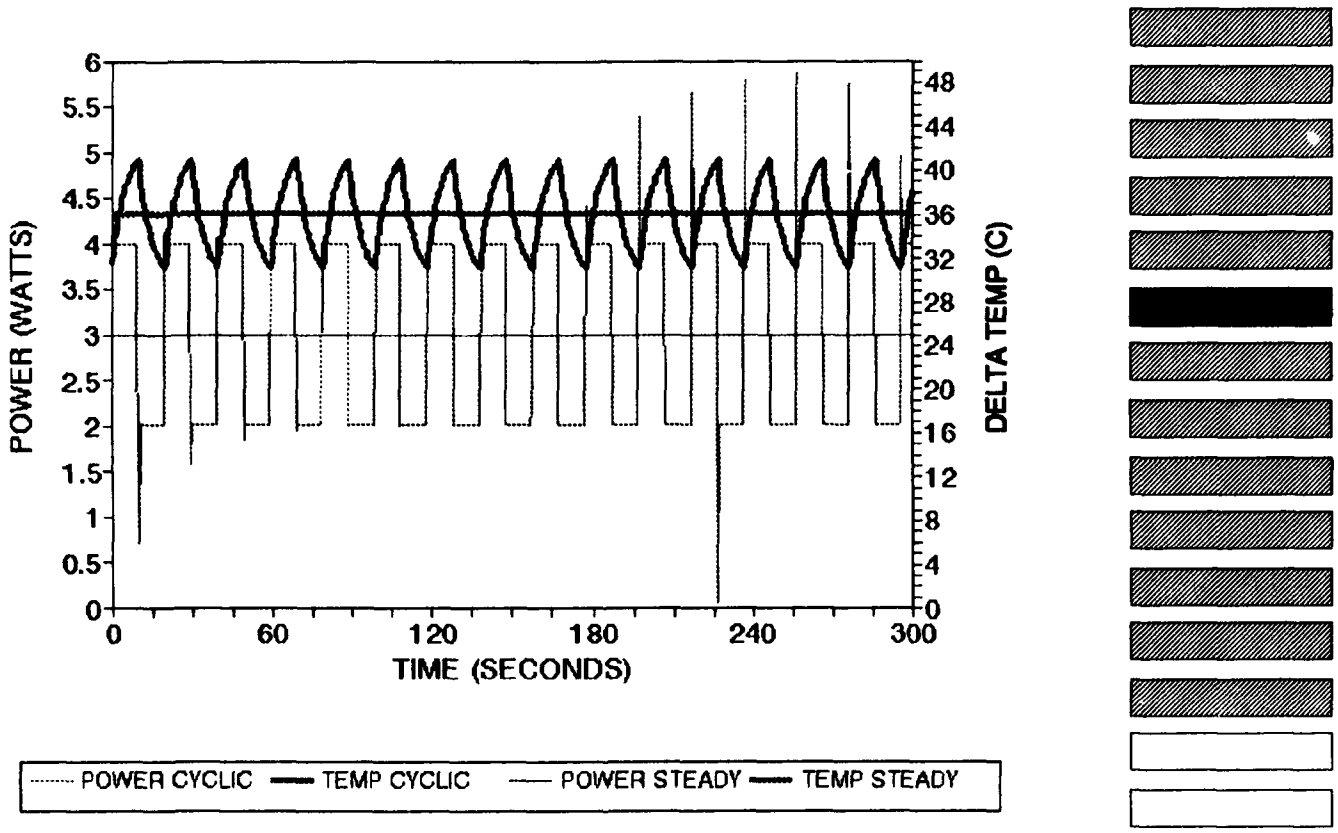

Figure QE. Time dependent transient power and delta temperature for square wave input, middle heater, heater configuration B21, ambient temperature 17.5°C.

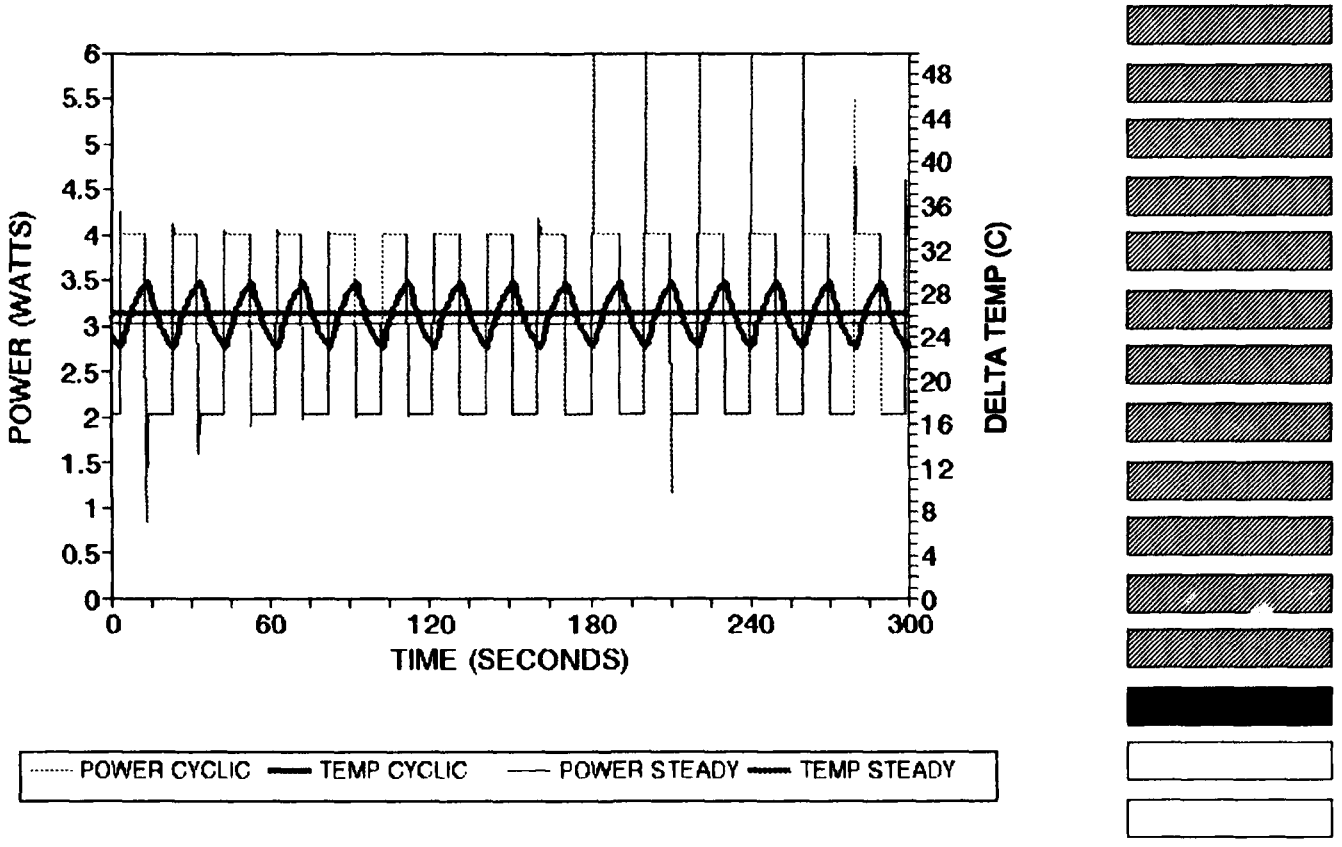

Figure QF. Time dependent transient power and delta temperature for square wave input, bottom heater, heater configuration B28, ambient temperature 17.5°C.

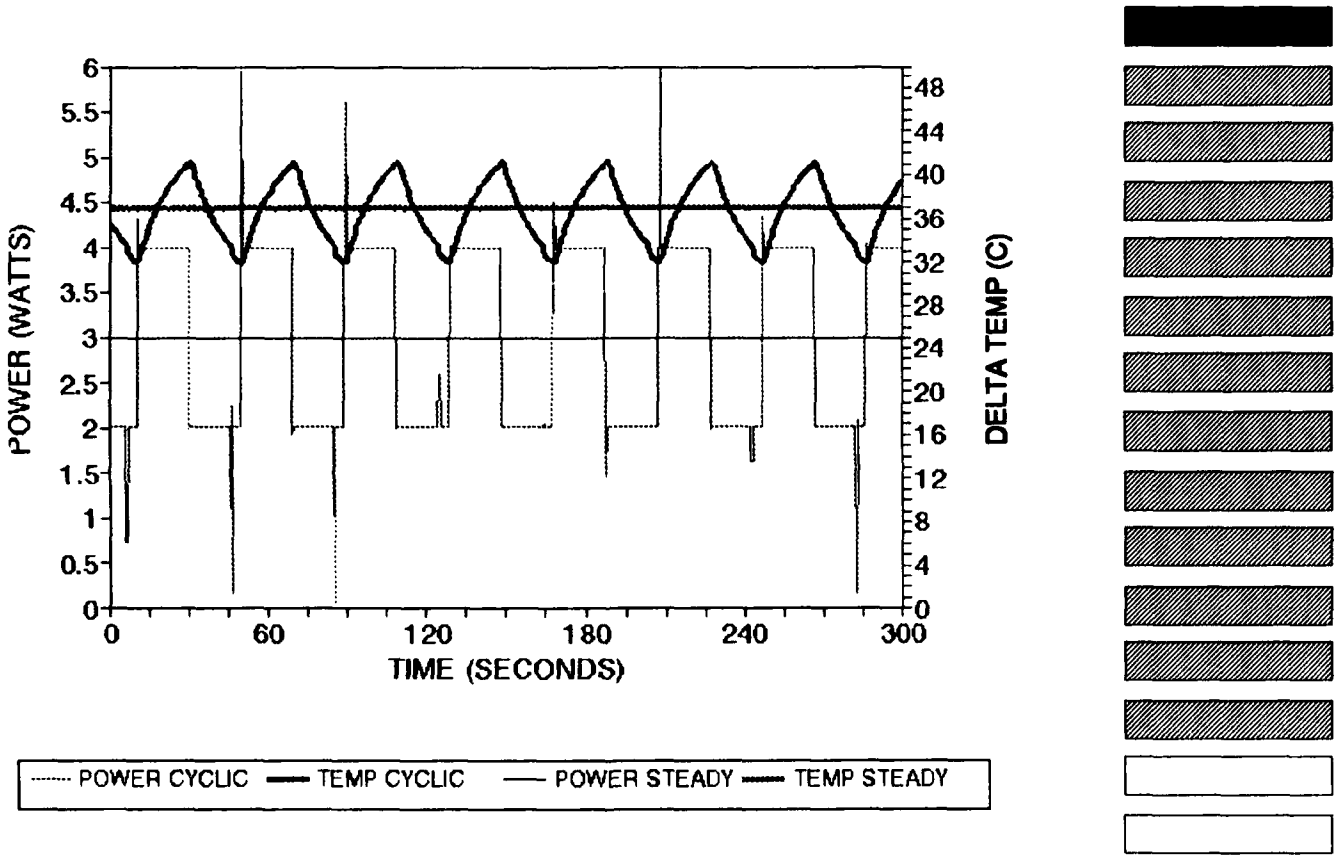

Figure QG. Time dependent transient power and delta temperature for square wave input, top heater, heater configuration B16, ambient temperature 17.5°C.

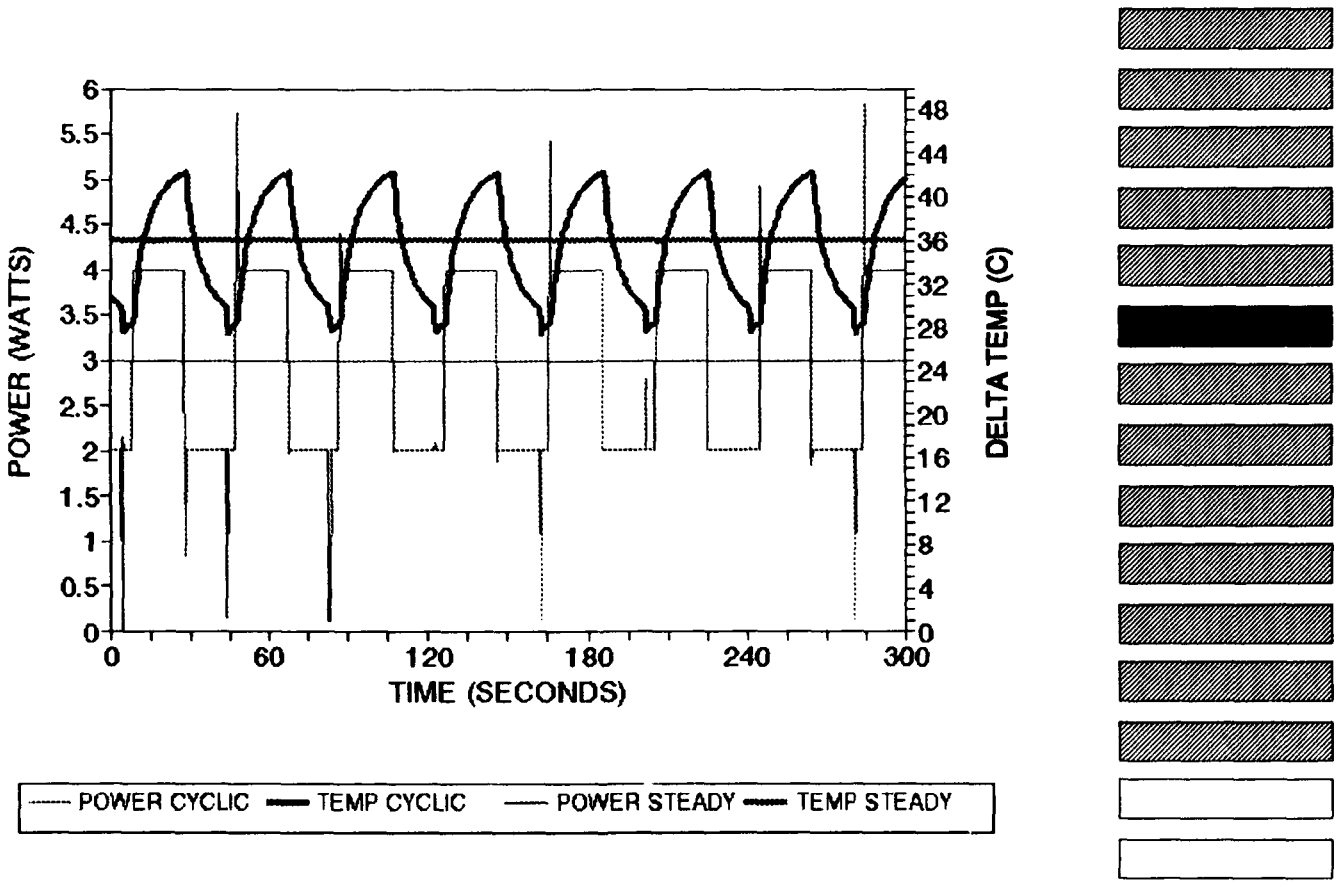

Figure QH. Time dependent transient power and delta temperature for square wave input, middle heater, heater configuration B21, ambient temperature 17.5°C.

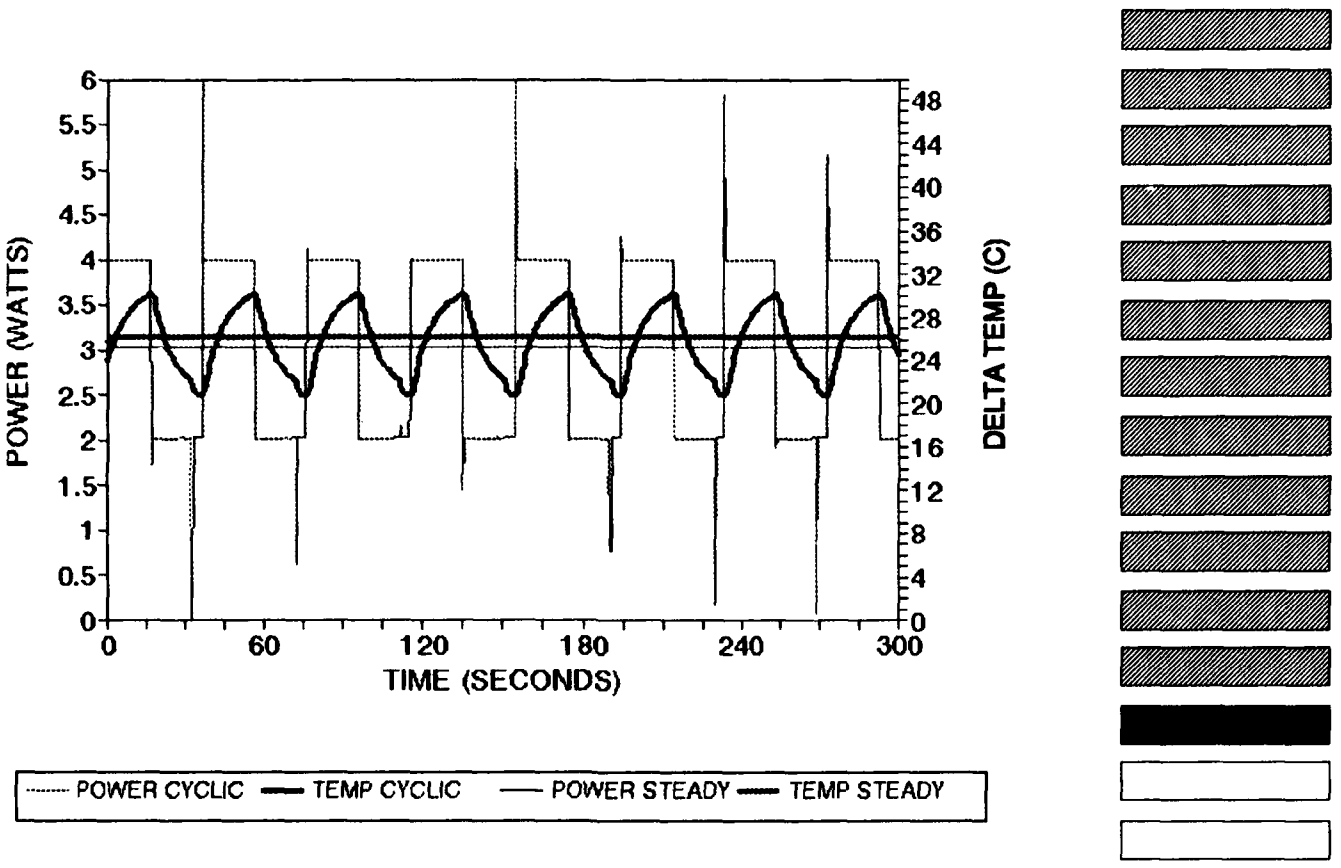

Figure QI. Time dependent transient power and delta temperature for square wave input, bottom heater, heater configuration B28, ambient temperature 17.5°C.

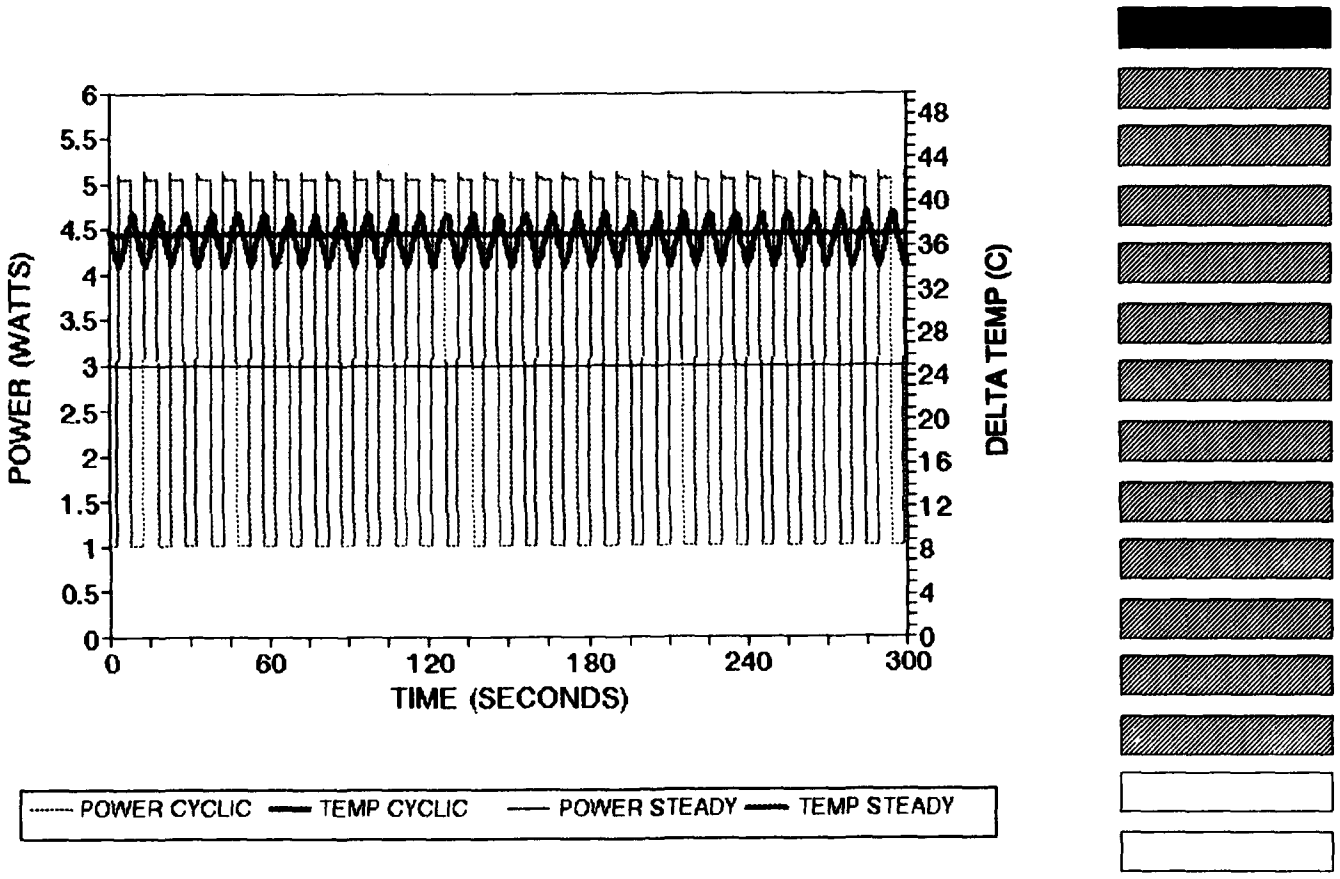

Figure RA. Time dependent transient power and delta temperature for square wave input, top heater, heater configuration B16, ambient temperature 17.5°C.

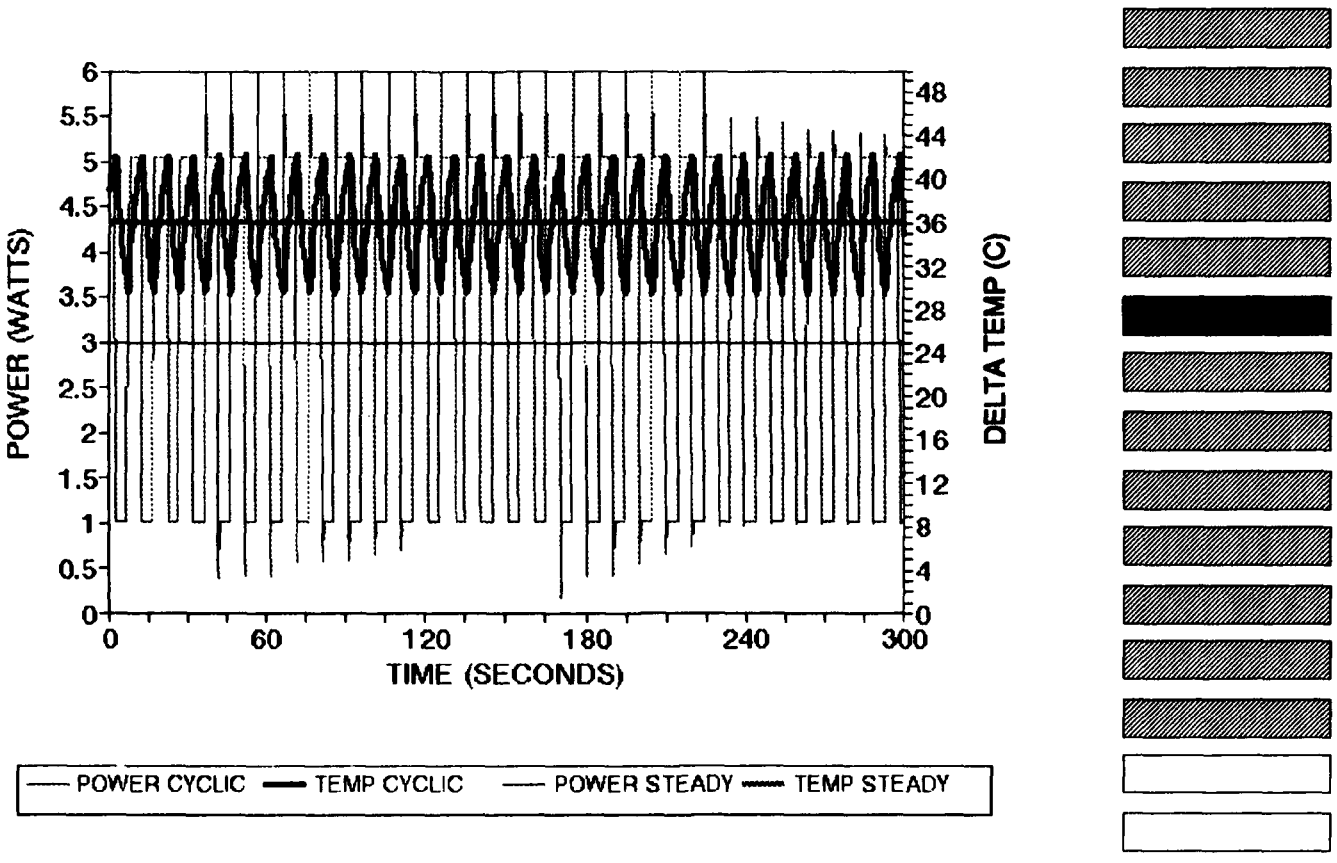

Figure RB. Time dependent transient power and delta temperature for square wave input, middle heater, heater configuration B21, ambient temperature 17.5°C.

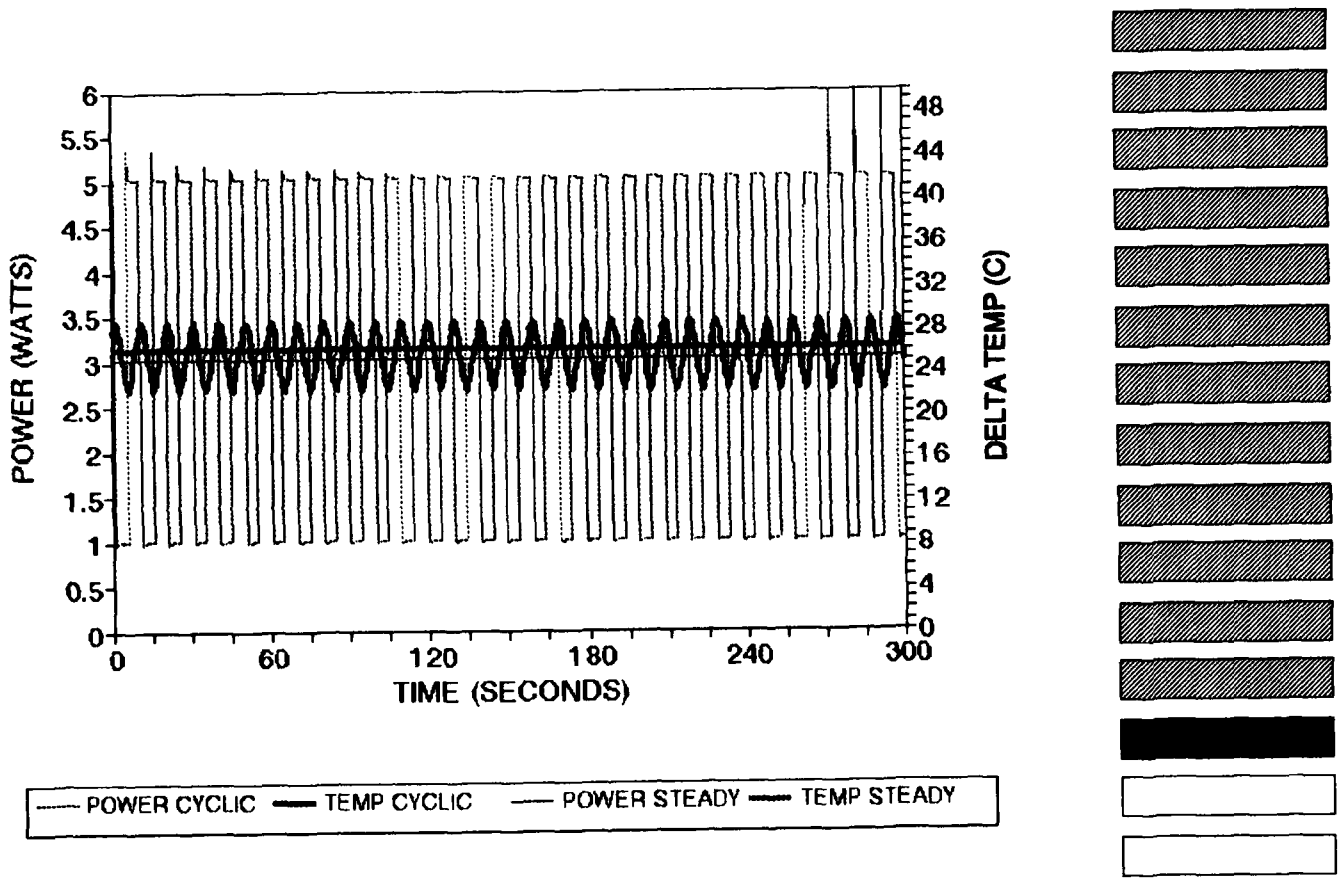

Figure RC. Time dependent transient power and delta temperature for square wave input, bottom heater, heater configuration B28, ambient temperature 17.6°C.

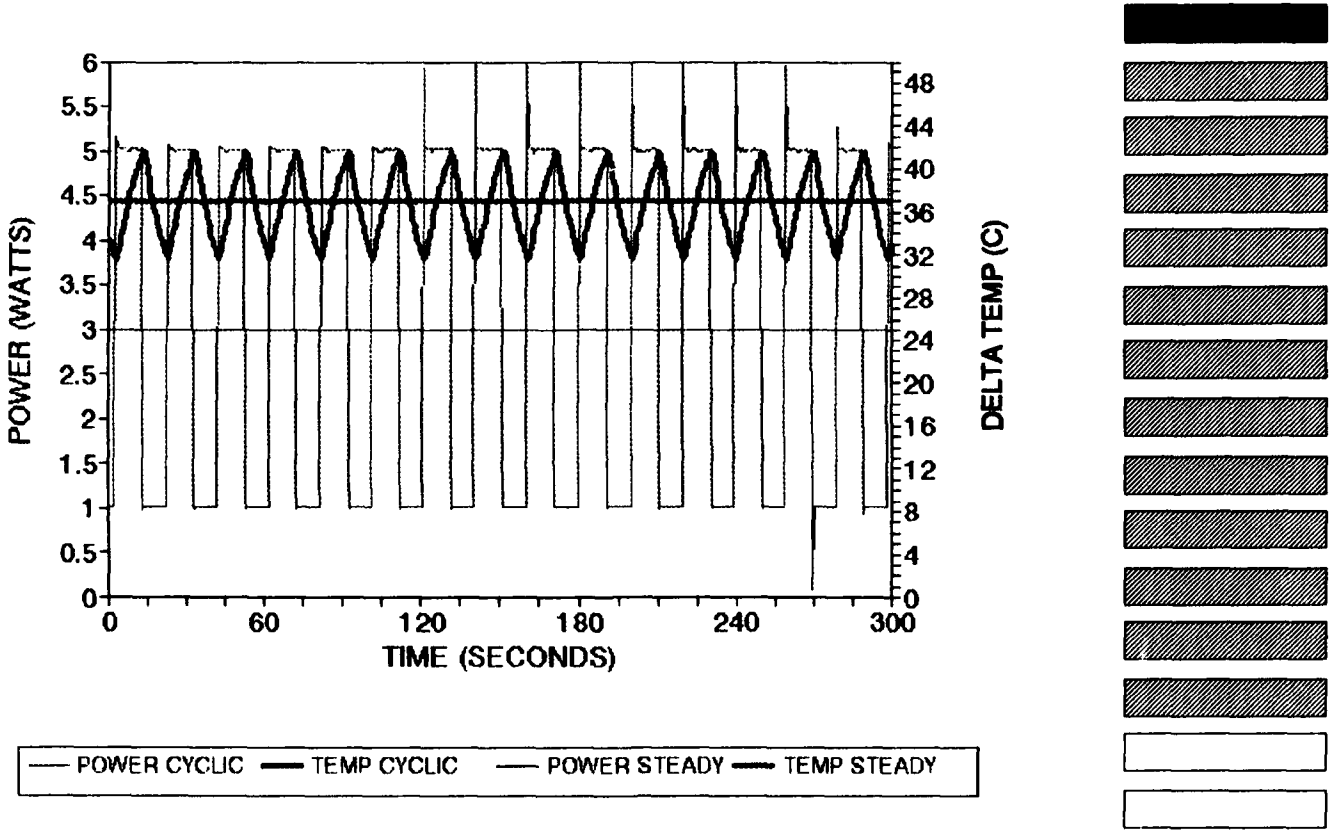

Figure RD. Time dependent transient power and delta temperature for square wave input, top heater, heater configuration B16, ambient temperature 17.6°C.

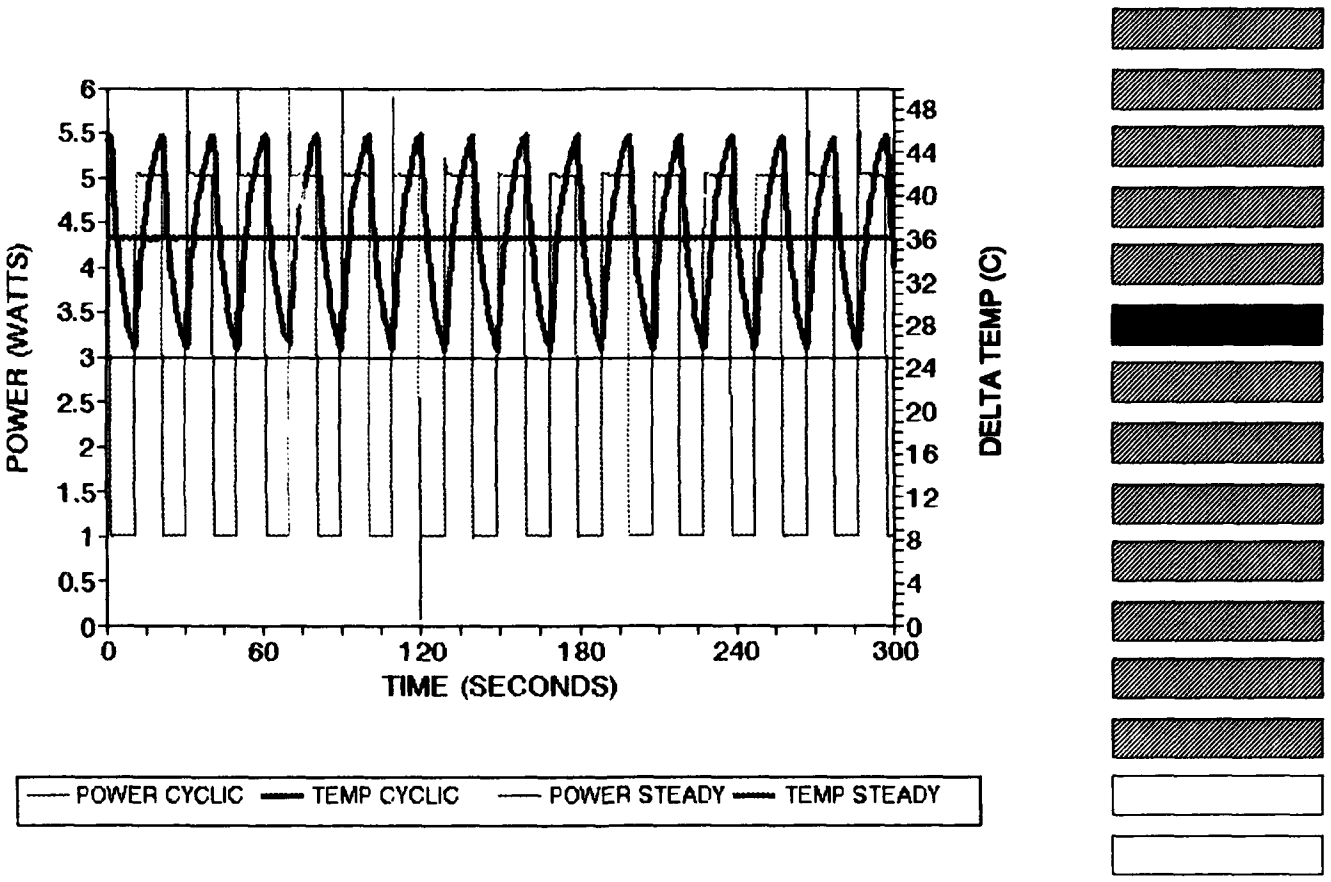

Figure RE. Time dependent transient power and delta temperature for square wave input, middle heater, heater configuration B21, ambient temperature 17.6°C.

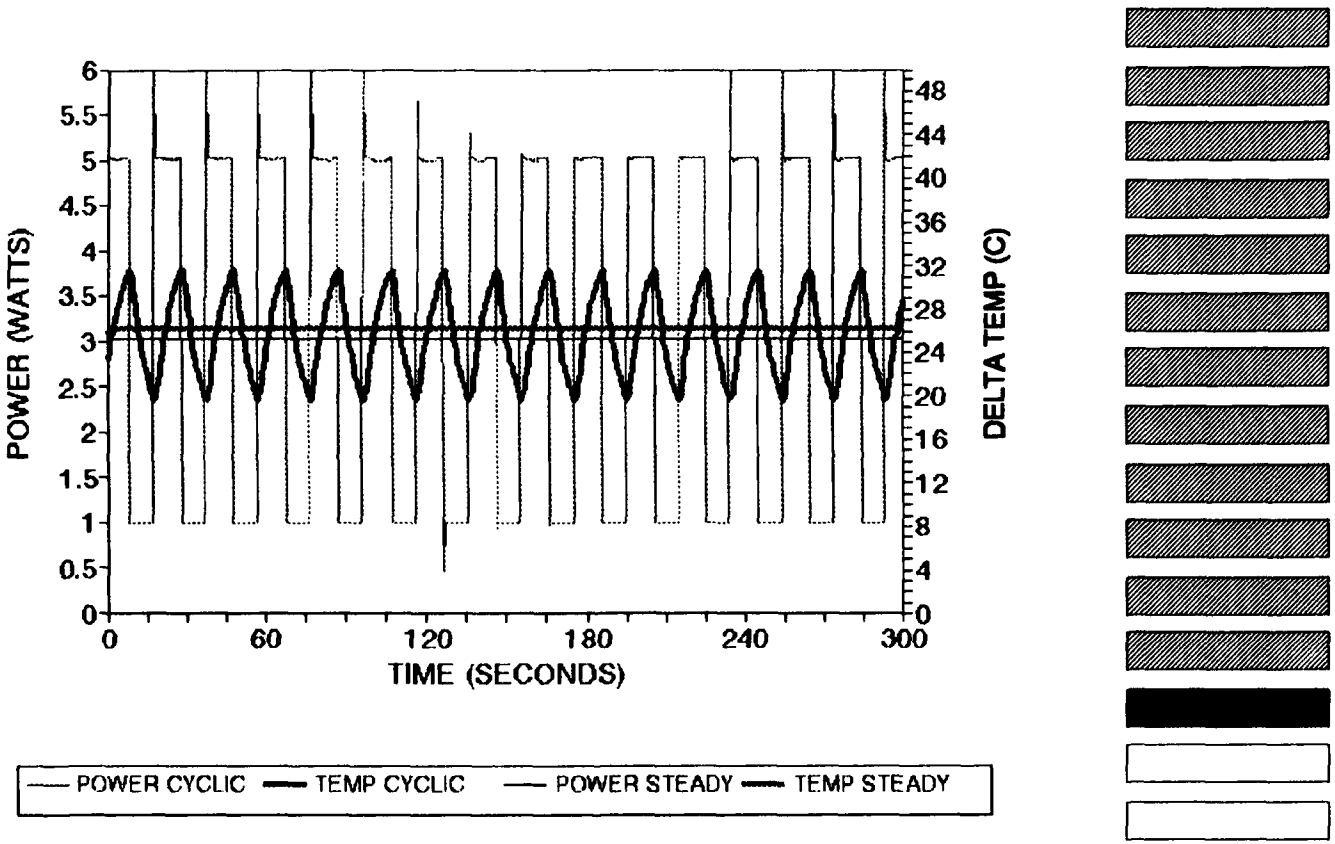

Figure RF. Time dependent transient power and delta temperature for square wave input, bottom heater, heater configuration B28, ambient temperature 17.6°C.

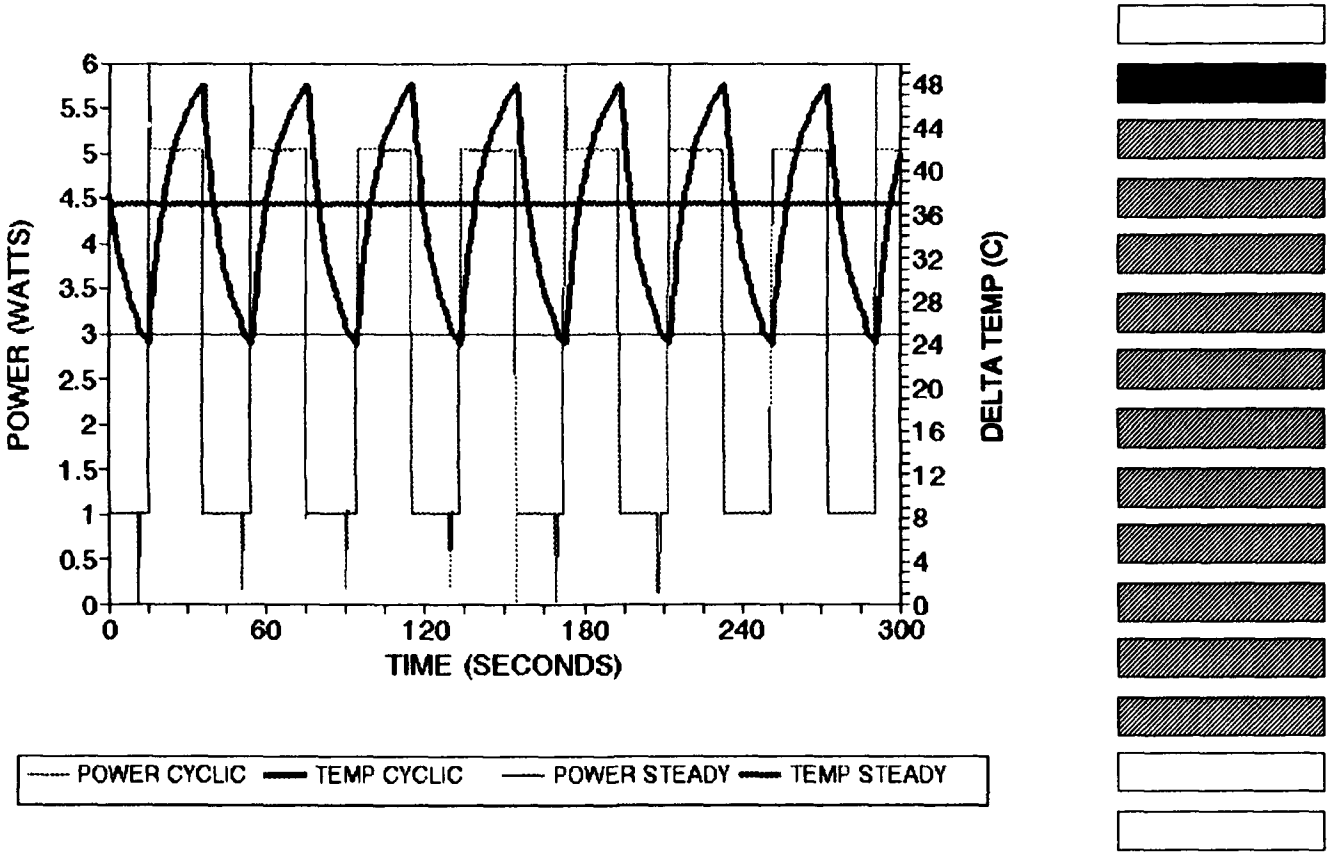

Figure RG. Time dependent transient power and delta temperature for square wave input, top heater, heater configuration C17, ambient temperature 17.6°C.

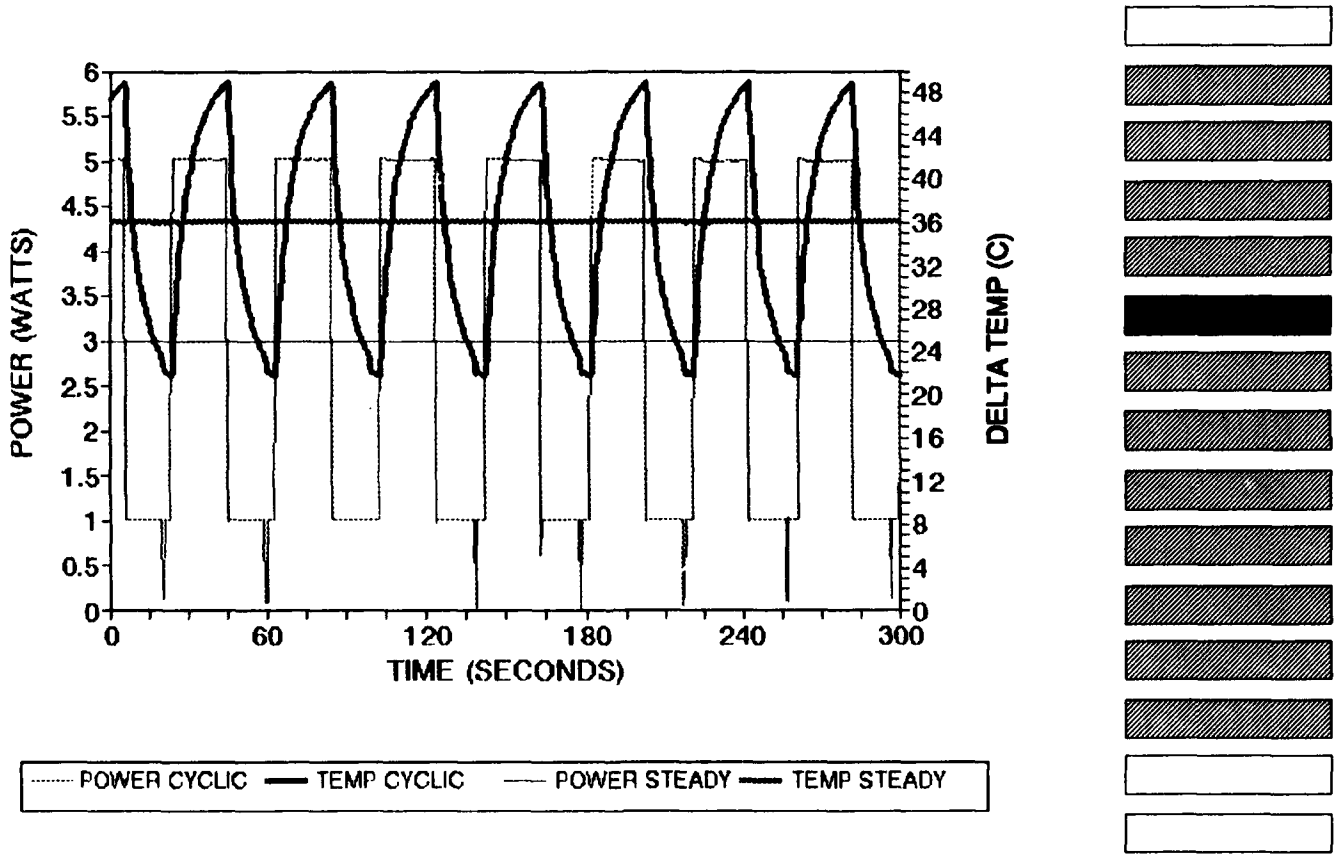

Figure RH. Time dependent transient power and delta temperature for square wave input, middle heater, heater configuration C21, ambient temperature 17.7°C.

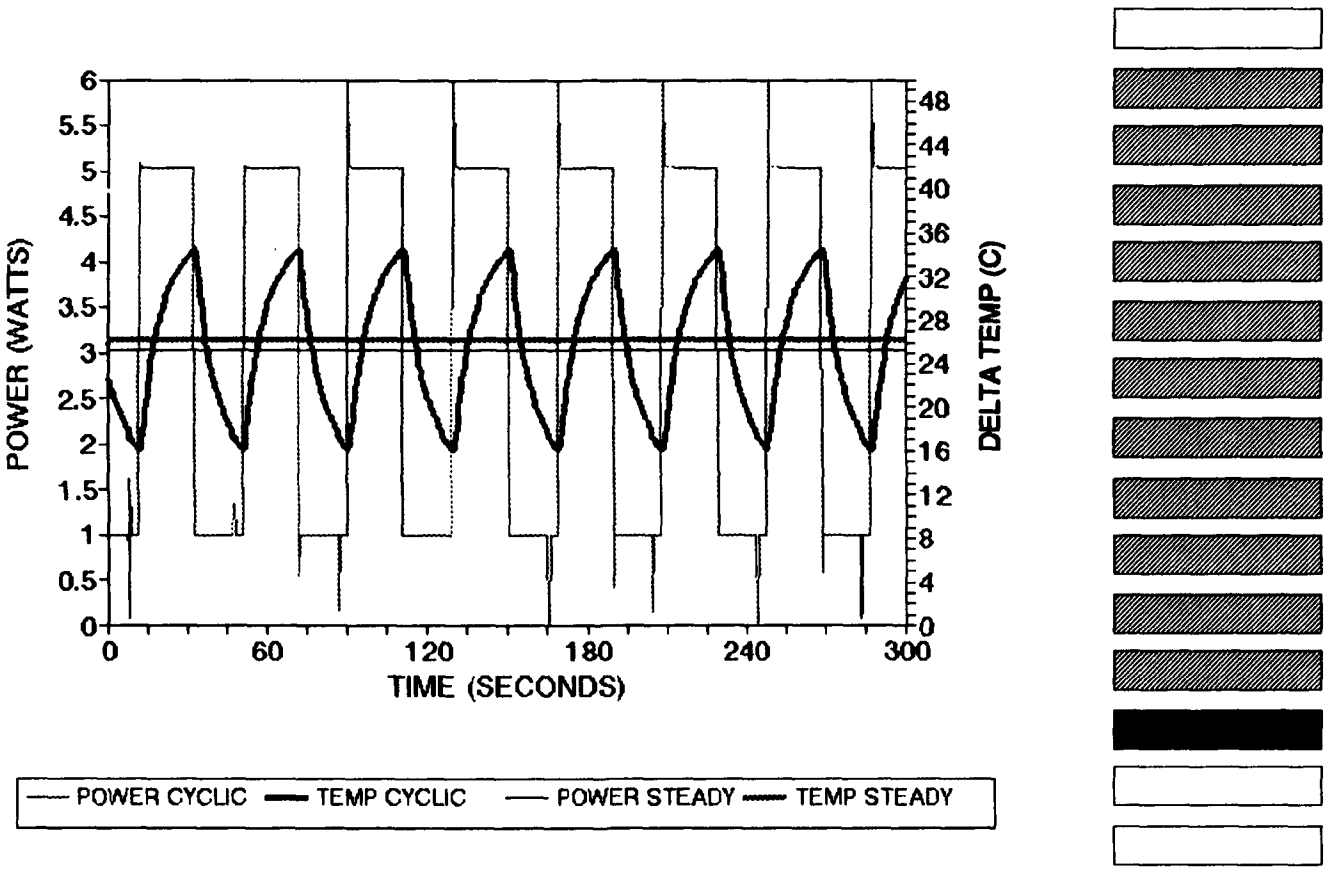

Figure RI. Time dependent transient power and delta temperature for square wave input, bottom heater, heater configuration C28, ambient temperature 17.7°C.

APPENDIX C:
TEMPERATURE AND POWER ACQUIISITION PROGRAM

```
10   !!!!!!!!!!!!!!!!!!!!!!!!!!!!!!!!!!!!!!!!!!!!!!!!!!!!!!!!!!!!!!!!
20   !!!    TEMPERATURE AND POWER TRANSIENT RESPOSE PROGRAM      !!!
30   !!!!!!!!!!!!!!!!!!!!!!!!!!!!!!!!!!!!!!!!!!!!!!!!!!!!!!!!!!!!!!!!
40   OPTION BASE 1
50   REAL T(2000),Volts(2000),Pow(2000),V(2000),Tyme(2000),Tsec(2000)
60   REAL Vminus(2000),Vplus(2000),Tminus(2000),Tplus(2000)
70   REAL V46(2000),V47(2000),V48(2000),V49(2000),V50(2000),V51(2000)
80   REAL Temp(3),Vamb(3)
90   FOR K=1 TO 2000
100  T(K)=0.
110  Volts(K)=0.
120  Pow(K)=0.
130  V(K)=0.
140  Tyme(K)=0.
150  Tsec(K)=0.
160  Vminus(K)=0.
170  Vplus(K)=0.
180  Tminus(K)=0.
190  Tplus(K)=0.
200  V46(K)=0.
210  V47(K)=0.
220  V48(K)=0.
230  V49(K)=0.
240  V50(K)=0.
250  V51(K)=0.
260  NEXT K
270 !
280  PRINTER IS CRT
290  !
300  INPUT "PLEASE INPUT THE NUMBER OF THE HEATER OF INTEREST",N
310  !
320  IF N=1 THEN
330     PRINT "THIS THERMOCOUPLE IS BAD, HOWEVER I CAN GIVE YOU THE"
340            PRINT "TEMPERATURE FOR HEATER NUMBER 31 WHICH IS
GEOMETRICALLY"
350     PRINT "SYMETERICAL TO HEATER 1"
360     PRINT " "
370     PRINT "PRESS Continue TO RESUME"
380     PAUSE
390  END IF
400  !
410  IF N=3 THEN
420     PRINT "THIS THERMOCOUPLE IS BAD HOWEVER I CAN GIVE YOU THE"
```

```
430    PRINT "AVERAGE TEMPERATURE OF THE THERMOCOUPLES ABOVE AND"
440    PRINT "BELOW"
450    PRINT " "
460    PRINT "PRESS Continue TO RESUME"
470    PAUSE
480  END IF
490  !
500  IF N=6 THEN
510    PRINT "THIS THERMOCOUPLE IS BAD HOWEVER I CAN GIVE YOU THE"
520    PRINT "AVERAGE TEMPERATURE OF THE THERMOCOUPLES ABOVE AND"
530    PRINT "BELOW"
540    PRINT " "
550    PRINT "PRESS Continue TO RESUME"
560    PAUSE
570  END IF
580  !
590  IF N=22 THEN
600    PRINT "THIS THERMOCOUPLE IS BAD HOWEVER I CAN GIVE YOU THE"
610    PRINT "AVERAGE TEMPERATURE OF THE THERMOCOUPLES ABOVE AND"
620    PRINT "BELOW"
630    PRINT " "
640    PRINT "PRESS Continue TO RESUME"
650    PAUSE
660  END IF
670  !
680  IF N=29 THEN
690    PRINT "THIS THERMOCOUPLE IS BAD HOWEVER I CAN GIVE YOU THE"
700    PRINT "AVERAGE TEMPERATURE OF THE THERMOCOUPLES ABOVE AND"
710    PRINT "BELOW"
720    PRINT " "
730    PRINT "PRESS Continue TO RESUME"
740    PAUSE
750  END IF
760  !
770  IF N=37 THEN
780    PRINT "THIS THERMOCOUPLE IS BAD HOWEVER I CAN GIVE YOU THE"
790    PRINT "AVERAGE TEMPERATURE OF THE THERMOCOUPLES ABOVE AND"
800    PRINT "BELOW"
810    PRINT " "
820    PRINT "PRESS Continue TO RESUME"
830    PAUSE
840  END IF
850  !
860  INPUT "PLEASE INUPT THE CYCLE TIME IN SECONDS",Np
870  INPUT "PLEASE INUPT THE MAX AND MIN VOLTAGE",Maxv,Minv
880  INPUT "PLEASE INUPT THE OUTPUT OF THE SIDE COLUMNS IN WATTS",Scp
890  IF Np<10 THEN GOTO 860
900  Wx=(Np/50)-1.0
910  IF Wx<=0 THEN Wx=0.
920  M=INT((60/Np)*250)+500
```

```
930  IF M>900 THEN M=900
940  !
950  Ti=TIMEDATE
960  FOR I=1 TO M
970  !
980  !OUTPUT 709;"RST"
990  !
1000 IF N=1 THEN
1010   OUTPUT 709;"CONFMEAS DCV,210,USE 0"
1020   ENTER 709;V(I)
1030   OUTPUT 709;"CONFMEAS DCV,315,USE 0"
1040   ENTER 709;Volts(I)
1050   OUTPUT 709;"CONFMEAS DCV,316,USE 0"
1060   ENTER 709;V46(I)
1070   GOTO 5590
1080 END IF
1090 !
1100 IF N=2 THEN
1110   OUTPUT 709;"CONFMEAS DCV,101,USE 0"
1120   ENTER 709;V(I)
1130   OUTPUT 709;"CONFMEAS DCV,314,USE 0"
1140   ENTER 709;Volts(I)
1150   OUTPUT 709;"CONFMEAS DCV,316,USE 0"
1160   ENTER 709;V46(I)
1170   GOTO 5590
1180 END IF
1190 !
1200 IF N=3 THEN
1210   OUTPUT 709;"CONFMEAS DCV,101,USE 0"
1220   ENTER 709;Vminus(I)
1230   OUTPUT 709;"CONFMEAS DCV,103,USE 0"
1240   ENTER 709;Vplus(I)
1250   OUTPUT 709;"CONFMEAS DCV,313,USE 0"
1260   ENTER 709;Volts(I)
1270   OUTPUT 709;"CONFMEAS DCV,316,USE 0"
1280   ENTER 709;V46(I)
1290   GOTO 5590
1300 END IF
1310 !
1320 IF N=4 THEN
1330   OUTPUT 709;"CONFMEAS DCV,103,USE 0"
1340   ENTER 709;V(I)
1350   OUTPUT 709;"CONFMEAS DCV,312,USE 0"
1360   ENTER 709;Volts(I)
1370   OUTPUT 709;"CONFMEAS DCV,316,USE 0"
1380   ENTER 709;V46(I)
1390   GOTO 5590
1400 END IF
1410 !
1420 IF N=5 THEN
```

```
1430   OUTPUT 709;"CONFMEAS DCV,104,USE 0"
1440   ENTER 709;V(I)
1450   OUTPUT 709;"CONFMEAS DCV,311,USE 0"
1460   ENTER 709;Volts(I)
1470   OUTPUT 709;"CONFMEAS DCV,316,USE 0"
1480   ENTER 709;V46(I)
1490   GOTO 5590
1500 END IF
1510 !
1520 IF N=6 THEN
1530   OUTPUT 709;"CONFMEAS DCV,104,USE 0"
1540   ENTER 709;Vminus(I)
1550   OUTPUT 709;"CONFMEAS DCV,106,USE 0"
1560   ENTER 709;Vplus(I)
1570   OUTPUT 709;"CONFMEAS DCV,310,USE 0"
1580   ENTER 709;Volts(I)
1590   OUTPUT 709;"CONFMEAS DCV,316,USE 0"
1600   ENTER 709;V46(I)
1610   GOTO 5590
1620 END IF
1630 !
1640 IF N=7 THEN
1650   OUTPUT 709;"CONFMEAS DCV,106,USE 0"
1660   ENTER 709;V(I)
1670   OUTPUT 709;"CONFMEAS DCV,309,USE 0"
1680   ENTER 709;Volts(I)
1690   OUTPUT 709;"CONFMEAS DCV,316,USE 0"
1700   ENTER 709;V46(I)
1710   GOTO 5590
1720 END IF
1730 !
1740 IF N=8 THEN
1750   OUTPUT 709;"CONFMEAS DCV,100,USE 0"
1760   ENTER 709;V(I)
1770   OUTPUT 709;"CONFMEAS DCV,308,USE 0"
1780   ENTER 709;Volts(I)
1790   OUTPUT 709;"CONFMEAS DCV,316,USE 0"
1800   ENTER 709;V46(I)
1810   GOTO 5590
1820 END IF
1830 !
1840 IF N=9 THEN
1850   OUTPUT 709;"CONFMEAS DCV,100,USE 0"
1860   ENTER 709;V(I)
1870   OUTPUT 709;"CONFMEAS DCV,403,USE 0"
1880   ENTER 709;Volts(I)
1890   OUTPUT 709;"CONFMEAS DCV,400,USE 0"
1900   ENTER 709;V47(I)
1910   GOTO 5590
1920 END IF
```

```
1930 !
1940 IF N=10 THEN
1950   OUTPUT 709;"CONFMEAS DCV,109,USE 0"
1960   ENTER 709;V(I)
1970   OUTPUT 709;"CONFMEAS DCV,404,USE 0"
1980   ENTER 709;Volts(I)
1990   OUTPUT 709;"CONFMEAS DCV,400,USE 0"
2000   ENTER 709;V47(I)
2010   GOTO 5590
2020 END IF
2030 !
2040 IF N=11 THEN
2050   OUTPUT 709;"CONFMEAS DCV,110,USE 0"
2060   ENTER 709;V(I)
2070   OUTPUT 709;"CONFMEAS DCV,405,USE 0"
2080   ENTER 709;Volts(I)
2090   OUTPUT 709;"CONFMEAS DCV,400,USE 0"
2100   ENTER 709;V47(I)
2110   GOTO 5590
2120 END IF
2130 !
2140 IF N=12 THEN
2150   OUTPUT 709;"CONFMEAS DCV,111,USE 0"
2160   ENTER 709;V(I)
2170   OUTPUT 709;"CONFMEAS DCV,406,USE 0"
2180   ENTER 709;Volts(I)
2190   OUTPUT 709;"CONFMEAS DCV,400,USE 0"
2200   ENTER 709;V47(I)
2210   GOTO 5590
2220 END IF
2230 !
2240 IF N=13 THEN
2250   OUTPUT 709;"CONFMEAS DCV,112,USE 0"
2260   ENTER 709;V(I)
2270   OUTPUT 709;"CONFMEAS DCV,407,USE 0"
2280   ENTER 709;Volts(I)
2290   OUTPUT 709;"CONFMEAS DCV,400,USE 0"
2300   ENTER 709;V47(I)
2310   GOTO 5590
2320 END IF
2330 !
2340 IF N=14 THEN
2350   OUTPUT 709;"CONFMEAS DCV,113,USE 0"
2360   ENTER 709;V(I)
2370   OUTPUT 709;"CONFMEAS DCV,408,USE 0"
2380   ENTER 709;Volts(I)
2390   OUTPUT 709;"CONFMEAS DCV,400,USE 0"
2400   ENTER 709;V47(I)
2410   GOTO 5590
2420 END IF
```

```
2430 !
2440 IF N=15 THEN
2450   OUTPUT 709;"CONFMEAS DCV,114,USE 0"
2460   ENTER 709;V(I)
2470   OUTPUT 709;"CONFMEAS DCV,409,USE 0"
2480   ENTER 709;Volts(I)
2490   OUTPUT 709;"CONFMEAS DCV,400,USE 0"
2500   ENTER 709;V47(I)
2510   GOTO 5590
2520 END IF
2530 !
2540 IF N=16 THEN
2550   OUTPUT 709;"CONFMEAS DCV,115,USE 0"
2560   ENTER 709;V(I)
2570   OUTPUT 709;"CONFMEAS DCV,410,USE 0"
2580   ENTER 709;Volts(I)
2590   OUTPUT 709;"CONFMEAS DCV,401,USE 0"
2600   ENTER 709;V48(I)
2610   GOTO 5590
2620 END IF
2630 !
2640 IF N=17 THEN
2650   OUTPUT 709;"CONFMEAS DCV,116,USE 0"
2660   ENTER 709;V(I)
2670   OUTPUT 709;"CONFMEAS DCV,411,USE 0"
2680   ENTER 709;Volts(I)
2690   OUTPUT 709;"CONFMEAS DCV,401,USE 0"
2700   ENTER 709;V48(I)
2710   GOTO 5590
2720 END IF
2730 !
2740 IF N=18 THEN
2750   OUTPUT 709;"CONFMEAS DCV,117,USE 0"
2760   ENTER 709;V(I)
2770   OUTPUT 709;"CONFMEAS DCV,412,USE 0"
2780   ENTER 709;Volts(I)
2790   OUTPUT 709;"CONFMEAS DCV,401,USE 0"
2800   ENTER 709;V48(I)
2810   GOTO 5590
2820 END IF
2830 !
2840 IF N=19 THEN
2850   OUTPUT 709;"CONFMEAS DCV,118,USE 0"
2860   ENTER 709;V(I)
2870   OUTPUT 709;"CONFMEAS DCV,413,USE 0"
2880   ENTER 709;Volts(I)
2890   OUTPUT 709;"CONFMEAS DCV,401,USE 0"
2900   ENTER 709;V48(I)
2910   GOTO 5590
2920 END IF
```

```
2930 !
2940 IF N=20 THEN
2950   OUTPUT 709;"CONFMEAS DCV,119,USE 0"
2960   ENTER 709;V(I)
2970   OUTPUT 709;"CONFMEAS DCV,414,USE 0"
2980   ENTER 709;Volts(I)
2990   OUTPUT 709;"CONFMEAS DCV,401,USE 0"
3000   ENTER 709;V48(I)
3010   GOTO 5590
3020 END IF
3030 !
3040 IF N=21 THEN
3050   OUTPUT 709;"CONFMEAS DCV,200,USE 0"
3060   ENTER 709;V(I)
3070   OUTPUT 709;"CONFMEAS DCV,415,USE 0"
3080   ENTER 709;Volts(I)
3090   OUTPUT 709;"CONFMEAS DCV,401,USE 0"
3100   ENTER 709;V48(I)
3110   GOTO 5590
3120 END IF
3130 !
3140 IF N=22 THEN
3150   OUTPUT 709;"CONFMEAS DCV,200,USE 0"
3160   ENTER 709;Vminus(I)
3170   OUTPUT 709;"CONFMEAS DCV,202,USE 0"
3180   ENTER 709;Vplus(I)
3190   OUTPUT 709;"CONFMEAS DCV,416,USE 0"
3200   ENTER 709;Volts(I)
3210   OUTPUT 709;"CONFMEAS DCV,401,USE 0"
3220   ENTER 709;V48(I)
3230   GOTO 5590
3240 END IF
3250 !
3260 IF N=23 THEN
3270   OUTPUT 709;"CONFMEAS DCV,202,USE 0"
3280   ENTER 709;V(I)
3290   OUTPUT 709;"CONFMEAS DCV,417,USE 0"
3300   ENTER 709;Volts(I)
3310   OUTPUT 709;"CONFMEAS DCV,401,USE 0"
3320   ENTER 709;V48(I)
3330   GOTO 5590
3340 END IF
3350 !
3360 IF N=24 THEN
3370   OUTPUT 709;"CONFMEAS DCV,203,USE 0"
3380   ENTER 709;V(I)
3390   OUTPUT 709;"CONFMEAS DCV,503,USE 0"
3400   ENTER 709;Volts(I)
3410   OUTPUT 709;"CONFMEAS DCV,500,USE 0"
3420   ENTER 709;V49(I)
```

```
3430   GOTO 5590
3440 END IF
3450 !
3460 IF N=25 THEN
3470   OUTPUT 709;"CONFMEAS DCV,204,USE 0"
3480   ENTER 709;V(I)
3490   OUTPUT 709;"CONFMEAS DCV,504,USE 0"
3500   ENTER 709;Volts(I)
3510   OUTPUT 709;"CONFMEAS DCV,500,USE 0"
3520   ENTER 709;V49(I)
3530   GOTO 5590
3540 END IF
3550 !
3560 IF N=26 THEN
3570   OUTPUT 709;"CONFMEAS DCV,205,USE 0"
3580   ENTER 709;V(I)
3590   OUTPUT 709;"CONFMEAS DCV,505,USE 0"
3600   ENTER 709;Volts(I)
3610   OUTPUT 709;"CONFMEAS DCV,500,USE 0"
3620   ENTER 709;V49(I)
3630   GOTO 5590
3640 END IF
3650 !
3660 IF N=27 THEN
3670   OUTPUT 709;"CONFMEAS DCV,206,USE 0"
3680   ENTER 709;V(I)
3690   OUTPUT 709;"CONFMEAS DCV,506,USE 0"
3700   ENTER 709;Volts(I)
3710   OUTPUT 709;"CONFMEAS DCV,500,USE 0"
3720   ENTER 709;V49(I)
3730   GOTO 5590
3740 END IF
3750 !
3760 IF N=28 THEN
3770   OUTPUT 709;"CONFMEAS DCV,207,USE 0"
3780   ENTER 709;V(I)
3790   OUTPUT 709;"CONFMEAS DCV,507,USE 0"
3800   ENTER 709;Volts(I)
3810   OUTPUT 709;"CONFMEAS DCV,500,USE 0"
3820   ENTER 709;V49(I)
3830   GOTO 5590
3840 END IF
3850 !
3860 IF N=29 THEN
3870   OUTPUT 709;"CONFMEAS DCV,207,USE 0"
3880   ENTER 709;Vminus(I)
3890   OUTPUT 709;"CONFMEAS DCV,209,USE 0"
3900   ENTER 709;Vplus(I)
3910   OUTPUT 709;"CONFMEAS DCV,508,USE 0"
3920   ENTER 709;Volts(I)
```

```
3930   OUTPUT 709;"CONFMEAS DCV,500,USE 0"
3940   ENTER 709;V49(I)
3950   GOTO 5590
3960  END IF
3970  !
3980  IF N=30 THEN
3990   OUTPUT 709;"CONFMEAS DCV,209,USE 0"
4000   ENTER 709;V(I)
4010   OUTPUT 709;"CONFMEAS DCV,509,USE 0"
4020   ENTER 709;Volts(I)
4030   OUTPUT 709;"CONFMEAS DCV,500,USE 0"
4040   ENTER 709;V49(I)
4050   GOTO 5590
4060  END IF
4070  !
4080  IF N=31 THEN
4090   OUTPUT 709;"CONFMEAS DCV,210,USE 0"
4100   ENTER 709;V(I)
4110   OUTPUT 709;"CONFMEAS DCV,510,USE 0"
4120   ENTER 709;Volts(I)
4130   OUTPUT 709;"CONFMEAS DCV,501,USE 0"
4140   ENTER 709;V50(I)
4150   GOTO 5590
4160  END IF
4170  !
4180  IF N=32 THEN
4190   OUTPUT 709;"CONFMEAS DCV,211,USE 0"
4200   ENTER 709;V(I)
4210   OUTPUT 709;"CONFMEAS DCV,511,USE 0"
4220   ENTER 709;Volts(I)
4230   OUTPUT 709;"CONFMEAS DCV,501,USE 0"
4240   ENTER 709;V50(I)
4250   GOTO 5590
4260  END IF
4270  !
4280  IF N=33 THEN
4290   OUTPUT 709;"CONFMEAS DCV,212,USE 0"
4300   ENTER 709;V(I)
4310   OUTPUT 709;"CONFMEAS DCV,512,USE 0"
4320   ENTER 709;Volts(I)
4330   OUTPUT 709;"CONFMEAS DCV,501,USE 0"
4340   ENTER 709;V50(I)
4350   GOTO 5590
4360  END IF
4370  !
4380  IF N=34 THEN
4390   OUTPUT 709;"CONFMEAS DCV,213,USE 0"
4400   ENTER 709;V(I)
4410   OUTPUT 709;"CONFMEAS DCV,513,USE 0"
4420   ENTER 709;Volts(I)
```

```
4430   OUTPUT 709;"CONFMEAS DCV,501,USE 0"
4440   ENTER 709;V50(I)
4450   GOTO 5590
4460  END IF
4470  !
4480  IF N=35 THEN
4490   OUTPUT 709;"CONFMEAS DCV,214,USE 0"
4500   ENTER 709;V(I)
4510   OUTPUT 709;"CONFMEAS DCV,514,USE 0"
4520   ENTER 709;Volts(I)
4530   OUTPUT 709;"CONFMEAS DCV,501,USE 0"
4540   ENTER 709;V50(I)
4550   GOTO 5590
4560  END IF
4570  !
4580  IF N=36 THEN
4590   OUTPUT 709;"CONFMEAS DCV,215,USE 0"
4600   ENTER 709;V(I)
4610   OUTPUT 709;"CONFMEAS DCV,515,USE 0"
4620   ENTER 709;Volts(I)
4630   OUTPUT 709;"CONFMEAS DCV,501,USE 0"
4640   ENTER 709;V50(I)
4650   GOTO 5590
4660  END IF
4670  !
4680  IF N=37 THEN
4690   OUTPUT 709;"CONFMEAS DCV,215,USE 0"
4700   ENTER 709;Vminus(I)
4710   OUTPUT 709;"CONFMEAS DCV,217,USE 0"
4720   ENTER 709;Vplus(I)
4730   OUTPUT 709;"CONFMEAS DCV,516,USE 0"
4740   ENTER 709;Volts(I)
4750   OUTPUT 709;"CONFMEAS DCV,501,USE 0"
4760   ENTER 709;V50(I)
4770   GOTO 5590
4780  END IF
4790  !
4800  IF N=38 THEN
4810   OUTPUT 709;"CONFMEAS DCV,217,USE 0"
4820   ENTER 709;V(I)
4830   OUTPUT 709;"CONFMEAS DCV,517,USE 0"
4840   ENTER 709;Volts(I)
4850   OUTPUT 709;"CONFMEAS DCV,501,USE 0"
4860   ENTER 709;V50(I)
4870   GOTO 5590
4880  END IF
4890  !
4900  IF N=39 THEN
4910   OUTPUT 709;"CONFMEAS DCV,218,USE 0"
4920   ENTER 709;V(I)
```

```
4930   OUTPUT 709;"CONFMEAS DCV,602,USE 0"
4940   ENTER 709;Volts(I)
4950   OUTPUT 709;"CONFMEAS DCV,600,USE 0"
4960   ENTER 709;V51(I)
4970   GOTO 5590
4980 END IF
4990 !
5000 IF N=40 THEN
5010   OUTPUT 709;"CONFMEAS DCV,219,USE 0"
5020   ENTER 709;V(I)
5030   OUTPUT 709;"CONFMEAS DCV,603,USE 0"
5040   ENTER 709;Volts(I)
5050   OUTPUT 709;"CONFMEAS DCV,600,USE 0"
5060   ENTER 709;V51(I)
5070   GOTO 5590
5080 END IF
5090 !
5100 IF N=41 THEN
5110   OUTPUT 709;"CONFMEAS DCV,300,USE 0"
5120   ENTER 709;V(I)
5130   OUTPUT 709;"CONFMEAS DCV,604,USE 0"
5140   ENTER 709;Volts(I)
5150   OUTPUT 709;"CONFMEAS DCV,600,USE 0"
5160   ENTER 709;V51(I)
5170   GOTO 5590
5180 END IF
5190 !
5200 IF N=42 THEN
5210   OUTPUT 709;"CONFMEAS DCV,301,USE 0"
5220   ENTER 709;V(I)
5230   OUTPUT 709;"CONFMEAS DCV,605,USE 0"
5240   ENTER 709;Volts(I)
5250   OUTPUT 709;"CONFMEAS DCV,600,USE 0"
5260   ENTER 709;V51(I)
5270   GOTO 5590
5280 END IF
5290 !
5300 IF N=43 THEN
5310   OUTPUT 709;"CONFMEAS DCV,302,USE 0"
5320   ENTER 709;V(I)
5330   OUTPUT 709;"CONFMEAS DCV,606,USE 0"
5340   ENTER 709;Volts(I)
5350   OUTPUT 709;"CONFMEAS DCV,600,USE 0"
5360   ENTER 709;V51(I)
5370   GOTO 5590
5380 END IF
5390 !
5400 IF N=44 THEN
5410   OUTPUT 709;"CONFMEAS DCV,303,USE 0"
5420   ENTER 709;V(I)
```

```
5430   OUTPUT 709;"CONFMEAS DCV,607,USE 0"
5440   ENTER 709;Volts(I)
5450   OUTPUT 709;"CONFMEAS DCV,600,USE 0"
5460   ENTER 709;V51(I)
5470   GOTO 5590
5480 END IF
5490 !
5500 IF N=45 THEN
5510   OUTPUT 709;"CONFMEAS DCV,304,USE 0"
5520   ENTER 709;V(I)
5530   OUTPUT 709;"CONFMEAS DCV,608,USE 0"
5540   ENTER 709;Volts(I)
5550   OUTPUT 709;"CONFMEAS DCV,600,USE 0"
5560   ENTER 709;V51(I)
5570 END IF
5580 !
5590 WAIT Wx
5600 !
5610 NEXT I
5620 !
5630 Tf=TIMEDATE
5640 !
5650 CLEAR SCREEN
5660 !
5670 BEEP 81.38,.5
5680 BEEP 2115.88,.5
5690 BEEP 3499.34,.5
5700 BEEP 5208.32,.5
5710 BEEP 3499.34,.5
5720 BEEP 2115.88,.5
5730 BEEP 81.38,.5
5740 !
5750 OUTPUT 709;"RST"
5760 !
5770 A=.0006797
5780 B=25825.1328
5790 C=607789.2467
5800 D=21952034.3364
5810 E=8370810996.1874
5820 !
5830 OUTPUT 709;"CONFMEAS DCV,317-319,USE 0"
5840 FOR I=1 TO 3
5850 ENTER 709;Vamb(I)
5860 Temp(I)=A+(B*Vamb(I))-(C*(Vamb(I)^2))-(D*(Vamb(I)^3))+(E*(Vamb(I)^4))
5870 NEXT I
5880 !
5890 Tamb=(Temp(1)+Temp(2)+Temp(3))/3
5900 !
5910 OUTPUT 709;"RST"
5920 FOR I=1 TO M
```

```
5930 !
5940 IF N=3 THEN GOTO 6040
5950 IF N=6 THEN GOTO 6040
5960 IF N=22 THEN GOTO 6040
5970 IF N=29 THEN GOTO 6040
5980 IF N=37 THEN GOTO 6040
5990 !
6000 T(I)=A+(B*V(I))-(C*(V(I)^2))-(D*(V(I)^3))+(E*(V(I)^4))
6010 !
6020 GOTO 6100
6030 !
6040 Tminus(I)=A+(B*Vminus(I))-(C*(Vminus(I)^2))-(D*(Vminus(I)^3))+(E*(Vminus(I)^4))
6050 !
6060 Tplus(I)=A+(B*Vplus(I))-(C*(Vplus(I)^2))-(D*(Vplus(I)^3))+(E*(Vplus(I)^4))
6070 T(I)=(Tminus(I)+Tplus(I))/2
6080 !
6090 !
6100 Resist=2.0
6110 R2=Resist*Resist
6120 IF N=2 THEN Pow(I)=(V46(I)-Volts(I))*(Volts(I)*(Resist+.4)-V46(I)*.4)/R2
6130 IF N=5 THEN Pow(I)=(V46(I)-Volts(I))*(Volts(I)*(Resist+.2)-V46(I)*.2)/R2
6140 IF N=9 THEN Pow(I)=(V47(I)-Volts(I))*(Volts(I)*(Resist+.3)-V47(I)*.3)/R2
6150 IF N=10 THEN Pow(I)=(V47(I)-Volts(I))*(Volts(I)*(Resist+.45)-V47(I)*.45)/R2
6160 IF N=18 THEN Pow(I)=(V48(I)-Volts(I))*(Volts(I)*(Resist+.55)-V48(I)*.55)/R2
6170 IF N=23 THEN Pow(I)=(V48(I)-Volts(I))*(Volts(I)*(Resist+.55)-V48(I)*.55)/R2
6180 IF N=24 THEN Pow(I)=(V49(I)-Volts(I))*(Volts(I)*(Resist+.10)-V49(I)*.10)/R2
6190 IF N=25 THEN Pow(I)=(V49(I)-Volts(I))*(Volts(I)*(Resist+.30)-V49(I)*.30)/R2
6200 IF N=32 THEN Pow(I)=(V50(I)-Volts(I))*(Volts(I)*(Resist+.60)-V50(I)*.60)/R2
6210 IF N=34 THEN Pow(I)=(V50(I)-Volts(I))*(Volts(I)*(Resist+.30)-V50(I)*.30)/R2
6220 IF N=35 THEN Pow(I)=(V50(I)-Volts(I))*(Volts(I)*(Resist+.60)-V50(I)*.60)/R2
6230 IF N=36 THEN Pow(I)=(V50(I)-Volts(I))*(Volts(I)*(Resist+.60)-V50(I)*.60)/R2
6240 IF N=37 THEN Pow(I)=(V50(I)-Volts(I))*(Volts(I)*(Resist+.60)-V50(I)*.60)/R2
6250 IF N=39 THEN Pow(I)=(V51(I)-Volts(I))*(Volts(I)*(Resist+.30)-V51(I)*.30)/R2
6260 IF N=40 THEN Pow(I)=(V51(I)-Volts(I))*(Volts(I)*(Resist+.30)-V51(I)*.30)/R2
6270 IF N=42 THEN Pow(I)=(V51(I)-Volts(I))*(Volts(I)*(Resist+.55)-V51(I)*.55)/R2
6280 IF N=43 THEN Pow(I)=(V51(I)-Volts(I))*(Volts(I)*(Resist+.45)-V51(I)*.45)/R2
6290 IF N=44 THEN Pow(I)=(V51(I)-Volts(I))*(Volts(I)*(Resist+.55)-V51(I)*.55)/R2
6300 IF N=25 THEN Pow(I)=(V49(I)-Volts(I))*(Volts(I)*(Resist+.3)-V49(I)*.3)/R2
6310 IF N=29 THEN Pow(I)=(V49(I)-Volts(I))*(Volts(I)*(Resist+.3)-V49(I)*.3)/R2
6320 IF N=30 THEN Pow(I)=(V49(I)-Volts(I))*(Volts(I)*(Resist+.3)-V49(I)*.3)/R2
6330 !
6340 Resist=1.972
6350 R2=Resist*Resist
6360 !
6370 IF N=15 THEN Pow(I)=(V47(I)-Volts(I))*(Volts(I)*(Resist+.2)-V47(I)*.2)/R2
6380 !
6390 Resist=1.9184
6400 R2=Resist*Resist
6410 !
6420 IF N=14 THEN Pow(I)=(V47(I)-Volts(I))*(Volts(I)*(Resist+.1)-V47(I)*.1)/R2
```

```
6430 !
6440 Resist=1.886
6450 R2=Resist*Resist
6460 !
6470 IF N=4 THEN Pow(I)=(V46(I)-Volts(I))*(Volts(I)*(Resist+.1)-V46(I)*.1)/R2
6480 IF N=6 THEN Pow(I)=(V46(I)-Volts(I))*(Volts(I)*(Resist+.1)-V46(I)*.1)/R2
6490 !
6500 Resist=1.862
6510 R2=Resist*Resist
6520 !
6530 IF N=27 THEN Pow(I)=(V49(I)-Volts(I))*(Volts(I)*(Resist+.5)-V49(I)*.5)/R2
6540 IF N=28 THEN Pow(I)=(V49(I)-Volts(I))*(Volts(I)*(Resist+0.)-V49(I)*0.)/R2
6550 IF N=31 THEN Pow(I)=(V50(I)-Volts(I))*(Volts(I)*(Resist+.65)-V50(I)*.65)/R2
6560 IF N=38 THEN Pow(I)=(V50(I)-Volts(I))*(Volts(I)*(Resist+.3)-V50(I)*.3)/R2
6570 !
6580 Resist=1.852
6590 R2=Resist*Resist
6600 !
6610 IF N=24 THEN Pow(I)=(V49(I)-Volts(I))*(Volts(I)*(Resist+.1)-V49(I)*.1)/R2
6620 IF N=33 THEN Pow(I)=(V50(I)-Volts(I))*(Volts(I)*(Resist+.7)-V50(I)*.7)/R2
6630 !
6640 Resist=1.8333
6650 R2=Resist*Resist
6660 !
6670 IF N=11 THEN Pow(I)=(V47(I)-Volts(I))*(Volts(I)*(Resist+.5)-V47(I)*.5)/R2
6680 IF N=12 THEN Pow(I)=(V47(I)-Volts(I))*(Volts(I)*(Resist+.1)-V47(I)*.1)/R2
6690 IF N=13 THEN Pow(I)=(V47(I)-Volts(I))*(Volts(I)*(Resist+.2)-V47(I)*.2)/R2
6700 IF N=41 THEN Pow(I)=(V51(I)-Volts(I))*(Volts(I)*(Resist+.1)-V51(I)*.1)/R2
6710 IF N=45 THEN Pow(I)=(V51(I)-Volts(I))*(Volts(I)*(Resist+.6)-V51(I)*.6)/R2
6720 !
6730 Resist=1.8182
6740 R2=Resist*Resist
6750 !
6760 IF N=21 THEN Pow(I)=(V48(I)-Volts(I))*(Volts(I)*(Resist+.7)-V48(I)*.7)/R2
6770 !
6780 Resist=1.8
6790 R2=Resist*Resist
6800 !
6810 IF N=8 THEN Pow(I)=(V46(I)-Volts(I))*(Volts(I)*(Resist+.2)-V46(I)*.2)/R2
6820 IF N=19 THEN Pow(I)=(V48(I)-Volts(I))*(Volts(I)*(Resist+.2)-V48(I)*.2)/R2
6830 IF N=20 THEN Pow(I)=(V48(I)-Volts(I))*(Volts(I)*(Resist+.7)-V48(I)*.7)/R2
6840 IF N=22 THEN Pow(I)=(V48(I)-Volts(I))*(Volts(I)*(Resist+.7)-V48(I)*.7)/R2
6850 !
6860 Resist=1.6667
6870 R2=Resist*Resist
6880 !
6890 IF N=1 THEN Pow(I)=(V46(I)-Volts(I))*(Volts(I)*(Resist+.3)-V46(I)*.3)/R2
6900 IF N=3 THEN Pow(I)=(V46(I)-Volts(I))*(Volts(I)*(Resist+.7)-V46(I)*.7)/R2
6910 IF N=7 THEN Pow(I)=(V46(I)-Volts(I))*(Volts(I)*(Resist+.2)-V46(I)*.2)/R2
6920 IF N=16 THEN Pow(I)=(V48(I)-Volts(I))*(Volts(I)*(Resist+.4)-V48(I)*.4)/R2
```

```
6930 IF N=17 THEN Pow(I)=(V48(I)-Volts(I))*(Volts(I)*(Resist+.4)-V48(I)*.4)/R2
6940 IF N=26 THEN Pow(I)=(V49(I)-Volts(I))*(Volts(I)*(Resist+.2)-V49(I)*.2)/R2
6950 !
6960 !
6970 NEXT I
6980 !
6990 PRINTER IS 9
7000 A$="TIME (MIN)"
7010 B$="TEMPERATURE C"
7020 C$="POWER WATT"
7030 D$="TIME (SEC)"
7040 E$="NUMBER"
7050 IF N=1 THEN
7060   PRINT "THIS THERMOCOUPLE IS BAD "
7070   PRINT " "
7080 END IF
7090 !
7100 IF N=3 THEN
7110   PRINT "THIS THERMOCOUPLE IS BAD "
7120   PRINT " "
7130 END IF
7140 !
7150 IF N=6 THEN
7160   PRINT "THIS THERMOCOUPLE IS BAD "
7170   PRINT " "
7180 END IF
7190 !
7200 IF N=22 THEN
7210   PRINT "THIS THERMOCOUPLE IS BAD "
7220   PRINT " "
7230 END IF
7240 !
7250 IF N=29 THEN
7260   PRINT "THIS THERMOCOUPLE IS BAD "
7270   PRINT " "
7280 END IF
7290 !
7300 IF N=37 THEN
7310   PRINT "THIS THERMOCOUPLE IS BAD "
7320   PRINT " "
7330 END IF
7340 !
7350 PRINT "TIME   ",TIME$(TIMEDATE)
7360 PRINT "DATE   ",DATE$(TIMEDATE)
7370 PRINT " "
7380 PRINT "HEATER NUMBER   ";N
7390 PRINT " "
7400 PRINT "CENTER COLUMN PARAMETERS"
7410 PRINT "CYCLE TIME ",Np
7420 PRINT "MAXIMUM VOLTAGE",Maxv
```

```
7430  PRINT "MINIMUM VOLTAGE",Minv
7440  PRINT " "
7450  PRINT "SIDE COLUMN PARATERMETERS"
7460  PRINT "OUTPUT",Scp,"WATTS"
7470  PRINT " "
7480  PRINT "Tamb =",Tamb
7490  PRINT " "
7500  PRINT USING "6A,2X,10A,4X,10A,4X,14A,2X,10A";E$,D$,A$,B$,C$
7510  Runtime=Tf-Ti
7520  !
7530  FOR I=1 TO M
7540  Tsec(I)=(I/M)*Runtime
7550  Tyme(I)=(I*Runtime/M)/60
7560  PRINT USING "1X,4Z,2X,7D.D,5X,4D.DD,11X,DD.DD,10X,DD.2D";I,Tsec(I),Tyme(I)
,T(I)-Tamb,Pow(I)
7570  WAIT 0.
7580  NEXT I
7590  BEEP 3011.06,1.
7600  BEEP 406.90,.3
7610  BEEP 3011.06,.3
7620  BEEP 406.90,.3
7630  END
```

APPENDIX D: PROGRAMS FOR THE HP 85 COMPUTER

```
10    !!!!!!!!!!!!!!!!!!!!!!!!!!!!!!!!!!!!!!
      !!
20    !        SQURE WAVE
30    !    TRANSIENT POWER PROGRAM
      !
40    !
50    !!!!!!!!!!!!!!!!!!!!!!!!!!!!!!!!!!!!!!
      !!
60    !
75    DIM V1(1399)
80    DISP "INPUT MAX VOLTAGE"
90    DISP "AND MIN VOLTAGE"
100   INPUT R1, R2
110   DISP "INPUT CYCLE TIME"
120   INPUT P
130   D=.05
135   P=P*1.13
140   Z=P/D
150   N=INT(Z)
160   K=INT(N/2)
220   FOR I=1 TO K
250   V1(I)=INT(R1*100)+2000
252   NEXT I
254   FOR I=K TO N
260   V1(I)=INT(R2*100)+2000
262   NEXT I
290   BEEP
300   FOR I=1 TO N
310   OUTPUT 706 USING "#,4D" ; V1(I)
330   NEXT I
340   GOTO 290
350   END
```

```
10   !!!!!!!!!!!!!!!!!!!!!!!!!!!!!!!!!!!!
20   !          TRIANGULAR WAVE
30   !    TRANSIENT POWER PROGRAM
     !
40   !
50   !!!!!!!!!!!!!!!!!!!!!!!!!!!!!!!!!!!!
     !!
60   !
70   DIM (E(1399)
75   DIM V1(1399)
80   DISP "INPUT MAX VOLTAGE"
90   DISP "AND MIN VOLTAGE"
100  INPUT R1, R2
110  DISP "INPUT CYCLE TIME"
120  INPUT P
130  D=.05
135  P=P*1.13
140  Z=P/D
150  N=INT(Z)
160  K=INT(N/2)
170  V1(K)=INT(R1*10)*10+2000
180  V1(0)=INT(R2*10)*10+2000
190  E(K)=R1
200  E(0)=R2
210  L=K-1
220  FOR I=1 TO K
230  E(I)=(R1-R2)/K+E(I-1)
240  E(N-1)=E(I)
250  V1(I)=INT(E(I)*100)+2000
260  V1(N-I)=V1(I)
270  NEXT I
280  M=N-1
290  BEEP
300  FOR I=0 TO M
310  OUTPUT 706 USING "#,4D" ; V1(I)
330  NEXT I
340  GOTO 290
350  END
```

```
10   !        CONSTANT
20   !    POWER SUPPLY PROGRAM
30   !
40   !
50   CLEAR
60   DISP "ENTER THE POWER SUPPLY 'S"
70   DISP "FULL SCALE OUTPUT VOLTAGE
80   INPUT F
90   IF F<0 THEN BEEF ISP "NEGATIVE VOLTAGE" @ GOTO 60
100  !
110  DISP "ENTER THE DESIRED OUTPUT VOLTAGE"
120  INPUT W
130  IF V<0 THEN BEEP ISP "NEGATIVE VOLTAGE NOT ALLOWED" @ GOTO 110
140  !
150  ! CALUCLATE PERCENT OF
160  ! POWER SUPPLY FULL SCALE
170  P=V/F*100
180  IF P>99.9 THEN BEEP ISP "VOLTAGE TOO LARGE" OTO 110
190  !
200  ! SELECT RANGE
210  IF P>9.99 THEN GOTO 280
220  !
230  ! LOW RANGE CALCULATIONS
240  M=INT(P*100+.5)
250  D=M+1000
260  GOTO 320
270  !
280  ! HIGH RANGE CALCULATIONS
290  M=INT(P*10+.5)
300  D=M+2000
310  !
320  OUTPUT 706 USING "#,4D" ; D
330  DISP "THE PROGRAMMED DATA WORD IS";D
340  GOTO 110
350  END
340  GOTO 290
350  END
```

APPENDIX E: SAMPLE UNCERTAINTY CALCULATIONS

Sample calculations are for the top heater location triangular wave power pattern baseline case; that is mean power input of 2.0 watts, amplitude 1.0 watts, and a frequency of pulsation of 0.050 Hz. The uncertainty is calculated by considering timewise jitter and bias components for each appropriate variable.

$$\bar{Nu} = \frac{Q_{conv} L}{kA(\Delta T)}$$

$$Q_{conv} = Q - Q_{cond}$$

$$\Delta T = T - T_{amb}$$

$$\frac{\delta \bar{Nu}}{\bar{Nu}} = \left[\left(\frac{\delta Q_{conv}}{Q_{conv}}\right)^2 + \left(\frac{\delta L}{L}\right)^2 + \left(\frac{\delta A}{A}\right)^2 + \left(\frac{\delta(\Delta T)}{\Delta T}\right)^2\right]^{\frac{1}{2}}$$

$$\delta Q_{conv} = \left[\left(\frac{\partial Q_{conv}}{\partial Q}\delta Q\right)^2 + \left(\frac{\partial Q_{conv}}{\partial Q_{cond}}\delta Q_{cond}\right)^2\right]^{\frac{1}{2}}$$

$$= \left[(\delta Q)^2 + (\delta Q_{cond})^2\right]^{\frac{1}{2}}$$

$$\delta(\Delta T)_{TWJ} = \left[\left(\frac{\partial(\Delta T)}{\partial T}\delta T\right)^2 + \left(\frac{\partial(\Delta T)}{\partial T_{amb}}\delta T_{amb}\right)^2\right]_{TWJ}^{\frac{1}{2}}$$

$$= \left[(\delta T)^2 + (\delta T_{amb})^2\right]^{\frac{1}{2}}$$

where:

$\bar{Nu}$ = 1.888

Q = 2.0 Watts

Q_{conv} = 1.93 Watts

Q_{cond} = 0.07 Watts

δQ_{BIAS} = 0.05 Watts

δQ_{TWJ} = 0.05 Watts

δQ_{cond} = 0.0035 Watts

L = 2.940×10^{-3} m

δL = 0.0

δA = 0.0

A = 186.4×10^{-6} m^2

ΔT = 20.04 K

$\delta \Delta T_{BIAS}$ = 0.1 K

δT_{TWJ} = 0.025 K

$(\delta T_{amb})_{TWJ}$ = 0.025 K

$$\delta Q_{conv} = \left[(0.05)^2_{BIAS} + (0.05)^2_{TWJ} + (0.0035)^2\right]^{\frac{1}{2}}$$

$$= 0.0708 \quad watts$$

$$\delta(\Delta T)_{TWJ} = \left[(0.025)^2 + (0.025)^2\right]^{\frac{1}{2}}$$

$$= 0.0354 \quad K$$

$$\delta(\Delta T)_{BIAS} = 0.1 \quad K$$

$$\frac{\delta \bar{Nu}}{\bar{Nu}} = \left[\left(\frac{.0708}{1.93}\right)^2 + 0.0 + 0.0 + \left(\frac{.0354}{20.4}\right)^2 + \left(\frac{.1}{20.4}\right)^2\right]^{\frac{1}{2}}$$

$$\frac{\delta \bar{Nu}}{\bar{Nu}} = 0.0371$$

$$\delta \bar{Nu} = 0.070$$

$$\bar{Nu} = 1.888 \pm 0.070$$

$$Gr = \frac{g\beta Q L^4}{kA\nu^2}$$

$$\frac{\delta \bar{Gr}}{\bar{Gr}} = \left[\left(\frac{\delta Q}{Q}\right)^2 + \left(\frac{\delta L^4}{L^4}\right)^2 + \left(\frac{\delta A}{A}\right)^2\right]^{\frac{1}{2}}$$

where:

$\bar{Gr}$ = 6808

Q = 2.0 watts

δQ_{BIAS} = 0.05 watts

δQ_{TWJ} = 0.05 watts

L^4 = 74.71×10^{-12} m^4

$\delta L^4 = 0.0$

$A = 186.4 \times 10^{-6}\ m^2$

$\delta A = 0.0$

$$\frac{\delta \bar{Gr}}{\bar{Gr}} = \left[\left(\frac{0.05}{2}\right)^2_{BIAS} + \left(\frac{0.05}{2}\right)^2_{TWJ} + 0.0 + 0.0\right]^{\frac{1}{2}}$$

$$\frac{\delta \bar{Gr}}{\bar{Gr}} = 0.0354$$

$$\delta \bar{Gr} = 240.7$$

$$\bar{Gr} = 6808 \pm 240.7$$

LIST OF REFERENCES

1. Bar-Cohen, A., and Kraus, A.D., "Advances in Thermal Modeling of Electronic Components and Systems," (1988)

2. Bar-Cohen, A., "Thermal Management of Electronic Components with Dielectric Liquids," *ASME/JSME Thermal Engineering Proceedings*, v. 2, pp. xv-xxxi, ASME 1991.

3. Incropera, F.P., and DeWitt, D.P., *Introduction to Heat Transfer*, 2d ed., John Wiley & Sons, 1985, 1990.

4. Sathe, S.B., and Joshi, Y., "Natural Convection Arising from a Heat Generating Substrate-Mounted Protreusion in a Liquid-Filled Two-Dimensional Enclosure," *Int J. Heat Mass Transfer*, v. 34, No. 8, pp. 2149-2163, 1991.

5. Haukenes, Larry O., "A Computational and Experimental Study of Flush Heat Sources in Liquids," Master's Thesis, Naval Postgraduate School, Monterey, California, June 1990.

6. Baker, E. "Liquid Immersion Cooling of Small Electronic Devices," *Microelectronics and Reliability*, v. 12, pp. 163-173, 1973.

7. Park, K., and Bergles, A., "Natural Convection Heat Transfer Characteristics of Simulated Microelectronic Chips," *ASME Journal of Heat Transfer*, v. 109, pp. 90-96, 1987.

8. Bar-Cohen, A., and Schweitzer, H., "Convective Immersion Cooling of Parallel Vertical Plates," *IEEE Transactions on Components, Hyfrids and Manufacturing Technology*, v. CHMT-8, pp. 343-351, 1985.

9. Kelleher, M., Knock, R., and Yang, K., "Laminar Natrual Convection in A Rectangular Enclosure Due To A Heated Protrusion on a Vertical Wall Part I: Experimental Investigation," *Proc. Second ASME/JSME Therm. Engr. Joint Conf.*, Honolulu, pp.169-177, 1987.

10. Lee, K., Kelleher, M., Knock, R., and Yang, K., "Laminar Natural Convection in A Rectangular Enclosure Due To A Heated Protrusion on A Verticla Wall Part II: Numerical Simulations," *Proc. Second ASME/JSME Therm. Engr. Jouint Conf.*, Honolulu, pp. 179-185, 1987.

11. Joshi, Y., Kelleher, M.,and Benedict, T., "Natural Convection Immewrsion Cooling of An Array of Simulated Chips in An Enclosure Filled With Dielectric Fluid," Presented at the XXth International Symposium of the International Center for Heat and Mass Transfer, Dubrovnic, Yugoslavia, 1988.

12. Joshi, Y., Willson, T., Hazard, and Hazard, S.J. III, "An Experimental Study of Natural Convection From an Array of Heated Protrusions on a Vertical Surface in Water," *Journal of Electronic Packaging*, v. 111, pp. 121-128, June 1989.

13. Joshi, Y., Willson, T., and Hazard, S.J. III, "An Experimental Study of Natural Convection Cooling of an Array of Heated Protrusions in a Vertical Channel in Water," *Journal of Electronic Packaging*, v. 111, pp. 33-40, March 1989.

14. Joshi, Y., and Paje, R., "Natural Convection Cooling of a Ceramic Substrate Mounted Leadless Chip Carrier in Dielectric Liquids," *Int. Comm. Heat Mass Transfer*, v. 18, pp. 39-47, 1991.

15. Joshi, Y., and Knight, L., "Natural Convection From a Column of Flush Heat Sorces in a Vertical Channel in Water," *Journal of Electronic Packaging*, v. 112, pp. 367-374, December 1990.

16. Gaiser, Alfred O., "Natural Convection Liquid Immersion Cooling of High Density Columns of Discrete Heat Sources in a Vertical Channel," Master's Thesis, Naval Postgraduate School, Monterey, California, June 1989.

17. Akdeniz, Erhan M., "Effects of Power Pulsations On Natural Convection From Discrete Heat Sources," Master's Thesis, Naval Postgraduate School, Monterey, California, March 1991.

INITIAL DISTRIBUTION LIST

		No. of Copies
1.	Defense Technical Information Center Cameron Station Alexandria, Virginia 22304-6145	2
2.	Library, Code 52 Naval Postgraduate School Monterey, California 93943-5002	2
3.	Prof. A.J. Healey, Code ME/Hy Department of Mechanical Engineering Naval Postgraduate School Monterey, California 93943-5000	1
4.	Prof. M.D. Kelleher, Code ME/Kk Department of Mechanical Engineering Naval Postgraduate School Monterey, California 93943-5000	1
5.	Prof. Y. Joshi, Code ME/Ji Deparment of Mechanical Engineering Naval Postgraduate School Monterey, California 93943-5000	2
6.	Prof. A.D. Kraus, Code EC/Ks Department of Elec. and Comp. Engineering Naval Postgraduate School Monterey, California 93943-5004	1
7.	Mr. Kip Hoffer Naval Weapons Support Center Code 6042 Crane, Indiana 47522	1

8. Mr. Tony Buechler 1
Naval Weapons Support Center
Code 6042
Crane, Indiana 47522

9. Naval Engineering Curricular Office, Code 34 1
Naval Postgraduate School
Monterey, California 93943-5004

10. Stephen Alan Larsen 1
8706 Arbor St.
Omaha, Nebraska 68124